



UNIVERSITY OF  
LIVERPOOL

**The tumorigenicity-promoting activity of C-FABP in prostate cancer  
cells depends on its fatty acid-binding ability**

THESIS SUBMITTED IN ACCORDANCE WITH THE REQUIREMENTS OF  
THE UNIVERSITY OF LIVERPOOL  
FOR THE DEGREE OF DOCTOR IN PHILOSOPHY

*By*

**Mohammed Imad Malki**

December 2011

**Department of Molecular and Clinical Cancer Medicine (Pathology)**

## ABSTRACT

Cutaneous fatty acid-binding protein (C-FABP) or FABP5, is a FABP family member that can bind to long chain fatty acids with high affinity. *C-FABP* was identified by our research group as a gene involved in malignant progression of prostate cancer and able to promote the growth of primary tumours and induce metastasis when transfected into rat benign Rama 37 model cells. It was demonstrated that C-FABP was a prognostic marker for patient outcome and a target of tumour-suppression for prostate cancer. As an initial step to understanding the complex molecular mechanisms involved in the cancer promoting activity of C-FABP, this study investigated the possible relationship between tumorigenicity-promoting activity of C-FABP and its fatty acid-binding capability. After single and double mutations were generated in the fatty acid binding motif of the C-FABP cDNA, wild type and mutant C-FABP cDNAs were excised from the mammalian vector pIRES2-EGFP and inserted into pBluescript cloning vector to generate a complimentary restriction sites at both ends of the cDNAs. The C-FABP cDNAs were excised from the pBluescript vector with *KpnI* and *PstI* and inserted into pQEs expression vector to form three constructs that express the wild type and two mutant C-FABPs (C-FABP-WT, C-FABP-R109A and C-FABP-R109/129A), respectively. SDS-PAGE and sequence analysis confirmed the correct insertion of C-FABPs into expression vector pQE. The pure recombinant proteins were subsequently produced and purified. The importance of fatty acid-binding activity to the cancer promoting function was assessed by comparing the cancer promoting abilities exerted by C-FABPs with different fatty acid-binding capabilities.

To test whether the recombinant proteins produced were biological active, the fatty acid binding ability of wild type and mutant C-FABPs were tested. When fatty acid binding ability of the wild type C-FABP is set at 1, the average fatty acid binding ability the C-FABP-R109A and C-FABP-R109/129A were significantly reduced to 0.32% and 0.09%, respectively (Student t-test,  $P < 0.005$ ). These results suggested that fatty acid binding ability of C-FABP depends on the structured integrity of the binding motif. Thus, changing one amino acid in the motif significantly reduced the fatty acid binding ability by 68%, and changing two amino acids almost completely abolished the fatty acid binding ability of C-FABP.

To access the importance of the structural integrity of the fatty acid binding motif to the tumorigenicity-promoting activity of C-FABP in prostate cancer, the effect of wild type and mutant C-FABPs on cell proliferation, invasion and colony formation as indication of tumourigenicity were analysed. The average growth rate of cells stimulated with C-FABP-WT was significantly increased by 17% (Student t-test,

$P<0.05$ ) when compared to control cells. Whereas, the average growth rate of cells stimulated with C-FABP-R109A and C-FABP-R109/129A were significantly reduced by 33% and 47%, respectively (Student t-test,  $P<0.005$ ) when compared to control cells. The invasiveness of cells stimulated with C-FABP-WT, C-FABP-R109, C-FABP-R109/129A and the control cells were  $256\pm40$ ,  $163\pm32$ ,  $80\pm26$  and  $96.6\pm15.2$ , respectively. The number of invaded cells stimulated with C-FABP-WT was the highest in all cell lines and more than 2.6-fold higher than the number of invaded cells from control (Student t-test,  $P<0.05$ ). The average number of colonies produced in the soft agar by selected cells stimulated with C-FABP-WT, C-FABP-R109A, C-FABP-R109/129A and control were  $1050\pm132.29$ ,  $283\pm76.38$ ,  $157\pm38.1$  and  $155\pm68.74$ , respectively. In comparison with the control, the average number of colonies produced by C-FABP-R109A stimulated cells was increased by 45% (Student t-test,  $P<0.01$ ) whereas the average number of colonies produced by C-FABP-R109/129A stimulated cells was at same level as the control cells (Student t-test,  $P>0.5$ ). The most significant change occurred in C-FABP-WT stimulated cells that produced more than a 6.7-fold (85%) increase in the number of colonies formed in soft agar when compared to controls (Student t-test,  $P<0.001$ ). These results showed that the increased wild type C-FABP stimulation in prostate cell line significantly increased cell proliferation, invasiveness, and tumorigenicity. Whereas, the increased expression of both mutant forms of C-FABP did not significantly affect these characteristics.

Overall, this study has confirmed that the biological potential of C-FABP to promote tumorigenicity of prostate cancer cells depends on its ability of binding to fatty acids. Thus, C-FABP may facilitate cancer development through a mechanism involving transportation of intracellular fatty acids into cells. These results were supported by our recent data obtained from *in-vivo* studies performed in a nude mouse model.

## DEDICATION

*To Prophet Mohammad, peace be upon him,  
to my parents, Abdulmoti & Houda,  
to my brothers Omar, Abdullah & Abdulawhab  
to my family and relatives in Syria  
to my Friends, in the UK, Syria & Sudan  
and to all Syrian Martyrs*

## ACKNOWLEDGMENTS

*All praise is due to God,  
the Creator and Sustainer of the Universe*

I would like to express my deepest gratitude and appreciation to my supervisors Professor Youqiang Ke and Professor Christopher Foster. They showed me an unequivocal perseverance, gave me so much time and enriched my work with invaluable comments.

In addition to my supervisors, many people assisted me to carry out this project. First and foremost, I would like to thank Dr. Shiva Forootan, Dr. Zhang Zhang Bao and Mrs. Carol Beesley for providing me with the first drops of genuine knowledge. They helped me with their experience and insightful feedback on the most experimental aspects of this research and also Mr. Tim Dickinson and Mrs. Pat Gerard for all the technical support they gave me. Moreover, I would like to express my grateful acknowledgment to the present and past Ph.D. students in Pathology Department, Drs Laleh, Shown and Rainy. They were around every day to give me good pieces of advice during my experiments. Also I would like to record my gratitude to Mr. Andy Dodson who helped me with the immunohistochemistry staining.

My greatest and sincerest gratitude and appreciation are due to my parents Dr. Abdulmoti Molki and Mrs. Houda Monadi to whom this work is dedicated. They spared no effort in helping me and for them today is a memorable day as they do feel the happiest whenever any one of their children takes a step ahead. Also I would like to express my grateful acknowledgment to my brothers; Omar, Abdullah and Abdalwahab for their endless love and encouragement during my studies.

I would like to express my thanks to Professor Ke's wife Mrs. Shuwen Yang and to my friends Afeef Aslam, Riyadh and Nabeel for taking care of my health and providing me with delicious foods during the recovery from appendectomy surgery.

I gratefully acknowledge the Overseas Research Students Award (ORS), University of Liverpool, the Prostate UK and the North West Cancer Research Fund (NWCRCF) for the financial support to this research project.

## **DECLARATION**

---

No portion of the work referred to in the thesis has been submitted in support of an application for another degree or qualification of this or any other university or other institute of learning.

---

## **DECLARATION OF ORIGINALITY**

---

This thesis is a product of my own work produced during my time at the Department of Molecular and Clinical Cancer Medicine (Pathology), University of Liverpool, between November 2008 and November 2011. All experiments presented in the results section were performed by myself with the exception of sections 3.2.3 to 3.2.5 of Chapter 3 which was done in parallel with Dr. Zhang Zhang Bao. The thesis was written by myself with guidance from my supervisors Professor Christopher Foster and Professor Youqiang Ke.

---

## THE AUTHOR

The author graduated in 2006 with a first class medical degree. Afterwards he was successfully awarded an MSc in Cellular Pathology from Manchester Metropolitan University in 2007. He then joined the School of Cancer Medicine at the University of Liverpool after being awarded an ORSAS scholarship for a PhD in Pathology with Professor Youqiang Ke and Professor Christopher Foster.

He presented the work developed during his PhD in the form of an oral presentations at the 53<sup>rd</sup> Annual Meeting of the Italian Cancer Society (SIC) Back to the Future: Translating Cancer Research from Bedside to Bench and Back, Turin, Italy, 19-22 October, 2011 (Awarded "EACR Prize" for best short talk presentation). Also, he was invited as a speaker in Blue Skies Forum on Prostate Cancer, Downing College, Cambridge University, 8<sup>th</sup> April 2011. The Author won a complimentary registration from European Association for Cancer Research (EACR) to attend the 1st EACR-OECI Joint Training Course "Molecular PATHOLOGY approach to cancer" 7<sup>th</sup> - 9<sup>th</sup> March 2011, Amsterdam, The Netherlands. In 2010, the Author's abstract, which was awarded the highest point, was selected for poster presentation at the 21<sup>st</sup> EACR meeting, 26-29<sup>th</sup> June 2010, Oslo, Norway.

## PUBLICATIONS

- ❖ **Malki M I\***, Bao Z Z\*, Forootan F S, Adamson J, Kamalian L, Zhang Y, Foster C S, Rudland P S, Ke Y Q. Tumorigenicity-promoting activity of C-FABP in prostate cancer cells depends on its fatty acid-binding capability. (Manuscript submitted).
- ❖ Zhang Y, Forootan S S, Kamalian L, Bao Z Z, **Malki M I**, Foster C S, Ke Y. (2011) Suppressing tumourigenicity of prostate cancer cells by inhibiting osteopontin. *International Journal of Oncology*. 38 (4). Page: 1083-9.
- ❖ **Malki, M I**, Forootan, S, Foster, C S & Ke, Y. Investigation of the Differentially Expressed C-FABP & FABP-pm in Human Prostate Tissues and Cell Lines: Histopathological and Molecular Biology Study. *European Journal of Cancer supplements* 8, no. 5 (2010) 155–170.
- ❖ **Malki, M I**, Bao, Z Z, Forootan, S, Foster, C S & Ke, Y. Tumourigenicity-promoting activity of C-FABP depends on its fatty acid-binding capability. The 53rd Annual Meeting of the Italian Cancer Society (SIC) Back to the Future: Translating Cancer Research from Bedside to Bench and Back. Turin, Italy, 19-22 October, 2011. (**Oral Presentation**)
- ❖ **Malki, M I**, Bao, Z Z., Forootan, S, Foster, C S & Ke, Y. Suppressing the malignant progression of prostate cancer by inhibiting the expression of C-FABP gene. Blue Skies Forum, Downing College, Cambridge University. 8 April 2011. (**Invited Speaker**)
- ❖ **Malki, M I**, Forootan, S, Foster, C S & Ke, Y. Investigation of the Differentially Expressed C-FABP & FABP-pm in Human Prostate Tissues and Cell Lines: Pathological and Molecular Biology Study. EACR-21. Oslo-Norway. 26-29 June 2010. (**Poster Presentation**)

\*Contributed equally to this study

## TABLE OF CONTENTS

ABSTRACT .....	2
DEDICATION .....	4
ACKNOWLEDGMENTS .....	5
DECLARATION .....	6
DECLARATION OF ORIGINALITY .....	6
THE AUTHOR .....	7
PUBLICATIONS .....	7
LIST OF FIGURES .....	20
LIST OF TABLES .....	25
LIST OF ABBREVIATIONS .....	27
1 INTRODUCTION .....	31
1.1 Epidemiology of prostate cancer .....	32
1.1.1 Incidence .....	32
1.1.2 Mortality.....	34
1.1.3 Survival .....	35
1.2 Risk Factors .....	36
1.2.1 Age .....	36
1.2.2 Race.....	37



1.2.3	Family history .....	37
1.2.4	Hormones .....	38
1.2.5	Other factors .....	39
1.3	The Pathology of Prostate Cancer .....	39
1.3.1	Anatomy of the prostate .....	39
1.3.2	Prostate Architecture .....	40
1.4	Prostate cancer initiation .....	41
1.4.1	Benign Prostatic Hyperplasia (BPH) .....	41
1.4.2	Prostatic Intraepithelial Neoplasia (PIN) .....	42
1.4.3	Gleason Score.....	43
1.5	Cell culture models.....	44
1.5.1	DU-145.....	45
1.5.2	LNCaP.....	46
1.5.3	PC-3 .....	46
1.6	Oncogenes and tumour suppressor genes in prostate cancer .....	47
1.6.1	Oncogenes .....	47
1.6.1.1	<i>Ras</i> oncogene .....	48
1.6.1.2	<i>C-myc</i> oncogene.....	49
1.6.1.3	HER-2 (C-ERB-R2, neu) .....	49
1.6.1.4	<i>Bcl-2</i> Oncogene.....	50
1.6.2	Tumour Suppressor genes .....	51

1.6.2.1	<i>Retinoblastoma (RB)</i> .....	52
1.6.2.2	<i>P53</i> .....	52
1.6.2.3	<i>Cadherin</i> .....	53
1.6.2.4	<i>KAI-1</i> .....	54
1.6.2.5	<i>NM23</i> .....	54
1.6.2.6	<i>CD44</i> .....	55
1.6.2.7	<i>PTEN</i> .....	56
1.7	Prostate Cancer Metastasis .....	57
1.7.1	Mechanisms of bone metastasis in prostate cancer.....	58
1.7.1.1	Osteoclastic bone resorption.....	58
1.7.1.2	Domination of the osteoblastic lesions .....	61
1.7.2	Androgens and Prostate Cancer .....	63
1.7.3	Androgen independence and prostate cancer .....	63
1.7.4	Progression to androgen independence .....	64
1.7.4.1	Pre-existing genetics changes in prostate cancer stem cells .....	65
1.7.4.2	Oncogenes and apoptosis inhibition .....	65
1.7.4.3	Ligand-independent AR activation .....	66
1.7.4.4	AR hypersensitivity .....	66
1.7.4.5	Changes of AR specificity (AR mutations) .....	67
1.7.4.6	Gene Fusions.....	68
1.7.4.7	Androgen synthesis in AIPC tissues .....	69

1.7.5	Androgen receptors and growth factors interactions .....	71
1.8	Angiogenesis .....	72
1.8.1	Vascular endothelial growth factor (VEGF) .....	72
1.8.2	The isoforms of VEGF.....	73
1.8.3	VEGF and prostate cancer .....	74
1.8.4	Other growth factors in Prostate cancer .....	75
1.9	Peroxisome proliferator-activated receptors.....	75
1.9.1	Structure of PPAR.....	76
1.9.2	PPAR $\beta/\delta$ .....	78
1.9.3	PPAR $\gamma$ .....	79
1.10	Fatty Acid, Fatty Acid Binding Proteins and Prostate Cancer .....	80
1.10.1	Introduction to Fatty Acid.....	80
1.10.2	Dietary fatty acid and prostate cancer .....	80
1.10.3	Fatty acid binding proteins (FABPs) .....	82
1.10.3.1	Fatty acid binding proteins (FABPs) family.....	82
1.10.3.2	Fatty acid binding proteins (FABPs) affinity and structure.....	84
1.10.3.3	Functions of FABPs.....	87
1.10.4	Cutaneous FABP (C-FABP) in prostate cancer .....	88
1.11	Scope of this thesis .....	90
1.11.1	Hypothesis.....	90
1.11.2	Aims .....	90

2	MATERIALS AND METHODS.....	91
2.1	Materials .....	92
2.2	General molecular biology methods.....	92
2.2.1	Calculation of DNA and RNA concentration .....	92
2.2.2	Ethanol precipitation of DNA and RNA .....	92
2.2.3	Agarose gel electrophoresis of DNA .....	93
2.2.4	Purification of DNA from agarose gels .....	93
2.2.5	Restriction Enzyme digestion of plasmid DNA.....	94
2.2.6	DNA ligation.....	95
2.2.7	cDNA sequencing .....	96
2.2.8	Transformation of competent bacteria with plasmid DNA.....	96
2.2.8.1	Preparation of competent bacterial cells .....	96
2.2.8.2	Transformation.....	97
2.2.8.3	Calculation of transformation efficiency .....	97
2.2.9	Isolation of plasmid DNA .....	98
2.2.9.1	Miniprep extraction of plasmid DNA.....	98
2.2.9.2	Midiprep extraction of plasmid DNA .....	99
2.3	Mutagenesis of C-FABP gene and construction of C-FABPs transfection vectors .....	100
2.3.1	Selection and mutagenic primers .....	104
2.3.2	Generation of the mutant plasmid DNA .....	104

2.3.3	Selection by restriction digestion .....	104
2.4	Cell culture .....	105
2.4.1	Routine cell culture .....	105
2.4.1.1	Thawing of cells.....	106
2.4.1.2	Sub-culture of cell lines .....	106
2.4.1.3	Counting cells .....	107
2.4.1.4	Freezing cells .....	107
2.5	Cell transfection .....	108
2.5.1	Stable transfection of the LNCaP cell line using GeneJammer .....	108
2.5.2	Transfected clone selection by cell image .....	109
2.5.3	Ring cloning of transfected cells.....	110
2.6	Molecular cloning.....	111
2.6.1	Phase 1: .....	111
2.6.1.1	Cloning into pBluescript II SK (+/-) Phagemids .....	111
2.6.1.2	Ethanol precipitation of DNA.....	113
2.6.1.3	Restriction Enzyme digestion of plasmid DNA .....	113
2.6.1.4	Agarose gel electrophoresis of DNA .....	114
2.6.1.5	Purification of DNA from agarose gels .....	114
2.6.1.6	Calculation of insert/vector ratio .....	115
2.6.1.7	DNA ligation.....	115
2.6.1.8	Transformation of competent bacteria with plasmid DNA .....	116

2.6.1.8.1	Preparation of competent bacterial cells .....	116
2.6.1.8.2	Transformation.....	117
2.6.1.9	Isolation of plasmid DNA.....	118
2.6.1.9.1	Miniprep extraction of plasmid DNA.....	118
2.6.1.9.2	Midiprep extraction of plasmid DNA.....	119
2.6.1.10	cDNA sequencing .....	120
2.6.2	Phase 2: .....	120
2.6.2.1	Cloning into pQE vectors .....	120
2.6.2.2	Restriction Enzyme digestion of plasmid DNA .....	123
2.6.2.3	Agarose gel electrophoresis of DNA .....	124
2.6.2.4	Purification of DNA from agarose gels .....	124
2.6.2.5	Calculation of insert/vector ratio .....	124
2.6.2.6	DNA ligation.....	125
2.6.2.7	Transformation of competent bacteria with plasmid DNA .....	126
2.6.2.7.1	Preparation of competent bacterial cells.....	126
2.6.2.7.2	Transformation.....	126
2.6.2.8	Isolation of plasmid DNA.....	127
2.6.2.9	cDNA sequencing .....	127
2.6.3	Expression and purification of recombinant C-FABP proteins .....	128
2.6.3.1	Growing <i>E. coli</i> and inducing expression.....	128
2.6.3.2	Protein purification .....	128

2.7	Analysis of protein expression using Western blot .....	131
2.7.1	Isolation of protein extracts from cultured cells .....	131
2.7.2	Determination of protein concentration .....	132
2.7.3	Equalization of protein samples for loading .....	132
2.7.4	Sodium dodecyl sulphate polyacrylamide protein gel electrophoresis (SDS-PAGE).....	132
2.7.5	Transfer of proteins from SDS gel to nitrocellulose membrane .....	134
2.7.6	Coomassie blue and PONCAUS staining .....	134
2.7.7	Immunoblotting for detection of protein expression.....	135
2.7.8	Immunoblotting for detection of $\beta$ -actin expression.....	136
2.8	Total RNA isolation .....	137
2.8.1	Reverse transcription polymerase chain reaction.....	138
2.8.1.1	First strand cDNA synthesis .....	138
2.8.1.2	Polymerase chain reaction .....	138
2.8.1.3	Real-time PCR .....	140
2.8.1.3.1	Real-time PCR primer design .....	141
2.8.2	Relative real-time PCR .....	142
2.8.2.1	Relative quantitation analysis .....	143
2.9	Fatty Acid Binding Assay .....	143
2.10	Fatty acid uptake assay .....	144
2.11	Cell proliferation assay .....	145

2.11.1	Preparation of growth curve.....	146
2.11.2	Assessing cell numbers using MTT assay .....	147
2.12	Cell migration assay in Boyden chamber system.....	148
2.13	Soft agar assay.....	149
2.14	Statistic methods.....	150
3	Generation of mutation in C-FABP cDNAs and Transfected them into LNCaP prostate cancer cells .....	152
3.1	Introduction .....	153
3.2	Results .....	154
3.2.1	Generation of mutations in <i>C-FABP</i> cDNA.....	154
3.2.2	Insertion of wild type C-FABP and mutant C-FABPs into a mammalian expression vector - pIRES <sub>2</sub> -EGFP .....	157
3.2.3	Detection of wild type and mutated C-FABP mRNAs in transfected LNCaP cells by RT-PCR .....	160
3.2.4	Expression of wild type and mutant C-FABP proteins in LNCaP cell line .....	164
3.2.5	Measurement of levels of wild type and mutant C-FABP mRNAs in different transfectants by Real-time PCR .....	168
3.3	Discussion .....	172
4	Production of recombinant C-FABPs and testing their fatty acid binding ability.. .....	175
4.1	Introduction .....	176



4.2	Results .....	178
4.2.1	Generation of complementary restriction sites .....	178
4.2.2	Confirmation of successful insertion of wild type and mutant cDNAs into pBluescript cloning vector.....	182
4.2.2.1	Sequence analysis of plasmid DNAs .....	182
4.2.3	Cloning of wild type and mutant C-FABPs into an expression vector pQEs .....	186
4.2.4	Confirmation of successful insertion of wild type and mutant C-FABP cDNAs into pQEs expression vector .....	189
4.2.4.1	Sequences analysis of plasmid DNAs .....	189
4.2.4.2	Confirmation of Correct reading frame for recombinant proteins production .....	190
4.2.5	Expression and purification of recombinant C-FABP proteins .....	196
4.2.5.1	Time course analysis of protein expression.....	196
4.2.5.2	Purification of 6xHis-tagged C-FABP proteins.....	198
4.2.6	Fatty acid binding assay for recombinant C-FABP proteins .....	199
4.3	Discussion .....	203
5	Effect of overexpression of recombinant wild type and mutant C-FABPs on tumorigenicity of prostate cancer cells .....	206
5.1	Introduction .....	207
5.2	Results .....	209

5.2.1	The effect of wild type and mutant C-FABPs on cellular fatty acid uptake .....	209
5.2.2	Effect of wild type and mutants C-FABPs on cell proliferation.....	211
5.2.2.1	LNCaP cell line.....	212
5.2.2.2	22RV1 Cell line .....	216
5.2.2.3	LNCaP-C4 <sub>2</sub> cell line .....	220
5.2.3	The effect of wild type and mutants C-FABPs on the invasiveness of the cells .....	224
5.2.4	Soft agar colony formation assay of recombinant C-FABP proteins.	228
5.2.4.1	LNCaP cell line.....	228
5.2.4.2	22RV1 cells line.....	231
5.2.4.3	LNCaP-C4 <sub>2</sub> cell line.....	235
5.3	Discussion .....	240
6	GENERAL DISCUSSION AND CONCLUSION.....	243
6.1	Discussion .....	244
6.2	Conclusion.....	258
6.3	Future work .....	262
7	REFERENCES .....	263
8	Appendices.....	289
8.1	Appendix 1 .....	290
8.1.1	Materials for general molecular Biology .....	290

8.1.2	Materials for transformation of competent bacteria.....	291
8.1.3	Materials for point mutation .....	292
8.1.4	Materials for PCR, RT-PCR and Real-time PCR .....	293
8.1.5	Materials for cell culture .....	294
8.1.6	Materials for Western blot .....	295
8.1.7	Materials for fatty acid uptake assay.....	296
8.1.8	Materials for fatty acid Binding assay .....	297
8.1.9	Materials for cell proliferation assay .....	297
8.1.10	Materials for cell invasion assay .....	298
8.1.11	Materials for soft agar assay .....	298
8.2	Appendix 2 .....	299
8.2.1	Media and Stock Solutions .....	299
8.2.1.1	Tissue culture .....	299
8.2.1.2	Qiagen Midi-prep plasmid extraction buffers.....	300
8.2.1.3	Wizard SV gel and PCR clean-up system buffers .....	301
8.2.1.4	Western blot buffers.....	302
8.3	Appendix 3 .....	303
8.4	Appendix 4 .....	306

## LIST OF FIGURES

Figure 1.1: prostate cancer, world age-standardised incidence and mortality rates, by world regions, 2008 (Jemal <i>et al</i> , 2008).....	33
Figure 1.2: number of deaths and age-specific mortality rates, prostate Cancer, UK, 2008 (Schroder <i>et al</i> , 2009).....	34
Figure 1.3: Age-standardised (European) mortality rates, prostate cancer 1971-2008 (Bosetti <i>et al</i> , 2008).....	35
Figure 1.4: prostate cancer Age standardised five-year survival rates in England and Wales (Rachet <i>et al</i> , 2009).....	36
Figure 1.5: The anatomy and zones of prostate gland (Abate-Shen and Shen, 2000). .....	40
Figure 1.6: Gleason grading system diagram (Humphrey, 2004).....	44
Figure 1.7: Schematics of original PC-3 cells and their derivatives (Sobel & Sadar, 2005). ....	47
Figure 1.8: The metastatic cascade of prostate cancer .....	57
Figure 1.9: Schematic representation of the putative interactions between prostate cancer cells and osteoblastic/osteoclastic cells in tumoral bone microenvironment (Mori <i>et al</i> , 2007). ....	59
Figure 1.10: The ratio of RANK ligand to osteoprotegerin determines the level of osteoclastogenesis (Mori <i>et al</i> , 2007).....	60
Figure 1.11: IGF-I-IFGBP3-ALS binds to IGF-IR to trigger a series of ligand-mediated activations including RAS-RAF-MAPK and PI3K-AKT signalling	

pathway, controlling cell proliferation and cell apoptosis, respectively (Piqueras <i>et al</i> , 2007). .....	62
Figure 1.12: The schematic view of the domain structure of PPARs. ....	76
Figure 1.13: Model for PPARs signalling pathway (Harmon <i>et al</i> , 2010). ....	78
Figure 1.14: Crystal structure of ligand-bound FABPs (Furuhashi & Hotamisligil, 2008). ....	85
Figure 1.15: Fingerprint for fatty acid binding proteins (Furuhashi & Hotamisligil, 2008). ....	86
Figure 1.16: Putative functions of FABPs in the cell (Furuhashi & Hotamisligil, 2008). ....	88
Figure 2.1: Circular maps and lists of features for the pBluescript II SK vector .....	102
Figure 2.2: Transformer site-directed mutagenesis strategy .....	103
Figure 2.3: Three mock-transfection controls .....	109
Figure 2.4: Circular maps and lists of features for the pIRES <sub>2</sub> -EGFP vector .....	110
Figure 2.5: Construction of QIAexpress expression vector. ....	112
Figure 2.7: PQE vectors for N-terminal 6xHis tag constructor. ....	122
Figure 2.8: purification of 6xHis-tagged proteins using QIAexpress. ....	129
Figure 2.9: SYBR Green Dye binds to the double stranded DNA and fluoresces... ..	141
Figure 3.1: Detection of mutations in C-FABP cDNA by sequencing analysis .....	156
Figure 3.2: The products of restriction enzyme digestion for the ligation reaction. ....	158
Figure 3.3: Identification of the recombinant DNAs by restriction enzyme digestion... ..	159
Figure 3.4: Green fluorescent emission images of successful transfected cells .....	161
Figure 3.5: Detection of mRNAs from transfected cell lines by RT-PCR.....	163

Figure 3.6: Detection of protein expression levels of wild type C-FABP in single cloned and pooled transfectant LNCaP cell lines .....	165
Figure 3.7: Detection of protein expression levels of wild type and mutant C-FABPs in pooled transfected LNCaP cell lines .....	167
Figure 3.8: Quality checks of total RNA samples by Agilent 2100 bioanalyzer .....	170
Figure 3.9: Relative level of C-FABP mRNA in transfectant and LNCaP cell lines...	171
Figure 4.1: the product of restriction enzyme digestion for the ligation reaction....	179
Figure 4.2: Linearization of the protein expressing vector .....	180
Figure 4.3: Digestion of vector DNAs .....	181
Figure 4.4: Insertion of C-FABP-WT cDNA into pBluescript cloning vector .....	183
Figure 4.5: Insertion of C-FABP-R109A cDNA into pBluescript II SK cloning vector.....	184
Figure 4.6: Insertion of C-FABP-R109/129A cDNA into pBluescript II SK cloning vector.....	185
Figure 4.7: the product of restriction enzyme digestion for the ligation reaction....	187
Figure 4.8: Digestion of vector DNAs .....	188
Figure 4.9: Sequencing primers for pQE vectors .....	190
Figure 4.10: confirmation of correct reading frame for recombinant C-FABP proteins production .....	192
Figure 4.11: Insertion of C-FABP-WT cDNA into pQE32 expression vector .....	193
Figure 4.12: Insertion of C-FABP-R109A cDNA into pQE32 expression vector...	194
Figure 4.13: Insertion of C-FABP-R109/129A cDNA into pQE32 expression vector .....	195
Figure 4.14: protein expression and time course for C-FABP-WT .....	197

Figure 4.15: Western blot analysis of the 6xHis-tagged wild type and mutant C-FABP proteins.....	199
Figure 4.16: Titration curves of DAUDA binding to C-FABP proteins.....	201
Figure 4.17: Displacement of DAUDA binding to three C-FABP proteins by natural fatty acids. ....	202
Figure 5.1: Fatty acid uptakes by C-FABP cDNAs at absence and presence of red fluorescence labelled LCFA.....	210
Figure 5.2: Relatives level of LCFA uptake by wild type and mutants C-FABP cDNAs.....	211
Figure 5.3: Standard curve for LNCaP cell line.....	213
Figure 5.4: Time course curve of proliferation rate for LNCaP cells stimulated by wild type and mutant C-FABP proteins .....	214
Figure 5.5: Standard curve for 22RV1 cell line .....	217
Figure 5.6: Time course curve of proliferation rate for 22RV1 cells stimulated by wild type and mutant C-FABP proteins .....	218
Figure 5.7: Standard curve for LNCaP-C4 <sub>2</sub> cell line.....	221
Figure 5.8: Time course curve of proliferation rate for LNCaP-C4 <sub>2</sub> cells stimulated by wild type and mutant C-FABP proteins .....	222
Figure 5.9: The images of invaded cells stimulated by C-FABP proteins on the lower filter surface of the Boyden Chamber .....	226
Figure 5.10: Number of cells invaded per field in the invasion assay .....	227
Figure 5.11: The colonies produced in soft agar by LNCaP cell stimulated with different C-FABPs .....	229

Figure 5.12: The effect of wild and mutants C-FABPs on colonies formation ability of LNCaP cells in soft agar .....	230
Figure 5.13: The colonies produced in soft agar by 22RV1 cells stimulated with different C-FABPs .....	233
Figure 5.14: The effect of wild and mutants C-FABPs on colonies formation ability of 22RV1 cells in soft agar .....	234
Figure 5.15: The colonies produced in soft agar by LNCaP-C4 <sub>2</sub> cells stimulated with different C-FABPs .....	237
Figure 5.16: The effect of wild type and mutants FABPs on colonies formation ability of LNCaP-C4 <sub>2</sub> in soft agar .....	238
Figure 6.1: Model for possible C-FABP signalling pathways in prostate cancer malignant progression. ....	259
Figure 8.1: Confirmation of insertion of C-FABP-WT cDNA into pQE32 .....	303
Figure 8.2: Confirmation of insertion of C-FABP-R109A cDNA into pQE32 .....	304
Figure 8.3: Confirmation of insertion of C-FABP-R109/129A into pQE32 .....	305



## LIST OF TABLES

Table 1.1: Prostate cancer: number of new cases and European-age standardised incidence rate (ASR), countries of the UK, 2008 (Baade <i>et al</i> , 2009).....	33
Table 1.2: General characteristics of DU-145, PC-3 and LNCaP parental cell lines (Sobel & Sadar, 2005).....	45
Table 1.3: Mechanisms of progression of prostate cancer to androgen independence (Schroder, 2008).....	64
Table 1.4: Family of FABPs (Furuhashi & Hotamisligil, 2008). ....	83
Table 2.1: The restriction enzyme digestion mixture (total volume 50µl) .....	94
Table 2.2: The ligation reaction mixture.....	95
Table 2.3: The restriction enzyme digestion mixture (total volume 25µl). ....	113
Table 2.4: The ligation reaction mixture.....	116
Table 2.5: The restriction enzyme digestion mixture (total volume 25µl). ....	123
Table 2.6: The ligation reaction mixture.....	125
Table 2.7: Primary and secondary antibodies used in Western blot. ....	136
Table 2.8: PCR mixture .....	139
Table 2.9: Real-time PCR program for amplification of short target DNAs (50-400bp)....	142
Table 5.1: Cell counts of C-FABPs at the end point of proliferation assay.....	215
Table 5.2: Cell counts of C-FABPs at the end point of proliferation assay.....	219
Table 5.3: Cell counts of C-FABPs at the end point of proliferation assay.....	223
Table 5.4: The number of invading cells that pass through the membrane. ....	225

Table 5.5: The numbers of colonies produced in soft agar by LNCaP cells stimulated by different C-FABPs .....	231
Table 5.6: The numbers of colonies produced in soft agar by 22RV1 cells stimulated with different C-FABPs .....	235
Table 5.7: The numbers of colonies produced in soft agar by LNCaP-C42 stimulated with different C-FABPs .....	239

## LIST OF ABBREVIATIONS

AF1	Activation function 1
AIPC	Androgen independent prostate cancer
ALS	Acid-labile subunit
AR	Androgen receptor
AREs	Androgen-responsive elements
bFGF	basic fibroblast growth factor
BPH	Benign Prostatic Hyperplasia
BRCA1	Carriers of the breast cancer 1
BSA	Bovine serum albumin
CAMs	Cell adhesion molecules
C-FABP	Cutaneous fatty acid binding protein
DAUDA	11-(dansylamino) undecanoic acid
DHT	Dihydrotestosterone
DMSO	Dimethyl sulfoxide
ECL	Enhanced chemiluminescence

ECM	Extra cellular matrix
EDTA	Ethylene diamine tetracetic acid
E-FABP	Epidermal fatty acid binding protein
EGF	Epidermal growth factor
EGFR	Epidermal growth factor receptor
ERK	Extracellular signal-regulated kinase
ET-1	Endothelin-1
FABPs	Fatty acid binding proteins
FBS	Foetal bovine serum
Flt-1	fms-like tyrosyl kinase-1
GnRH	Gonadotropin-releasing hormone
Grb2	Growth factor receptor-binding protein 2
GS	Gleason Score
HIF	Hypoxia-induced factor
HPC1	Hereditary prostate cancer gene 1
HSL	Hormone-sensitive lipase
IFGBP3	Insulin-like growth factor binding protein-3

IGF	Insulin-like growth factor
IPTG	Isopropyl- $\beta$ -D-1-thiogalactopyranoside
KDR	Kinase insert domain receptor
KGF	Keratinocyte growth factor
LB	Lysogeny broth
LBD	Ligand binding domain
LCFA	Long chain fatty acid
LUTS	Lower urinary tract symptoms
MAPK	Mitogen-activated protein kinase
MVD	Microvessel density
Ni-NTA	Nickel-nitrilotriacetic acid
PAGE	Polycrylamide gel electrophoresis
PCAP	Predisposing to prostatic cancer
PI3K	Phosphorylates phosphatidylinositol 3'-kinase
PIN	Prostatic Intraepithelial Neoplasia
PlGF	Placental growth factor
PPARs	Peroxisome proliferator-activated receptors

PPRE	Peroxisome proliferator response element
PSA	Prostate specific antigen
PTEN	Phosphatase and tensin homologue
PTHrP	Parathyroid hormone related protein
PUFA	Polyunsaturated fatty acids
RANK	Receptor Activator of Nuclear Factor
RB	Retinoblastoma
RXR	Retinoic acid receptor
SOB	Super optimal broth
SOC	SOB medium plus glucose
TBS	Tris buffered saline
uPA	urokinase-type plasminogen activator
VEGF	Vascular endothelial growth factor

# **1 INTRODUCTION**

## 1.1 Epidemiology of prostate cancer

### 1.1.1 Incidence

Prostate cancer is the most frequently diagnosed non-cutaneous male malignancy and is the second cause of cancer-related death in men in most Western countries. In 2008, there were 37,051 new cases of prostate cancer diagnosed in the UK (Table 1.1). Worldwide, it is estimated that 913,000 men were diagnosed with prostate cancer in 2008, and more than two-thirds of cases were diagnosed in developed countries (Figure 1.1). The highest rates were in Australia/New Zealand, Western Europe and USA while the Asian countries have the lowest rates (Figure 1.1) (Jemal *et al*, 2008). Different screening methods, diet and environment, family history and genetic factors all contribute to this variation.

The apparent rise in incidence rates is almost certainly of the introduction of serum-based assays for prostate specific antigen (PSA) together with other clinical examinations. PSA is normally present in blood at very low levels up to 4.0 ng/ml. PSA is usually used as one of the primary methods to diagnose the disease at an early stage. As a result, survival rate has improved in recent decades, mostly because the improved diagnosis and screening procedures have lead to discovery of organ-confined tumours (Tanaka *et al*, 2010). However, elevated levels of PSA (more than 4.0 ng/ml) may suggest although not confirmed the presence of prostate cancer. In addition, tumour metastasis also occurs in patients with prostate cancer who have normal PSA level.



**Table 1.1:** Prostate cancer: number of new cases and European-age standardised incidence rate (ASR), countries of the UK, 2008 (Baade *et al*, 2009).

	England	Scotland	Wales	Northern Ireland	United Kingdom
<b>Cases</b>	<b>30,893</b>	<b>2,716</b>	<b>2,480</b>	<b>962</b>	<b>37,051</b>
Crude Rate	122	108.6	169.9	110.5	122.9
<b>ASR</b>	<b>97.5</b>	<b>85.7</b>	<b>119.9</b>	<b>103.8</b>	<b>97.9</b>
ASR - LCL	96.4	82.5	115.2	97.2	96.9
ASR - UCL	98.6	88.9	124.6	110.3	98.9

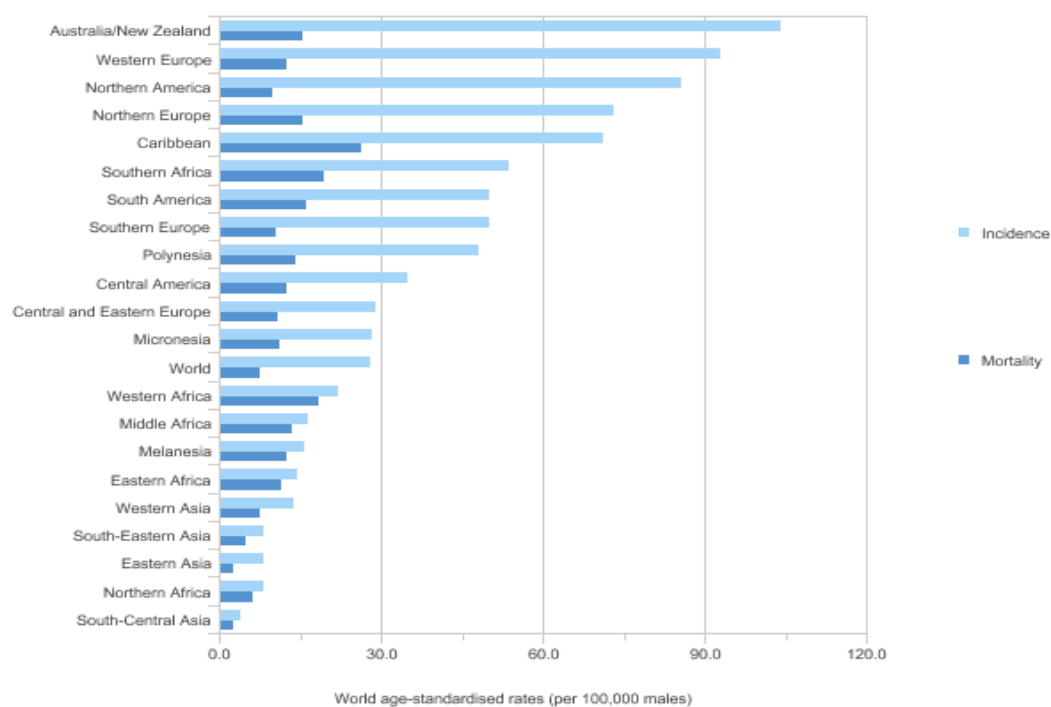


**Figure 1.1:** prostate cancer, world age-standardised incidence and mortality rates, by world regions, 2008 (Jemal *et al*, 2008).

### 1.1.2 Mortality

Prostate cancer accounts for around 12% of male deaths from cancer in the UK and is the second most common cause of cancer death in men after lung cancer. Ninety-three Percent of prostate cancer deaths occur in men aged 65 and over (Figure 1.2) (Edwards *et al*, 2005).

Prostate cancer mortality in the UK was fairly stable during the 1970s but began to increase in the early 1980s (Figure 1.3). Mortality peaked in the early 1990s when the European age-standardised death rate reached 30 per 100,000 in 1992. Since then there has been a slight fall in the rates and in 2008 the European age-standardised rate was 24 per 100,000. This was the first sustained decrease in annual death rates for thirty years (Bosetti *et al*, 2008).

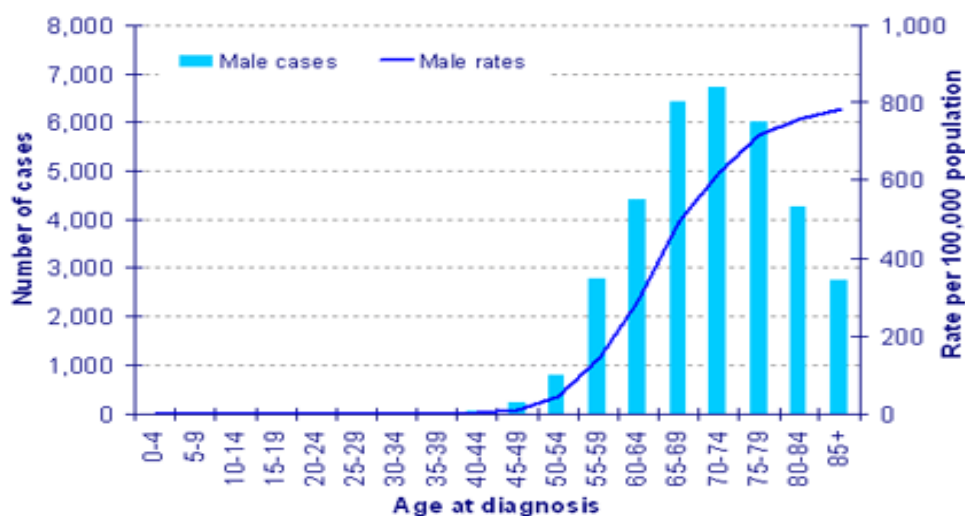


**Figure 1.2: number of deaths and age-specific mortality rates, prostate Cancer, UK, 2008 (Schroder *et al*, 2009).**

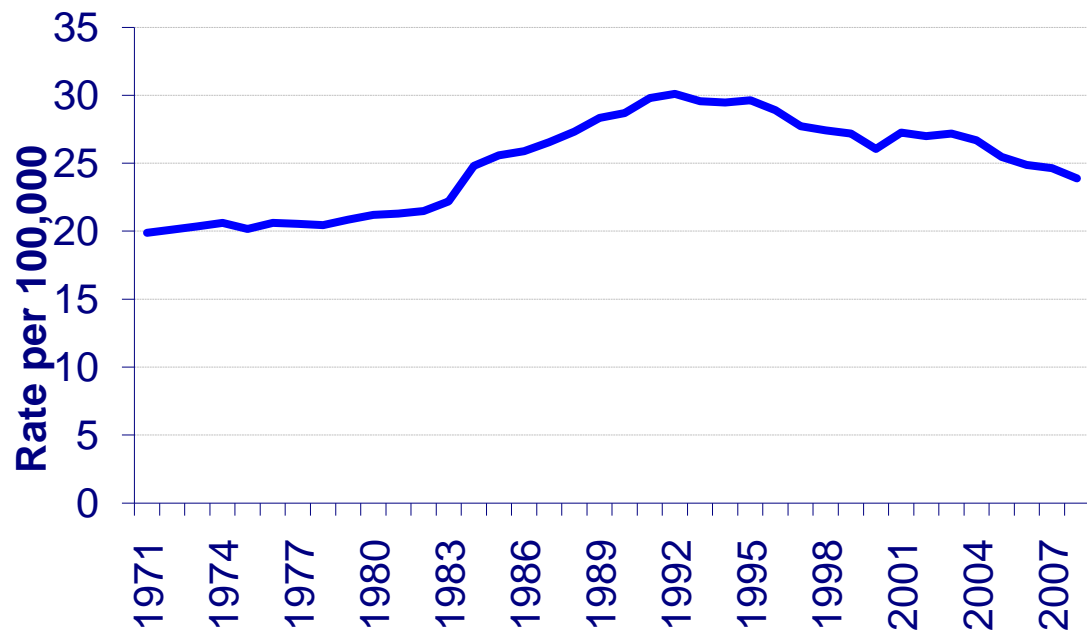


**Figure 1.3: Age-standardised (European) mortality rates, prostate cancer 1971-2008 (Bosetti *et al*, 2008).**

### 1.1.3 Survival

Five year survival rates for prostate cancer have improved from around 31% for patients diagnosed in 1971-75 to 77% in 2001-2006 in England and Wales (Figure 1.4) (Rachet *et al*, 2009). The latest survival statistics for Scottish men show that five-year relative survival rates have increased from 37% for patients diagnosed in 1977-81 to 60% for patients diagnosed in 1996-2000 (Brewster *et al*, 2000).

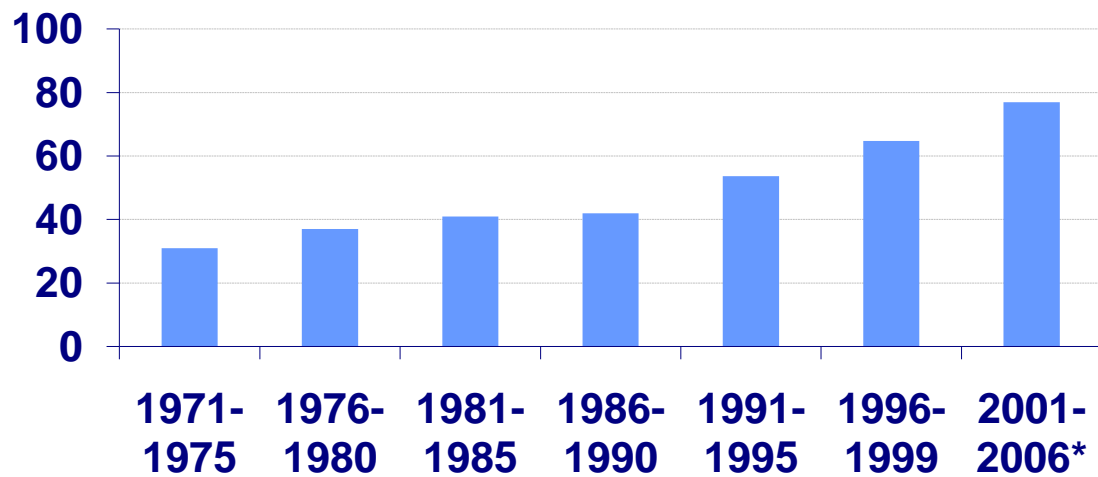


**Figure 1.4: prostate cancer Age standardised five-year survival rates in England and Wales (Rachet *et al*, 2009).**

## 1.2 Risk Factors

### 1.2.1 Age

Age is an important risk factor for prostate cancer (Figure 1.2). Prostate cancer is rarely seen in men younger than 40 years, the incidence rises rapidly with each decade thereafter. The possibility of developing prostate cancer varies with age, being 13.7% for the age group of 60-79 years, 2.2% for those aged 40-59 and 0.005% in those younger than 39 years (Merrill & Bird, 2002). In addition, the probability of finding prostate cancer when performing autopsies in deceased people is much higher, at about 20% in men between the age of 50 and 60 years and increasing to 50% in men between 70 and 80 years old (Lunenfeld, 2002).

### 1.2.2 Race

Variations in both incidence and death rates around the world from prostate cancer have been reported amongst different races. In the UK, the risk of being diagnosed or dying from prostate for black Caribbean and black African men is approximately two to three times higher than that for white men, while Asians annually have the lowest incidence rate of prostate cancer (Jemal *et al*, 2008). The differences in prostate cancer risk by race may reflect genetic variation, dietary habit, and even the methods used to detect the cancer and determine the incidences. In recent years, prostate cancer incidence has risen considerably in many countries, including countries in which prostate cancer was previously considered low. Although changes in lifestyle cannot be excluded, the rate of change is too fast to be concerned solely by alterations in life style.

### 1.2.3 Family history

There is an increase in incidence of prostate cancer in persons with a history of prostate cancer in their family (about two to four times higher than in control population). Those with a family history of prostate cancer tend to have their disease diagnosed six years earlier than control (Bratt, 2002). Family history and hereditary factors are estimated to be important in 5-10% of all prostate cancers, and 40% of those cancers diagnosed below the age of 55. However, the clinical presentation of a family history of prostate cancer does not indicate cancer presenting at an early age, and there is no difference in stage or grade.

Some of the genetic loci identified by linkage studied include hereditary prostate cancer gene 1 (HPC1) on chromosome 1q23-25, predisposing to prostatic cancer

(PCAP) on chromosome 1q42-43, cancer of the prostate and brain (CAPB) on chromosome 17p, locus on chromosome 8p22-23 and HPC2 on chromosome 17p (Makridakis & Reichardt, 2004). In a study of Scandinavian twins, higher prostate cancer concordance rates were found for monozygotic twins versus dizygotic twins, suggesting a genetic influence on risk (Lichtenstein *et al*, 2000).

Prostate cancer was also reported to occur at a higher rate in families with other cancers such as breast cancer. Carriers of the breast cancer 1 (BRCA1) gene had twice the incidence of prostate cancer of non-carriers (Tulinius *et al*, 1992). Those families with hereditary prostate cancer also had higher incidence of central nervous system tumours (Isaacs *et al*, 1995).

#### **1.2.4 Hormones**

Androgens play an important role both in development and growth of the prostate gland and its over-expression also play an important role of prostate cancer development. It has been suggested that altered hormone metabolism may play a role in the progression of prostate cancer from histologic to clinically significant (Attar *et al*, 2009). Indeed, Hsing (2001) showed that testosterone levels was higher in patients with prostate cancer than control (Hsing, 2001), although, another study has been unable to confirm this (Shaneyfelt *et al*, 2000). It has been found that the level of serum testosterone in young black men is approximately 15% higher than that in their white counterparts, and this difference may explain the increased risk of prostate cancer in black men (Sasagawa & Nakada, 2001). It has also been shown that testosterone metabolism is different in American/European men when compared with Japanese men (Sasagawa & Nakada, 2001). Japanese men have a lower 5-alpha

reductase activity, which may help explain their lower incidence of clinical prostate cancer. Although, hormones play an important role in normal and cancerous prostate physiology, their relationship to risk of prostate cancer remains undefined.

### **1.2.5 Other factors**

The association of prostate cancer with other risk factors have been evaluated in a number of studies. However, the statistic data for risk factors such as socioeconomic status, occupation, cigarette smoking, alcohol consumption and vasectomy were not convincing that these risk factors resulted in an increasing incidence of prostate cancer. In contrast, some studies have shown increase in risk of prostate cancer with an increase in number of sexual partners (Rosenblatt *et al*, 2001).

## **1.3 The Pathology of Prostate Cancer**

### **1.3.1 Anatomy of the prostate**

The prostate gland is an ovoid shaped gland located at the base of the bladder, surrounding the proximal urethra. The human prostate consists of four morphological regions comprising of two peripheral zones, a central zone and a fibromuscular zone (Figure 1.5). The peripheral zones together consist of approximately 70% of the total tissue mass of the gland. They are very susceptible to inflammation and it is within these zones that mature prostate tumour cells are commonly located. The central zone makes up 25% of the total tissue mass of the prostate gland and it is very resistant to inflammation and to prostatic carcinoma. The transitional zone, making up 5% of the total prostate tissue mass and it is the most common site of Benign

Prostatic Hyperplasia (BPH) while the fibromuscular zone is responsible for secretion of prostatic fluids during ejaculation by initiating muscular contractions (Abate-Shen & Shen, 2000).

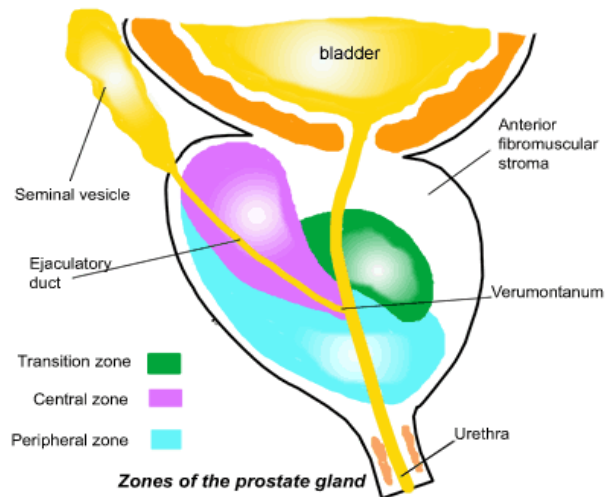


**Figure 1.5: The anatomy and zones of prostate gland (Abate-Shen and Shen, 2000).**

### 1.3.2 Prostate Architecture

The normal prostate composes of different cell types that can be distinguished by their cytokeratin (CK) and cluster differentiation (CD) expression pattern. Three main cell types are discernible within normal, mature prostatic epithelium-basal, secretory luminal and neuroendocrine. The luminal or glandular cells constitute the exocrine compartment of the prostate, secreting prostate specific antigen (PSA) and prostatic acid phosphate (PAP) into the glandular lumina. They express high levels of the androgen receptor (AR), and depend on androgens for their survival (Collins & Maitland, 2006). They also express CK 8 and CK 18.



In contrast, basal cells are relatively undifferentiated and lack secretory activity. These cells rest on the basement membrane and are able to express CKs 5 and 14 as well as CD44 (Bonkhoff & Remberger, 1996). A study by Collins and Maitland (2006) reported that basal cells express low/undetectable levels of AR and are independent of androgens for their survival (Collins & Maitland, 2006). However, they do express autocrine factors such as *Bcl-2* which has a protective function against DNA damage (Rizzo *et al*, 2005).

The third cell type is neuroendocrine cells. These cells are found in the epithelium of the acini and in ducts of all parts of the gland. The major type of neuroendocrine cells contains serotonin, thyroid stimulating hormone and chromogranin A. neuroendocrine cells are terminally differentiated, post-mitotic cell types that are androgen insensitive (Bui & Reiter, 1998), and can also express neuropeptide Y. Therefore, the immunoreactivity to neuropeptide Y was demonstrated in up to 75% of prostate cancer, suggesting a role in growth and expansion of prostate cancer (Ruscica *et al*, 2007).

## **1.4 Prostate cancer initiation**

### **1.4.1 Benign Prostatic Hyperplasia (BPH)**

Benign Prostatic Hyperplasia (BPH) defines as non malignant overgrowth of prostate tissue. BPH and prostate cancer are often found concurrently, and there are some similarities between these two lesions. Both are age related disease and both require androgen stimulation. However, BPH is not a precursor of prostate cancer (Sausville

& Naslund, 2010). BPH develops in the transition zone, a ring of tissue around the urethra and its growth is inward toward the prostate's core, constantly tightening around the urethra and associated with lower urinary tract symptoms (LUTS). Most of prostate carcinomas, on the other hand, begin in the outer peripheral zone of the prostate and invade the surrounding tissues. Although the pathogenesis of BPH is still poorly understood, some studies indicated that BPH is related to hormonal changes that occur as men age (Wise & Ostad, 2001).

#### **1.4.2 Prostatic Intraepithelial Neoplasia (PIN)**

Prostatic Intraepithelial Neoplasia (PIN) refers to a sub stage of cellular transformation from a normal to a malignant prostatic epithelium (Foster *et al*, 1999). In the UK, over a million biopsies are studied to detect 198,500 new cases of prostate cancer annually. PIN represents abnormal proliferation of malignant cells without invasion into surrounding stroma, and can be characterized by a variety of architectural and cytological aspects (Foster & Ke, 1997) resulting in minimal changes to modifications that make it undistinguishable from carcinoma (Montironi *et al*, 2000).

A study by Berry *et al* (2008) identified PIN lesions by histological studies of prostate cancer tissues (Berry *et al*, 2008). These lesions were grouped into a series of four architectural types: Tufting, Micropapillary, Cribriform and flat and are mainly located in the peripheral zone of the prostate. Likewise, the morphological appearances can be as low grade or high grade PIN. A low grade PIN lesion is often a well differentiated early invasive tumour with a high percentage of basal cells

whereas the high grade lesions form poorly differentiated tumours with a secretory luminal cell population (Bonkhoff & Remberger, 1996).

Chromosomal mutation studies (Ayala & Ro, 2007; Joniau *et al*, 2005) have shown that high grade PIN is multifocal and endures the same chromosomal mutations observed in early invasive carcinoma. The appearance of high grade PIN generally precedes the manifestation of carcinoma by approximately 20 years and is an important morphological marker for detection of potential carcinoma of the prostate.

### 1.4.3 Gleason Score

Gleason Score (GS), the histological grading system of prostate cancer proposed by Dr. David Gleason in 1966 as a method for evaluating the prognosis of men with prostate cancer. GS is widely used for morphological tumour grading prostate cancer (Molinie, 2008). The GS is a sum of primary (greater 50% of total pattern seen) grade which represents the majority of tumour and secondary (less than 50%, but greater than 5% of total pattern seen) grade which represents the minority of tumour. The Combined GS is a number ranging from 2 – 10 (Molinie, 2008). The Gleason grade is a prostate cancer assess system depend on subjective microscopic determination, ranges from 1 – 5, representing the degree of loss of normal glandular tissue architecture. Thus grade 1 is the least aggressive and Grade 5 is the most aggressive cancer (Figure 1.6).

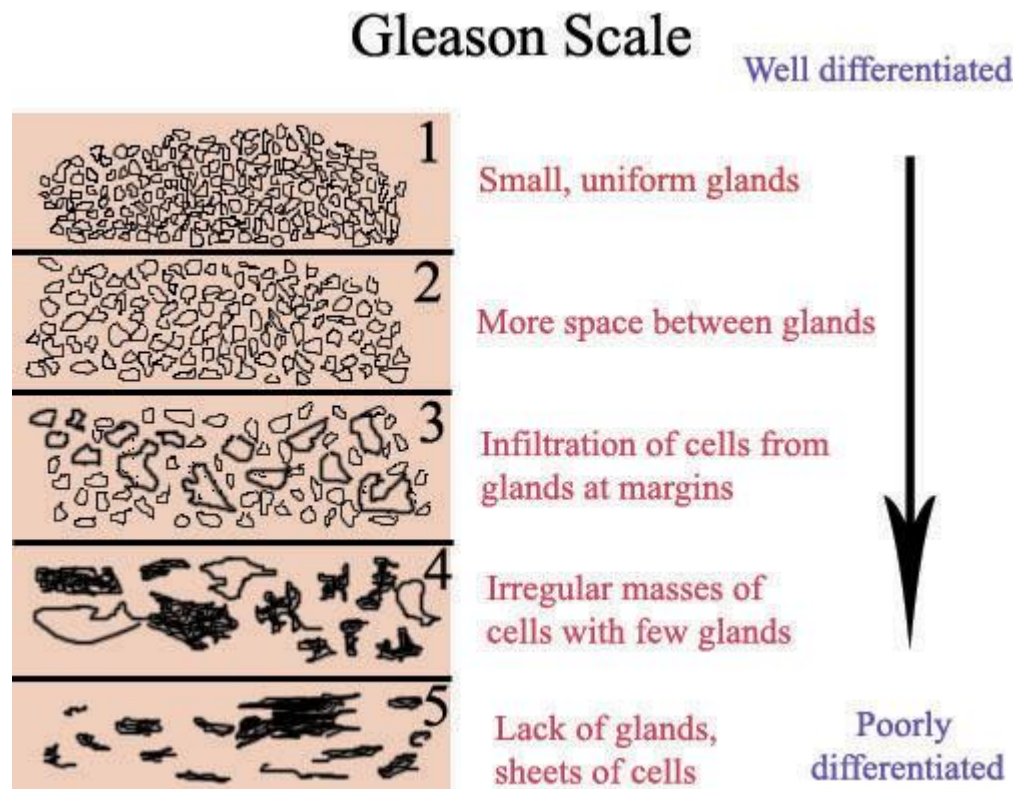


**Figure 1.6: Gleason grading system diagram (Humphrey, 2004).**

*The subjective microscopic determination of the loss of normal prostate glandular structure caused by cancer is graded by number ranged from 1 to 5, with 5 being the worst grade possible.*

## 1.5 Cell culture models

The three cell lines DU-145, PC-3 and LNCaP are the most widely used cells in prostate cancer research (Table 1.2). These cells have also been used to address various problems encountered in understanding and treating cancer progression and metastasis.

**Table 1.2: General characteristics of DU-145, PC-3 and LNCaP parental cell lines (Sobel & Sadar, 2005)**

	<b>DU-145</b>	<b>PC-3/PC-3M</b>	<b>LNCaP</b>
<b>Androgen sensitive</b>	No	No	Yes/No*
<b>PSA</b>	No	No	RNA and protein
<b>hK2</b>	No	No	RNA and protein
<b>AR</b>	No	No	RNA and protein
<b>Derivation</b>	Brain	Vertebra	Lymph node

\*some sublines have become androgen insensitive

### 1.5.1 DU-145

DU-145 was the first prostate cancer cell line to be established in tissue culture. It was derived from a moderately-differentiated brain metastasis (Sobel & Sadar, 2005). DU-145 cell express low level of prostatic acid phosphatase (PAP) and fail to express androgen receptor (AR), prostate specific antigen (PSA) and kallikrein (hK2) (Sobel & Sadar, 2005). They also express intermediate filament proteins and cytokeratins (CKs) 7, 8, 9 and 19, but not cytokeratin 5 and 14 (van Bokhoven *et al*, 2003). The cell population doubling time of Du-145 is approximately 34 hours. It grows slowly in soft agar but produces sizable colonies when seeded at  $1 \times 10^{3-5}$  cells per dish. Animal studies showed that the tumour, when inoculated into SCID mice, results in metastases to liver, lung, spleen, adrenals, kidneys and lymph nodes (Bastide *et al*, 2002).

### 1.5.2 LNCaP

LNCaP cells were isolated from a needle aspiration biopsy of a lymph node metastatic lesion (Sobel & Sadar, 2005). LNCaP cells express a high affinity nuclear androgen receptor and respond to androgens that stimulate their growth. The cell population doubling time of LNCaP is 60 hours. Animal studies showed that tumours are formed earlier in male than in female mice, indicating a probable androgen-dependant characteristic (Zheng *et al*, 2010). LNCaP cells express CK8 and 18, and express a wild type TP53.

### 1.5.3 PC-3

The PC-3 cell lines (Figure 1.7) were originally derived from a poorly-differentiated prostate cancer metastasis in bone (Sobel & Sadar, 2005). The cells have a doubling time of approximately 33 hours and grow readily in female nude mice, indicating their androgen-independent character. Treatment with the mitogens insulin or parathyroid hormone and growth factors such as EGF and FGF fails to stimulate their growth. PC-3 cells express CKs 5, 8 and 18, and contain a frame-shift mutation in TP53 that results in a premature stop codon (van Bokhoven *et al*, 2003). Based on PC-3 cell growth in xenografts, PC3-M cells were isolated with more aggressive features than their parental cells. Other sublines, including PC3-M2, PC3-M-pro4 and PC3-M-LN4 with increased levels of malignancy were also generated. All PC-3 cells and their derivatives (Figure 1.7) are androgen independent, and do not express PSA, RNA or protein (Sobel & Sadar, 2005).

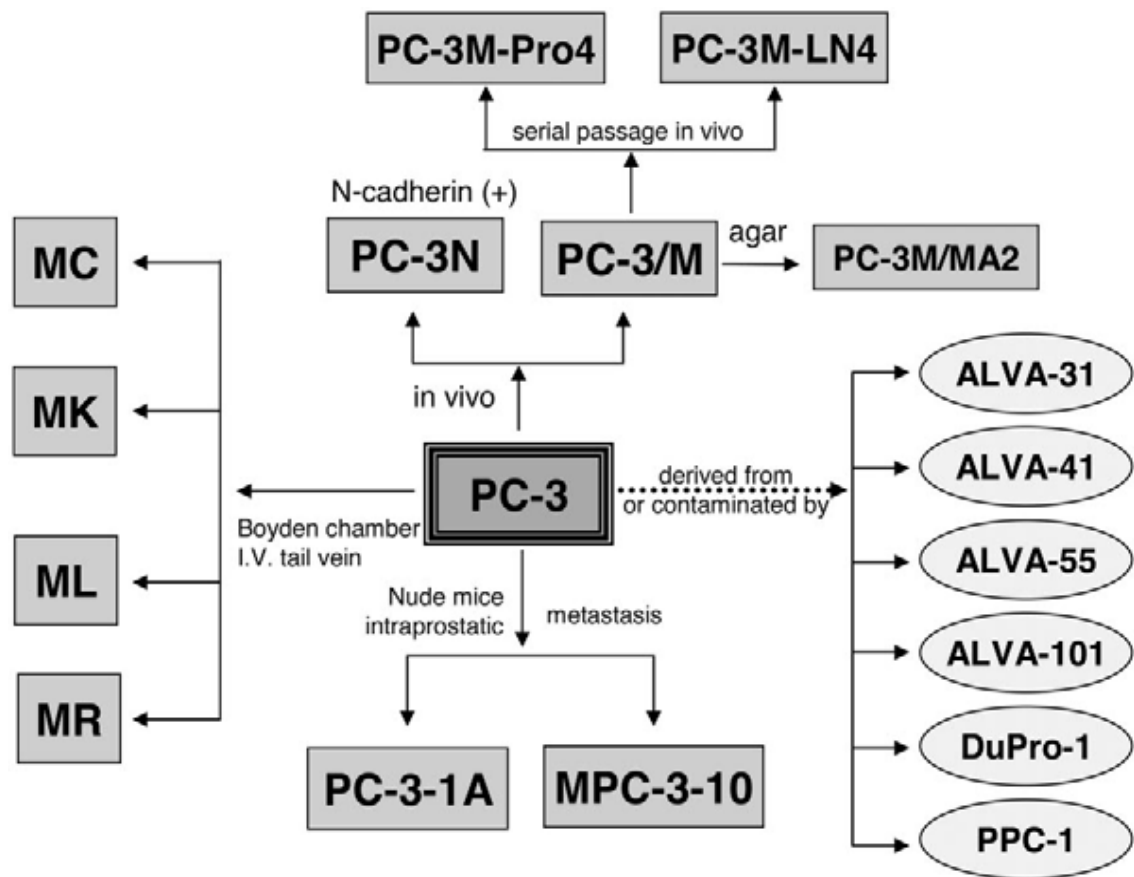


Figure 1.7: Schematics of original PC-3 cells and their derivatives (Sobel & Sadar, 2005).

## 1.6 Oncogenes and tumour suppressor genes in prostate cancer

### 1.6.1 Oncogenes

Proto-oncogenes are a group of genes that cause normal cells to become cancerous when they are mutated. Proto-oncogenes are involved in regulating cell proliferation, single transduction, differentiation and execution of mitogenic signals, usually via a translated protein product (Weinstein & Joe, 2006).

Many oncogenes have been implicated in the development of various types of human malignancies. In prostate cancer, the most frequently studied oncogenes are genes of

*Ras* family, *C-myc*, *bcl-2*, and *HER-2*. Thus, none of these oncogenes have been correlated conclusively with the initiation or progression of prostate cancer.

#### 1.6.1.1 *Ras* oncogene

The *Ras* family gene, including *H-Ras*, *K-Ras* and *N-Ras* has been widely studied in prostate cancer. *Ras* genes encode the G-protein (21kD) that connect receptor tyrosine kinases on the cell surface with their downstream effectors, *Raf*, *MEK* (mitogen-activated kinas/extracellular signal-regulated kinase) and *ERK* (extracellular signal-regulated kinase) (Gioeli, 2005). *Ras* oncogene is activated by missense point mutation and altered p21 stimulated cell proliferation in the absence of external signals. Abnormalities of the signal pathway occur in many cancers, although a very limited number of clinical cases have been reported in prostate cancer gene mutation in Western countries. There appears to be a racial variation. For instance, *Ras* gene mutation were relatively uncommon in prostate cancer in the United States (Gumerlock *et al*, 1991). In contrast, the rate of mutation is 26% in Japanese prostate cancer suggesting that such mutation is racially-distributed. Nevertheless, the p21 mediated signalling pathway is a key role in prostate cancer, which was activated by growth factors as a portion of their signalling pathway. Moreover, activation of *Ras* can induce androgen independent growth of prostate cancer cells and stimulate the activation of androgen-response genes through *Raf* and *MEK* mediated pathway in androgen-dependent and androgen-independent cells (Gioeli, 2005).

At mRNA level, the increased expression of *Ras* was reported both in rat prostatic dysplasia (Yu *et al*, 1993) and human primary tumours, as well as prostate cancer



cell lines (Shields *et al*, 2000). However, the *Ras* mRNA expression was not correlated with tumour progression.

#### **1.6.1.2 *C-myc* oncogene**

The *c-myc* oncogene is located on chromosome 8 at 8q24 and plays an important role in regulation of cell proliferation, cell differentiation and apoptosis (Grandori *et al*, 2000). This well known oncogene, characterised as a transcription factor, increase its copy numbered by amplification or/and chromosomal gain (Ferrara, 2004). A number of studies have reported that *c-myc* mRNA is elevated in prostate cancer, compared to normal prostate tissues or BPH, and that there is a trend on the enhanced *c-myc* expression with increased tumour grades (Gurel *et al*, 2008; Williams *et al*, 2005). These results indicated that the amplification of *c-myc* may be a potential marker for prostate cancer progression. However, Zhang *et al* (2000) did not detect the over-expression of *c-myc* gene in prostate cancer by in-situ hybridisation (Zhang *et al*, 2000).

#### **1.6.1.3 HER-2 (C-ERB-R2, neu)**

The *HER* kinase family, which includes epidermal growth factor receptor (*EGFR*) and human epidermal growth factor receptor (*HER2*), are receptor-and receptor- like transmembrane proteins that are activated in some human tumours (Hynes & Lane, 2005). The gene encoding the *HER2* protein is amplified in 20% to 25% of breast cancer patients and an anti *HER2* antibody, trastuzamb, has verified to be useful in their treatment (Slamon *et al*, 2001). It has been reported that over expression of *HER2* may contribute to androgen independence in prostate cancer (Craft *et al*, 1999). They showed that *HER2* can activate the androgen receptor pathway in

absence of ligands like steroid hormones. In addition, casodex, an androgen antagonist, blocks the effects of growth factors but not *HER2* on androgen receptor functions. This indicates that either *HER2* signalling cascade produces a molecule that binds at competitively higher affinity than casodex, or *HER2* activates androgen receptor function on fresh non-optimal androgen receptor ligand binding domains rather than to enhance androgen receptor function on high-affinity binding sites. Another group found that *HER2* expression correlated with advanced stages of prostate cancer and higher Gleason scores (Katsumata *et al*, 1992). Nevertheless, reports on frequencies of *HER2* over-expression in prostate cancer are controversial.

#### 1.6.1.4 *Bcl-2* Oncogene

*Bcl-2* located on chromosome 18q21.33/18q21.3. It prevents programmed cell death and is thought to be a key gene for the regulation of cell life and death (Catz & Johnson, 2003). In the prostate gland, *Bcl-2* is normally expressed in basal epithelial cells which are not affected by androgen deprivation but not in prostatic secretory epithelial cells (Matsushima *et al*, 1996; Raffo *et al*, 1995). Furthermore, McDonnell *et al* (1992) reported that *Bcl-2* is undetectable in 13 of 19 androgen dependent prostate tumours. In contrast, 77% of androgen-independent cancers display high levels of *Bcl-2* reactivity, indicating that *Bcl-2* might be involved in the progression from androgen –dependence to independence. Abeele *et al* (2002) suggested that the function of *Bcl-2* might be associated with its ability to regulate nuclear and systolic  $\text{Ca}^{2+}$  in prostate carcinoma cells (Abeele *et al*, 2002). Several studies have suggested that *Bcl-2* expression increase with grade and stage, and is a potential biomarker for early prostate cancer (Foster *et al*, 1999) and in advanced hormone-refectory prostate cancer (Quinn *et al*, 2005). However, low level and high level *Bcl-2* expression were

also observed in prostate cancer after treatment by radical prostatectomy alone (Amirghofran *et al*, 2005).

### 1.6.2 Tumour Suppressor genes

A tumour suppressor gene is a gene can protect normal cells from progressing to form a malignant tumour cell through their regulation function in cell. Absence of a tumour suppresser gene may allow tumorigenesis with restrained progression to metastasis (Knudson, 2001). Unlike oncogene, tumour suppressor genes generally follow the 'two-hit hypothesis', which implies that the mutation in both alleles of double stranded DNA, before being permissive for tumorigenesis or metastasis (Knudson, 1971). This is due to the fact that if only one allele for the gene is damaged, then the second can still produce the correct protein. Hence, mutant tumour suppressor's alleles are usually recessive whereas mutant oncogene alleles are typically dominant.

'Gatekeeper' genes are tumour suppressor genes that directly regulate the growth of tumours by inhibiting cell proliferation or promoting cell death. Mutation or deletion of such a gene increase the probability of tumour formation, such as *PTEN* (Ali, 2000). 'Caretaker' genes like *BRCA1/BRCA2* (Levitt & Hickson, 2002), are tumour suppressor genes that normally repair DNA damage. Individuals with mutation of 'Gatekeeper' genes are at great risk of developing tumour. Furthermore, metastasis suppressor genes, are considered to be a gene that can prevent tumour cells from progressing to metastasis and eventually prevent tumour cells from spreading, such as *NM23* and *CD44* (Liu *et al*, 2002; Lombardi, 2006).

### 1.6.2.1 *Retinoblastoma (RB)*

Retinoblastoma (*RB*) gene was the first tumour suppressor gene identified and was reported by Knudson *et al* in 1971 (Knudson, 1971). *RB* is located on the long arm of chromosome 13q and has been implicated in tumorigenesis of the DU-145 prostate cancer cell line. The *RB* gene product functions to suppress cell division by preventing cells in G1 phase from entering S phase. Replacement of the wild type *RB* gene led to decreased tumorigenesis of the cell line in nude mice (Bookstein *et al*, 1990). A study by Taneja *et al* (2001) reported that 16.4% of *RB* gene mutations in primary human prostate cancer were detected by polymerase chain reaction (PCR) – single stranded conformation polymorphism (SSCP) analysis, suggesting that structural alteration of the *RB* gene is involved in progression steps of prostate carcinogenesis (Taneja *et al*, 2001).

### 1.6.2.2 *P53*

*P53* is a nuclear phosphoprotein (53 KDa) encoded by gene *TP53* located on chromosome 17p13. The protein product of *P53* gene has been shown to control cell cycle progression, DNA repair and cell survival (Shi *et al*, 2002). *P53* has been found in three of five prostate cancer cell lines (Isaacs *et al*, 1991). In the PC-3 cell lines, the alteration of *P53* gene has been detected on DNA, mRNA and protein levels (Rubin *et al*, 1991). Several studies described that alteration in *P53* gene is clearly associated with progressive disease, like metastasis to bone and androgen-independent growth (Burchardt *et al*, 2001; Shi *et al*, 2004). However, Brooks *et al* (1996) considered that point mutation of *P53* gene may be an infrequent event in the oncogenesis of untreated prostate cancer (Brooks *et al*, 1996).

### 1.6.2.3 Cadherin

Cadherin is a member of the family of cell adhesion molecules (CAMs) that include occludins, integrins, and a variety of immunoglobulin-like molecules. All are cell-surface proteins and play a variety of roles in cell recognition, contact inhibition and cell-cell adhesion. The E-cadherins encoded by CDH1 located on chromosome 16q22.1, is a calcium dependent, homophilic cell-cell adhesion molecule that drive morphogenetic rearrangements and maintain the integrity of epithelial layers via the formation of adherens junction (Lilien *et al*, 2002). The expression of E-cadherin was decreased in a various high grade carcinomas with more aggressive phenotype, including prostate cancer (Umbas *et al*, 1997). N-cadherin is just like E-cadherin a type-I cadherin encoded by gene CDH2 located on chromosome 18q11.2. While E-cadherin is mostly expressed in epithelial cells, N-cadherin is expressed in various cell types including nerve, myocardial and mesenchymal cells. It was believed that E-cadherin promotes epithelial cell-epithelial cell adhesion by interacting with E-cadherin molecules on opposing cell surface (Hajra & Fearon, 2002), while N-cadherin promotes epithelial cell-stromal cell adhesion.

Controversial gene expression of E-cadherin was found in prostate cancer different stages, in which loss of expression of E-cadherin was found in localised prostate cancer with increased N-cadherin, while high expression of E-cadherin in metastasis (Rubin *et al*, 2001; Tomita *et al*, 2000). However, re-expression of E-cadherin was also found in primary breast cancer transition to metastasis. Recent studies showed a single polymorphism was found on allele A of E-cadherin promoter region with 70% decreased transcription of allele A in prostate cancer (Lindstrom *et al*, 2005), that

may explain decreased E-cadherin expression in localised prostate cancer not in metastasis.

Although several studies suggested that a significant effect for E-cadherin expression in prostate cancer (Dhanasekaran *et al*, 2001), it is still difficult to use E-cadherin in clinical trial. This is partly due to heterogeneous expression in prostate carcinoma. Thus, as a potential marker, E-cadherin may be used in combination with other biomarker.

#### **1.6.2.4 *KAI-1***

*KAI-1* is a metastasis suppressor gene isolated by Alu-PCR techniques from human chromosome 11p11.2 and shown to suppress metastasis when introduced into Dunning rat AT6.1 prostate cancer cells. *KAI-1* encodes a plasma membrane glycoprotein belonging to the TM4 superfamily (Jackson *et al*, 2003), with four transmembrane domains and a large N-glycosylated motif. It is believed to play a key role in cell-cell interaction or in extra cellular matrix binding and suggested as a tumour suppressor gene. In addition, the protein product of the gene is reported to be reduced in human cell lines derived from metastatic prostate cancer (Dong *et al*, 1995). Interestingly, Schulz *et al* (2003) have shown that expression of *KAI-1* is directly activated by *p53*, and loss of immunoreactivity of both *KAI-1* and *p53* resulted in poor overall survival of prostate cancer patients (reviewed in (Schulz *et al*, 2003)).

#### **1.6.2.5 *NM23***

*NM23* located on chromosome 17q21.3, encodes a nucleoside diphosphate kinase that was reported to be a tumour suppressor gene (Kauffman *et al*, 2003), involved in

the proliferation and differentiation of several cancers. Several studies correlated low expression of *NM23* with poor prognosis and survival, lymph node infiltration and histopathological indicators of high metastatic potential, in a number of cancer types (Hartsough & Steeg, 2000). However, the role of *NM23* needs to be clarified in prostate cancer. Evidence from some studies showed that the high level expression of *NM23* was found in prostate metastasis sites by immunohistochemical staining analysis (Igawa *et al*, 1996). Another study displayed over-expression of *NM23* in PIN suggesting that over-expression of *NM23* represents an early event in the development of prostate cancer and its decreased expression might be associated with later prostate cancer metastases (Myers *et al*, 1996).

#### **1.6.2.6 CD44**

The *CD44* gene located at 11p13 chromosome encodes a transmembrane glycoprotein. It is an important tumour metastasis suppressor gene in prostate cancer (Ponta *et al*, 2003) which also plays a role in normal prostatic epithelial cell differentiation. Both protein and mRNA studied demonstrated that *CD44* expressed strongly in basal cells and moderately in luminal cells in benign acini (Noordzij *et al*, 1997; Omara-Opyene *et al*, 2004). Moreover, *CD44* protein has been found in benign prostatic tissues and in 60% of primary prostate cancer with about 14% of metastasis expressing low level of *CD44* (Aaltomaa *et al*, 2000). De Marzo *et al* (1998) strongly correlated loss of *CD44* with high grade and invasive prostate cancer (De Marzo *et al*, 1998). In the AT3.1 rat prostate cancer cell-line, transfection-induced expression of *CD44* can suppress tumour metastasis but not affect tumorigenesis (Noordzij *et al*, 1999). Verkaik *et al* (2000) suggested that hypermethylation at the promoter region

of *CD44* may block gene transcription in prostate cancer eventually and, reducing protein expression of *CD44* (Verkaik *et al*, 2000).

#### 1.6.2.7 *PTEN*

The gene *PTEN* (phosphatase and tensin homologue) is a 47-KDa dual-specificity phosphatase with homology both to the protein tyrosine phosphatase family and two cytoskeleton proteins, tensin and auxilin. The tyrosine phosphatase family plays an important role in regulating cell signal transduction and in cell transformation (Tell *et al*, 2004). Homozygous deletions of *PTEN* have been detected in up to 10% of locally confined cancers and metastasis (Verhagen *et al*, 2006) also in 30% of prostate cancer cell lines and xenografts (Vlietstra *et al*, 1998). *PTEN* point mutations have been demonstrated in 2 to 10% of primary prostate cancer (Dong *et al*, 2001), and 30% to 60% of metastases (Dong *et al*, 2001; McMenamin *et al*, 1999), suggesting that *PTEN* could be a marker for prostate cancer metastasis, as well as for metastatic potential. The mechanism of *PTEN* acting as a tumour suppressor gene may involve inhibition of the phosphatidylinositol-3-kinase- protein B (PI3K-AKT) signalling pathway that is important for cell-cycle progression and cell- survival (Davies *et al*, 1999). Further studies demonstrated that the up-regulation of AKT activation is significantly associated with decreased survival, and therefore *PTEN* loss is a possible route by which this may occur (McCall *et al*, 2008).



## 1.7 Prostate Cancer Metastasis

Metastasis is defined as the process, by which malignant prostatic epithelial cells leave the primary tumour and travel to distant sites through circulatory system and there establish secondary tumours. This is a multi-step process that consists of a series of sequential events involving complex interaction between the cancer cells and their environment. After the initial neoplastic transformation of cells, metastasis is thought to involve the following steps (Figure 1.8) (Arya *et al*, 2006).

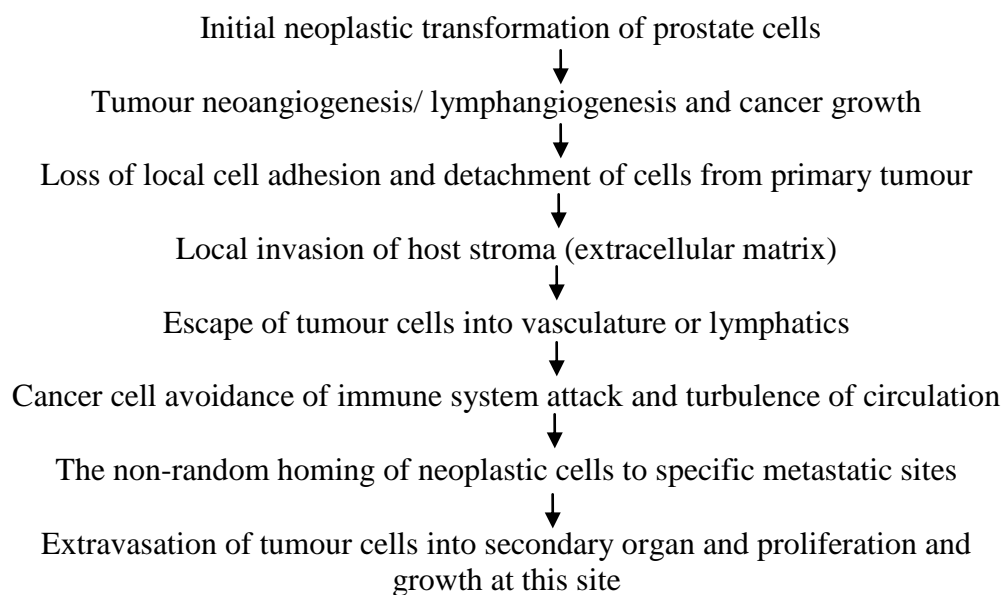


**Figure 1.8: The metastatic cascade of prostate cancer**

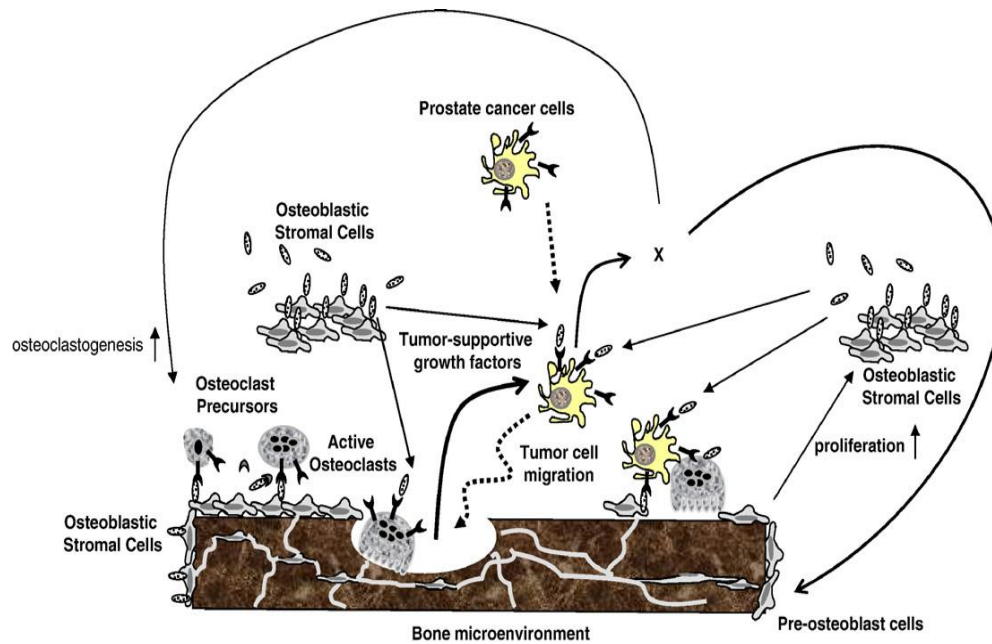
*After the initial neoplastic transformation of cells, metastasis is thought to involve multiple steps. The cell has to detach from the local primary tumour tissue architecture and invade the surrounding tissue, leading to invasive growth. Motile cells then have to enter the bloodstream and travel in the vascular network to reach a distant location. Then the cell must be able to leave the bloodstream and invade into the target tissue and proliferate at the target site.*

### **1.7.1 Mechanisms of bone metastasis in prostate cancer**



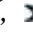
The skeleton is a preferred site for prostate and breast cancer metastasis. The studies demonstrated that approximately 90% of advanced prostate cancer metastasize to bone (Kingsley *et al*, 2007). Within the skeleton, metastases present as two types of lesions: osteoblastic or osteolytic. These lesions result from an imbalance between osteoblast-mediated bone formation and osteoclast-mediated bone resorption (Kingsley *et al*, 2007).

#### **1.7.1.1 Osteoclastic bone resorption**

The first important steps of prostate cancer cells metastasis to the bone is the activation of osteoclasts resorption which results in not only allowing the seeding of cancer cells but also releasing survival and growth factors that promote prostate cancer metastasis (Kingsley *et al*, 2007). Among these factors, the most prominent is the Receptor Activator of Nuclear Factor -  $\kappa$ B ligand (RANK ligand) produced by osteoblastic cells (Figure 1.9).



**Figure 1.9: Schematic representation of the putative interactions between prostate cancer cells and osteoblastic/osteoclastic cells in tumoral bone microenvironment (Mori *et al*, 2007).**

*RANK-positive prostate tumour cells preferentially target bone microenvironment where it is rich in RANKL. In tumoral bone environment, RANKL produced by osteoblasts and bone stromal cells has two potential targets: osteoclasts/osteoclast precursors and prostate cancer cells. RANKL acts as a 'soil' factor that facilitates prostate cancer metastasis development in bone by activating both kinds of RANK-positive cells. : RANKL, : RANK, : OPG, X: soluble factor(s) produced by prostate cancer cells.*

RANK ligand is mainly located on the surface of osteoblasts and bind to its specific receptor (RANKR) which is expressed on the surface of the osteoclastic precursors.

The studies showed that osteotropic factors such as parathyroid hormone, 1, 25-

dihydroxyvitamin D3, and parathyroid hormone can induce osteoclast formation and activation by up-regulation of RANKR (Penno *et al*, 2009). Osteoprotegerin, a member of tumour necrosis factor receptors, acts as a competitive inhibitor against RANK ligand binding RANKR and thus blocks the RANKR - RANK ligand interaction (Cairns *et al*, 1997). On the other hand, some controversial results demonstrated that osteoprotegerin also bind to tumour necrosis factor related apoptosis inducing ligand results in inhibition of cancer cell apoptosis (Holen *et al*, 2002). Nevertheless, osteoprotegerin remarkably decreases prostate cancer metastasis to bones because it inhibits bone resorption (Mori *et al*, 2007). Therefore, the development of competitive antibodies, such as recombinant osteoprotegerin, against RANK ligand can be potential treatments for bone metastasis (Figure 1.10).

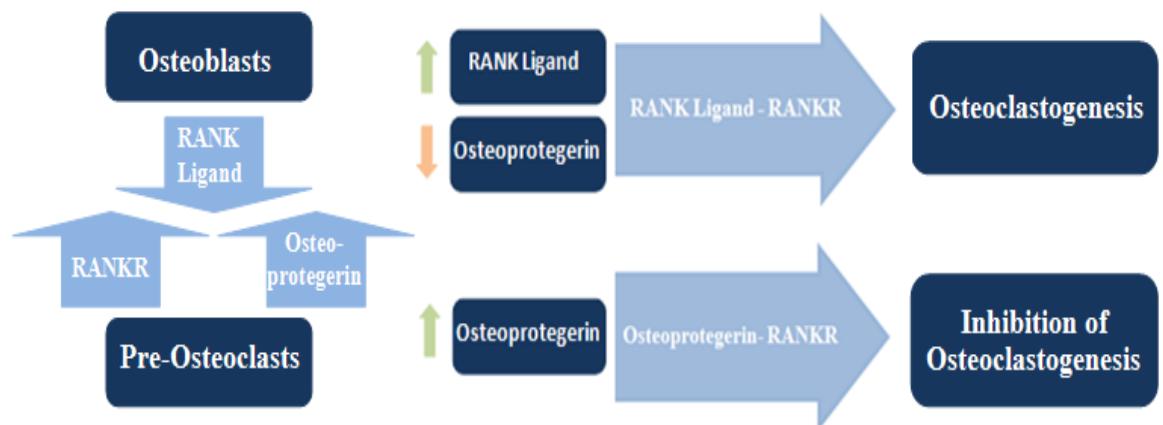


**Figure 1.10: The ratio of RANK ligand to osteoprotegerin determines the level of osteoclastogenesis (Mori *et al*, 2007).**

### 1.7.1.2 Domination of the osteoblastic lesions

Osteoblasts are bone forming cells which come from mesenchymal stem cells (Arya *et al*, 2006). Many factors can regulate the growth, survival and differentiation of osteoblasts, such as Endothelin-1 (ET-1), basic fibroblast growth factor (bFGF), Insulin-like growth factor (IGF) and Parathyroid hormone related protein (PTHrP). Some of them are also produced by metastatic prostate cancer cells.

ET-1, a peptide of 21 amino acid residues, is synthesized in vascular endothelial cells. It is involved in angiogenesis, the formation of the new bone and osteoblastic bone metastasis (Medinger *et al*, 2003). The previous studies demonstrate that ET-1 is one of the most over-expressed factors in osteoblast and can increase prostate cancer cell proliferation probably by enhancing the mitogenic effects of IGF and epidermal growth factor. Recent studies showed that overexpress ET-1 can up-regulate the vascular endothelial growth factor (VEGF) expression through the endothelin receptor A in osteoblast and thus could act as an angiogenic factor in the formation of bone metastasis (Medinger *et al*, 2003).

IGF-1 plays an important role in cell proliferation and inhibiting cell apoptosis in prostate cancer. Insulin-like growth factor binding protein-3 (IFGBP3) together with acid-labile subunit (ALS) binds IGF-1 (75% - 90% of circulating IGF-1) and the ligands binding trigger the downstream pathway of IGF-1 receptor (IGF-1R). The ligands binding activate the intrinsic tyrosine kinase of IGF-1R which results in phosphorylation of IGF-1R substrates - insulin receptor substrate-1 (IRS1), Src- and collagen-homology (SHC) and growth factor receptor-binding protein 2 (Grb2). Then, these phosphorylated factors active with *Ras – Raf – mitogen-activated protein kinase (MAPK)* cascade, which result in increasing cell proliferation (Piqueras *et al*,

2007). The IRS-1 also phosphorylates phosphatidylinositol 3'-kinase (*PI3K*) and *AKT*, which promotes anti-apoptotic survival of the cancer cells as shown in (Figure 1.11). In addition, it has been reported that elevated concentration of urokinase-type plasminogen activator (uPA) which is produced by prostate cancer cells also stimulates the local activity of IGF-1, therefore, increasing prostate cancer cells proliferation and inducing the osteoblastic reaction.

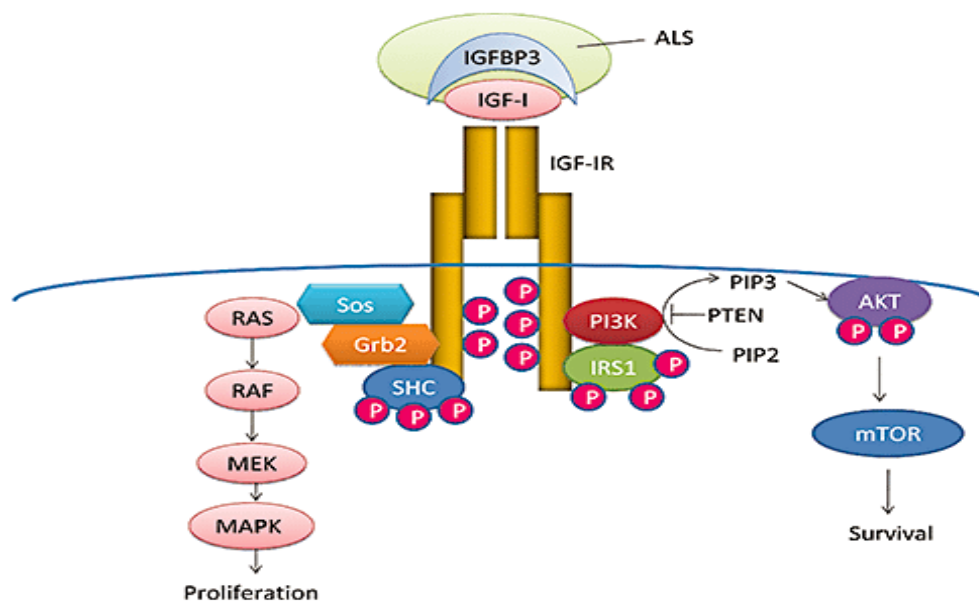


**Figure 1.11: IGF-I-IGFBP3-ALS binds to IGF-IR to trigger a series of ligand-mediated activations including RAS-RAF-MAPK and PI3K-AKT signalling pathway, controlling cell proliferation and cell apoptosis, respectively (Piqueras *et al*, 2007).**

### 1.7.2 Androgens and Prostate Cancer

Androgens are male steroid hormones, such as testosterone, that control the development and maintenance of masculine characteristics. Androgens are synthesized primarily in testes, under the regulation of luteinizing hormone, which is itself regulated by the levels of gonadotropin-releasing hormone (GnRH). Adrenal glands and some peripheral tissues including the prostate, also produce certain amount of androgens. Testosterone is the principle androgen and circulates mostly (98%) bound to sex hormone-binding globulin and albumin. At intracellular level, Testosterone is enzymatically converted to a more potent metabolite dihydrotestosterone (DHT); both steroids bind to the androgen receptor (AR), a ligand regulated transcription factor in the nuclear hormone receptor super family. Liganded-AR binds to the androgen response elements located in the regulatory regions of a variety of genes, many of which are involved in the growth, survival and differentiation of prostate cells (Attar *et al*, 2009).

### 1.7.3 Androgen independence and prostate cancer

Androgens play a major role in promoting the development and progression of prostate cancer. As a result, androgen ablation (blockade of androgen action) through the androgen receptor (AR) has been the cornerstone of treatment of advanced prostate cancer (Miyamoto *et al*, 2004). Therefore, prostate cancer is treated based on a unique characteristic, in that it is exquisitely dependent on androgen for development, growth and survival (Culig & Bartsch, 2006). Androgen ablation triggers cell death or cell cycle arrest of prostate cancer cells (Balk, 2002). Thus, androgen ablation remains the primary course of treatment for all patients with prostatic cancer (Sowery *et al*, 2007). The androgen-blockage therapy is initially

effective, and result in disease remission. However, recurrent tumours arise within a median period of 2-3 years, and in these recurrent tumour cells androgen signalling has been inappropriately restored (Feldman & Feldman, 2001).

#### 1.7.4 Progression to androgen independence

Progression to androgen independence is frequently signalled by a rise of Prostate Specific Antigen (PSA) under endocrine treatment and usually followed by cancer cell metastasis (Schroder, 2008). However, a total of seven mechanisms can be identified that are related to progression to androgen independence (Table 1.3). Five of those are dependent on the androgen receptor (AR), which is present or over-expressed in androgen independent prostate cancer (AIPC) cell (Schroder, 2008).

**Table 1.3: Mechanisms of progression of prostate cancer to androgen independence (Schroder, 2008)**

<b>Cause of Androgen independence</b>	<b>AR-dependent change</b>	<b>Example of Mechanisms of Androgen Independence</b>
Genetic Change in PC cells	No	Malignant epithelial stem cells
Bypassing the AR	No	Inhibition of apoptosis
Ligand-independent AR activation	Yes	GF function as ligands
AR hypersensitivity	Yes	Amplified AR hypersensitivity AR increased DHT
Change of AR specificity by mutation	Yes	Stimulation by non androgens (antagonists)



#### **1.7.4.1 Pre-existing genetics changes in prostate cancer stem cells**

Several studies (Coffey & Isaacs, 1981; Isaacs, 1999) postulated that androgen independence of prostate cancer was due to a selective growth advantage of pre-existing hormone-independent clonal populations of pre-existing, hormone-independent stem cells. The total population of prostate cancer cells in this setting is considered to be a mixture of hormone-dependent and hormone-independent cells from the time of initiation of the malignancy. Progression to hormone independence would then be explained by proliferation the hormone- independent cell population due to a growth advantage originating from suppression by androgen ablation of the growth of hormone-dependant cancer cells.

#### **1.7.4.2 Oncogenes and apoptosis inhibition**

Another Androgen and AR-independent mechanism plays an important role in clinical settings. This mechanism includes the activation of oncogenes, the suppression of tumour suppressor genes, such as the over expression of *Bcl-2*, which is part of a mechanism capable of inhibiting apoptosis. McDonnell *et al* (1992) found that *Bcl-2* was undetectable in 13 of 19 cases of AIPC tissue. In contrast, some other studies showed high levels of *Bcl-2* staining. In normal human prostate *Bcl-2* expression was limited to the basal epithelial cells (McDonnell *et al*, 1992). However, the observation of these findings does not establish a casual relationship. In contrast, (Revelos *et al*, 2005) found that expression of *Bcl-2* in prostate cancer cells was an independent predictor of treatment failure in localised disease. *Bcl-2* has been regarded as a therapeutic target in hormone refractory prostate cancer and antisense therapy was also developed for the mouse double minute 2 (MDM2) oncogene (Chi, 2005).

Inactivation of the *PTEN* tumour suppressor gene was found to be associated with locally progressive prostate cancer (Verhagen *et al*, 2006). Also, knock-down of both alleles of *PTEN* in mouse prostate resulted in successful induction of prostate cancer in an animal that did not usually develop this disease. The resulting cell proliferation was not accompanied by reduced apoptosis indicating that the proliferative mechanism is independent of the *Bcl2* cascade (Ma *et al*, 2005).

#### **1.7.4.3 Ligand-independent AR activation**

It was suggested (Culig *et al*, 1994b) that AR can be activated by insulin-like growth factor 1 (IGF-1), keratinocyte growth factor (KGF) and the epidermal growth factor (EGF). It was also showed that these growth factors were over expressed in some prostatic cancers and that antiandrogen bicalutamide blocks the IGF-induced AR activation. Receptor tyrosine kinase activated pathways have been targeted by several new drugs including Herceptin with limited activity in AIPC (Ziada *et al*, 2004).

Although these described mechanisms appeared to have no direct relation to androgen regulation, the intriguing finding that AR is expressed in most AIPC tissue suggests that different mechanisms may overlap (Dorff *et al*, 2006). Other authors have shown that the androgen-binding capacity of the AR in AIPC cells is unchanged (Ruizeveld de Winter *et al*, 1994). This leads to review of those potential mechanisms of progression to AIPC that are dependent on AR.

#### **1.7.4.4 AR hypersensitivity**

Amplification of AR leading to increased sensitivity and response to very low levels of androgens was found in about a third of tissues derived from hormone-

independent prostate cancer (Koivisto *et al*, 1997) and it was positively related to increased progression measured by the proliferation marker Ki67 (Haapala *et al*, 2007). Hypersensitivity of the AR may also explain the antiandrogens treatment failure resulting from an imbalance of the increased number of receptor molecules and the available number of competing molecules of the antiandrogen in the nucleus (de Jong *et al*, 1992). Moreover, increased intraprostatic levels of androgens due to increased production of DHT in the prostate as suggested by (Labrie *et al*, 2005) or changes of the sensitivity of AR (Gregory *et al*, 2001) will have the same results; stimulation of growth due to activation of AR.

#### **1.7.4.5 Changes of AR specificity (AR mutations)**

The AR gene is located on the X chromosome. Germline mutations leading to a loss of AR function and the clinical androgen insensitivity syndrome are not infrequent. Complete loss of AR function is compatible with life (Quigley *et al*, 1995). However, due in part to the heterogeneity of tumours, the incidence of somatic mutation is not fully known. What is clear however is that the primary tumours have a low level of androgen receptor mutations compared to metastatic tumours after androgen ablation therapy (Marcelli *et al*, 2000). These findings suggest that gaining such mutations may be a driving factor leading to androgen independence. These results contrast with another study which reported that accumulated mutations during androgen deprivation were already acquired in metastatic tumours, and were not instigated by androgen ablation (Cher *et al*., 1996).

A study by (Veldscholte *et al*, 1992) discovered a mutation leading to a functional change of the AR in the LNCaP cell line. This mutation resulted in substitution of

alanine for threonine at position 877 of the AR (the T877A mutation) gene. The presence of this mutation changes the growth inhibitory effect of the same substance. At present, it remains uncertain how frequently AR mutation lead to androgen insensitivity in a clinical setting. Experiments relating to the use of castration or an luteinizing hormone-releasing hormone (LHRH) agonist in combination with an antiandrogen as initial treatment in prostate cancer has shown that flutamide withdrawal may lead to clinical remission in about 30% of cases with duration of 3 to 4 months (Feldman & Feldman, 2001). AR mutations seem to be at least in part due to the selective pressure exerted by the use of antiandrogens. A study by (Taplin *et al*, 1999) identified the T877a mutation in 5 of 16 patients who received maximal androgen blockade using flutamide. Later, in a study of 48 specimens obtained from bone marrow metastases of prostate cancer progressing under endocrine treatment, 5 (10%) had a mutation in the hormone-binding domain (Taplin *et al*, 2003).

#### **1.7.4.6 Gene Fusions**

Gene fusion between the androgen-dependant *TMPRSS2* gene and oncogenes of the ETS family were described by Tomlins *et al* (Tomlins *et al*, 2005). Such fusions may play a role in the initiation or promotion of prostate cancer and may also provide a mechanism for explaining the progression of clinical prostate cancer from the hormone dependent to the hormone independent state. The fused gene was formed through the binding of the activated AR to the androgen responsive element of *TMPRSS2*. In this way, the activated AR actually mediates the fusion of an oncogene. Presence of the fusion mainly between *TMPRSS2*, and the *ERG* or *ETV1* members of the *ETS* oncogenes family were observed in both hormone dependent and hormone independent prostate cancer xenograft lines (Hermans *et al*, 2006).

One recent study of 165 patients treated by radical prostatectomy revealed that one of the gene fusions was found in every 81 (49.1%) of cases. Also, after adjusting for grade, stage and PSA level, the hazard ratio for PSA recurrence of gene-positive cases was 8.6%. This is the only large clinical study suggesting that the *TMPRSS2-ERG* gene fusion is an independent prognostic parameter in locally confined prostate cancer (Nam *et al*, 2007). In contrast, (Demichelis *et al*, 2007) showed that the *TMPRSS2-ERG* fusion was present more frequently in lethal prostate cancer prospectively treated by watchful waiting (cumulative incidence ratio 2.6,  $P < 0.01$ ). The *TMPRSS2-ERG* gene fusion has also been identified in 21% of 19 evaluated high-grade prostatic intraepithelial neoplasia (PIN) lesions (Cerveira *et al*, 2006).

Although there is theoretical potential for *TMPRSS2-ERG* oncogene family gene fusions to be related to prostate cancer progression to androgen independence, direct causal clinical evidence for the involvement of this mechanism is not available at present.

#### **1.7.4.7 Androgen synthesis in AIPC tissues**

In 1991, van der Kwast *et al* showed that almost consistently the AR studied by immunohistochemistry remained over-expressed in primary prostate cancer tissue that was progressive under endocrine treatment (van der Kwast *et al*, 1991). The study was based on freshly obtained and frozen tissue in 17 cases of local progression under endocrine treatment requiring transurethral prostatic resection. In 13 of the 17 examined specimens at least 80% of the nuclei of tumour cells were AR positive. Only one case was completely AR negative. Shortly thereafter it was confirmed that the AR in AIPC tissue was structurally intact and has a normal

binding capacity (Ruizeveld de Winter *et al*, 1994). The other finding, the fact that PSA still serves as a prognostic marker in AIPC despite castration levels of serum androgens, has always been suggestive of remaining androgen activity that is not counteracted by castration or the use of LHRH agonist. The promoter region of the PSA gene contains several androgen-responsive elements (AREs); PSA expression, therefore, requires an activated AR.

These findings provide links to recent developments that show that high androgen levels are preserved in tissues derived from metastases of patients with AIPC suggesting a high level of endocrine activity. Stanbrough *et al* (Stanbrough *et al*, 2006) studied 33 prostate cancer specimens that were obtained from bone marrow metastases and preserved by snap freezing. The study showed an increased expression of number genes involved in the androgenic part of the steroid metabolism included the genes 3 $\beta$ HSD2, AKR1C3, SRD5A1, as well as AKR1C1, C2 and UGT2B15. These genes all encode for enzymes that are involved in the androgen synthesis from the level of pregnenolone and progesterone on downward. The AR was found to be a 5.8 fold over expressed. Moreover, over-expression was also seen for SRD5A1, the gene that encode for 5- $\alpha$ -reductase type 1 but not type 2 which is predominant in tissue of benign prostatic hyperplasia (BPH).

More recently these data were confirmed in a study of six cases of AIPC with metastases disease. Tissue from bone metastases was obtained by warm autopsy and immediately frozen. This study showed levels of DHT that were equivalent to non-castrated prostate cancer tissue. Testosterone level, however, was found to be 3.8 times higher than that in prostate cancer tissue from non-androgen deprived patients. The transcripts for enzymes of androgen synthesis including cytochrome P17A, aldo-

keto reductase 1 C3 (AKR1CK), 3 $\beta$  hydroxysteroid dehydrogenase-2 (3 $\beta$ HSD2) and the gene encoding for 5- $\alpha$ -reductase type 2 (5- $\alpha$ -R2) were significantly up regulated in the metastatic samples. The data suggest that both the increased synthesis and degradation of androgen occurred in AIPC tissues (Mostaghel *et al*, 2009).

### 1.7.5 Androgen receptors and growth factors interactions

Although AR is playing a key role in all phases of prostate carcinogenesis, a number of other signalling pathways, and their interaction with AR signalling, are also critically implicated in prostate cancer, especially in advanced cancer cells.

Several growth factors such as, insulin-like growth factor (IGF), Keratinocyte growth factor (KGF) and epidermal growth factor (EGF), can increase AR transactivation under absence or low levels of androgen (Culig *et al*, 1996; Culig *et al*, 1994a). A study by Gregory *et.al* suggested that EGF increased level of transcriptional intermediary factor 2/glucocorticoid receptor interacting protein 1 through mitogen activated protein kinase (MAPK) signalling pathway and promote AR transcriptional response in prostate cancer cells (Gregory *et al*, 2004). Another angiogenesis growth factor, vascular endothelial growth factor (VEGF), has been frequently studied recently. The elevated expression of VEGF, which resulted in promoting vascular growth and endothelial cell proliferation, was found in androgen-stimulated prostate growth (Joseph *et al*, 1997). Other reports also showed that functions of VEGF were activated through hypoxia-induced factor (HIF) regulated by androgens and/or androgen receptor (Boddy *et al*, 2005). Further studies demonstrated the significant correlation between HIF expression with AR and VEGF expression, and provided firm support for this control system (Banham *et al*, 2007). Understanding of such

cross-talk between AR cascade and growth factors signalling may provide new opportunities for therapy of aggressive prostate cancer.

## **1.8 Angiogenesis**

Angiogenesis is a process involving the growth of new capillaries from pre-existing blood vessels. Angiogenesis repairs damaged tissue when wounds are healing; therefore, normal cells can switch on the growth of blood vessel by releasing angiogenic factors (Folkman, 2002). In contrast, they also can produce antiangiogenic factors which switch blood vessel growth off (Carmeliet & Jain, 2000). Tumour angiogenesis is defined as: cancer cells stimulate the growth of hundreds of capillaries from the nearby blood vessels which grow around and/or into the tumour to establish an independent supply of nutrients and oxygen. Angiogenesis is not only important to tumour development but also a critical step in tumour metastasis. The immature, highly permeable blood vessels, which have little basement membrane and few intercellular junctional complexes, provide efficient route of exit for tumour cells to leave the primary site, enter the blood stream, travel to another part of the body and begin to grow there.

### **1.8.1 Vascular endothelial growth factor (VEGF)**

There are at least five members of the vascular endothelial growth factor (VEGF) family which exist in man: VEGF-A (usually referred to as VEGF), VEGF-B, VEGF-C and VEGF-D and a structurally related molecule, placental growth factor (PlGF). All members of VEGF family are crucial important angiogenic factors which primarily target vascular endothelial cells. They promote new blood vessel formation



by binding tyrosine kinase receptors (also known as VEGF receptors) located on cell surface. Three VEGF receptors have been recognized: VEGFR-1 or fms-like tyrosyl kinase-1(Flt-1), VEGFR-2 or Kinase insert domain receptor (KDR/Flk-1) and VEGFR-3 or Flt-4. Both VEGF and VEGF-B bind to VEGFR-1. VEGFR-1 is involved in the organization of development of blood vessel, haematopoiesis and enhances VEGF-induced VEGFR-2 signaling during abnormal angiogenesis. VEGF but not VEGF-2 binds to VEGFR-2 results in promoting cell proliferation, mitosis, vascular permeability and angiogenesis, whereas VEGF-C and VEGF-D are ligands for VEGFR-3, which stimulates lymphangiogenesis (Ferrara, 2004).

### 1.8.2 The isoforms of VEGF

VEGF is a ~45kDa homodimeric heparin-binding glycoprotein which was firstly identified by Senger *et al.* in 1983. VEGF gene consists of 8 exons separated by 7 introns and is located at chromosome 6p21.3 (Aragon-Ching & Dahut, 2009). So far, there are 12 VEGF isoforms which have been divided into two families according to their terminal exon (exon 8) splice site: the proximal splice site, designated as VEGF<sub>xxx</sub> or distal splice site, designated as VEGF<sub>xxx</sub>b (Nowak *et al.*, 2008). The identified multiple proteins of VEGF expressed in human tissues and cells are named as VEGF<sub>121</sub>, VEGF<sub>121</sub>b, VEGF<sub>145</sub>, VEGF<sub>145</sub>b, VEGF<sub>165</sub>, VEGF<sub>165</sub>b, VEGF<sub>189</sub>, VEGF<sub>189</sub>b and VEGF<sub>206</sub> according to the different number of amino acids. VEGF<sub>121</sub> is thought to be the most diffusible isoform due to the absence of a heparin-binding domain. VEGF<sub>165</sub> is the predominant VEGF isoform secreted by different types of cells. VEGF<sub>165</sub> not only exists in diffusible location but also remains bound to the cell surface and the extra cellular matrix (ECM). However, the larger isoforms such

as VEGF<sub>189</sub> and VEGF<sub>206</sub> with high affinity to heparin remain localized within ECM (Ferrara, 2004).

### 1.8.3 VEGF and prostate cancer

Most of the tumour cells secrete VEGF *in vitro* indicating that VEGF may play a crucial role in tumour angiogenesis. This has been confirmed by *in situ* hybridization studies which demonstrated that VEGF mRNA is expressed in the majority of human carcinomas such as breast cancer, lung cancer, bladder cancer and ovary cancer (Ferrara, 2004). In prostate, VEGF is expressed differently between normal, benign and prostate cancer cells. It has been reported that the expression of VEGF mRNA was detected in PIN, and poorly differentiated tissues, but not in normal prostate tissue (Huss *et al*, 2001). Further studies also showed that the microvessel density (MVD) was increased significantly in metastatic prostate cancer samples when compared with non-metastatic prostate cancer tissues (Kitagawa *et al*, 2005). In addition, higher expression of hypoxia-inducible factor (HIF), a key regulator of VEGF expression, was detected in malignant prostate cancer compared with the adjacent normal and benign prostate tissue (Du *et al*, 2003). Clinical studies revealed that the level of VEGF expression in serum, plasma or urine was correlated with higher Gleason grade, metastasis and disease-specific survival (Bok *et al*, 2001; Duque *et al*, 1999). On the other hand, inhibition of VEGFR-1 and VEGFR-2 using AZD-2171 (Cediranib, AstraZeneca) induced tumour shrinkage in 56.5% of patients (13 out of 23 patients with measurable disease) with 4 meeting the criteria for partial response (Aragon-Ching & Dahut, 2009). These results indicated that VEGF played a dual role in prostate cancer at both the early initiating stage and the later stage for tumour progression and metastasis. VEGF interacts with VEGF-2 to stimulate

endothelial cell proliferation through the mitogen activated protein kinase (MAPK) pathway and promote vascular permeability, and subsequently with VEGFR-1 to assist the organization of new capillary tubes.

#### **1.8.4 Other growth factors in Prostate cancer**

Several growth factors, such as insulin-like growth factor (IGF) and epidermal growth factor (EGF) were found to increase the trans-activation potential of AR in prostate cancer. Epidemiological studies suggested that there is a correlation between the increased risk of developing prostate cancer and the high serum level of IGF-1 or low levels of IGFBP-3, a serum protein that regulates the binding of free IGF-1 to IGF receptor (IGFR) (Chan *et al*, 1998). However, these findings have not been successfully demonstrated by some other studies (Chen *et al*, 2005).

The EGFR is expressed in 40-80% of malignant prostate cancer cells and this increased expression was correlated with high Gleason score and tumour progression from an androgen-dependent to an androgen-independent state (Syed & Tolcher, 2003). EGF was shown to activate the transcriptional activity of AR by either increasing the expression levels or stimulating the activity of the AR co-activators in prostate cancer cells. Therefore, EGF is thought to promote malignant progression and metastasis of advanced prostate cancer (Reddy *et al*, 2006).

### **1.9 Peroxisome proliferator-activated receptors**

Peroxisome proliferator-activated receptors (PPARs) are part of the nuclear receptors family of transcription factors and identified originally in *Xenopus* frogs as receptors

that induce the proliferation of peroxisome in cells in the early 1990s (Han *et al*, 2008). The functional role of these ligand activated transcription factors is involved in regulating fatty acid catabolism, lipid storage and glucose metabolism in the body. There are three isoforms of PPARs: PPAR $\alpha$ , PPAR $\beta/\delta$  and PPAR $\gamma$ . They are expressed in various tissues and play different roles.

### 1.9.1 Structure of PPAR

Despite the location and functional differences, PPAR isoforms share similar structure and functional domains. Like other nuclear receptors, PPARs are composed of four major domains: A/B, C, D and E/F (Figure 1.12).

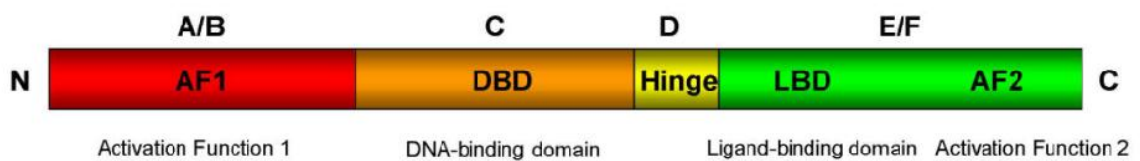


**Figure 1.12: The schematic view of the domain structure of PPARs.**

The N-terminal region of PPARs contains A/B domains which are different in both length and amino acid sequences. The A/B domain contains a transactive domain, which is independent of the presence, is termed activation function 1 (AF1). The activity of this domain can be regulated by protein kinase phosphorylation (Stephen *et al*, 2004). The C domain, which is the most conserved region amongst the PPARs, consists of a DNA binding domain (DBD). This domain contains two typical zinc

finger motifs which bind to specific sequences of DNA and are responsible for binding PPAR to peroxisome proliferator response element (PPRE) within the promoter region of the target gene. The D domain is a highly flexible hinge region. The C-terminal region of PPAR is an E/F domain which contains ligand binding domain (LBD) and ligand dependent activation domain (AF2). The LBD of PPARs consists 13  $\alpha$  helices and a  $\beta$  sheet forming a hydrophobic pocket which is about twice as large as other nuclear receptors (Peters & Gonzalez, 2009). This region is important for activation of PPAR binding to the PPRE and also plays an important role in nuclear localization. In addition, some studies demonstrated that PPARs could be activated by a variety of fatty acids at certain concentrations (Keller *et al*, 1993). PPARs form heterodimers with the 9-*cis* retinoic acid receptor (RXR), which result in a conformational change of both receptors, allowing the heterodimers to bind to the PPRE DNA promoter region containing repeat motifs (AGGTCA<sub>n</sub>AGGTCA) and regulate the gene transcription (Figure 1.13).

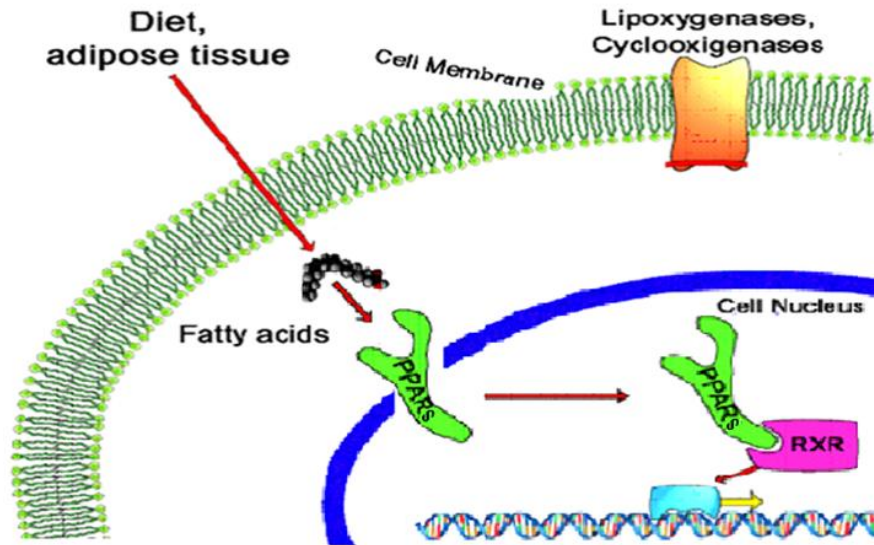


Figure 1.13: Model for PPARs signalling pathway (Harmon *et al*, 2010).

### 1.9.2 PPAR $\beta/\delta$

PPAR  $\beta/\delta$  is expressed ubiquitously throughout the body with different levels in different cell types. PPAR  $\beta/\delta$  can be activated by natural ligands, such as fatty acids, retinoid acids and prostaglandins as well as synthetic ligands including GW501516, GW0742 and L165041. Several studies demonstrate that PPAR  $\beta/\delta$  plays an important role in cell proliferation, differentiation and apoptosis. Activation of PPAR  $\beta/\delta$  can stimulate cell proliferation in colon cancer, liver cancer, lung cancer and breast cancer cell lines (Peters & Gonzalez, 2009). It has also been reported that PPAR  $\beta/\delta$  increases cell proliferation in PNT2 and LNCaP but not in DU145 and PC-3 prostate cancer cell lines (Stephen *et al*, 2004). However, the data on the role of PPAR  $\beta/\delta$  in cell proliferation are inconsistent and controversial. In addition, a number of recent studies suggest that activation of PPAR  $\beta/\delta$  with GW501516 can also stimulate angiogenesis by enhancing the expression of VEGF (Han *et al*, 2008;

Piqueras *et al.*, 2007). Strong evidence suggests that ligand activation of PPAR  $\beta/\delta$  can enhance the expression of 3-phosphoinositide dependent protein kinase 1 (PDK1) and subsequently activate the downstream protein kinase B (AKT) by phosphorylation. Activation of the PDK1/AKT signalling pathway has a direct effect on cell apoptosis through phosphorylation of the *BCL-2* family member *BCL-2* associated death promoter (BAD) thereby suppressing cell apoptosis and promoting cell survival. Schug *et al.* also suggested that PDK1/AKT anti-apoptosis signalling pathway regulated by PPAR  $\beta/\delta$  (Schug *et al.*, 2007a). A recent study by Morgan *et al.* (2010) showed that PPAR  $\beta/\delta$  directly induce the expression of C-FABP through a functional PPRE within the promoter region of the C-FABP gene. They also showed that activation of the C-FABP/ PPAR  $\beta/\delta$  pathway enhances the proliferation of malignant prostate cancer cell line PC3M, and that downregulation of either protein inhibits growth of these cells (Morgan *et al.*, 2010). Moreover, these results revealed the existence of a positive feedback loop that enhances the transcriptional activities of the C-FABP/ PPAR  $\beta/\delta$  pathway in prostate cancer cells, and they indicate that these activities support prostate carcinoma cell proliferation and tumourigenicity.

### 1.9.3 PPAR $\gamma$

PPAR $\gamma$  has been the most extensively studied isoform of PPAR family. It is mainly expressed in adipose tissues and plays a crucial role in adipocyte differentiation and lipid metabolism. Previous observation showed that PPAR $\gamma$  ligands promote the VEGF production in bladder and prostate cancer cells (Fauconnet *et al.*, 2002; Haslmayer *et al.*, 2002). Analogous findings were also reported by Cho *et al.* who detected a significant increase in VEGF and its receptors in epithelial cells treated with PPAR $\gamma$  synthetic ligand, thiazolidinediones. In addition, activation of PPAR $\gamma$

also stimulates the tumour formation in colon cancer (Pino *et al*, 2004). On the other hand, there are several lines of evidence to support that PPAR $\gamma$  ligand activations are capable of inhibiting angiogenesis progression under certain conditions. It is suspected that the various times and doses of PPAR $\gamma$  ligand treatment or the variety of organisms and cells examined may lead to such discrepancies.

## **1.10 Fatty Acid, Fatty Acid Binding Proteins and Prostate Cancer**

### **1.10.1 Introduction to Fatty Acid**

Fatty acid (FA) trafficking in cells is a complex and dynamic process that affects many aspects of cellular function. FAs functioning both as an energy source and as signals for metabolic regulation, acting through enzymatic and transcriptional networks to modulate gene expression, growth and survival pathways, and inflammatory and metabolic responses (Hotamisligil, 2006). Furthermore, FAs, particularly linoleic and arachidonic acids, can be metabolized into a diversified large family of bioactive lipid mediators called eicosanoids, which may function as pro and anti-inflammatory mediators. In particular, the cyclopentenone prostaglandins, such as PGA1, PGA2 and PGJ2, have potent anti-inflammatory effects through the inhibition of inflammatory kinase pathways (Serhan, 2007).

### **1.10.2 Dietary fatty acid and prostate cancer**

The incidence of latent cancer is uniform around the globe. However, western developed nations have a higher incidence of clinical prostate cancer. Giving that approximately 40% of total energy intake is obtained from fat in a westernised diet,



this provides a rationale for studying the link between dietary fat intake and prostate cancer (Das *et al*, 2001).

Epidemiological studies (Maeda *et al*, 2003; Newberry *et al*, 2006) showed a link between prostate cancer and two main factors; age and diet. Such studies suggested that the difference in prostate cancer incidence between western countries and Japan was a direct link to the type and quantity of fatty acids ingested. It was shown that an increase in incidence of an individual from a country of a relatively low prostate cancer risk to that from a country of high prostate cancer risk.

The human body is capable of synthesising certain FAs. Yet those acquired solely through diet defined as “essential” fatty acids. These make up precursors of two classes of polyunsaturated fatty acids, linoleic acid- an omega 6 fatty acid derived from vegetable, seed and corn oils, and alpha-linolenic acid- an omega 3 fatty acid derived mainly from fish oils. The methods by which polyunsaturated fatty acids (PUFA), such as eicosanoids, are thought to influence and promote cancer progression is not fully understood, however it is suggested that conversion of the precursor linoleic acids into arachidonic acid by desaturation plays an integral part. Arachidonic acid is catalysed into prostaglandin and thromboxanes by the cyclooxygenase enzyme. Studies have shown the existence of two forms of cyclooxygenase enzyme. Cox-1, which is constitutively active and Cox-2, an inducible gene observed to be over expressed/up regulated in prostate cancer biopsies (Fosslien, 2000). In contrast, fish oils containing eicosapentaenoic acid and lipoxygenase, thereby producing series 3 and 5 prostaglandins which reportedly cause less tissue inflammation, and reduce the production of the more active arachidonic acid metabolites (Newberry *et al*, 2008).

### 1.10.3 Fatty acid binding proteins (FABPs)

Intracellular lipid chaperones known as FABPs are a group of molecules that coordinate lipid responses in cells and are also strongly linked to metabolic and inflammatory pathways (Chmurzyńska, 2006). FABPs are abundantly expressed 14-15 kDa proteins that reversibly bind hydrophobic ligands, such as saturated and unsaturated long chain fatty acids, eicosanoids and other lipids, with high affinity (Zimmerman & Veerkamp, 2002). FABPs are found across species from *Drosophila melanogaster* and *Caenorhabditis elegans* to mice and humans, demonstrating strong evolutionary conservation. However, little is known about their exact biological functions and mechanisms of actions. Studies in cultured cells have suggested potential action of FABPs in fatty acid import, storage and export as well as cholesterol and phospholipid metabolism (Chmurzyńska, 2006; Haunerland & Spener, 2004).

Recently, through the use of various genetic and chemical models in cells as well as whole animals, the FABPs have been shown to be central to lipid-mediated processes and related metabolic and immune response pathways. In addition, they have also highlighted their considerable potential as therapeutic targets for a range of associated disorders, including obesity, diabetes and atherosclerosis (Furuhashi & Hotamisligil, 2008).

#### 1.10.3.1 Fatty acid binding proteins (FABPs) family

Different types of FABPs can be divided into two main groups (Glatz & van der Vusse, 1996): those associated with the plasma membrane (FABPpm) and those located intracellularly or in cytoplasm (C-FABP). So far nine tissue-specific

cytoplasmic FABPs have been identified Table 1.4 (Furuhashi & Hotamisligil, 2008).

**Table 1.4: Family of FABPs (Furuhashi & Hotamisligil, 2008).**

Gene	Common name	Alternative names	Expression	Chromosomal location		
				<i>Homo sapiens</i>	<i>Mus musculus</i>	<i>Rattus norvegicus</i>
<i>Fabp1</i>	Liver FABP	L-FABP	Liver, intestine, pancreas, kidney, lung, stomach	2p11	6 C1	4q32
<i>Fabp2</i>	Intestinal FABP	I-FABP	Intestine, liver	4q28–q31	3 G1	2q42
<i>Fabp3</i>	Heart FABP	H-FABP, MDGI	Heart, skeletal muscle, brain, kidney, lung, stomach, testis, aorta, adrenal gland, mammary gland, placenta, ovary, brown adipose tissue	1p32–p33	4 D2.2	5q36
<i>Fabp4</i>	Adipocyte FABP	A-FABP, aP2	Adipocyte, macrophage, dendritic cell	8q21	3 A1	2q23
<i>Fabp5</i>	Epidermal FABP	E-FABP, PA-FABP, mal1	Skin, tongue, adipocyte, macrophage, dendritic cell, mammary gland, brain, intestine, kidney, liver, lung, heart, skeletal muscle, testis, retina, lens, spleen	8q21.13	3 A1-3	2
<i>Fabp6</i>	Ileal FABP	II-FABP, I-BABP, gastrotropin	Ileum, ovary, adrenal gland, stomach	5q33.3–q34	11 B1.1	10q21
<i>Fabp7</i>	Brain FABP	B-FABP, MRC	Brain, glia cell, retina, mammary gland	6q22–q23	10 B4	20q11
<i>Fabp8</i>	Myelin FABP	M-FABP, PMP2	Peripheral nervous system, Schwann cell	8q21.3–q22.1	3 A1	2q23
<i>Fabp9</i>	Testis FABP	T-FABP	Testis, salivary gland, mammary gland	8q21.13	3 A2	2q23

### 1.10.3.2 Fatty acid binding proteins (FABPs) affinity and structure

Several FABP isoforms have been structurally investigated through isolated recombinant proteins by X-ray crystallography and nuclear magnetic resonance. FABPs have an extremely wide range of sequences diversity ranging from 15% to 70% sequence identity between different members (Chmurzyńska, 2006). However, all known FABPs share almost identical three dimensional structures (Figure 1.14). Common to all FABPs is a 10-stranded antiparallel  $\beta$ -barrel structure, which is formed by two orthogonal five-stranded  $\beta$ -barrels, the opening of which is framed on one side by the N-terminal helix-loop-helix “cap” domain, and fatty acids are bound to the interior cavity. The conserved fingerprint, providing a signature for all FABPs, has recently been revealed as shown in Figure 1.15.

All FABPs bind long-chain fatty acids with differences in ligand selectivity, binding affinity and binding mechanisms as a result of small structural differences between isoforms. In general, the more hydrophobic the ligand is the tighter the binding affinity with the exception of unsaturated fatty acids. It is also possible that the needs of target cells determine the affinity and even selectivity of the major isoforms present in different sites. For example, B-FABP is highly selective for very long-chain fatty acids such as docosahexanoic acid (Balendiran *et al*, 2000). On the other hand, L-FABP exhibits binding capacity for a broad range of ligands from lysophospholipids to haem (Coe & Bernlohr, 1998).

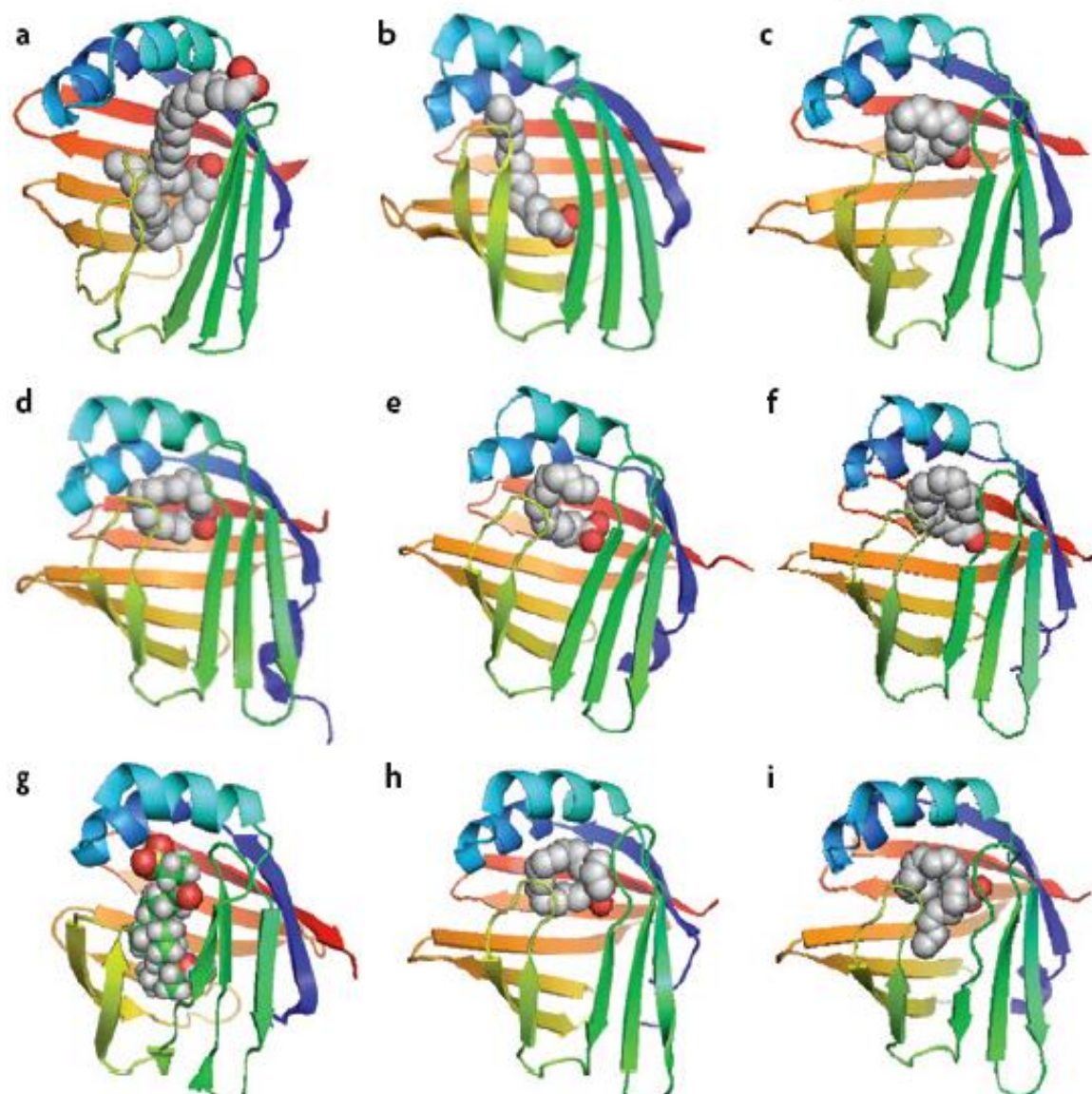


**Figure 1.14: Crystal structure of ligand-bound FABPs (Furuhashi & Hotamisligil, 2008).**

*Ligand-binding FABPs are shown above (The figures were created using PyMOL).*

*(a) FABP1 (Protein Data Bank (PDB) code: 1lfo); (b) FABP2 (PDB code: 2ifb); (c) FABP3 (PDB code: 2hmb); (d) FABP4 (PDB code: 2ifb); (e) FABP5 (PDB code: 1b56); (f) FABP8: (PDB code: 1pmp); (g) FABP6: (PDB code: 1o1v); (h&i) FABP7: (PDB code: 1fe3 & 1fdq).*

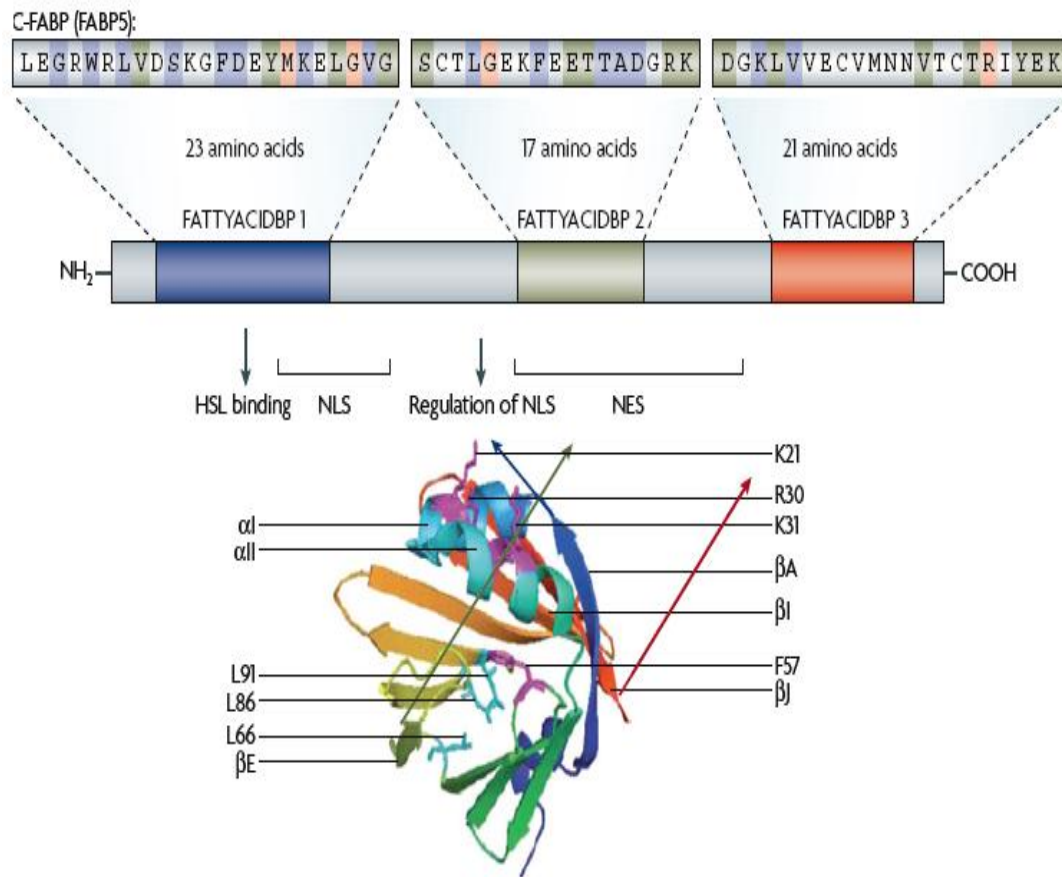


**Figure 1.15: Fingerprint for fatty acid binding proteins (Furuhashi & Hotamisligil, 2008).**

Three highly conserved motifs are presented with the ribbon diagram. FATTYACIDBP1 (blue ribbon) forms part of first  $\beta$  strands ( $\beta A$ ). It also includes a nuclear localization signal (NLS) and a hormone-sensitive lipase (HSL) binding site. The nuclear export signal (NES) domain is located in FATTYACIDBP2 (green ribbon) which includes  $\beta$  sheet 4 and 5 ( $\beta E$ ). FATTYACIDBP3 (red ribbon) encodes  $\beta$  sheet 9 ( $\beta I$ ) and 10 ( $\beta J$ ). The key amino acids are also marked with blue, green and red respectively.

### 1.10.3.3 Functions of FABPs

Numerous functions have been proposed for FABPs. As lipid chaperones, FABPs may actively facilitate the transport of lipids to specific compartments in the cells, such as to the lipid droplet for storage, to the endoplasmic reticulum for signalling, trafficking and membrane synthesis, to the mitochondria or peroxisome for oxidation, to cytosolic or other enzymes to regulate their activity, to the nucleus for lipid-mediated transcriptional regulation, or even to the outside of cells to signal in an autocrine or paracrine manner (Figure 1.16).

FABPs content in most cells is generally promotional to the rates of fatty acid metabolisms. FABPs are also involved in conversion of fatty acids to eicosanoid intermediates and in stabilizations of leukotrienes (Zimmer *et al*, 2004). Furthermore, a direct protein-protein interaction between hormone-sensitive lipase (HSL) activity and A-FABP or E-FABP in adipocytes has been also reported (Hertzel *et al*, 2002). In general, the interacting protein partners for FABPs are poorly understood, and the searches for such proteins with conventional approaches have not been fruitful. However, movement of FABPs into the nucleus and interaction with nuclear hormone receptors is possible, and this mechanism might potentially deliver ligands to this protein family (Gillilan *et al*, 2007).

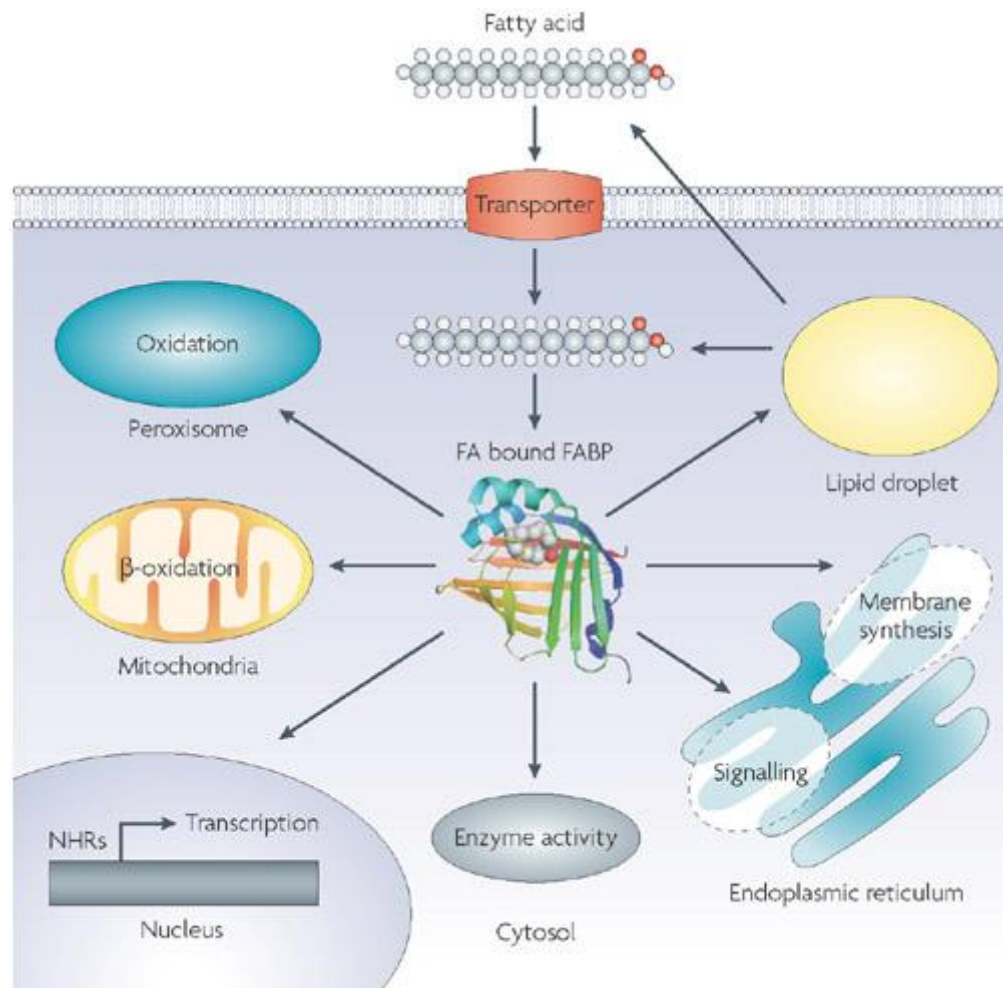


**Figure 1.16: Putative functions of FABPs in the cell (Furuhashi & Hotamisligil, 2008).**

#### 1.10.4 Cutaneous FABP (C-FABP) in prostate cancer

C-FABP is also called Epidermal FABP (E-FABP) or Psoriasis-associated FABP (PA-FABP). C-FABP is a 15 KDa cytosolic protein of the fatty acid binding protein, which binds with high affinity to long chain fatty acid. In addition to skin, C-FABP expression has been identified in the endothelial cells of the placenta, heart, skeletal muscle, small intestine, renal medulla and in the goblet cells of the lung (Masouye *et al*, 1996). In addition to breast tissues, increased levels of C-FABP have also been



detected in the malignant tumours of bladder and pancreas (Celis *et al*, 1999; Sinha *et al*, 1999), indicating that C-FABP may also play a role in malignant progression in these cells. Although the precise role of C-FABP in these tissues is not clear, it is likely to be involved in binding and transporting intracellular fatty acids, some of which are signalling molecules reported to be involved in carcinogenesis (Glatz & van der Vusse, 1996).

Our previous studies (Jing *et al*, 2000) have found that the *C-FABP* gene was overexpressed in malignant breast and prostate epithelial cell lines, when *C-FABP* gene was transfected into the benign rat Rama 37 model cells and the tranfectants subsequently inoculated into Wistar Furth rats, a significant number of animals developed metastasis. Further studies demonstrated that C-FABP promoted tumorigenesis and metastasis of prostate cancer cells by facilitating angiogenesis through up-regulating *VEGF* gene (Jackson *et al*, 2002; Soker *et al*, 2001). These results indicated that there may be a fatty acid signalling initiated pathway that leads to metastasis in prostate cancer and C-FABP and VEGF are all important factors in this possible pathway.

Suppression of C-FABP expression by antisense transfection in PC-3M cells decreased the invasive capacity *in vitro* and reduced the tumourigenicity *in vivo*. Moreover, the suppression of VEGF expression has also been detected in these transfected cell lines (Adamson *et al*, 2003). These results indicated that over-expression of C-FABP may stimulate the expression of VEGF and subsequently promote the angiogenesis to facilitate tumour formation and metastasis. Recent studies by Morgan *et.al* also confirmed that suppressing the expression of C-FABP in PC-3M cells using siRNA silencing technique resulted the significant reduction of

tumorigenicity both *in vitro* and *in vivo* (Morgan *et al*, 2008). However, how exactly C-FABP elevates the expression of VEGF is still unclear.

## **1.11 Scope of this thesis**

### **1.11.1 Hypothesis**

This thesis tests hypothesis that the tumour-promoting activity of C-FABP depends on its fatty acid binding and transporting function which is dependant of structural integrity of fatty acid binding motif.

### **1.11.2 Aims**

To investigate the relationship between the tumorigenicity-promoting function of C-FABP and its fatty acid binding ability by performing following set of experiments:

- ❖ Generation of mutation in C-FABP cDNAs and transfected them into LNCaP prostate cancer cells.
- ❖ Production of recombinant C-FABPs and testing their fatty acid binding ability.
- ❖ Study the effect of over-expression of recombinant wild type and mutant C-FABPs on tumorigenicity of prostate cancer cells.

## **2 MATERIALS AND METHODS**

## **2.1 Materials**

All materials and preparation of stock solutions used in this thesis are summarised in Appendices 1 and 2.

## **2.2 General molecular biology methods**

### **2.2.1 Calculation of DNA and RNA concentration**

The DNA or RNA samples were examined for concentration and quality using the NanoDrop ND-1000 spectrophotometer. Nucleic acid sample (1µl) was loaded onto the lower measurement pedestal. After closing the sampling arm, the spectral measurement was initiated using the operating software on the computer. The DNA or RNA sample concentration was presented on the screen in ng/µl based on absorbance at 260nm using the modified Beer-Lambert equation. The purity of the sample was also assessed using ratio of absorbance at 260nm and 280nm. A ratio of ~1.8 was generally accepted as pure for DNA; a ratio of ~2.0 was generally accepted as pure for RNA.

### **2.2.2 Ethanol precipitation of DNA and RNA**

The DNA or RNA to be precipitated was mixed with 2.5 volumes of chilled 4°C temperature absolute ethanol and 10% volumes of 3M sodium acetate (pH5.2). The mixture was mixed gently by inversion and incubated at –80°C overnight for DNA or RNA to precipitate. The DNA or RNA was pelleted by centrifuging at 16,000 xg at 4°C in a microcentrifuge for 20 minutes. The supernatant was removed and the pellet was washed by 100µl of pre-chilled 70% (v/v) ethanol. The DNA or RNA was

recentrifuged at 16,000xg at 4°C for 15 minutes and the supernatant was decanted. The DNA or RNA was air dried and resuspended in sterile DEPC-treated water.

### **2.2.3 Agarose gel electrophoresis of DNA**

Agarose gel electrophoresis was performed in 1xTBE buffer (0.089M Tris-base, 0.089M boric acid, 0.002M EDTA pH8.0). The agarose concentration of the gel was 0.8% to 2.0% (w/v) according to DNA size. The agarose was dissolved in 200ml of 1xTBE buffer by microwave heating for 2 minutes and cooled to 40-50°C. Then, 10µl of 500ng/ml ethidium bromide was added for visualisation. The gel mixture was poured and placed at 4°C to solidify. DNA samples were prepared by adding 5x agarose gel loading buffer [0.25% (w/v) bromophenol blue, 0.25% (w/v) xylene cyanol FF, 30% (v/v) glycerol in water] to a 1x concentration and loaded into the gel alongside DNA size marker. The gel was run for 50 minutes at 90V and visualised on a UV transilluminator.

### **2.2.4 Purification of DNA from agarose gels**

DNA fragments were separated using agarose gel electrophoresis (section 2.2.3). The required fragments were visualised by ethidium bromide and excised using a sterile blade. Each excised gel slice was weighed and three times the volume of buffer QG was added. Then, the mixture was dissolved in a 50°C water bath for 10 minutes with occasional vortex mixing. The melted agarose and DNA solution was applied to a QIAquick spin column and centrifuged for 1 minute at 16,000xg in a microcentrifuge

and the flow through was discarded. The membrane, bound with DNA, was washed by passing through 750 $\mu$ l of buffer PE and re-centrifuged for a further minute to remove any residue. The DNA was eluted from the column by adding 30 $\mu$ l of distilled water and quantified as described above. The DNA was stored at  $-20^{\circ}\text{C}$  until needed.

### 2.2.5 Restriction Enzyme digestion of plasmid DNA

Plasmid DNA was digested with two different restriction enzymes (*Xho*I and *Pst*I) to check for the presence of insert or to produce the DNA fragment for ligation. The restriction enzyme digest mixture was prepared as shown in Table 2.1.

Water	35 $\mu$ l
10x NEBuffer 3	5 $\mu$ l
<i>Xho</i> I 20units/ $\mu$ l	1 $\mu$ l
<i>Pst</i> I 20units/ $\mu$ l	1 $\mu$ l
BSA 10 $\mu$ g/ $\mu$ l	5 $\mu$ l
DNA 1 $\mu$ g/ $\mu$ l	3 $\mu$ l

**Table 2.1: The restriction enzyme digestion mixture (total volume 50 $\mu$ l)**

The restriction enzyme digest mixture was incubated at  $37^{\circ}\text{C}$  for 2 hours to allow complete digestion of template DNA. Then, the enzyme reaction was inactivated by heating to  $68^{\circ}\text{C}$  for 10 minutes and the products were analysed by gel electrophoresis.

### 2.2.6 DNA ligation

Fragments of DNA were removed from pBluescript vector using restriction enzyme digestion (section 2.1.5) and inserted into transfection vector pIRES2-EGFP by ligation reaction using T4 DNA ligase. The ligation mixture was prepared as shown in Table 2.2.

Insert DNA (180ng/ $\mu$ l)	2 $\mu$ l
Vector DNA ( 110ng/ $\mu$ l)	1 $\mu$ l
2x quick Ligation buffer	10 $\mu$ l
T4 DNA Ligase (400 cohesive end units)	1 $\mu$ l
H <sub>2</sub> O	6 $\mu$ l
Total volume	20 $\mu$ l

**Table 2.2: The ligation reaction mixture**

After overnight incubation at 4°C, 5 $\mu$ l of ligation mixture was transformed into competent bacterial cells (section 2.1.8). Recombinant DNA was recovered from bacterial cells using a Qiagen miniprep or midiprep kit (section 2.1.9).

### 2.2.7 cDNA sequencing

Recombinant plasmid DNAs or cDNA sequences generated by reverse transcription polymerase chain reaction (RT-PCR) were sent for nucleotide sequencing at the School of Tropical Medicine, University of Liverpool. Sequencing was carried out by using a big dye terminator cycle sequencing reaction kit with an ABI prism 377 automated DNA sequencer. Sequence alignment was determined by using BioEdit for searching Genbank (BLAST).

### 2.2.8 Transformation of competent bacteria with plasmid DNA

#### 2.2.8.1 Preparation of competent bacterial cells

*E.coli* (DH5 $\alpha$ ) glycerol stock was streaked onto an LB-agar plate and incubated at 37°C overnight. On the following day, a single colony was inoculated into a conical flask containing 10mls LB broth and incubated at 37°C overnight with shaking at 225xg. Then, 1ml of overnight culture was transferred into 100ml of SOB medium (2% w/v bactotryptone, 0.5% w/v yeast extract, 10mM NaCl, and 2.5mM KCl) and incubated at 37°C with shaking at 225xg until the OD<sub>550</sub> reached 0.4. The culture solution was split into 8x 12ml aliquots and placed on ice to cool for 10 minutes. The DH5 $\alpha$  bacteria were pelleted by centrifuging at 2500xg for 10 minutes at 4°C and the supernatant was discarded. The bacterial cell pellets were resuspended in 8.25ml of pre-cooled RF1 buffer (100mM KCl, 50mM MgCl<sub>2</sub>.4H<sub>2</sub>O, 30mM KCl, 10mM CaCl<sub>2</sub> and 15% v/v glycerol, pH6.8) and incubated on ice for 10 minutes. After a further centrifuging at 2500xg for 10 minutes at 4°C, the cell pellet was resuspended in 2ml of RF2 buffer (10mM MOPS, 10mM KCl, 75mM CaCl<sub>2</sub>.2H<sub>2</sub>O and 15% v/v



glycerol, pH6.8). The DH5 $\alpha$  bacteria solution was dispensed into 1ml aliquots in cryovials, frozen in liquid nitrogen and transferred immediately to  $-80^{\circ}\text{C}$  freezer for storage.

#### **2.2.8.2 Transformation**

A vial of DH5 $\alpha$  competent cells was removed from the  $-80^{\circ}\text{C}$  and thawed on ice. Then, 50ng of plasmid DNA or 10 $\mu\text{l}$  of the ligation mixture was added to 50 $\mu\text{l}$  of competent DH5 $\alpha$  cells, mixed by flicking gently and incubated on ice for 30 minutes. The cells were heat shocked at  $42^{\circ}\text{C}$  for exactly 90 seconds and placed on ice for a further 2mins followed by adding 800 $\mu\text{l}$  of SOC (2% w/v bactotryptone, 0.5% w/v yeast extract, 10mM NaCl, 10mM MgCl<sub>2</sub>, 10mM MgSO<sub>4</sub>, 2.5mM KCl, 20mM glucose) and incubated  $37^{\circ}\text{C}$  for 1 hour in a shaking incubator at 225xg. Transformed bacteria solution (200 $\mu\text{l}$ ) was plated onto LB plates containing 50 $\mu\text{g}/\text{ml}$  ampicillin or 30 $\mu\text{g}/\text{ml}$  kanamycin for antibiotic selection and incubated at  $37^{\circ}\text{C}$  overnight. Finally, colonies were picked from the plate and grown in LB broth containing antibiotic at  $37^{\circ}\text{C}$ , 225xg overnight and plasmid minipreps were conducted.

#### **2.2.8.3 Calculation of transformation efficiency**

Transformation efficiency is the number of transformed cells (transformants) generated by 1 $\mu\text{g}$  of supercoiled plasmid DNA in a transformation reaction. Transformation efficiency is calculated as follows:

## **2.2.9 Isolation of plasmid DNA**

Plasmid DNA was isolated using Qiagen extraction kits.

### **2.2.9.1 Miniprep extraction of plasmid DNA**

Overnight cultured bacteria (5ml) in LB medium containing antibiotic harvested by centrifuging at 6,000xg for 1min and the supernatant removed. The cell pellet was resuspended in 250µl of suspension buffer P1 (50mM Tris-HCl pH8.0, 10mM EDTA and 100µg/ml RNaseA) by vortexing, followed by adding 250µl of cell lysis buffer P2 (200mM NaOH and 1% w/v SDS) and mixed by gentle inversion of the microcentrifuge tube six times. Then, 350µl of neutralisation buffer N3 (4.2M Gu-HCl, 0.9M potassium acetate pH4.8) was added and mixed by gentle inversion of the microcentrifuge tube six times. The mixture was centrifuged at 13,000xg for 10 minutes and the supernatant was loaded to a miniprep spin column. The column was centrifuged at 13,000xg for 1 minute and the flow through was discarded. The column was then washed by adding 750µl of wash buffer PE (10mM Tris-HCl pH7.5 and 80% ethanol) and centrifuged at 13,000xg for 1 minute. After removing the flow through, the spin column was centrifuged for an additional minute to remove residual wash buffer. The column was placed in a clean 1.5ml microcentrifuge tube and 30µl of distilled water was added to the centre. After 1min incubation at RT, the plasmid DNA was eluted by centrifuging at 13,000xg for 1 minute. The concentration and

quality of the DNA were examined as described in section 2.1.1 and isolated plasmid DNA was stored in a -20°C freezer.

#### **2.2.9.2 Midiprep extraction of plasmid DNA**

A single colony of transformed DH5 $\alpha$  bacteria was transferred into flasks containing 10ml of LB medium with antibiotic and left to grow overnight at 37°C, 225xg. The overnight cultured bacterial cells (5ml) were then transferred to 200ml LB medium containing antibiotic and incubated for 5 additional hours at 37°C, 225xg. The transformed bacterial cells were harvested by centrifuging at 6,000xg for 10min at 4°C and the supernatant was removed. The cell pellet was resuspended in 4ml of buffer P1 (50mM Tris-HCl pH8.0, 10mM EDTA, 100 $\mu$ g/ml RNase A) by vortexing until no clump remained. The bacterial cells were lysed by adding 4ml of lysis buffer P2 (200mM NaOH, 1% w/v SDS), gently mixed by six times inversion. After incubation at RT for 5mins, 4ml of pre-chilled P3 neutralising buffer (3.0M potassium acetate pH5.5) was added and the mixture was mixed by inverting six times, incubated on ice for 15mins and then centrifuged at 16,000xg, 11°C for 30mins. The supernatant containing plasmid DNA was transferred to a clean 30ml centrifuge tube and re-centrifuged at 16,000xg, 11°C for further 15mins. In the mean while, a Qiagen midiprep column was equilibrated by applying 4ml of equilibration buffer QBT (750mM NaCl, 50mM MOPS pH 7.0 and 15% v/v isopropanol) and allowed to empty by gravity flow. Once the Qiagen midiprep column was equilibrated, the cleared supernatant containing plasmid DNA was loaded into the column and allowed to flow under gravity. The column was washed twice with 10ml

of wash buffer QC (1.0M NaCl, 50mM MOPS pH 7.0, 15% v/v isopropanol) and the plasmid DNA was eluted from the column using 5ml of elution buffer QF (1.25 M NaCl, 50mM Tris-HCl pH 8.5, 15% v/v isopropanol). The eluted DNA was precipitated by adding 3.5ml of isopropanol, mixed and centrifuged at 4°C, 11,000xg for 30mins. The supernatant was carefully removed and the pellet was washed with 2ml of 70% (v/v) ethanol and centrifuged at RT, 11,000xg for 10mins. After removing the supernatant, the pellet was air-dried for 10mins and the plasmid DNA was then dissolved in 200µl of nuclease-free water. The concentration and quality of the DNA were examined as described in section 2.1.1 and the isolated plasmid DNA was stored at -20°C

### **2.3 Mutagenesis of C-FABP gene and construction of C-FABPs transfection vectors**

A 436 base pair fragment of the protein coding region of C-FABP was amplified by RT-PCR from total mRNA isolated from PC-3M cells. The amplified C-FABP product was T-A cloned into a PGEM-Teasy plasmid and then transferred into pBluescript II SK vector as shown in Figure 2.1. Transformer<sup>tm</sup> Site-Directed Mutagenesis Kit was used to generate one or two point mutations to the C-FABP gene. The transformer mutagenesis strategy, as shown in Figure 2.2, can not only introduce single or multiple specific base mutations with high efficiencies (70-90%) but also has the advantage of avoiding subcloning and using single-stranded vectors or specialized double-stranded plasmids. Furthermore, the use of T4 DNA polymerase instead of PCR reduces the risk of generating spurious mutations.

First, the mutagenic primer and the selection primer containing a mutation in a restriction enzyme site were annealed to one strand of the denatured double-stranded plasmid.

Second, after DNA extension, ligation and a primary selection by restriction digest the mixture of mutated and unmutated plasmids is transformed into a *mutS E.coli* strain defective in mismatch repair.

Third, the DNA was isolated from pooled transformants and digested with the selective restriction enzyme.

Finally, the digested DNA was transformed into DH5 $\alpha$  bacterial cells and the mutated plasmid was recovered by midiprep extraction.

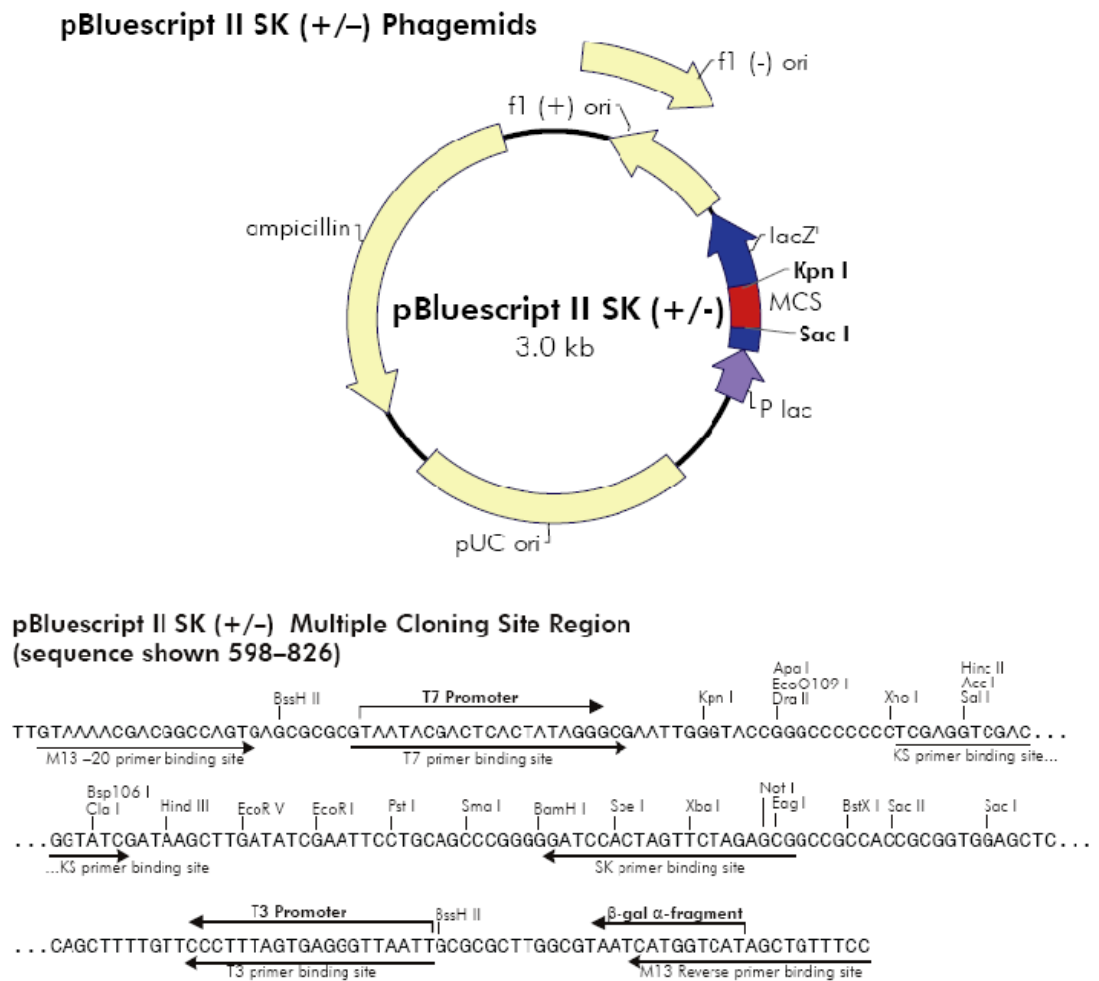


**Figure 2.1: Circular maps and lists of features for the pBluescript II SK vector**

The *pBluescript II SK* vector contains an ampicillin selection marker which is essential for Transformer site-directed mutagenesis kit because the bacterial strain *BMH 71-18 mutS* has a *Tn10* transposon and therefore is tetracycline resistant. The efficiency of the chosen restriction enzyme digestion has been examined at a low DNA concentration (0.1 µg/30 µl) before the mutagenesis assay procedure.

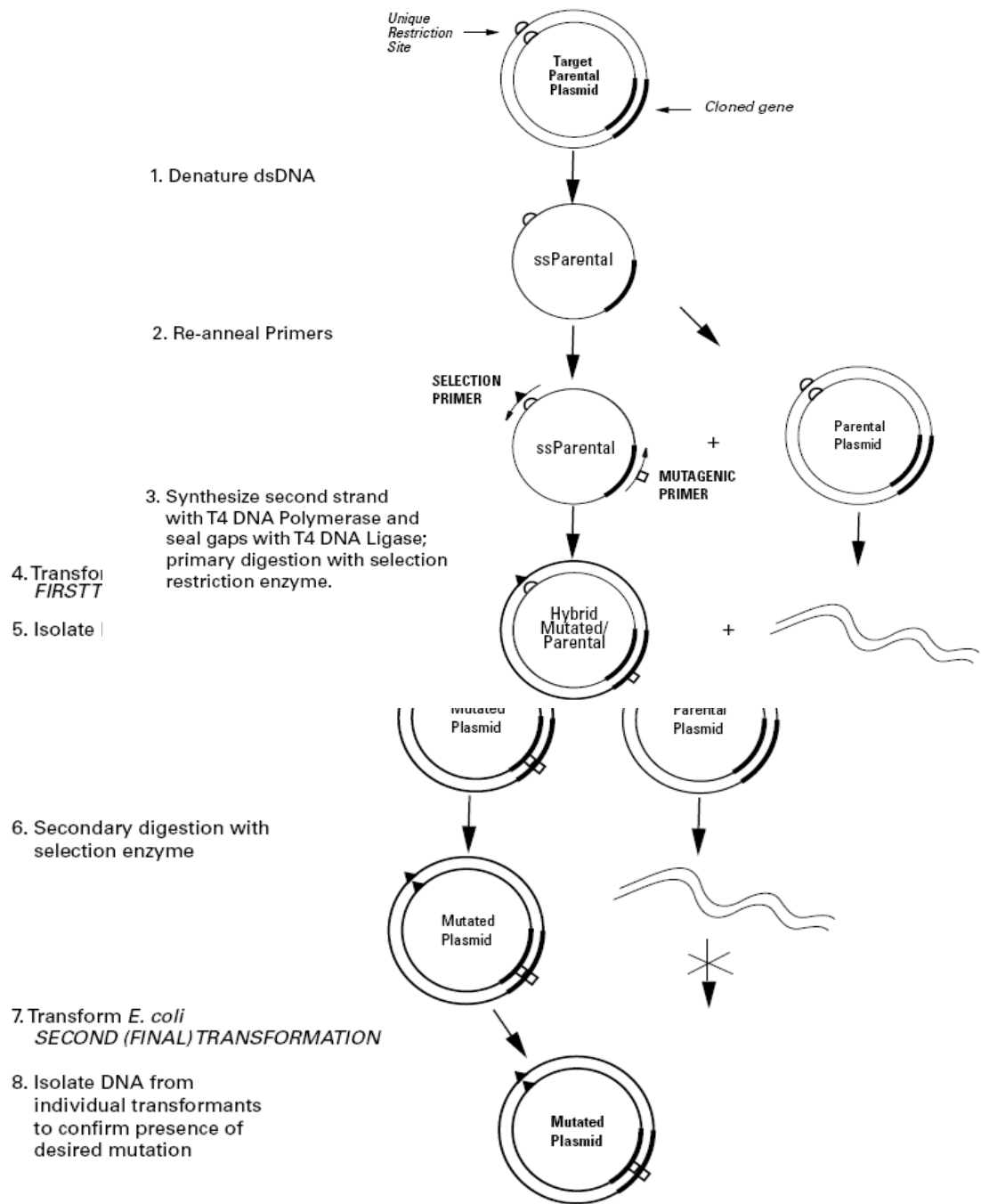


**Figure 2.2: Transformer site-directed mutagenesis strategy**

(The picture is taken from Clontech transformer site-directed mutagenesis kit user manual).

### 2.3.1 Selection and mutagenic primers

Selection primer: 5'- CAAGATCTCGATGGCGGTGGCG-3'

Mutagenic primer (R109A): 5'- CGTGTTATGTCGTTTTAACTTTC -3'

Mutagenic primer (R129A): 5'- GTGGACATGACGCTAGATAC -3'

The changed base pairs of the selection and mutagenic primers are underlined. All primers were synthesized with an incorporated 5' phosphate.

### 2.3.2 Generation of the mutant plasmid DNA

The primer/plasmid annealing reaction mixture was prepared with 2µl of 10x annealing buffer (200mM Tris-HCl pH7.5, 100mM MgCl<sub>2</sub>, 500mM NaCl), 0.1µg plasmid DNA, 2µl of 0.1µg/µl selection primer, 2µl of 0.1µg/µl mutagenic primer (the selection and mutagenic primers are listed in section 2.2.1.) and nuclease-free water (adjust to a total volume of 20µl). After denaturation at 100°C for 3 minutes, the reaction mixture was immediately placed on ice for 5 minutes. Then, the reaction mixture was supplemented with 3µl of 10x synthesis buffer, 1µl of T4 DNA polymerase (3units/µl), 1µl of T4 DNA ligase (2.84 WEISS units/µl), 5µl of nuclease-free water and incubated at 37°C for 2 hours to synthesize the mutant DNA strand. The reaction was stopped by heating at 70°C for 8 minutes and cool to RT.

### 2.3.3 Selection by restriction digestion

The DNA in synthesis/ligation mixture was ethanol precipitated (section 2.2.2) and resuspended in restriction enzyme digestion mixture with 0.5µl of *Not*I (20units/µl),



3µl of 10x NEBuffer3 and 26.5µl of nuclease-free water for primary selection. The reaction mixture was incubated at 37°C for 2 hours and heated at 70°C for 5 minutes to stop the digestion. Then, 11µl of the digested plasmid DNA was used to transform BMH 71-18 *mutS* competent cells (section 2.2). The mixed plasmid pool was isolated using miniprep (section 2.1.9) and digested with *NotI* restriction enzyme. The digested plasmid DNA was used to transform DH5α competent cells followed the same procedure as for the first transformation. The mutant DNA was recovered by miniprep or midiprep and the mutation was verified by directly sequencing the mutagenized region as previously described in section 2.2.1 The mutagenic primer (R109A) was applied to introduce single mutation and the double mutations were generated using both mutagenic primer (R109A) and mutagenic primer (R129A).

## 2.4 Cell culture

### 2.4.1 Routine cell culture

All routine cell culture manipulations took place in a tissue culture hood located in the Tissue Culture Laboratory. Cells were cultured in 75cm<sup>2</sup> cell culture flasks and maintained at 37°C in a humidified incubator which contains 5% (v/v) CO<sub>2</sub>. LNCaP cells were cultured in XGI1640 nutrient medium supplemented with 10% (v/v) Foetal calf serum (FCS), 2mM L-glutamine, 1mM Sodium pyruvate, 100IU penicillin/streptomycin (PEN-STREP), 5µg/ml 5-αdihydroxytestosterone and 5µg/ml hydrocortisone. LNCaP-C4<sub>2</sub> and 22RV-1 cells were cultured in XGI1640 nutrient medium supplemented with 10% (v/v) Foetal calf serum (FCS), 2mM L-

glutamine and 100IU penicillin/streptomycin (PEN-STREP). All routine culture media were replaced every alternate day.

#### **2.4.1.1 Thawing of cells**

Cryogenic vials of cells were defrosted in a water bath at 37°C and immediately transferred into a universal tube with 20ml of complete cell culture medium. The cells were then pelleted by centrifugation at 900xg lasting for 3 minutes. Then, the supernatant was discarded and the pellet was resuspended in a suitable volume of complete medium containing 10% FCS. Finally, cells were plated out in a 75cm<sup>2</sup> cell culture flask and maintained within a controlled atmosphere of 5% CO<sub>2</sub> at 37°C.

#### **2.4.1.2 Sub-culture of cell lines**

Cells cultured to approximately 70-80% confluence were passaged to allow continuous growth. Medium was completely removed from the flasks. Cell cultures were washed by phosphate buffered saline (PBS) and incubated at 37°C with 3.5ml of 2.5% (v/v) trypsin/versene solution for a period 4 minutes or until the cells had rounded up and were starting to detach from the culture dish. The trypsin/versene solution was inactivated by adding 10ml of complete medium. The cells were then transferred to a universal tube and centrifuged at 900xg for 3 minutes. The supernatant was removed and cells were resuspended in cell culture medium. The cells were aliquotted at the required concentration and maintained within a controlled atmosphere of 5% CO<sub>2</sub> at 37°C.

#### 2.4.1.3 Counting cells

The number of cells was calculated by using an improved Neubauer double counting chambers haemocytometer. Cells were detached as described previously. After thoroughly mixed, 10µl of cell suspension was loaded to a counting chamber of haemocytometer with 9 (3x3) squares. Then, cells were counted in four corner squares under the microscope. The total number of cells is calculated using the equation listed below:

Total number of cells = Average cell count per square x Dilution x  $10^4$  x Total volume (ml)

#### 2.4.1.4 Freezing cells

Cells were selected for freezing when they were approximately 70-80% confluence. Before freezing, the cell culture medium was replaced with fresh medium for 24 hours. The cells were detached as described in 2.4.1.2 and resuspended in 10ml of completed medium. Then, the total number of cells was counted as mentioned in 2.4.1.3. The cells were re-centrifuged at 900 xg for 3 minutes. The supernatant was removed and the cell pellet was broken up by repeated pipetting with freezing medium (Complete medium with 7.5% (v/v) DMSO) to give a concentration of  $1 \times 10^6$  cells/ml. Aliquots (1ml) of the cell suspension were pipetted into cryogenic vials and placed into a nalgene cryo-preserved box containing 250ml of isopropyl alcohol. The box stored in a freezer at  $-80^{\circ}\text{C}$  overnight before cryogenic vials transferred for long term storage in liquid nitrogen.

## 2.5 Cell transfection

### 2.5.1 Stable transfection of the LNCaP cell line using GeneJammer

A polyamine based method of transfection (GeneJammer) was used to insert pIRES<sub>2</sub>-EGFP into LNCaP cells. Prior to transfection, LNCaP cells ( $2 \times 10^5$ ) were seeded in a 6-well tissue culture plate and the cells were grown overnight in complete LNCaP culture medium to reach 50-70% confluence. In the mean time, 97  $\mu$ l of sterile, room temperature (RT), serum-free, antibiotic-free XGI medium was transferred to a 1.5ml eppendorf tube and supplemented with 3  $\mu$ l GeneJammer transfection reagent. After incubation for 5mins at RT, 2  $\mu$ g of DNA was added to the diluted GeneJammer transfection reagent and mixed gently. The mixture was incubated at RT for 30 minutes and added dropwise to the wells of the 6-well tissue culture plate. Then, the transfection mixture was distributed evenly by rock the plate back and forth. The control transfections were also performed as shown in Figure 2.3. After incubation in standard growth conditions for 48 hours, cells were split into 5 separate 9cm cell culture plate and cultured in selective medium containing 0.5mg/ml Geneticin for 10 days. The Geneticin was removed and the surviving transfected clones were allowed to recover in routine medium for one week.

<b>(A) Cell Control</b> No reagent No DNA	<b>(B) Reagent Control</b> 6 $\mu$ l reagent No DNA	<b>(C) DNA Control</b> No reagent 1 $\mu$ g DNA
<b>(D) 3:2 ratio</b> 3 $\mu$ l reagent 2 $\mu$ g DNA	<b>(E) 3:2 ratio</b> 3 $\mu$ l reagent 2 $\mu$ g DNA	<b>(F) 3:2 ratio</b> 3 $\mu$ l reagent 2 $\mu$ g DNA

**Figure 2.3: Three mock-transfection controls**

*Three mock-transfection controls were performed by putting cells through the transfection procedure without adding GeneJammer transfection reagent or DNA or both of them.*

### 2.5.2 Transfected clone selection by cell image

Cells were then re-cultured in selective medium for a further 3-4 weeks until the cells in control transfection died out and healthy cell clones had formed in the cell culture plate. As pIRES<sub>2</sub>-EGFP vector (Figure 2.4) contained the enhanced green fluorescent protein (EGFP) coding region, successfully transfected cell colonies with the expression of fluorescent marker were detected under a fluorescence microscope. Because the proportion of cells transfected within a population is relatively low (less than 10%), the ring cloning methodology was used to isolate colonies. For each batch transfectants, 5 colonies with best expression of EGFP were marked on the down-side of 9cm plate for ring cloning.

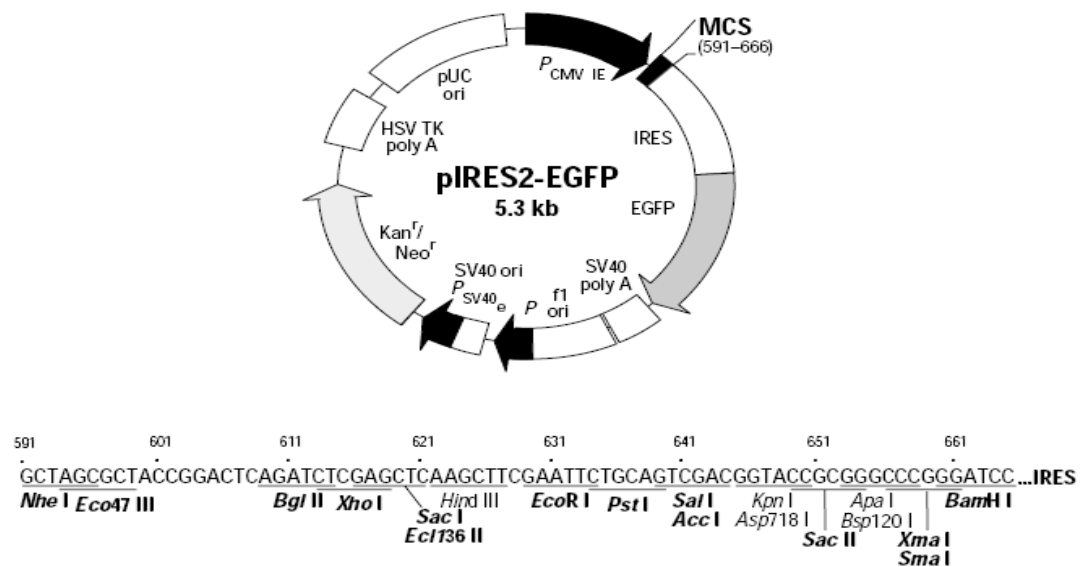


**Figure 2.4: Circular maps and lists of features for the pIRES<sub>2</sub>-EGFP vector**

(The vector map is taken from Clontech transformer site-directed mutagenesis kit user manual).

### 2.5.3 Ring cloning of transfected cells

The tops of 1ml pipette tips were cut to enlarge the cloning rings and sterilised by autoclaving. The selective medium from the transfectant plates was removed and the plates were washed with PBS. Using forceps, cloning rings were dipped in silicon grease and placed over the colonies. The small amount of silicon grease allowed the rings to adhere to the plate and formed a watertight seal around the colony. Then, 100µl of 2.5% (v/v) trypsin/versene solution was added to isolated colonies and incubated for 6 minutes or until the cells were rounded-up. The detached cells were transferred to a 1.5ml Eppendorf tube and the trypsin inactivated by adding an equal volume of routine cell culture medium. The cells were centrifuged for 3 minutes at

900xg. After remove of supernatant, the cell pellet was resuspended in 1ml selective culture medium containing 0.5mg/ml geneticin and plated into a 24-well plate and maintained within a controlled atmosphere of 5% CO<sub>2</sub> at 37°C.

## 2.6 Molecular cloning

Cloning technique is a powerful tool for the *in-vitro* studies of gene expression, structure and function. In this study, a fragment of the C-FABP-WT, C-FABP-R109A (single mutant) and C-FABP-R109/129A (Double mutant) were inserted into an expression vector. The vector-gene construct was transformed into the host *E.coli* cells for further manipulation of the C-FABPs fragments.

### 2.6.1 Phase 1:

#### 2.6.1.1 Cloning into pBluescript II SK (+/-) Phagemids

The pIRES2-CFABP-WT, pIRES2-CFABP-R109, C-FABP-R109/129A and pIRES2-EGFP (vector only) were inserted in to a plasmid vector, the vector used was pBluescript II SK (+/-) Phagemids supplied by Qiagen. The pBluescript II SK (+/-) Phagemids vector is circular and contains multiple unique restriction enzymes recognition sites as well as T7 and T3 promoters, the choice of promoter used to initiate transcription determines which strand of the insert cloned into the victor will be transcribed. The vector contains ampicillin and  $\beta$ -galactosidase resistance genes. The restriction map of the poly cloning region of the vector is shown in Figure 2.1. Ligation of the pIRES2-CFABP wild type and mutants into the pBluescript vector

and subsequent transformation of the *E.coli* bacteria cells were carried out according to the manufacturer's the QIAexpressionist (Qiagen, Duesseldorf, Germany) Figure 2.5. The molar ratio of vector insert used for the reaction was 10:1. The ligation reaction described in Table 2.4 was incubated overnight at 14°C. A self ligation reaction containing all the above components except for the pIRES2-EGFP (vector only) was used as a positive control. After completion of the ligation reaction mixtures were stored at -20°C until further use.

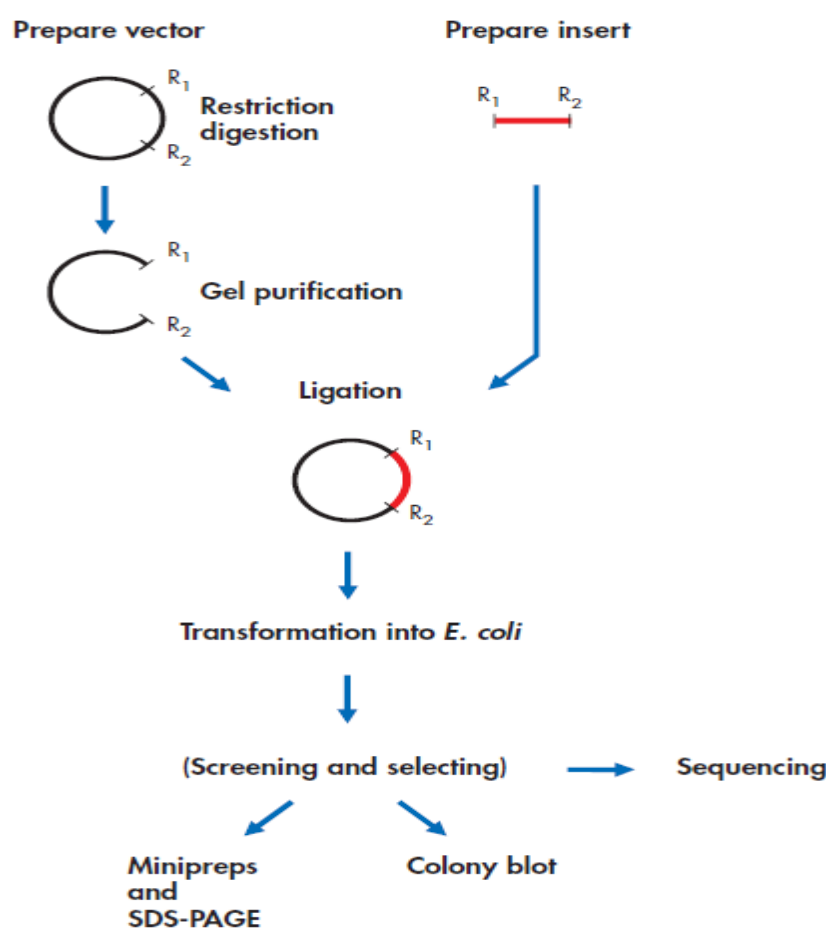


**Figure 2.5: Construction of QIAexpress expression vector.**

(The picture is taken from QIAexpress Ni-NTA Fast Start Handbook)

\* $R_1$  and  $R_2$ : restriction sites.



### 2.6.1.2 Ethanol precipitation of DNA

The DNA to be precipitated was mixed with 2.5 volumes of chilled state temperature absolute ethanol and 10% volumes of 3M sodium acetate (pH5.2). The mixture was mixed gently by inversion and incubated at  $-80^{\circ}\text{C}$  freezer overnight for DNA to precipitate. The precipitated DNA was pelleted by centrifuge at 16,000 xg at  $4^{\circ}\text{C}$  in a microcentrifuge for 20 mins. The supernatant was removed and the pellet was washed by 100 $\mu\text{l}$  of pre-chilled 70% (v/v) ethanol. The DNA was recentrifuged at 16,000xg at  $4^{\circ}\text{C}$  for 15 mins and the supernatant was decanted. The DNA was air dried and resuspended in sterile DEPC-treated water.

### 2.6.1.3 Restriction Enzyme digestion of plasmid DNA

Plasmid DNA was digested with two different restriction enzymes (*XhoI* and *PstI*) to check for the presence of insert and to produce DNA fragment for ligation. The restriction enzyme digest mixture was prepared as shown in Table 2.3.

	WT	Single Mutant (R)	Double Mutant (RR)	PBluescript
Water	13.5 $\mu\text{l}$	14.8 $\mu\text{l}$	13 $\mu\text{l}$	13 $\mu\text{l}$
10x NEBuffer 3	2.5 $\mu\text{l}$	2.5 $\mu\text{l}$	2.5 $\mu\text{l}$	2.5 $\mu\text{l}$
<i>XhoI</i> 20units/ $\mu\text{l}$	1 $\mu\text{l}$	1 $\mu\text{l}$	1 $\mu\text{l}$	1 $\mu\text{l}$
<i>PstI</i> 20units/ $\mu\text{l}$	1 $\mu\text{l}$	1 $\mu\text{l}$	1 $\mu\text{l}$	1 $\mu\text{l}$
DNA 1.5 $\mu\text{g}$	7 $\mu\text{l}$	5.7 $\mu\text{l}$	7.5 $\mu\text{l}$	7.5 $\mu\text{l}$

**Table 2.3: The restriction enzyme digestion mixture (total volume 25 $\mu\text{l}$ ).**

The restriction enzyme digest mixture was incubated at 37°C for 2 hours to allow complete digestion of the template DNA. Then, the enzyme reaction was inactivated by heating to 68°C for 10 minutes and the products were analysed by gel electrophoresis.

#### **2.6.1.4 Agarose gel electrophoresis of DNA**

Agarose gel electrophoresis was carried out in 1xTBE buffer (0.089M Tris-base, 0.089M Boric acid, 0.002M EDTA pH8.0). The agarose concentration of the gel was 0.8% to 2.0% (w/v) according to DNA size. The agarose was dissolved in 200ml of 1xTBE buffer by microwave heating for 2mins and cooled to 40-50°C. Then, 10µl of 500ng/ml ethidium bromide was added for visualisation. The gel mixture was poured and placed at 4°C to solidify. DNA samples were prepared by adding 5x agarose gel loading buffer (0.25% (w/v) bromophenol blue, 0.25% (w/v) xylene cyanol FF, 30% (v/v) glycerol in water) to a 1x concentration and loaded into the gel alongside DNA size marker. The gel was run for 50mins at 90V and visualised on a UV transilluminator.

#### **2.6.1.5 Purification of DNA from agarose gels**

DNA fragments were separated using agarose gel electrophoresis as described previously in section 2.5.1.4. The required fragments were visualised by ethidium bromide and excised using a sterile blade. Each excised gel slice was weighed and three times the volume of buffer QG was added. Then, the mixture was dissolved in a 50°C water bath for 10 mins with occasional vortex mixing. The melted agarose and DNA solution was applied to a QIAquick spin column and centrifuged for 1 minute

at 16,000 xg in a microcentrifuge and the flow through was discarded. The membrane, bound with DNA, was washed by passing through 750µl of buffer PE and re-centrifuged for a further minute to remove any residue. The DNA was eluted from the column by adding 30µl of distilled water and quantified as described above. The DNA was stored at -20°C until needed

#### **2.6.1.6 Calculation of insert/vector ratio**

The insert to vector molar ratio can have a significant effect on the outcome of a ligation and subsequent transformation step. Molar ratios can vary from a 1:1 insert to vector molar ratio to 10:1. In this study, 10:1 insert to vector molar ratio has been the most suitable according to formula below:

---

#### **2.6.1.7 DNA ligation**

Fragments of DNA were removed from pBluescript vector using restriction enzyme digestion as described in section 2.5.1.3 and inserted into transfection vector pIRES2-EGFP by ligation reaction using T4 DNA ligase. The ligation mixture was prepared as shown in Table 2.4.

	WT	R	RR
Insert DNA (180ng/ $\mu$ l)	9 $\mu$ l	9 $\mu$ l	9 $\mu$ l
Vector DNA ( 110ng/ $\mu$ l)	1 $\mu$ l	1 $\mu$ l	1 $\mu$ l
10x quick Ligation buffer	2 $\mu$ l	2 $\mu$ l	2 $\mu$ l
T4 DNA Ligase ( 400 cohesive end units	1 $\mu$ l	1 $\mu$ l	1 $\mu$ l
H <sub>2</sub> O	7 $\mu$ l	7 $\mu$ l	7 $\mu$ l
Total volume	20 $\mu$ l	20 $\mu$ l	20 $\mu$ l

**Table 2.4: The ligation reaction mixture**

*WT: C-FABP-WT, R: C-FABP-R109A and RR: C-FABP-R109/129A. Undigested pBluescript used as a control.*

After overnight incubation at 4°C, 5 $\mu$ l of ligation mixture was transformed into competent bacterial cells as described in section 2.5.1.8. The recombinant DNA was recovered from bacterial cells using a Qiagen miniprep or midiprep kit as described in section 2.5.1.9.

### 2.6.1.8 Transformation of competent bacteria with plasmid DNA

#### 2.6.1.8.1 Preparation of competent bacterial cells

*E.coli* (DH5 $\alpha$ ) glycerol stock was streaked onto LB-agar plate and incubated at 37°C overnight. On the following day, a single colony was inoculated into a conical flask containing 10mls LB broth and incubated at 37°C overnight with shaking at 225xg. Then, 1ml of overnight culture was transferred into 100ml of SOB medium (2% w/v

bactotryptone, 0.5% w/v yeast extract, 10mM NaCl, and 2.5mM KCl) and incubated at 37°C with shaking at 225xg until the OD550 reached 0.4. The culture solution was split into 8x 12ml aliquots and placed on ice to cool for 10mins. The DH5 $\alpha$  bacteria were pelleted by centrifuging at 2500xg for 10mins at 4°C and the supernatant was discarded. The bacterial cell pellets were resuspended in 8.25ml of pre-cooled RF1 buffer (100mM KCl, 50mM MgCl<sub>2</sub>·4H<sub>2</sub>O, 30mM KCl, 10mM CaCl<sub>2</sub> and 15% v/v glycerol, pH6.8) and incubated on ice for 10mins. After a further centrifuging at 2500xg for 10mins at 4°C, the cell pellet was resuspended in 2ml of RF2 buffer (10mM MOPS, 10mM KCl, 75mM CaCl<sub>2</sub>·2H<sub>2</sub>O and 15% v/v glycerol, pH6.8). The DH5 $\alpha$  bacteria solution was dispensed into 1ml aliquots in cryovials, frozen in liquid nitrogen and transferred immediately to -80°C for storage.

#### 2.6.1.8.2 Transformation

A vial of DH5 $\alpha$  competent cells was removed from the -80° C and thawed on ice. Then, 50ng of plasmid DNA or 10 $\mu$ l of the ligation mixture was added to 50 $\mu$ l of competent DH5 $\alpha$  cells, mixed by flicking gently and incubated on ice for 30mins. The cells were heat shocked at 42°C for exactly 90 seconds and placed on ice for a further 2mins followed by adding 800 $\mu$ l of SOC (2% w/v bactotryptone, 0.5% w/v yeast extract, 10mM NaCl, 10mM MgCl<sub>2</sub>, 10mM MgSO<sub>4</sub>, 2.5mM KCl, 20mM glucose) and incubated 37°C for 1 hour in a shaking incubator at 225xg. Transformed bacteria solution (200 $\mu$ l) was plated onto LB plates containing 50 $\mu$ g/ml ampicillin or 30 $\mu$ g/ml kanamycin for antibiotic selection and incubated at 37°C overnight. Finally, colonies were picked from the plate and grown in LB broth

containing antibiotic at 37°C, 225xg overnight and plasmid minipreps were conducted. Transformation efficiency was calculated (section 2.1.8.3).

#### **2.6.1.9 Isolation of plasmid DNA**

Plasmid DNA was isolated using Qiagen extraction kits.

##### **2.6.1.9.1 Miniprep extraction of plasmid DNA**

The overnight cultured bacteria (5ml) in LB medium containing antibiotic was harvested by centrifuging at 6,000xg for 1min and the supernatant was removed. The cell pellet was resuspended in 250µl of cell suspension buffer P1 (50mM Tris-HCl pH8.0, 10mM EDTA and 100µg/ml RNaseA) by vortexing, followed by adding 250µl of cell lysis buffer P2 (200mM NaOH and 1% w/v SDS) and mixed by gentle inversion of the microcentrifuge tube six times. Then, 350µl of neutralisation buffer N3 (4.2M Gu-HCl, 0.9M potassium acetate pH4.8) was added and mixed by gentle inversion of the microcentrifuge tube six times. The mixture was centrifuged at 13,000xg for 10 minutes and the supernatant was loaded to a miniprep spin column. The column was centrifuged at 13,000xg for 1min and the flow through discarded. The column was then washed by adding 750µl of wash buffer PE (10mM Tris-HCl pH7.5 and 80% ethanol) and centrifuged at 13,000xg for 1 minute. After removing the flow through, the spin column was centrifuged for an additional minute to remove residual wash buffer. The column was placed in a clean 1.5ml microcentrifuge tube and 30µl of distilled water was added to the centre. After 1 minute incubation at RT, the plasmid DNA was eluted by centrifuging at 13,000xg

for 1 minute. The concentration and quality of the DNA were examined as described in section 2.1.1 and isolated plasmid DNA was stored in a -20°C.

#### **2.6.1.9.2 Midiprep extraction of plasmid DNA**

A single colony of transformed DH5 $\alpha$  bacteria was transferred into flasks containing 10ml of LB medium with antibiotic and left to grow overnight at 37°C, 225xg. The overnight cultured bacterial cells (5ml) were then transferred to 200ml LB medium containing antibiotic and incubated for 5 additional hours at 37°C, 225xg. The transformed bacterial cells were harvested by centrifuging at 6,000xg for 10 minutes at 4°C and the supernatant was removed. The cell pellet was resuspended in 4ml of buffer P1 (50mM Tris-HCl pH8.0, 10mM EDTA, 100 $\mu$ g/ml RNase A) by vortexing until no clump remained. The bacterial cells were lysed by adding 4ml of lysis buffer P2 (200mM NaOH, 1% w/v SDS), gently mixed by six times inversion. After incubation at RT for 5 minutes, 4ml of pre-chilled P3 neutralising buffer (3.0M potassium acetate pH5.5) was added and the mixture was mixed by inverting six times, incubated on ice for 15 minutes and then centrifuged at 16,000xg, 11°C for 30mins. The supernatant containing plasmid DNA was transferred to a clean 30ml centrifuge tube and re-centrifuged at 16,000xg, 11°C for further 15 minutes. In the mean while, a Qiagen midiprep column was equilibrated by applying 4ml of equilibration buffer QBT (750mM NaCl, 50mM MOPS pH 7.0 and 15% v/v isopropanol) and allowed to empty by gravity flow. Once the Qiagen midiprep column was equilibrated, the cleared supernatant containing plasmid DNA was loaded into the column and allowed to flow under gravity. The column was washed

twice with 10ml of wash buffer QC (1.0M NaCl, 50mM MOPS pH 7.0, 15% v/v isopropanol) and the plasmid DNA was eluted from the column using 5ml of elution buffer QF (1.25 M NaCl, 50mM Tris-HCl pH 8.5, 15% v/v isopropanol). The eluted DNA was precipitated by adding 3.5ml of isopropanol, mixed and centrifuged at 4°C, 11,000xg for 30mins. The supernatant was carefully removed and the pellet was washed with 2ml of 70% (v/v) ethanol and centrifuged at RT, 11,000xg for 10mins. After removing the supernatant, the pellet was air-dried for 10 minutes and the plasmid DNA was then dissolved in 200µl of nuclease-free water. The concentration and quality of the DNA were examined as described in section 2.1.1 and the isolated plasmid DNA was stored at -20°C.

#### **2.6.1.10 cDNA sequencing**

Recombinant plasmid DNAs were sent for nucleotide sequencing at the Cogenics Technologies<sup>TM</sup> (Essex, UK), 100ng/µl (10µl) of each purified DNA was analysed. Appropriate primers were used according to Cogenics Technologies protocol. Sequence alignment was determined by using BioEdit for searching Genbank (BLAST).

### **2.6.2 Phase 2:**

#### **2.6.2.1 Cloning into pQE vectors**

The CFABP-WT, CFABP-R109A and C-FABP-R109/129A cDNAs were excised from pBluescript cloning vector and inserted into pQEs expression vector (pQE-30,



pQE-31 and pQE-32). The high-level expression of 6xHis-tagged proteins in *E.coli* using pQE vectors is based on the T5 promoter transcription-translation system. The pQE vectors are circular and contain 6xHis-tag coding sequence either 5' or 3' to the cloning region as well as T5 promoter (optimized promoter) and two *lac* operator sequences which increase *lac* repressor binding and ensure efficient repression of the powerful T5 promoter. The vector contains  $\beta$ -lactamase (*bla*) conferring resistance to ampicillin at 100 $\mu$ g/ml. The restriction map of the poly cloning region of the vector is shown in Figure 2.6. Ligation of the pBluescript-CFABP wild type and mutants into the pQE vectors and subsequent transformation of the *E.coli* bacteria (BL21) cells were carried out according to the manufacturer's the QIAexpressionist (Qiagen, Duesseldorf, Germany). The molar ratio of vector insert used for the reaction was 10:1. The ligation reaction described in Table 2.6 was incubated overnight at 14°C. A self ligation reaction containing all the above components except for the pQE (vector only) was used as a positive control. After completion of the ligation reaction mixtures were stored at -20°C until further use.

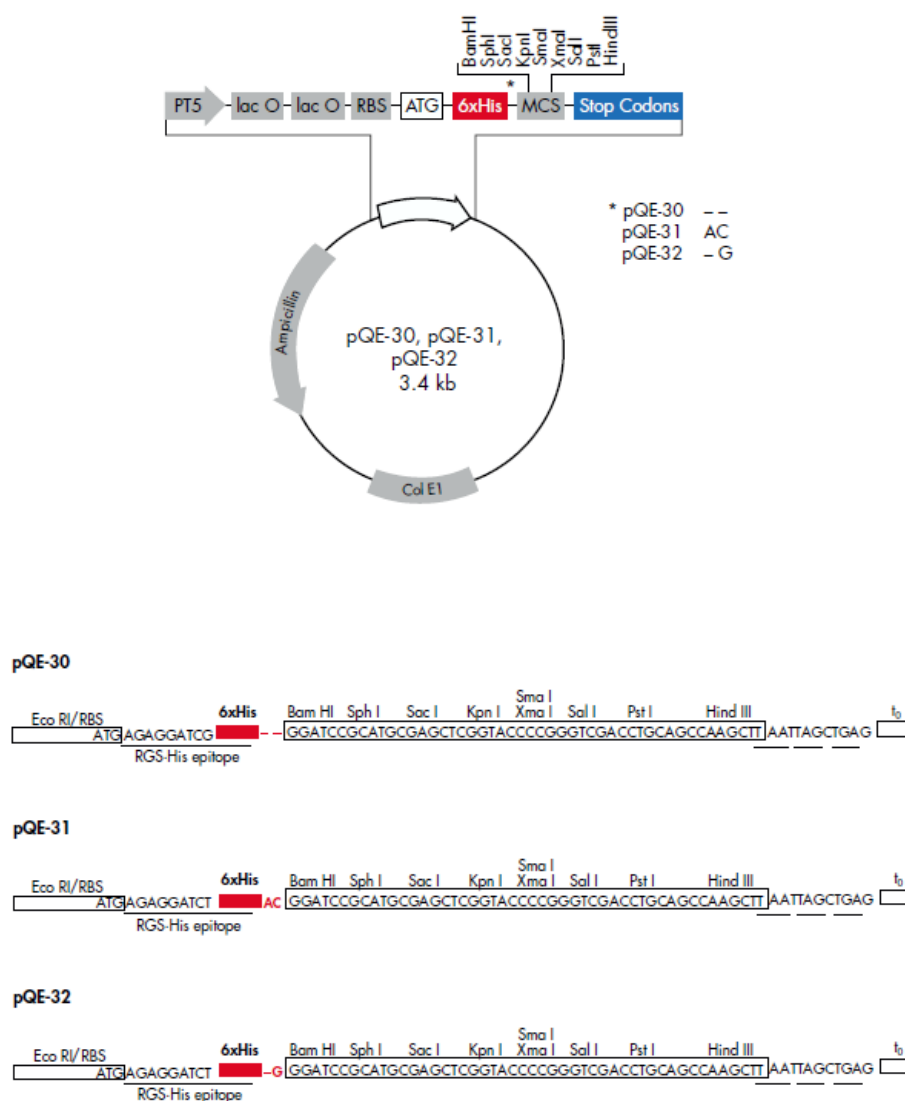


**Figure 2.6: PQE vectors for N-terminal 6xHis tag constructor.**

(The vector map is taken from *QIAexpress Ni-NTA Fast Start Handbook*) PT5: T5 promoter, lac O: lac operator, ATG: start codon, MCS: multiple cloning sites with restrictions site indicated.

### 2.6.2.2 Restriction Enzyme digestion of plasmid DNA

Plasmid DNA was digested with two different restriction enzymes (*Pst*I and *Kpn*I) to check for the presence of insert or to produce the DNA fragment for ligation. The restriction enzyme digest mixture was prepared as shown in Table 2.5.

	<b>pBlue-CFABP-WT</b>	<b>pQE-30</b>	<b>pQE-31</b>	<b>pQE-32</b>
Water	15µl	14.5µl	2.3µl	2.3µl
10x NEBuffer 1	3µl	3µl	3µl	3µl
<i>Kpn</i> I 20units/µl	1.5µl	1.5µl	1.5µl	1.5µl
<i>Pst</i> I 20units/µl	1.5µl	1.5µl	1.5µl	1.5µl
DNA 1.5µg	4µl	4.5µl	16.7µl	16.7µl

	<b>pBlue-CFABP-R109A</b>	<b>pBlue-CFABP-R109/129A</b>	<b>pQE-32</b>
Water	17µl	17µl	12µl
10x NEBuffer 1	3µl	3µl	3µl
<i>Kpn</i> I 20units/µl	1.5µl	1.5µl	1.5µl
<i>Pst</i> I 20units/µl	1.5µl	1.5µl	1.5µl
DNA 1.5µg	2µl	2µl	7µl

**Table 2.5: The restriction enzyme digestion mixture (total volume 25µl).**

The restriction enzyme digest mixture was incubated at 37°C for 2 hours to allow complete digestion of the template DNA. Then, the enzyme reaction was inactivated by heating to 68°C for 10 minutes and the products were analysed by gel electrophoresis.

### **2.6.2.3 Agarose gel electrophoresis of DNA**

Agarose gel electrophoresis was performed as described in section 2.6.1.4.

### **2.6.2.4 Purification of DNA from agarose gels**

DNA fragments were separated using agarose gel electrophoresis as described previously in section 2.6.1.5.

### **2.6.2.5 Calculation of insert/vector ratio**

The insert to vector molar ratio can have a significant effect on the outcome of a ligation and subsequent transformation step. Molar ratios can vary from a 1:1 insert to vector molar ratio to 10:1. In this study, 10:1 insert to vector molar ratio has been the most suitable according to formula below:

---

### 2.6.2.6 DNA ligation

Fragments of DNA were removed from pBluescript-CFABPs (wild type and mutants) vector using restriction enzyme digestion as described in section 2.5.2.2 and inserted into transfection vectors pQE by ligation reaction using T4 DNA ligase. The ligation mixture was prepared as shown in Table 2.6.

	WT	R	RR
Insert DNA	6µl	16µl	16µl
Vector DNA (PQE-30, 31 & 32)	2µl	2µl	1µl
10x quick Ligation buffer	2µl	1µl	2µl
T4 DNA Ligase ( 400 cohesive end units	1µl	1µl	1µl
H <sub>2</sub> O	9µl	-	-
Total volume	20µl	20µl	20µl

**Table 2.6: The ligation reaction mixture.**

*WT: wild type, R: Single Mutant and RR: double mutant. Undigested pBluescript used as a control.*

After overnight incubation at 4°C, 5µl of ligation mixture was transformed into competent bacterial cells as described in section 2.5.2.7. The recombinant DNA was recovered from bacterial cells using a Qiagen miniprep or midiprep kit as described in section 2.5.1.9.

### 2.6.2.7 Transformation of competent bacteria with plasmid DNA

#### 2.6.2.7.1 Preparation of competent bacterial cells

*E.coli* (BL21) glycerol stock obtained from Qiagen was streaked onto LB-agar plate and incubated at 37°C overnight. On the following day, a single colony was inoculated into a conical flask containing 10mls LB broth and incubated at 37°C overnight with shaking at 225xg. Then, 1ml of overnight culture was transferred into 100ml of SOB medium (2% w/v bactotryptone, 0.5% w/v yeast extract, 10mM NaCl, and 2.5mM KCl) and incubated at 37°C with shaking at 225xg until the OD<sub>550</sub> reached 0.4. The culture solution was split into 8x 12ml aliquots and placed on ice to cool for 10mins. The DH5α bacteria were pelleted by centrifuging at 2500xg for 10mins at 4°C and the supernatant was discarded. The bacterial cell pellets were resuspended in 8.25ml of pre-cooled RF1 buffer (100mM KCl, 50mM MgCl<sub>2</sub>·4H<sub>2</sub>O, 30mM KCl, 10mM CaCl<sub>2</sub> and 15% v/v glycerol, pH6.8) and incubated on ice for 10mins. After a further centrifuging at 2500xg for 10mins at 4°C, the cell pellet was resuspended in 2ml of RF2 buffer (10mM MOPS, 10mM KCl, 75mM CaCl<sub>2</sub>·2H<sub>2</sub>O and 15% v/v glycerol, pH6.8). The BL21 bacteria solution was dispensed into 1ml aliquots in cryovials, frozen in liquid nitrogen and transferred immediately to -80°C for storage.

#### 2.6.2.7.2 Transformation

A vial of BL21 competent cells was removed from the -80° C freezers and thawed on ice. Then, 50ng of plasmid DNA or 10μl of the ligation mixture was added to 50μl of competent DH5α cells, mixed by flicking gently and incubated on ice for 30mins. The cells were heat shocked at 42°C for exactly 90 seconds and placed on ice for a

further 2mins followed by adding 800µl of SOC (2% w/v bactotryptone, 0.5% w/v yeast extract, 10mM NaCl, 10mM MgCl<sub>2</sub>, 10mM MgSO<sub>4</sub>, 2.5mM KCl, 20mM glucose) and incubated 37°C for 1 hour in a shaking incubator at 225xg. Transformed bacteria solution (200µl) was plated onto LB plates containing 50µg/ml ampicillin and 25µg/ml kanamycin for antibiotic selection and incubated at 37°C overnight. Finally, colonies were picked from the plate and grown in LB broth containing antibiotic at 37°C, 225xg overnight and plasmid minipreps were conducted. Transformation efficiency was calculated as described in section 2.1.8.3.

#### **2.6.2.8 Isolation of plasmid DNA**

The isolation of plasmid DNA was conducted using extraction kits provided by Qiagen.

Miniprep and Midiprep extraction of plasmid DNA were examined as described in section 2.5.1.9.

#### **2.6.2.9 cDNA sequencing**

The recombinant plasmid DNAs were sent for nucleotide sequencing at the Cogenics Technologies<sup>TM</sup> (Essex, UK), 100ng/µl (10µl) of each purified DNA was analysed. Appropriate primers were used according to Cogenics Technologies protocol. Sequence alignment was determined by using BioEdit for searching Genbank (BLAST).

### 2.6.3 Expression and purification of recombinant C-FABP proteins

The expression and purification of C-FABP recombinant proteins conducted using QIAexpress Ni-NTA Fast Start kits provided by Qiagen (for purification and detection of recombinant 6xHis-tagged proteins).

#### 2.6.3.1 Growing *E. coli* and inducing expression

- Using a sterile toothpick, a single colony was picked from selective antibiotic LB agar plate and inoculated into a 10ml LB medium containing 50µg/ml ampicillin in a 50ml flask and incubated at 37°C overnight.
- 250ml of pre-warmed media with ampicillin was inoculated with 10ml of the overnight bacterial culture and grow at 37°C with vigorous shaking until an OD<sub>600</sub> of 0.6 was reached (30-60 minutes). 0.5ml sample was taken immediately before induction (this sample was the non-induced control).
- Expression was induced by adding IPTG (Isopropylthiogalactoside) (Appendix 1 & 2) to a final concentration of 1mM. A second 0.5ml was collected (this sample was the induced control).
- Culture was incubated for an additional 4 hours.
- Cells were harvested by centrifugation at 4000xg for 20 minutes.
- Cell pellets were stored overnight at -20°C until further use.

#### 2.6.3.2 Protein purification

Purification of 6xHis-tagged proteins under denaturing condition was conducted according to Ni-NTA Fast Start kits provided by Qiagen (Figure 2.7).



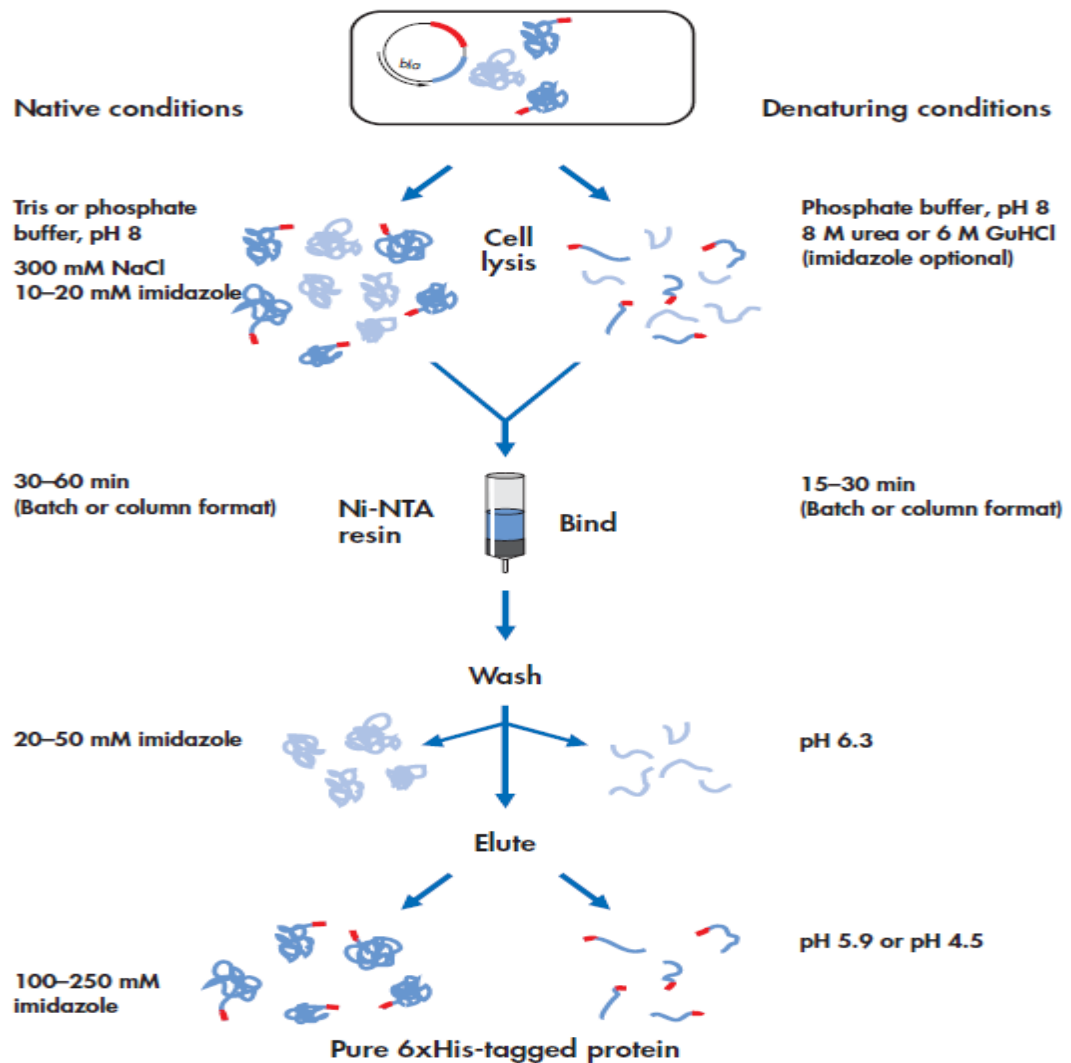


**Figure 2.7: purification of 6xHis-tagged proteins using QIAexpress.**

*(The picture is taken from QIAexpress Ni-NTA Fast Start Handbook)*

### Protocol

The material used for the purification process and solution preparations are summarised in Appendix 1 & 2.

Step 1	Cell pellets were resuspended in 10ml denaturing lysis buffer (pH 8.0)
Step 2	Cell suspensions were incubated at RT (15-25°C) for 60 min. After an hour cell suspensions were mixed 2-3 times by gently swirling the suspensions (lysis was completed when the suspension is translucent).
Step 3	Lysates were centrifuged at 14000xg for 30 min at RT to pellet the cellular debris (the supernatants contain the recombinant protein). 5µl 2x SDS-PAGE sample buffer was added to a 5µl aliquot of the supernatant and stored at -20°C for SDS-PAGE analysis
Step 4	The resin in a fast star column was gently resuspended by inverting it several times. The seal at the outlet of the column was broken, screw cap was opened, and the storage buffer allowed draining out.
Step 5	The cell lysate supernatants were applied to the column. The flow-through fractions were collected and 5µl 2x SDS-PAGE sample buffer was added to a 5µl aliquot of the flow-through fractions and stored at -20°C for SDS-PAGE analysis
Step 6	Columns were washed 2 times with 4ml of denaturing wash buffer (pH 6.3) and both wash fractions were collected. 5µl 2x SDS-PAGE sample buffer was added to a 5µl aliquot of each wash fraction and stored at -20°C for SDS-PAGE analysis
Step 7	Bound 6xHis-tagged proteins were eluted with 1ml aliquots of

	denaturing elution buffer (pH 4.5) and each elution fraction was collected in a separate tube. 5µl 2x SDS-PAGE sample buffer was added to a 5µl aliquot of each elution fractions and stored at -20°C for SDS-PAGE analysis
Step 8	All fractions were analysed by SDS-PAGE.

## 2.7 Analysis of protein expression using Western blot

### 2.7.1 Isolation of protein extracts from cultured cells

Cells were selected for protein isolation when they were grown to approximately 80% confluence. The cells were detached (section 2.4.1.3) and suspended in 10ml of completed medium to inactive the trypsin. Cells suspension was transferred to a 25 ml sterile universal tube and centrifuged at 900 xg for 3 minutes. The supernatant was decanted and the cells were washed with PBS which was removed by centrifuging. The cells was lysed by adding CelLytic-M reagent and incubated on a roller mixer for 15 minutes at RT ( $5 \times 10^6$  cells / 100µl). The mixture was transferred into a 1.5ml microcentrifuge tube and then centrifuged for 20 minutes at 10,000xg to pellet the cellular debris. The supernatant was harvested into a fresh microcentrifuge tube and the pellet was discarded.

### **2.7.2 Determination of protein concentration**

The concentration of protein extract was quantified using the Bradford dye-binding assay. The dye reagent was diluted 5-fold by adding distilled water (Bradford reagent: H<sub>2</sub>O = 1:4) and filtered through Whatman 540 paper. A concentration standard curve was created by measuring the absorbance (595nm) of a serial dilution of BSA standards (from 50µg/µl to 500µg/µl) after 20 minutes incubation with Bradford reagent. Protein samples were also diluted by PBS and incubation with Bradford reagent for 15 minutes before measuring the absorbance at 595nm. The sample concentration was calculated using the equation from established standard curve.

### **2.7.3 Equalization of protein samples for loading**

Protein samples were quantified before loading using Bradford dye-binding assay as described in section 2.7.2. Distilled water was added to samples to make sure an equal amount of total protein in all samples. After equalization 5x sample loading buffer was added and the protein samples were heated for 10 minutes, chilled on ice for 2 minutes and centrifuged before loading in to the SDS gel.

### **2.7.4 Sodium dodecyl sulphate polyacrylamide protein gel electrophoresis (SDS-PAGE)**

The apparatus used for SDS-PAGE was the Bio-Rad Mini Protein II cell (Bio-Rad Laboratories Ltd, UK). The 10.2cm x 8.3cm glass plate was placed on a clean dry surface. Two 0.75mm spacers were placed along the edges of the plate and the

10.2cm x 7.3cm plate was placed on top of the spacers so that it was flush with one end of the long plate. Plates were secured with the sandwich clamps and the assembled gel sandwich placed in the alignment slot of the casting stand ensuring that plates and spacers were flush at the bottom and that a good seal was obtained.

A 12.5% resolving gel was made by adding 10mls of Next Gel (Appendix 2) to 60 $\mu$ l of 10% ammonium persulphate (APS) and 6 $\mu$ l TEMED and the gel immediately poured using a glass pipette and an electric pipette filler (Drummond laser) until approximately the edge of the plastic comb. At this stage it was very important to pour the solution smoothly in order to avoid air bubbles. The 10 well x 0.75mm comb was immediately placed in the gel until all teeth were completely covered by the solution. The gel was allowed to polymerise for 40 minutes and the comb removed by slowly pulling it vertically upwards. The newly formed wells were then carefully rinsed with distilled water. The gel was released from the casting stand and inserted into the buffer chamber securely. Approximately about 500mls of running buffer (Appendix 2) were added to the chamber.

Five minutes before the loading gel was ready equal amounts of each sample protein along with a positive control were placed into separate thin walled Eppendorf tubes and lowered into heater. At the end of this period the samples were carefully loaded using a Hamilton microliter 700 series syringe, (Hamilton Company, Reno, USA) which was thoroughly rinsed with boiling water between each sample. Pre-stained electrophoresis standards of various molecular weights were added to the first well (Bio-Rad Laboratories Ltd, Herts, UK). The lid was placed on the lower buffer chamber, the cell connected to the BioRad power pack 200 (Bio-Rad Laboratories Ltd, Herts, UK) and electrophoresis was performed in 500ml 1x next gel running

buffer (25ml next gel running buffer and 500ml distilled water ) at 200 volts until the dye front had reached the end of the next gel.

### **2.7.5 Transfer of proteins from SDS gel to nitrocellulose membrane**

Separated Proteins were transferred from SDS gel to a nitrocellulose membrane using the BioRad mini trans-blot system. Six sheets of Whatman 3mm filter paper and the nitrocellulose membrane were cut according to the size of the SDS gel and soaked in 1x transfer buffer for 5 minutes. The cassette, with black side down, was placed on a tray containing transfer buffer and assembles the cassette in following order (from black side): a pre-wet fiber pad, three sheets of Whatman filter paper, equilibrated SDS gel, nitrocellulose membrane, three sheets of Whatman filter paper and another pre-wet fiber pad. The air bubbles were removed from each step using a glass roller. The transfer was performed at 100V, 4°C for 1.5 hours in pre-chilled 1x transfer buffer.

### **2.7.6 Coomassie blue and PONCAUS staining**

After transfer, the gel was stained with coomassie blue (Severn Biotech Ltd, UK) for an hour and washed with distilled water shaking slowly overnight, then dried using a vacuum gel-drier (Flowgen, Nottingham, UK) at 70°C for 4-5 hours.

After transfer, the membrane was stained with 10% PONCEUS solution (Sigma, USA) for 2 minutes and washed with TBST for 10 minutes to visualise the protein bands. Efficiency of the transfer was assessed through both staining methods.

### **2.7.7 Immunoblotting for detection of protein expression**

The nitrocellulose membrane containing the proteins was blocked with 10ml of 5% blocking solution (5g Milk dissolved in 100ml TBST) for an hour at room temperature on a gentle agitation to prevent non-specific binding of the primary antibody. The membrane was then incubated on a shaker with a primary antibody in an appropriate concentration (Table 2.7) at 4°C overnight. The following day, the membrane was washed with 1x T-TBS 4 times for 10 minutes each time to remove unbound primary antibody and incubated with a secondary antibody in an appropriate concentration (Table 2.7) for an hour at room temperature. Then, the membrane was washed with 1x T-TBS 4 times for 10 minutes each time again. The probed antigens on the membrane were visualized by incubation in ECL reagents (2ml of Reagent A was mixed with 50µl of solution B) for 5 minutes at room temperature. Chemiluminescent images were recorded on Kodak films with 0.5-10 minute's exposure. The films were developed and fixed in the dark room.

Target Protein	Primary Antibody	Secondary Antibody
C-FABP	Monoclonal Rabbit Anti-human C-FABP (1:500) (Hycult <sup>R</sup> Biotech)	Polyclonal Swine Anti-rabbit Immunoglobulins/HRP (1:5000) (Abcam)
6xHis-tagged protein	Penta-his antibody Binding (1:1000) (Qiagen)	Polyclonal Swine Anti-rabbit Immunoglobulins/HRP (1:5000) (Abcam)
$\beta$ -Actin	Monoclonal Mouse Anti- $\beta$ -Actin (1:5000) (Abcam)	Polyclonal Rabbit Anti-mouse Immunoglobulins/HRP (1:20000) (Abcam)

**Table 2.7: Primary and secondary antibodies used in Western blot.**

### 2.7.8 Immunoblotting for detection of $\beta$ -actin expression

Consistently expressed  $\beta$ -actin antibody was used to normalise any loading variations.

After target protein expression detection by ECL, the membrane washed in 1x T-TBS, agitated overnight. Then the membrane was incubated in 10ml of 5% blocking solution for 30 minutes before incubation with  $\beta$ -actin antibody in a 1:5000 dilution for 30 minutes at room temperature. This was followed by three washes with 1x T-TBS for 10 minutes each then the secondary antibody was added and incubated for



30 minutes at room temperature in 1:20000 dilution. Blots were washed three times with 1x T-TBS again and bound  $\beta$ -actin probes were visualised using the advanced ECL detection system.

To standardize the loading difference, the level of  $\beta$ -actin expression was examined. The expression level (EL) of each target protein was calibrated using the formula listed below:

## 2.8 Total RNA isolation

Total RNA was isolated from cultured cells using the RNAeasy Mini Kit. Two 75cm<sup>2</sup> flasks cells were cultured to 70-80% confluence and harvested as described in section 2.4.1.2. The cells were washed with PBS which was removed by centrifuging at RT, 900xg for 3 minutes and 350 $\mu$ l buffer RLT containing 3.5 $\mu$ l  $\beta$ -Mercaptoethanol was added to lyse the cells. The cell lysate was then homogenised by centrifuging through a PrepEase filter unit at 16,000xg for 1 minute and precipitated in one volume of 70% ethanol. The resulting solution was transferred to an RNAeasy mini column sitting in a 2ml collection tube and centrifuge for 30 seconds at 11,000xg. The column was then washed by 700 $\mu$ l buffers RW1 and twice with 500 $\mu$ l RPE buffer by centrifuging at 11,000xg for 30 seconds. The RNeasy spin column was centrifuged again at 16,000xg for 1 minute to eliminate any carryover buffer. After 30 $\mu$ l of RNase free water was added, the RNeasy spin column was

incubated at RT for 1 minute. Finally, the total RNA was eluted by centrifuging the column for 1 minute at 16,000xg. The total RNA yield and purity was determined by NanoDrop ND-1000 spectrophotometer as mentioned in section 2.2.1.

## **2.8.1 Reverse transcription polymerase chain reaction**

### **2.8.1.1 First strand cDNA synthesis**

First strand cDNA was synthesized using total RNA isolated from LNCaP cells as described in section 2.7. Total RNA (3µg) was mixed with 1µl of 50µM Oligo (dT)<sub>20</sub> primer and 2µl of dNTP mixture (10mM each dATP, dCTP, dGTP, dTTP at neutral pH). After the volume was adjusted to 13µl with nuclease-free water, the mixed solution was incubated at 65°C for 5 minutes and chilled on ice for 1 minute. Then, the solution was mixed with 4µl of 5x first strand buffer, 1µl of 0.1M DTT, 1µl of RNaseOUT (40units/µl) and 1µl of SuperScriptIII reverse transcriptase (200units/µl). The reaction mixture was incubated at 50°C for one hour, followed by incubation at 70°C for 15 minutes to inactivate the reaction. The First strand cDNA was used as a template for amplification.

### **2.8.1.2 Polymerase chain reaction**

Polymerase chain reaction (PCR) was performed to amplify a specific region of the DNA template. The forward and reverse primers for C-FABP are listed as below:

Forward primers sequence: 5'- ACCATGGCCACAGTTCAGCA -3'

Reverse primers sequence: 5'- CCTGTCCAAAGTGATGATGGAA -3'

The DNA template was amplified in a total volume of 50 $\mu$ l reaction mixture as shown in Table 2.8.

DNA template	50-200ng
10x PCR buffer	5 $\mu$ l
MgCl <sub>2</sub> (25mM)	3 $\mu$ l
Forward primer (10 $\mu$ M)	1 $\mu$ l
Reverse primer (10 $\mu$ M)	1 $\mu$ l
dNTPs mixture (10mM each)	1 $\mu$ l
<i>Taq</i> polymerase ( 5U / $\mu$ l)	1 $\mu$ l
Nuclease-free water	Up to 50 $\mu$ l

**Table 2.8: PCR mixture**

The reaction was incubated in a thermal cycler at 95°C for 5 minutes, followed by 35 cycles of PCR amplification, each cycle consisting of denaturing: 95°C for 30 seconds; annealing: 55°C for 45 seconds; extension: 72°C for 1 minute, followed by one cycle incubation at 72°C for 5 minutes and then maintained the reaction at 4°C. PCR amplification products were analysed by agarose gel electrophoresis and purified as previously described in section 2.2.3 and 2.2.4.

### 2.8.1.3 Real-time PCR

The real-time PCR, also known as quantitative real time polymerase chain reaction (qPCR), was applied in order to quantify the level of C-FABP mRNA in the transfected LNCaP cells. Traditional PCR or RT-PCR uses agarose gel electrophoresis for detection of amplified DNA fragments at the end of the reaction. However, real-time PCR is designed to collect data in the exponential growth phase when the reaction is in progress, which significantly increased the accuracy for DNA and RNA quantitation compare to the traditional PCR or RT-PCR.

Several methods exist for real-time quantitation of amplification products, including fluorescence resonance energy transfer techniques using fluorescently labelled molecular beacons, SYBR Green I. During the PCR amplification, the fluorescence of SYBR Green I increases 100- to 200-fold when bound to double stranded DNA as presented in Figure 2.8. The number of amplicons generated is directly proportional to the increase in reporter fluorescent signal which was detected at the end of the elongation step of the PCR reaction by Chromo4 fluorescence detector.

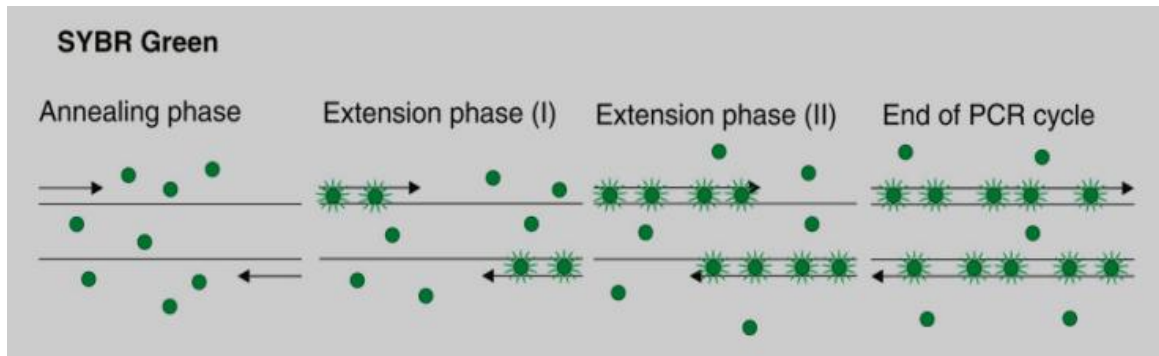


**Figure 2.8: SYBR Green Dye binds to the double stranded DNA and fluoresces**

#### 2.8.1.3.1 Real-time PCR primer design

The real-time PCR primers were designed spanning exon-exon junctions of C-FABP gene in order to avoid amplifying any genomic DNA contamination. The size of PCR amplicon was limited to between 50bp to 200bp and the primers self complementarity and hair pins was also checked as SYBR Green Dye bound to all double stranded PCR products, including non-specific PCR products. Similarly, the house-keeping gene,  $\beta$  actin primers were designed as listed below:

Real-time PCR primers for C-FABP

Forward primers sequence: 5'- CATTGGTTCAGCATCAGGAG -3'

Reverse primers sequence: 5'- TTCATGACACACTCCACCACT -3'

Real-time PCR primers for  $\beta$  actin

Forward primers sequence: 5'- CTGGTGCCTGGGGCG -3'

Reverse primers sequence: 5'- AGCCTCGCCTTTGCCGA - 3'

### 2.8.2 Relative real-time PCR

The total RNAs were extracted from each cell line using RNAeasy Mini Kit as described in section 2.8 and reverse transcribe 1µg of total RNA to cDNA using SuperScriptIII reverse transcriptase as mentioned in section 2.8.1.1. The real-time PCR mixture for both C-FABP and  $\beta$  actin was prepared with 5µl of 2× Brilliant SYBR Green qPCR master mix (containing SureStart Taq DNA polymerase, dNTPs mixture, MgCl<sub>2</sub> and optimized buffer), 1µl of forward primer, 1µl of reverse primer, 1µl of cDNA generated by reverse transcription and 2µl of nuclease-free water. After gentle mix, the reactions were centrifuged briefly and placed to a real-time PCR thermocycler. The real-time PCR program is listed in Table 2.9.

	Temperature	Time
Step1 Denaturation	95°C	15mins
Step2 Denaturation	94°C	15 seconds
Step3 Annealing	60°C	30 seconds
Step4 Extension	72°C	30 seconds
Step5 Plate reading	57°C	15 seconds
Step6 Go back to step 2 and repeat 38 cycles		
Step7 Final extension	72°C	10mins
Step8 Melting curve	65-95°C	1°C increment for 10mins

**Table 2.9: Real-time PCR program for amplification of short target DNAs (50-400bp)**

### 2.8.2.1 Relative quantitation analysis

Melting curve analysis was performed to detect the presence of nonspecific products and the primer dimers. The relative fold differences of C-FABP mRNA between transfected cell lines and parental cell line LNCaP were obtained using the formula listed below (Pfaffl, 2001) :

$$\text{Relative fold difference} = 2^{-\Delta\Delta C_t}$$

$\Delta C_t$  was calculated as the average  $C_t$  for the gene of interest minus the average  $C_t$  for the house keeping gene,  $\beta$  actin.

$\Delta\Delta C_t$  was calculated as the  $\Delta C_t$  of the test sample minus the  $\Delta C_t$  of the calibrator sample

## 2.9 Fatty Acid Binding Assay

In order to monitor the fatty acid-binding activity, the fatty acid dissociation constant of three recombinant C-FABP proteins was determined by following the changes in fluorescence by increasing the concentration of fluorescent fatty acid analogue 11-(dansylamino) undecanoic acid (DAUDA) (Hagan *et al*, 2008). The excitation wavelength used for DAUDA was 345 nm. A stock solution of 10mM DAUDA in ethanol, kept in the dark at  $-20^{\circ}\text{C}$ , was freshly diluted in PBS to 1mM or 0.1mM before use in fluorescence experiments. The protein concentration was 2 $\mu\text{M}$  in 1ml of PBS at  $20^{\circ}\text{C}$ . Fluorescence data were subtracted for the blank values (sample without proteins) and fitted by standard non-linear regression techniques (ORIGIN

software version 6.1, Origin Lab Corporation, MA) to a single non-compatible binding model to estimate the apparent dissociation constant ( $K_d$ ) and maximal fluorescence intensity ( $F_{max}$ ). Competitive experiments were designed to reveal a possible difference in affinity of the three C-FABP proteins for the various natural fatty acids. The myristic, palmitic, oleic and linoleic acids were stored and diluted as described above for DAUDA. In these experiments, the binding of 2 $\mu$ M DAUDA to 2 $\mu$ M proteins was performed in the presence or absence of 2 $\mu$ M of each fatty acid.

## 2.10 Fatty acid uptake assay

Fatty acid uptake assay was designed in order to test long chain fatty acid (LCFA) uptake kinetics in different LNCaP cells containing fatty acid transporters. Conventional protocols utilizing radioactivity often require cell lysis and processing at very low temperature. Whereas, uptake of fluorescently-labelled fatty acids requires neither radioisotope usage nor cell lysis and also the fluorescence intensity in each individual cell can be measured by flow cytometry precisely. The red fluorescence-labelled LCFA, BODIPY 558/568C<sub>12</sub> (4, 4-difluoro-5-(2-thienyl)-4-bora-3a, 4a-diaza-s-indacene-3-dodecanoic acid), was used as the analogue of natural LCFA in the fatty acid uptake assay. BODIPY analogue behaves much like natural fatty acids: it becomes activated by acyl-CoA attachment; is incorporated into triglycerides; and accumulates in intracellular lipid droplets. In addition, the BODIPY analogue is also known as the substrate for fatty acid transporters since its uptake by adipocytes and can be competed by natural LCFA.



Cultured cells ( $1 \times 10^5$  cells, already treated by  $15 \mu\text{M}$  recombinant C-FABPs) in 2ml routine culture medium were seeded into 6-well plates and incubated at  $37^\circ\text{C}$ , 5%  $\text{CO}_2$  overnight. After replacing the medium with 2ml of solution containing  $25 \mu\text{g}$  BODIPY 558/568C<sub>12</sub> in  $200 \mu\text{m}$  BSA/PBS, the cells were incubated for 30 minutes at  $37^\circ\text{C}$ , 5%  $\text{CO}_2$ . The fatty acid uptake was stopped by removal of BODIPY fatty acid solution followed by addition of 3ml of an ice-cold stop solution (PBS containing 0.5% BSA). The stop solution was discharged after 2 minutes and the culture plates were washed another two times by fresh ice-cold stop solution. Then, cells were detached using 2.5% (V/V) trypsin/versene at  $4^\circ\text{C}$  and the fluorescence intensity of each cell line was measured with an EPICS XL Cytometer at the wave length of 570 nm to assess the fatty acid uptakes.

## 2.11 Cell proliferation assay

Proliferation is an important biological process for maintaining cell growth and tissue homeostasis. Cell growth is defined as the increase in cell number that occurs as the net number of cells gained by proliferative activity and offset by the net cell loss by apoptosis and necrosis. Cell proliferation results from the action of the cell cycle. Includes interphase (G1, S and G2 phases) and mitosis phases (M). Proliferative activity (Pich *et al*, 2004) defines the rate of the cell cycle, and represents the relation between cell generations time (T) and the cells committed to the cycle such as the growth fraction time (G). High proliferative activity can be the result of either a high growth fraction or a short generation time.

### 2.11.1 Preparation of growth curve

LNCaP, LNCaP-C4<sub>2</sub> and 22RV-1 cells were grown to 70-80% confluence in 175cm<sup>2</sup> flasks and harvested as previously outlined and resuspended in 10ml of complete culture medium. Each cell line was counted using a hemocytometer as previously mentioned in section 2.3.1.3 and was made up in 5x10<sup>5</sup>/ml in 4mls of complete culture medium. A standard growth curves was prepared in serial dilution at: 6.25x10<sup>3</sup>/ml, 1.25x10<sup>4</sup>/ml, 2.5x10<sup>4</sup>/ml, 5x10<sup>4</sup>/ml, 1x10<sup>5</sup>/ml, 2.5x10<sup>5</sup>/ml and 5x10<sup>5</sup>/ml. Then, 200µl of cell suspension from each dilution was plated into a 96-well plate in triplicate. Each cell line requires its own standard curve.

In the mean time, two sets of cells for proliferation assay were also prepared at the concentration of 5x10<sup>4</sup>/ml. Similar as preparation of standard curve;

Cell suspensions were treated with 15µM recombinant C-FABP wild type and mutants only.

Cell suspensions were treated with 15µM recombinant C-FABP wild type and mutants and further stimulated with 10µM of Myristic acid (natural fatty acid).

All suspensions were plated into six separate 96 well plates in triplicate. After overnight incubation with 5% CO<sub>2</sub> at 37°C, the cell growth of the standard curve and first experimental day analysed by the MTT assay as described in section 2.11.2. The cell proliferation assay was set to run for six days at each plate per day.

### 2.11.2 Assessing cell numbers using MTT assay

MTT is a yellow coloured chemical and it entered into the mitochondria of the cells. In mitochondria, MTT is oxidised into an insoluble blue dye known as formazan which forms blue crystals in the cytoplasm. The crystals are dissolved by adding DMSO and leave a coloured liquid, which is directly proportional to the number of cells present. The optical density (OD) of the cell population colour is measured accurately with a Multiscan plate reader at 570nm. For each cell line, a standard curve was constructed by plotting OD (570nm) against the number of cells. The cell number of the test samples was determined from the standard curve.

MTT stock solution is prepared at a concentration of 5mg/ml (100mg MTT in 20ml PBS) and stored at 4°C. At each time point (every 24 hours), 50µl of MTT stock solution was added to each well in a 96-well plate and the cells were incubated at 37°C, 5% CO<sub>2</sub> for 4 hours. The cell culture medium and MTT is removed gently to avoid disturbing cells followed by adding 200µl of DMSO to each well including blank control wells mixed by pipetting up and down. The plate was incubated for a further 10 minutes at 37°C, 5% CO<sub>2</sub> and read at 570nm in the optical density plate reader. The growth rate for each cell line is quantified against the standard curve to obtain the number of cells/well in each day for six days. Graphs of cell number/time were plotted.

## 2.12 Cell migration assay in Boyden chamber system

The Boyden chamber system was used to examine the difference in invasive ability in cell lines stimulating by wild-type and mutant C-FABPs. The results are often variable, as many factors are involved in the assay, including the number of cells added to the upper chamber, the duration of the assay and the way to measure the number of the cells (Kassis *et al*, 1999). Therefore, it is important for the system gives reproducible results by setting up an optimized procedure considering the variables mentioned above. All materials used in this section can be found in Appendix 1 and 2.

Cells to be used in invasion assay were cultured in flasks until 70-80% confluent. Cell invasion assays performed out using a modified Boyden chamber system. Wells of the 24-wells plate were divided into upper and lower compartment by 6.5mm diameter polycarbonate membrane containing 8µm pores. The polycarbonate filters were wetted with 200µl XGI medium for 30 minutes and the medium was removed followed by adding further 100µl XGI medium containing 30µg of matrigel to the upper side of the filters. The plates were incubated at 37°C, 5% CO<sub>2</sub> for 2 hours to allow the matrigel solidification. The assays were set up with 1x10<sup>5</sup> cells in the upper compartment in 200µl of 2% (v/v) FCS growth medium, 500µl of 10% (v/v) FCS growth medium and 10µM natural fatty acid (Myristic acid) was placed to the lower chamber. After 24 hours incubation at 37°C, 5% CO<sub>2</sub>, the cells remaining in the upper side of the filters were removed gently by cotton swabs and the cells attached to the lower side of the filter were fixed and stained by crystal violet reagent. None

of cell was found in lower compartment indicated that all cells invaded through the matrigel coated filter were attached to the lower side of the filter. The numbers of the invaded cells were counted under microscope. The results were finally normalized by the cell number in the 24-well plate after 20 hours incubation because the cells after trypsinisation may vary in viability. In this way, the cell motilities measured from different cell lines were more comparable. The results are the mean  $\pm$  SD of three separate experiments.

### 2.13 Soft agar assay

Soft agar assay was designed in order to examine the tumorigenicity of each cell lines in anchorage-independent environment. To perform the assays, 2g of low-melting agarose was added to 100ml of distilled water to make-up final concentration 2% ( $^{W/V}$ ). The low melting agarose was sterilized by autoclaving and placed in a water bath at 45°C to prevent agarose from solidifying until required. The assay was carried out in 6-well plates which were pre-coated with 2ml of 2% (w/v) low melting point agarose in routine culture medium with 10% (v/v) FCS and the mixture solidified in refrigerator at 4°C for 10mins. LNCaP, LNCaP-C4<sub>2</sub> and 22RV-1 cells were routinely grown to 70-80% confluent in flasks, detached and counted as previously described in section 2.4.1.2 and 2.4.1.3. Cells were washed once by centrifugation and resuspended in routine culture medium with 10% (v/v) FCS at the concentration of  $2 \times 10^4$ /ml. Two sets of cell suspensions were prepared:

Cell suspensions were treated with 15 $\mu$ M recombinant C-FABP wild type and mutants only.

Cell suspensions were treated with 15 $\mu$ M recombinant C-FABP wild type and mutants and further stimulated with 10 $\mu$ M of Myristic acid (natural fatty acid).

The cell suspensions were mixed with 2% low melting point agarose in a ratio of 1:1 and 2ml of mixtures were seeded to the pre-coated wells to make the final cell concentration at  $1 \times 10^4$  per well. The plates were placed at 4°C until solidified. Once the top layer was set, the 6-well plates were placed in the incubator at 37°C, 5% CO<sub>2</sub> for 4-6 weeks. During this period, 2 drops of routine culture medium were added to each well twice a week to keep the soft agar moist. At the end of the soft agar assay, colonies were dyed by adding 2ml of MTT (5mg/ml) followed by incubation at 37°C, 5% CO<sub>2</sub> for 2 hours. Colonies larger than 150 $\mu$ m in diameters were counted by the GelCount.

## 2.14 Statistic methods

The Student's t-test is the most commonly used method to evaluate the differences in averages between two groups. In this thesis, the Student's t-test was used to compare any differences observed between each experimental group and the control group. The results from most of assays were statistically assessed using the Student's t-test. For all Students's t-test calculated by online calculator (<http://www.graphpad.com/quickcalcs/ttest1.cfm>), the *P*-value less than 0.05 was regarded as statistical significance.

The fatty acid binding assay, fluorescence data were subtracted for the blank values (samples without proteins) and fitted by standard non-linear regression techniques (ORIGIN software version 6.1, Origin Lab Corporation, MA) to a single non-competitive binding model to estimate the apparent dissociation constant ( $K_d$ ) and maximal fluorescence intensity ( $F_{max}$ ).

### **3 Generation of mutation in C-FABP cDNAs and Transfected them into LNCaP prostate cancer cells**



### 3.1 Introduction

Cutaneous fatty acid binding protein (C-FABP) is a FABP family member binding to long chain fatty acids with high affinity. *C-FABP* was identified by our research group as a gene involved in malignant progression of prostate cancer and able to promote the growth of primary tumours and induce metastasis when transfected into rat benign Rama 37 model cells (Jing *et al*, 2000). Further, it was demonstrated that C-FABP was a prognostic marker for patient outcome and a target of tumour-suppression for prostate cancer (Adamson *et al*, 2003).

Several studies indicated that C-FABP might promote the malignant progression of prostate cancer by up-regulating the expression of the gene for vascular endothelial growth factor (VEGF), a potent factor for angiogenesis which is essential for growth and expansion of solid tumours (Adamson *et al*, 2003; Chen *et al*, 2000; Jing *et al*, 2001). However, the mechanism by which C-FABP up-regulates the expression of VEGF remains unclear. Since the common biological function of FABPs, including C-FABP, is to transport the intracellular fatty acids into cells, therefore it is interesting to know whether the tumorigenicity-promoting function of C-FABP is related to its activity of transporting fatty acids. It has been confirmed that there are three key amino acids (Arg<sup>109</sup>, Arg<sup>129</sup>, and Tyr<sup>131</sup>) of C-FABP, which are highly conserved amongst the FABP protein family, and which are responsible for binding to the carboxylate group in the fatty acids (Vorum *et al*, 1998). Mutation of one or two of the three key amino acids would either partially or completely deprive of C-FABP fatty acid-binding ability.

In order to investigate whether binding to fatty acids is essential for C-FABP to promote cancer malignant progression, one and two site-directed point mutations were introduced to the C-FABP cDNA region which contains the fatty acid-binding motif. The mammalian expression vector pIRES2-EGFP containing wild type and mutated C-FABP cDNAs were transfected respectively into the LNCaP prostate cancer cells, which did not express C-FABP prior to the transfection, to establish cell lines expressing wild type C-FABP and mutated C-FABPs

## 3.2 Results

### 3.2.1 Generation of mutations in *C-FABP* cDNA

Point mutations were introduced into fatty acid binding domain of the *C-FABP* cDNA using Transformer<sup>tm</sup> Site-Directed Mutagenesis Kit (Chapter 2). The pBluescript II SK vectors containing wild type, single-mutation and double-mutated *C-FABP* cDNA were transformed into DH5 $\alpha$  *E.coli* competent cells respectively for amplification. After overnight incubation at 37°C, 225xg, the plasmid vectors were isolated from DH5 $\alpha$  cells using midiprep and the presence of mutations were confirmed by nucleotide sequence analysis using specific *C-FABP* cDNA forward and reverse primers (Chapter 2). The construct harboring wild type of *C-FABP* cDNA was designated as C-FABP-WT. Those containing the single and double-mutated *C-FABP* cDNAs were denoted as C-FABP-109A and C-FABP-109/129A, respectively.

As showing in Figure 3.1, sequencing analysis results demonstrated that the sequence of the *C-FABP* cDNA region containing the first mutation site was successfully altered by converting Arginine 109 to Alanine 109. Thus the triplet AGA was changed into GCA. In the second mutation site the triplet CGG was changed into GCG by replacing Arginine 129 with Alanine 129. In the construct of C-FABP-109A, only one amino acid was changed in first mutation site and no change was made in second mutation site. In the construct of C-FABP-109/129A, amino acids in both mutation sites were changed.

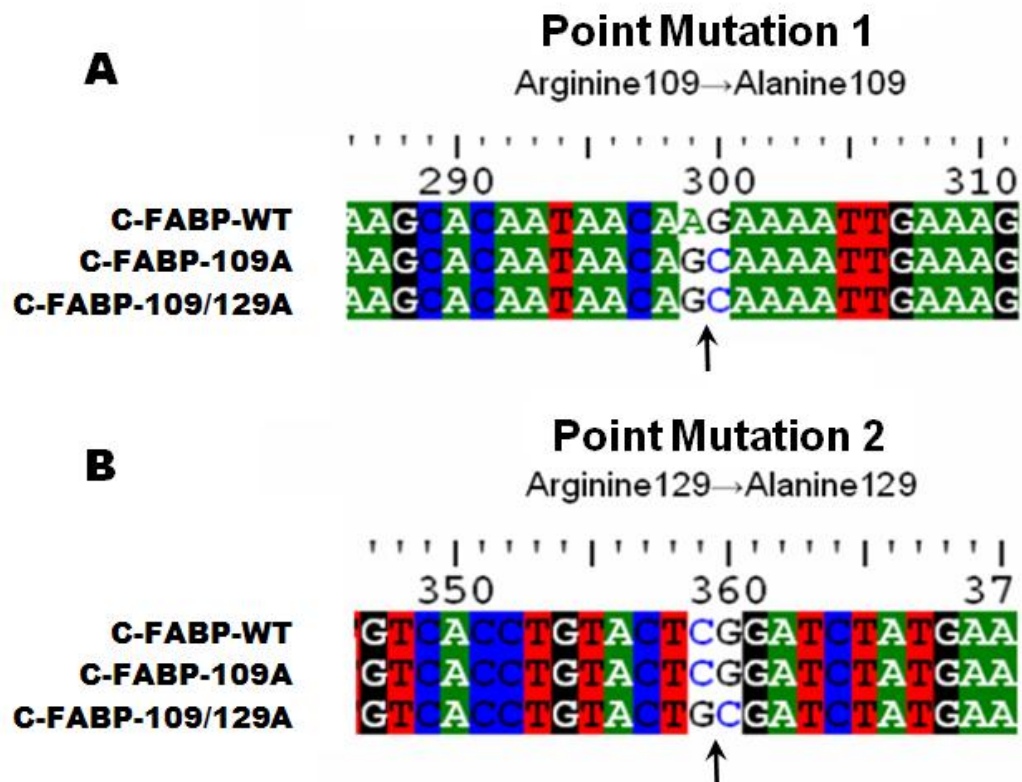


**Figure 3.1: Detection of mutations in C-FABP cDNA by sequencing analysis**

(A) Point mutation in first site is shown in panel A. The Alanine (GCA), mutated from Arginine (AGA), is presented both in C-FABP-109A and C-FABP-109/129A constructs. (B) Point mutation in second site is shown in panel B. The Alanine (GCG), converted from Arginine (CGG), is presented in C-FABP-109/129A but not in single-mutated C-FABP, C-FABP-109A and C-FABP-WT constructs.

### 3.2.2 Insertion of wild type C-FABP and mutant C-FABPs into a mammalian expression vector - pIRES<sub>2</sub>-EGFP

The C-FABP-WT, C-FABP-109A and C-FABP-109/129A cDNAs were removed from pBluescript II SK vector by restriction enzyme digestion using *XhoI/PstI* restriction enzymes. The products of restriction enzyme digestion were separated by agarose gel electrophoresis (1%) as presented in Figure 3.2A. The DNA fragments of C-FABP-WT, C-FABP-109A and C-FABP-109/129A were recovered from agarose gel respectively as described in Chapter 2 section 2.2.1.4. The mammalian expression vector pIRES<sub>2</sub>-EGFP was linearized using *XhoI/PstI* restriction enzymes as shown in Figure 3.3A and purified from agarose gel. The purified DNA fragment of wild type and mutant C-FABPs were inserted into pIRES<sub>2</sub>-EGFP vector respectively using T4 DNA ligase. The recombinant DNAs were transformed into DH5 $\alpha$  bacterial cells and plated onto LB plates in the presence of antibiotics (50 $\mu$ g/ml ampicillin). Single colonies of transformed DH5 $\alpha$  bacteria were transferred into flasks containing 10ml of LB medium with 50 $\mu$ g/ml ampicillin and left to grow overnight at 37°C, 225xg. The overnight cultured bacterial cells (5ml) were harvested and the pIRES<sub>2</sub>-EGFP vectors containing C-FABP-WT, C-FABP-109A and C-FABP-109/129A were isolated from bacterial cells respectively using miniprep as described in Chapter 2 section 2.2.3.1. The ligation was examined using restriction enzyme digestion as shown in Figure 3.3B. The sequencing analysis also confirmed the presence of the insertions in pIRES<sub>2</sub>-EGFP vector.

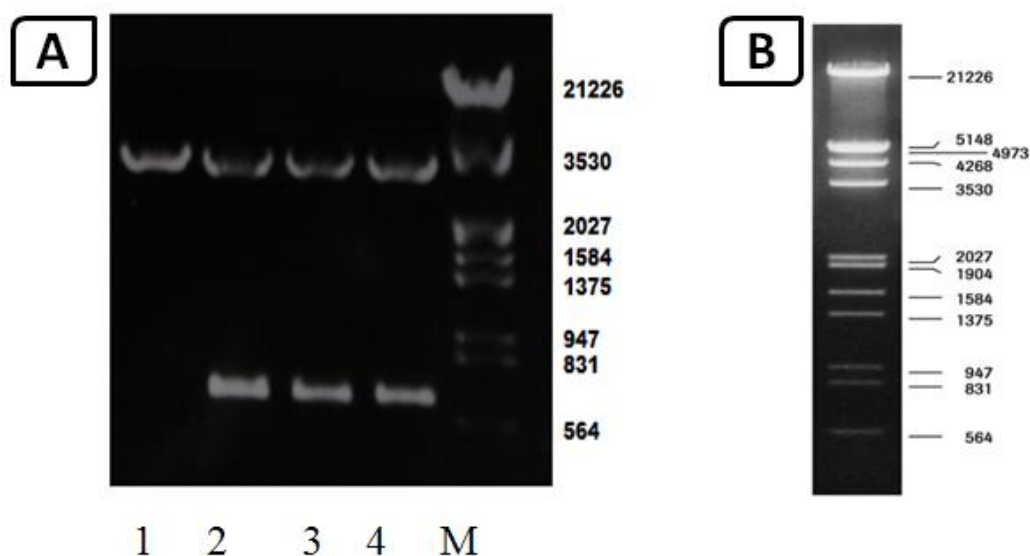


**Figure 3.2: The products of restriction enzyme digestion for the ligation reaction**

(A) After DNA sequencing analysis, the pBluescript II SK vector containing C-FABP-WT (Lane 2), C-FABP-109A (Lane 3) and C-FABP-109/129A (Lane 4) was digested by *XhoI/PstI* for the ligation reaction. The control vector digested by *XhoI/PstI* is presented in lane 1. For lanes 2, 3 and 4, the bottom band represents DNA fragment of C-FABP-WT, C-FABP-109A and C-FABP-109/129A respectively. The top band in lanes 1, 2, 3, and 4 represents digested pBluescript II SK vector (3.0 kb). (B) The DNA standard marker is denoted in number of base pairs.

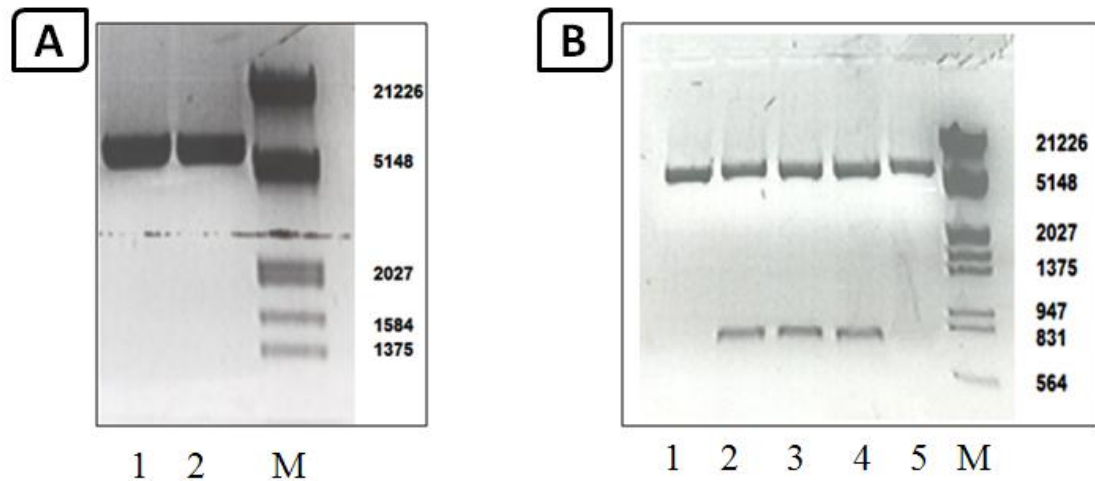


**Figure 3.3: Identification of the recombinant DNAs by restriction enzyme digestion**

(A) Two restriction enzyme digestions (Lanes 1 and 2) of mammalian expression vector pIRES2-EGFP (5.3 kb) using *XhoI/PstI* restriction enzymes to linearize the plasmid for the ligation reaction. (B) After ligation reaction, the recombinant DNAs were digested using *XhoI/BamHI* to assure that the DNA fragment of C-FABP-WT, C-FABP-109A and C-FABP-109/129A was inserted into the vector. The empty pIRES2-EGFP vector was used as control in lane 1. The vector containing C-FABP-WT digested with *BamHI* was shown in lane 5 for comparison with the recombinant DNAs digested with *XhoI/PstI* restriction enzymes. For lanes 2, 3 and 4, the bottom band represents DNA fragment of C-FABP-WT, C-FABP-109A and C-FABP-109/129A respectively. The top band in lanes 1, 2, 3, 4, and 5 represents digested pIRES2-EGFP vector. In panel A and B, the DNA standard marker in lane M is denoted in number of base pairs.

### 3.2.3 Detection of wild type and mutated C-FABP mRNAs in transfected LNCaP cells by RT-PCR

LNCaP cells were stably transfected with the empty pIRES2-EGFP vector containing C-FABP-WT or one of the two mutated C-FABP: C-FABP-109A and C-FABP-109/129A using a polyamine based transfection reagent. The cell line transfected with C-FABP-WT, C-FABP-109A, C-FABP-109/129A and the empty pIRES2-EGFP vector were designated LNCaP-WT, LNCaP-R109A, LNCaP-R109/129A and LNCaP-V.

It was difficult to establish transfected clones as LNCaP cells had an extremely low survival rate when plated at very low concentrations in tissue culture flask (Bennett *et al*, 1997). Furthermore, the Geneticin also significantly slowed the growth rate of the transfected cells in selection step which makes the formation of transfected clones more difficult. In order to overcome the difficulties in generating LNCaP clones, the modified transfection method was developed using GeneJammer transfection reagent which is a proprietary formulation of polyamine offering high efficiency with low cytotoxicity. After selection step, the surviving clones were analyzed by fluorescence microscopy as described in Chapter 2 section 2.2.6.2.

The successful transfected clones for LNCaP-WT, LNCaP-R109A, LNCaP-R109/129A and LNCaP-V were isolated using ring clone and cultured in selective medium separately. The pool of wild type C-FABP and mutant C-FABP transfected clones was also established by random selection of five single clones. The abundant green fluorescence images for pooled transfected cell lines were presented Figure 3.4 confirmed the expression of recombinant pIRES2-EGFP vectors. For LNCaP-WT,



LNCaP-R109/129A and LNCaP-V transfected cell lines, the fluorescence-positive cells represented a subset of approximately 90% of the whole population. For LNCaP-R109A, approximately 80% of cells displayed strong green fluorescent emission and about 10% of LNCaP-R109A transfectant expressed less green fluorescence. The rest 10% populations of all four pooled transfected cell lines were fluorescence-negative. The fluorescence-positive cell population stayed at same level when increased the concentration of Geneticin or removed the antibiotic for a period of time (4 weeks). Similar observations were found in single cloned transfectants.

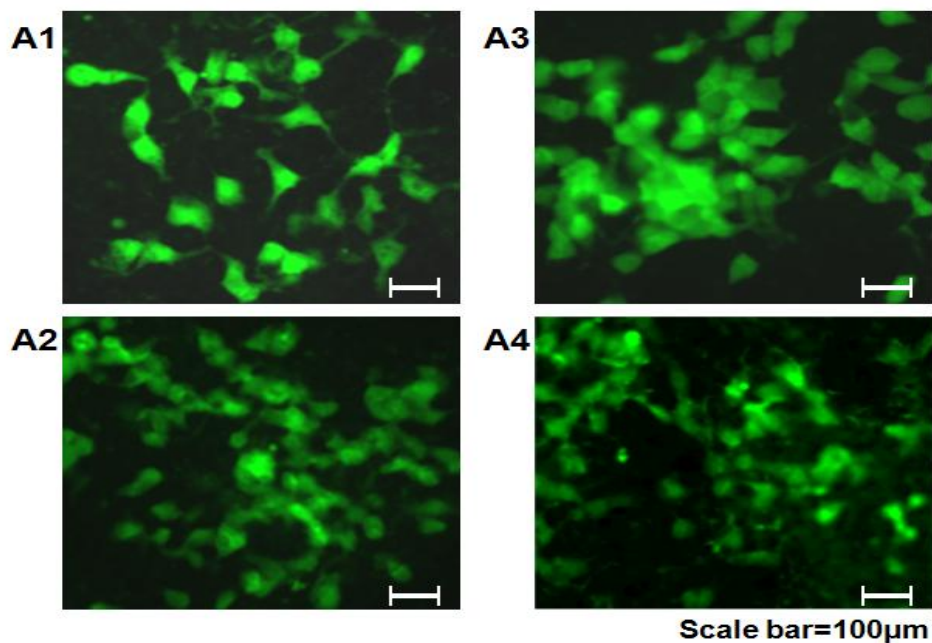


**Figure 3.4: Green fluorescent emission images of successful transfected cells**

*The green fluorescence images of pooled LNCaP-WT, LNCaP-R109A, LNCaP-R109/129A and LNCaP-V are shown in panel A1, A2, A3 and A4 respectively. All four cell lines appeared strong green fluorescence confirmed the expression of recombinant pIRES2-EGFP vectors.*

To confirm the presence of the wild type and mutated C-FABP mRNAs existence in the transfected cell lines, total RNA was isolated from each pooled clones of transfectants. The total RNAs were amplified by PCR using a specific C-FABP forward primer which was listed in Chapter 2 section 2.2.9.2 and a specific pIRES2-EGFP plasmid reverse primer to ensure the amplification products were from the transgenes instead of the endogenous gene for C-FABP. The products of PCR amplification were analysed by agarose gel electrophoresis as shown in Figure 3.5. No band was detected in PCR amplification without reverse transcriptase indicating that the amplified bands were not arising from total RNA isolation. The RT-PCR products on the agarose gel were excised and purified as mentioned in Chapter 2 and send for sequencing analysis (Liverpool University, School of tropical Medicine, Sequencing Unit).

The RT-PCR products of LNCaP-R109A and LNCaP-R109/129A were the same size as LNCaP-WT (623kb). In contrast, no band was detected in LNCaP-V and negative control amplifications. Subsequent nucleotide sequencing also confirmed the presence of C-FABP-WT, C-FABP-109A, and C-FABP-109/129A.

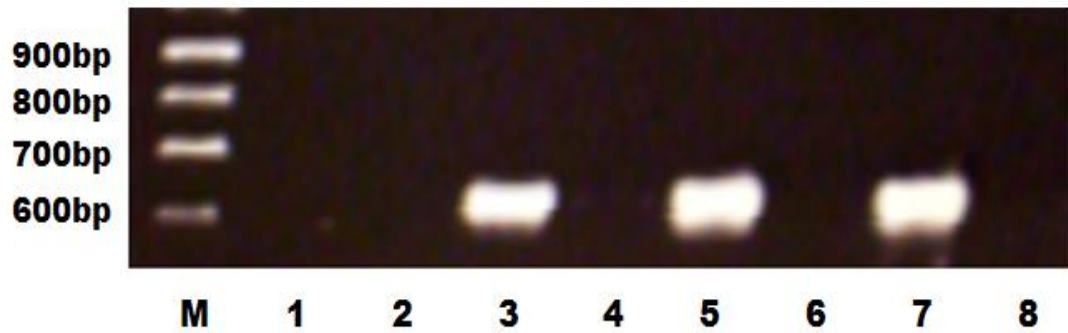


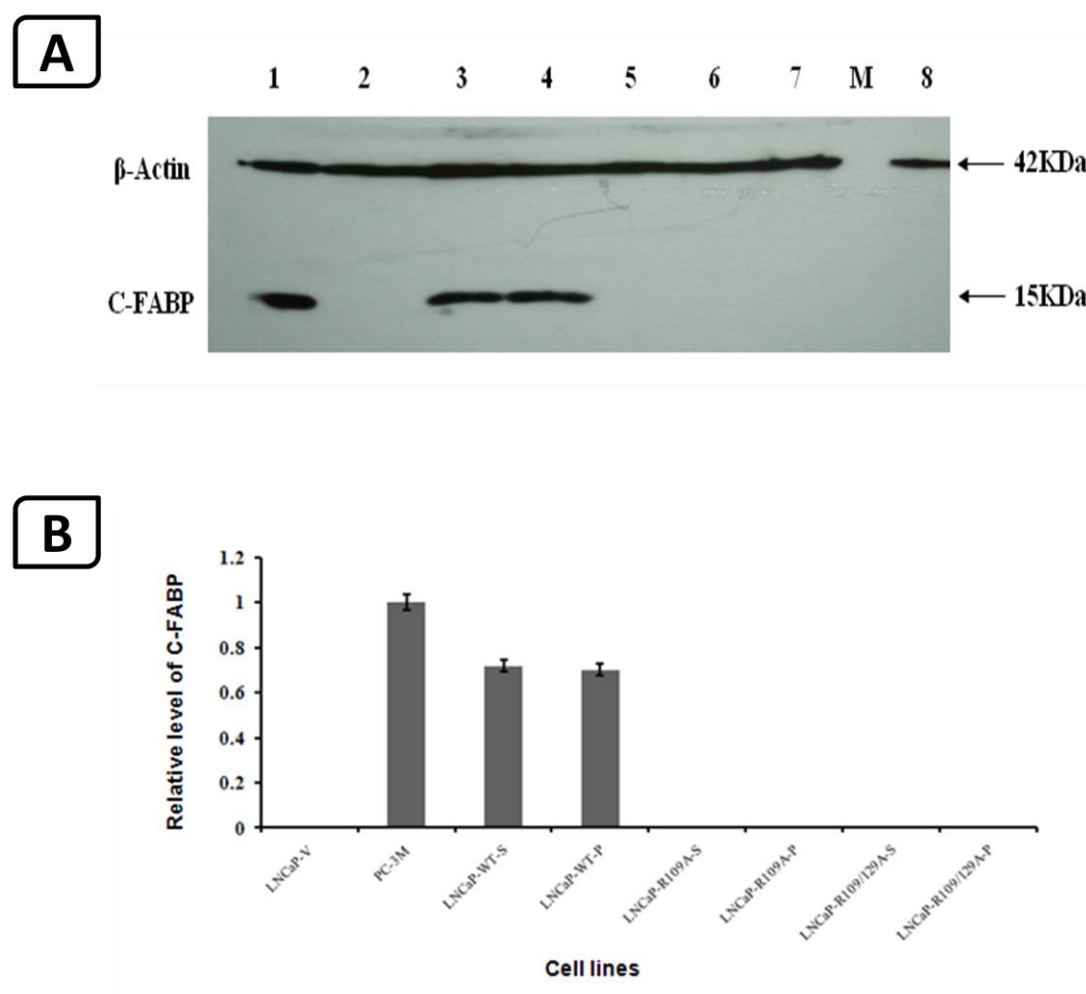
**Figure 3.5: Detection of mRNAs from transfected cell lines by RT-PCR**

Reverse transcriptase PCR was carried out using the Taq polymerase with specific primers to amplify the wild type and mutated C-FABP gene. Total RNAs were isolated from LNCaP cell line (Lane 1) and transfected cell lines LNCaP-V (Lane 2), LNCaP-WT (Lanes 3 and 4), LNCaP-R109A (Lanes 5 and 6) and LNCaP-R109/129A (Lane 7 and 8). Negative controls are presented in lanes 4, 6 and 8 in which the reverse transcriptase was omitted. The PCR products were analyzed on a 2% agarose/EtBr gel in 1xTBE buffer alongside 100 base pair ladder DNA marker (Lane M).

### 3.2.4 Expression of wild type and mutant C-FABP proteins in LNCaP cell line

Levels of wild type and mutant C-FABP proteins expressed in transfected LNCaP cells were examined by Western Blot as described in Chapter 2. The LNCaP-V cells and highly malignant prostate cancer cells, PC-3M were used as negative and positive control respectively. The C-FABP specific primary antibody used in Western Blot analysis was provided by Dr. Hiroshi Fujii, Niigata University, Japan. The level of  $\beta$ -actin expression in each cell line was also examined and used as loading control. The C-FABP expression in transfectant cells was quantified by relating to that in positive control cells using scanning densitometry.

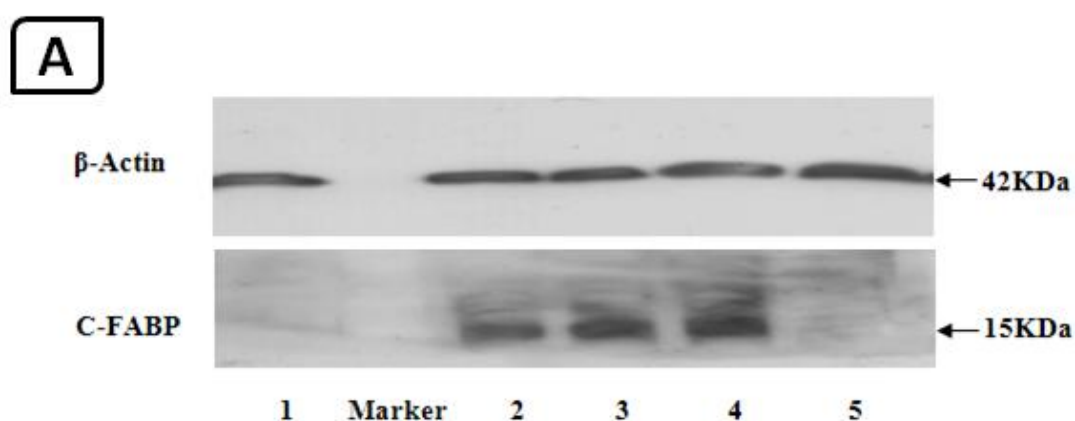
The expression of wild type C-FABP (15 KDa) in LNCaP-WT and PC-3M cells are shown in Figure 3.6A and B. When the level of C-FABP expression in positive control PC-3M cells was set as 1, the level of C-FABP in LNCaP-WT was significantly increased (Students t-test  $P < 0.05$ ) to approximately 70% of that in the PC-3M cells. No band was observed in LNCaP-R109A, LNCaP-R109/129A and LNCaP-V. In addition, no significant difference was detected in wild type C-FABP levels between single cloned and pooled LNCaP-WT cells (Students t-test  $P > 0.05$ ). The expression of  $\beta$ -actin, served as a loading control, is also examined as shown in Figure 3.6A at the size of 42 KDa.



**Figure 3.6: Detection of protein expression levels of wild type C-FABP in single cloned and pooled transfectant LNCaP cell lines**

(A) Cellular lysates from three individual cloned (Lanes 3, 5 and 7) and three pooled (Lane 4, 6 and 8) of transfectant lines: LNCaP-WT (Lanes 3 and 4), LNCaP-R109A (Lanes 5 and 6) and LNCaP-109/129A (Lanes 7 and 8), were subjected to Western blot analysis. C-FABP protein band was recognized by a monoclonal anti-human C-FABP antibody and visualized as described in Chapter 2 section 2.2.7. The  $\beta$ -actin antibody was used to correct the possible loading artifacts. (B) The relative levels of C-FABP expression in different transfectants. The results (mean S.D. of three experiments) were obtained by densitometry analysis of the band intensities.

Both wild type and mutant C-FABPs were picked up using a rabbit polyclonal anti-human C-FABP antibody. It was observed that intensities of the bands in LNCaP-WT, LNCaP-109A and LNCaP-109/129A were very similar, whereas the expression of C-FABP in control cell line LNCaP-V and parental cell line LNCaP is barely detectable as shown in Figure 3.7. The  $\beta$ -actin protein expression level in each cell lines, served as a loading control, was also presented. Further relative quantifications by scanning densitometry were shown in Figure 3.7. When wild type C-FABP expression in LNCaP-WT was set as 1, the level of mutant C-FABPs were 1.09 and 0.946 in LNCaP-R109A and LNCaP-109/129A cells respectively. No significant expression differences have been found between the level of wild type C-FABP and level of mutant C-FABPs (Students t-test  $P>0.05$ ) in the transfectants. LNCaP-V with empty pIRES2-EGFP vector and parental LNCaP cells exhibited undetectable level of C-FABP.



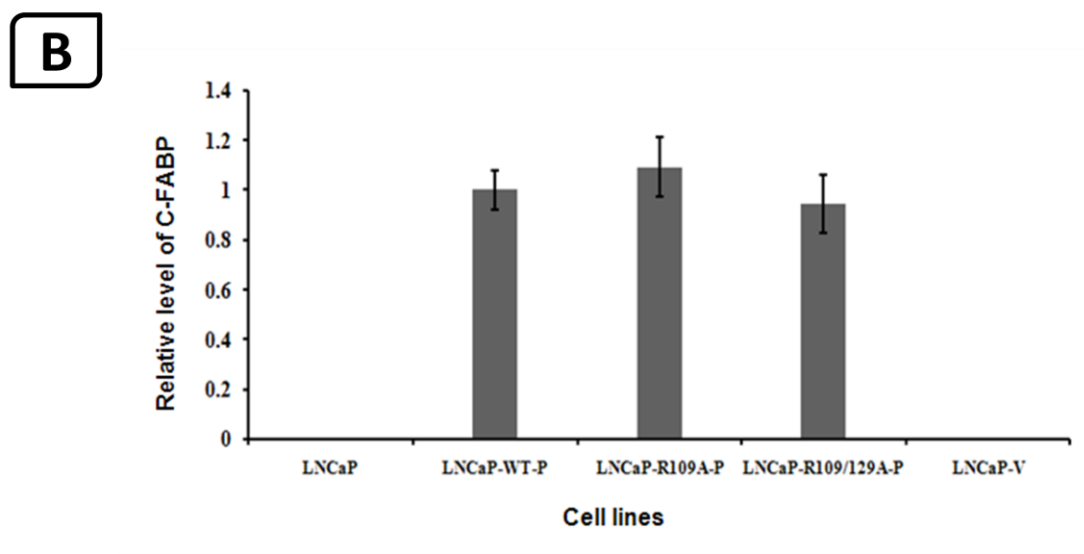


**Figure 3.7: Detection of protein expression levels of wild type and mutant C-FABPs in pooled transfected LNCaP cell lines**

(A) The mutant C-FABP proteins in LNCaP-R109A cells (Lane 2) and LNCaP-109/129A cells (Lane 3) were recognized using a polyclonal anti-human C-FABP antibody. The wild type C-FABP in LNCaP-WT cells (Lane 1) was also detected by the antibody. LNCaP-V and LNCaP cells were used as negative control in Lane 4 and 5 respectively.

(B) The mean and S.D. of the relative band intensities of each cloned and pooled cell lines from three individual experiments.

### **3.2.5 Measurement of levels of wild type and mutant C-FABP mRNAs in different transfectants by Real-time PCR**

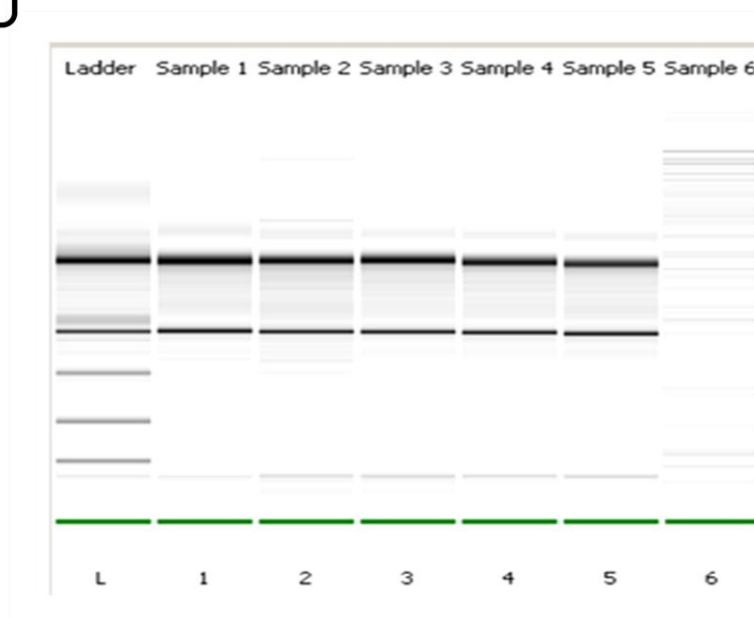
To confirm that the transfected wild type and different mutant cDNAs were expressed, the relative C-FABP mRNA levels in each transfectant cell line was measured by real-time PCR. The parental cells, LNCaP were used as the calibrator. Total RNAs from each cell lines were isolated routinely and purified by RNeasy Mini column.

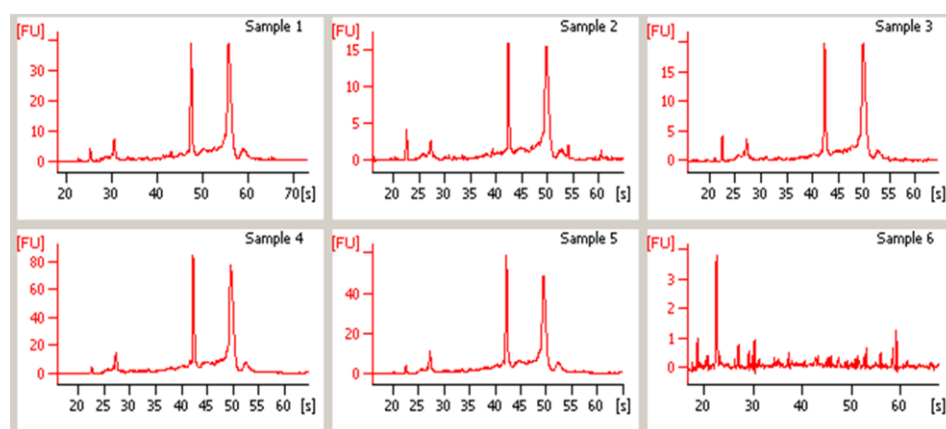
As poor quality RNA samples can lead to spurious Real-time PCR results, the integrity and quality of the total RNAs were determined by Agilent 2100 bioanalyzer using RNA 6000 Nano Kit. The results (as shown in Figure 3.8A) were analyzed by the 2100 Expert Software and visual output were confirmed that the isolated total RNAs were in high quality with both rRNA bands (18S/28S) distinguishable as shown in Figure 3.8B. The RNA integrity numbers (RIN) for each isolated RNA were between 9.0 to 9.6 out of 10 and no degradation was observed. The RNA concentration of each sample was also calculated by the 2100 Expert Software.

After RNA purification, relative quantification real-time PCR was performed to measure the mRNA levels of wild type and mutant C-FABPs using exon-exon junction primers as described in Chapter 2 section 2.2.10. Figure 3.9 summarizes the relative level of C-FABP mRNA in total RNA isolated from each pooled cell line. The LNCaP-WT, LNCaP-R109A and LNCaP-R109/129A cell line showed a significant increase in the relative C-FABP mRNA level when compared to parental cell line LNCaP. When the C-FABP mRNA level in the parental cell line LNCaP



was set at 1, the levels of expression was  $137.5 \pm 18.1$ ,  $114.1 \pm 15.6$ , and  $115 \pm 25.2$  in LNCaP-WT, LNCaP-R109A and LNCaP-R109/129A, respectively. On the other hand, the C-FABP mRNA level in LNCaP-V cells was only slightly increased. The C-FABP mRNA level between LNCaP-R109A and LNCaP-R109/129A did not show significant difference (Students t-test  $P > 0.05$ ). Similarly, no difference was found when they compared to LNCaP-WT (Students t-test  $P > 0.05$ ). However, the relative levels of C-FABP mRNA expressed in all three transfectant lines (LNCaP-WT, LNCaP-R109A and LNCaP-R109/129A) were significantly increased when compared to the control LNCaP-V cells (Students t-test  $P < 0.05$ ).

**A**

**B**

**Figure 3.8: Quality checks of total RNA samples by Agilent 2100 bioanalyzer**

The quality and quantification of total RNA were assessed using the RNA 6000 Nano LabChip on Agilent 2100 bioanalyzer. The gel electropherogram images for LNCaP-WT (Lane 1), LNCaP-R109A (Lane 2), LNCaP-R109/129A (Lane 3), LNCaP-V (Lane 4) and LNCaP (Lane 5) were shown in panel A. The fluorescence plots with two peaks of 18S and 28S ribosomal RNAs of each sample were shown in panel B. The qualities of RNAs were presented by RINs which were calculated from the plots.

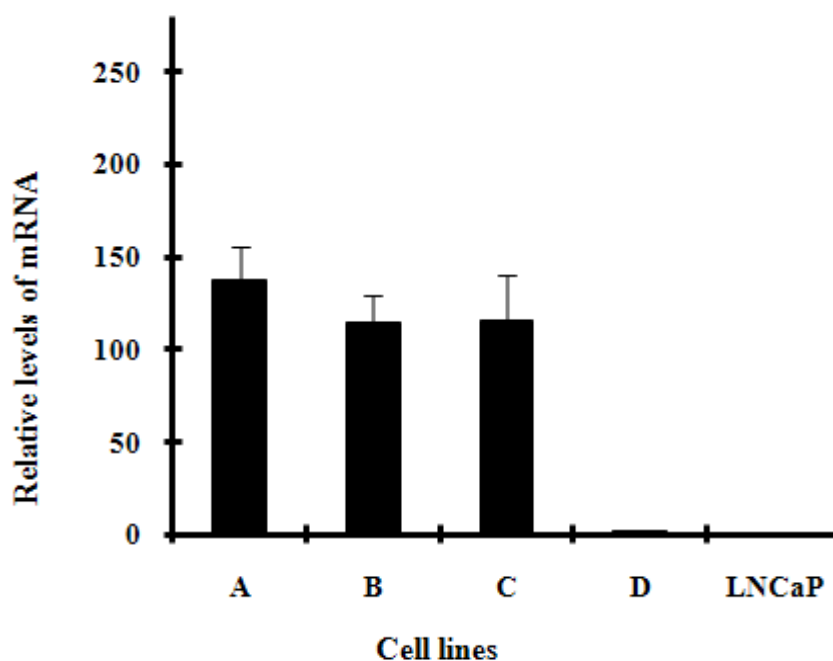


**Figure 3.9: Relative level of C-FABP mRNA in transfectant and LNCaP cell lines**

*The Real-time PCR products of LNCaP-WT (A), LNCaP-R109A (B), LNCaP-R109/129A (C), LNCaP-V (D) and LNCaP (LNCaP) were analyzed by Chromo4 fluorescence detector. The mean and S.D. of relative C-FABP mRNA level for each cell line from three individual experiment were shown in the bar chart. LNCaP cells were used as calibrator.*

### 3.3 Discussion

C-FABP is a member of FABP family which binds with high affinity to long chain fatty acid. It has been revealed that over-expression of C-FABP may promote VEGF to facilitate angiogenesis which contributed to tumour progression such as tumour formation and metastasis (Adamson *et al*, 2003; Jing *et al*, 2001). However, the exact mechanism remains unclear. In order to establish transfectants expressing mutant forms of C-FABP which are not able to bind to fatty acids, point mutations were introduced to two key amino acids (Arg<sup>109</sup> and Arg<sup>129</sup>) which are responsible for fatty acid-binding in *C-FABP* gene. As a result, the relationship between the fatty acid binding capacity and the tumour promoting function can be assessed by investigating whether the transfectants expressing mutant C-FABP can still promote tumour growth.

Two mutated gene have been successfully generated from the wild type C-FABP gene using Transformer<sup>tm</sup> Site-Directed Mutagenesis Kit: (1) C-FABP-109A where Arginine 109 was converted to Alanine 109; (2) C-FABP-109/129A where Arginine 109 and Arginine 129 were converted to Alanine 109 and Alanine 129. The point mutations in both mutated genes were confirmed by sequencing analysis. Then, the wild type and mutant C-FABPs were transferred into a mammalian expression vector pIRES2-EGFP with enhanced green fluorescent protein coding region using *XhoI* and *PstI* restriction digestion enzymes. The pIRES2-EGFP empty vector and vectors containing C-FABP-WT, C-FABP-109A, and C-FABP-109/129A were transfected

into LNCaP cells to create transfected cell lines LNCaP-V, LNCaP-WT, LNCaP-R109A and LNCaP-R109/129A respectively.

LNCaP cell line, established from a needle aspiration biopsy of the lymph node of male patient with diagnosed metastatic prostate carcinoma, is a widely used androgen sensitive human prostate cancer model cell line (Horoszewicz *et al*, 1983a). Two properties of LNCaP cells make them a particularly difficult cell line to generate transfectants compared to other cell lines firstly; LNCaP cells have a low growth rate and a tendency to form aggregates. Secondly; LNCaP cells have a poor survival rate when seeded at low concentration in tissue culture plate (Bennett *et al*, 1997), which can significantly affect the efficiency of transfection as the cell colonies were developed from a single transfected cell. To overcome the difficulties in cloning LNCaP cells, the modified transfection method was carried out using a polyamine based transfection reagent, GeneJammer which provided a higher transfection efficiency and lower cytotoxicity to LNCaP cells compared to calcium phosphate method (Orth *et al*, 2008). The transfected cell lines were selected by 0.5mg/ml antibiotic G418 for 10 days in a 75cm<sup>2</sup> tissue culture flask. Then, the G418 was removed and 500µl of untransfected LNCaP cells at a concentration of 2x10<sup>4</sup>cells/ml were seeded into the flask as a feeder layer. The cells were allowed to grow in routine culture medium until cellular confluence reached at 80%. Then, the cells were re-select followed the same procedure as for the first selection. After 5 round selections, the cells were maintained in selective culture medium and successfully transfected colonies were determined by green fluorescence imaging and recovered by ring cloning.

Transfectant lines: LNCaP-WT transfected with wild type C-FABP, LNCaP-R109A transfected with single site mutated C-FABP, LNCaP-R109/129A transfected with double site mutated C-FABP and LNCaP-V (control) transfected with pIRES2-EGFP vector only were successfully generated. The wild type or mutant C-FABP cDNAs in each transfected cell line were examined by RT-PCR. The Western Blot assays were applied to determine the protein level of C-FABP-WT, C-FABP-R109A and C-FABP-R109/129A in each transfected cell line. The results demonstrated that expression level of C-FABP-WT in pooled LNCaP-WT cells and mutant C-FABPs in pooled LNCaP-R109A and LNCaP-109/129A cells were at similar level, which indicated that these transfectants were suitable for comparison. However, there is no C-FABP cDNA or protein has been detected in LNCaP cells transfected with empty vector and parental cells indicating that transfected with pIRES2-EGFP vector did not change the expression level of C-FABP. The same pattern of relative C-FABP mRNA level obtained by Real-time PCR analysis also confirmed the Western Blot results.

The results in this chapter demonstrated the successful establishment of transfected cell lines with expression of wild type or mutant C-FABPs. However, the effect of wild type or mutant C-FABP expression prostate cells is unknown. These aspects such as recombinant protein of mutant and wild-type C-FABP will be produced in *E.coli* cells and purified as described in Chapter 2 and fatty acid-binding assay will be conducted in order to monitor the fatty acid-binding activity, both will be examined and presented in the Chapter 4.

## **4 Production of recombinant C-FABPs and testing their fatty acid binding ability**

## 4.1 Introduction

In Chapter 3, four transfected LNCaP cell lines with expression of wild type and mutant C-FABPs were successfully established to generate transfectants with different fatty acids uptake capacities. To reveal whether the fatty acid binding ability is essential for C-FABP to promote cancer development and progression, fatty acid binding ability of recombinant wild type and mutant types of C-FABPs produced by cancer cells were measured and compared. In this Chapter, recombinant proteins of mutant and wild type C-FABPs were produced in *E. coli* cells and purified according to the procedure described in Chapter 2 so that the fatty acid binding activity of these proteins can be clearly monitored.

Long chain fatty acids are not only served as metabolic fuel but also act as endogenous ligands for nuclear receptors such as PPAR (Furuhashi & Hotamisligil, 2008). Within the cells, it is possible that excessive amount of intracellular fatty acids may contribute to both breast and prostate cancer risk and disease progression (Collett *et al*, 2000; Hughes-Fulford *et al*, 2001). Although the three key amino acids conserved in FABPs were suggested to be the fatty acid binding site, direct evidence on the effect of changing this site on fatty acid binding ability of C-FABP is lacking. Thus, it is important to examine the fatty acids binding-capacities of recombinant wild type and mutant C-FABP proteins.

In order to establish a construct to express a wild type and mutant type of C-FABPs, the cDNAs were cloned into expression vector pQEs then since there is no restriction site from pQEs can be directly used. The C-FABP cDNAs excised out from a pIRES2-EGFP construct by *XhoI/KpnI* restriction enzymes and first inserted into



pBluescript II SK vector so that desired restrict sites can be generated then existed out with *KpnI* and *PstI* which are located in multiple cloning sites of the expression vector pQEs. Thus C-FABP cDNAs from pBluescript II SK can be directly inserted into the pQEs to form 3 constructs capable of expressing C-FABP-WT, C-FABP-R109 and C-FABP-R109/129A respectively. The recombinant His<sub>6</sub>-tagged protein of wild type and mutant C-FABPs were expressed and purified using QIAexpress Ni-NTA Fast Start kits (for purification and detection of recombinant 6xHis-tagged proteins). Single protein bands with molecular masses of ~ 14 KDa were observed for recombinant C-FABPs when subjected to SDS-PAGE analysis. The fatty acid binding capability of three C-FABP proteins was examined by using the environment-sensitive fluorescent fatty acid analogue DAUDA that alters its fluorescence emission spectra and intensities on entry into binding proteins.

Since the biological activity of C-FABP in normal condition is to bind to fatty acids and to transport them into cells, it is important to understand whether the ability of binding to fatty acids is related to the tumorigenicity promoting function of C-FABP in experiments of this Chapter. Firstly, generation of construct expressing wild type and mutant C-FABPs cDNA and cloning the expression construct into *E.coli* cells. Then expressed and purified the His<sub>6</sub>-tagged protein of wild type and mutant C-FABPs and analysed the C-FABP proteins by sequencing analysis and SDS-PAGE. Thirdly, monitor the fatty acid binding capability of three C-FABP proteins by fatty acid binding assay.

## 4.2 Results

### 4.2.1 Generation of complementary restriction sites

The cDNAs for C-FABP-WT, C-FABP-R109A and C-FABPR109/129A were cut out from three pIRES2-EGFP by restriction enzyme digestion using *XhoI* and *PstI*. The products of restriction enzyme digestion were separated by agarose gel electrophoresis (1%) as presented in Figure 4.1. The DNA fragments of C-FABP-WT, C-FABP-109A and C-FABP-109/129A were recovered from agarose gel respectively as described in Chapter 2. The expression vector pBluescript II SK was linearized using *XhoI/PstI* restriction enzymes as shown in Figure 4.2 and purified from agarose gel. The purified DNA fragment of wild type and mutant C-FABPs were inserted into pBluescript II SK vector respectively using T4 DNA ligase. The recombinant DNAs were transformed into DH5 $\alpha$  bacterial cells and plated onto LB plates in the presence of antibiotics (50 $\mu$ g/ml ampicillin). Single colonies of transformed DH5 $\alpha$  bacteria were transferred into flasks containing 10ml of LB medium with 50 $\mu$ g/ml ampicillin and incubated overnight at 37°C, 225xg. The overnight cultured bacterial cells (5ml) were harvested and the pBluescript II SK vectors containing C-FABP-WT, C-FABP-109A and C-FABP-109/129A were isolated from bacterial cells respectively using miniprep as described in Chapter 2. The ligation was examined using restriction enzyme digestion as shown in Figure 4.3. The sequencing analysis confirmed the presence of the insertions in pBluescript II SK vector as shown in Figure 4.4 - Figure 4.6.

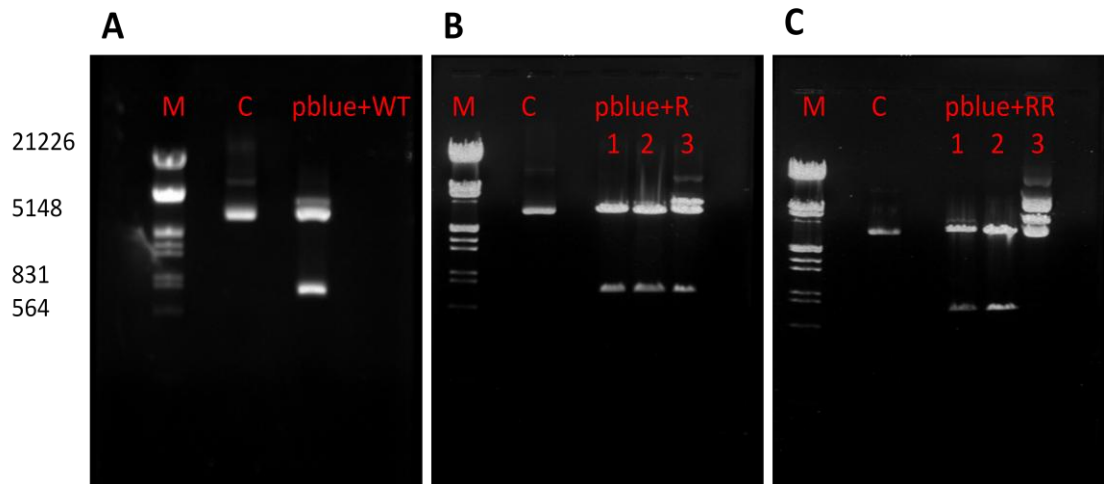


**Figure 4.1: the product of restriction enzyme digestion for the ligation reaction**

After DNA sequencing analysis, the pBluescript II SK vector containing C-FABP-WT (A), C-FABP-109A (B) and C-FABP-109/129A (C) was digested by *XhoI/PstI* for the ligation reaction. The control vector digested by *XhoI/PstI* is presented in control lanes. The bottom bands represent DNA fragment of C-FABP-WT, C-FABP-109A and C-FABP-109/129A respectively. The top bands represent digested pBluescript II SK vector (3.0 kb). \*M: marker; C: Control; pblue+WT,R and RR: Ligated pBluescript and C-FABP-WT, C-FABP-109A and C-FABP-109/129A respectively.

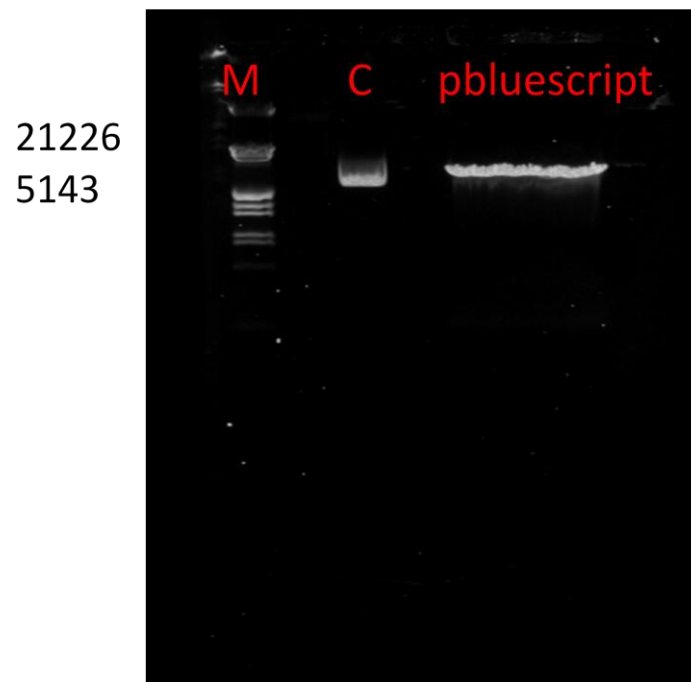


**Figure 4.2: Linearization of the protein expressing vector**

*Two restriction enzyme digestions (Lanes 1 and 2) of mammalian expression vector pBluescript II SK (5.3 kb) using XhoI/PstI restriction enzymes to linearize the plasmid for the ligation reaction.*

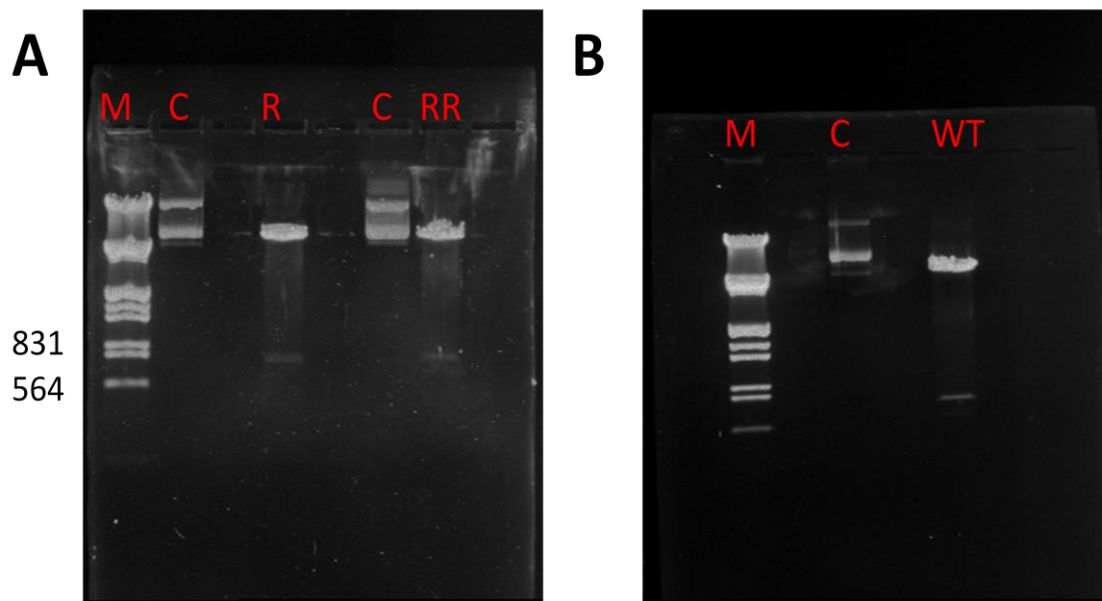


**Figure 4.3: Digestion of vector DNAs**

To generate a cohesive end with the insert, the DNAs were digested using *XhoI* /*PstI* which is complimentary to the sequence on both ends of the C-FABP CDNAs. After ligation reaction, the recombinant DNAs were double digested using *XhoI* /*PstI* to confirm that the DNA fragment of C-FABP-WT (B), C-FABP-109A and C-FABP-109/129A (A) was inserted into the vector. The undigested pBluescript II SK vector was used as control as shown in control lanes. (A) The bottom bands represent DNA fragment of C-FABP-109A and C-FABP-109/129A respectively. The top bands represent digested pBluescript II SK vector. (B) The bottom band represents DNA fragment of C-FABP-WT. The top band represents digested pBluescript II SK vector. In panel A and B, the DNA standard marker in lane M is denoted in number of base pairs.

## 4.2.2 Confirmation of successful insertion of wild type and mutant cDNAs into pBluescript cloning vector

### 4.2.2.1 Sequence analysis of plasmid DNAs

The ligation reaction was transfected into *E.coli* cells and the colonies have the cloning vector was selected and the total DNA from *E.coli* cell purified and subjected to sequencing analysis. The sequence obtained from the cloning vector was shown in Figure 4.4 - Figure 4.6. Total DNAs were sent for sequencing at the Cogenics Technologies<sup>TM</sup> (Essex, UK), 100ng/μl (10μl) of each purified DNA was analysed. M13F and M13R primers were used according to Cogenics Technologies. Sequence alignment was determined by using BioEdit for searching Genbank (BLAST).

Forward sequence (M13F)

5'- GTTTTCCCAGTCACGACGTTGTA-3'

Reverse sequence (M13R)

5'- CAGGAAACAGCTATGACC -3'

```

GAATTGGGTACCGGGCCCCCCTCGAGATCTTCGAATTCGGCTTACCGCCGACGCAGA
CCCCTCTCTGCACGCCAGCCGCCGCCGACCCACCATGGCCACAGTTCAGCAGCTGGAA
GGAAGATGGCGCCTGGTGGACAGCAAAGGCTTTGATGAATACATGAAGGAGCTAGGA
GTGGGAATAGCTTTGCGAAAAATGGGCGCAATGGCCAAGCCAGATTGTATCATCACTT
GTGATGGTAAAAACCTCACCATAAAAACTGAGAGCACTTTGAAAACAACACAGTTTTTC
TTGTACCCTGGGAGAGAAGTTTGAAGAAACCACAGCTGATGGCAGAAAAACTCAGAC
TGTCTGCAACTTTACAGATGGTGCATTGGTTTCAGCATCAGGAGTGGGATGGGAAGGAA
AGCACAATAACAAGAAAATTGAAAGATGGGAACTAGTGGTGGAGTGTGTCATGAAC
AATGTCACCTGTACTCGGATCTATGAAAAAGTAGAATAAAAAATTCCATCATCACTTTGGA
CAGGAGTTAATTAAGAGAACGACCAAGCTCAGTTCAATGAGCAAATCTCCATACTGTTT
CTTTCTTTTTTTTTTCACTACTGTGTTCAATTATCTTTATCATAAACATTTTACATGCAGCTA
TTTCAAAGTGTGTTGGATTAATTAGGATCATCCCTTTGGTTAATAAATAAATGTGTTTGTG
CTAAAGCCGAATTCCGCGGCCGCAGGCCTCTAGAGTCGACCTGCAGCCCGGGGGATC
CACTAGTTCTAGAGCGGCCGCCACCGCGGTGGAGCTCCAGCTTTTGTTCCTTTAGTG
AGGGTTAATTGCGCGCTTGGCGTAATCATGGTCATAGCTGTTTCCTGTGTGAAATTGTTA
TCCGCTCACAATTCCACACAACATACGAGCCGGAAGCATAAAGTGTAAGCCTGGGGT
GCCTAATGAGTGAGCTAACTCACATTAATTTGCGTTGCGCTCACTGCCCGCTTCCAGTC
GGGAAACCTGTCGTGCCAGCTGCATTAATGAATCGCCACGCGCGGGGAGGAGGCGG
TTTGCATATTGGGCGCTCTTCCGCTTCTCGCTCACTGACTCGCTGCGCTCGTCGTC

```

**Figure 4.4: Insertion of C-FABP-WT cDNA into pBluescript cloning vector**

*Sequence alignment was determined by using BioEdit for searching Genbank (BLAST) (appendix 3). The sequences marked in red colour are C-FABP-WT (insert) while the sequences marked in black colour are pBluescript (vector). The sequences marked in blue colour are multiple restriction sites as GGTACC represents KpnI, CTCGAG represents XhoI and CTGCAG represents PstI.*

```

GGNTCTTGGGCGATTGGGTACCGGGCCCCCCTCGAGATCTTCGAATTCGGCTTACCGC
CGACGCAGACCCCTCTCTGCACGCCAGCCCGCCGCACCCACCATGGCCACAGTTCAG
CAGCTGGAAGGAAGATGGCGCCTGGTGGACAGCAAAGGCTTTGATGAATACATGAAG
GAGCTAGGAGTGGGAATAGCTTTGCGAAAAATGGGCGCAATGGCCAAGCCAGATTGTA
TCATCACTTGTGATGGTAAAAACCTCACCATAAAAACTGAGAGCACTTTGAAAACAACA
CAGTTTTCTTGTACCCTGGGAGAGAAGTTTGAAGAAACCACAGCTGATGGCAGAAAAA
CTCAGACTGTCTGCAACTTTACAGATGGTGCATTGGTTCAGCATCAGGAGTGGGATGGG
AAGGAAAGCACAATAACAGGCAAAATTGAAAGATGGGAAACTAGTGGTGGAGTGTGTCA
TGAACAATGTACCTGTACTCGGATCTATGAAAAAGTAGAATAAAAAATTCCATCATCACTT
TGGACAGGAGTTAATTAAGAGAACGACCAAGCTCAGTTCAATGAGCAAATCTCCATACT
GTTTCTTTCTTTTTTTTTTTCATTACTGTGTTCAATTATCTTTATCATAAACATTTTACATGCA
GCTATTTCAAAGTGTGTTGGATTAATTAGGATCATCCCTTTGGTTAATAAATAAATGTGTT
TGTGCTAAAGCCGAATTCCGCGGCCGCGAGGCCTCTAGAGTCGACCTGCAGCCCGGGGG
ATCCACTAGTTCTAGAGCGGCCGCCACCGCGGTGGAGCTCCAGCTTTTGTTCCTTTAG
TGAGGGTTAATTGCGCGCTTGCGTAATCATGGTCATAGCTGTTTCTGTGTGAAATTGT
TATCCGCTCACAATCCACACAACATACGAGCCGGAAGCATAAAGTGTAAGCCTGGGG
TGCC

```

**Figure 4.5: Insertion of C-FABP-R109A cDNA into pBluescript II SK cloning vector**

Sequence alignment was determined by using BioEdit for searching Genbank (BLAST) (appendix 3). The sequences marked in red colour are C-FABP-R109A (insert) while the sequences marked in black colour are pBluescript (vector). The sequences marked in blue colour are multiple restriction sites as GGTACC represents *KpnI*, CTCGAG represents *XhoI* and CTGCAG represents *PstI*. GC represents single mutation (The Alanine GCA, mutated from Arginine AGA).



```

GGNTCTTGGGCGATTGGGTACCGGGCCCCCCTCGAGATCTTCGAATTCGGCTTACCGC
CGACGCAGACCCCTCTCTGCACGCCAGCCCGCCCGCACCCACCATGGCCACAGTTCAG
CAGCTGGAAGGAAGATGGCGCCTGGTGGACAGCAAAGGCTTTGATGAATACATGAAG
GAGCTAGGAGTGGGAATAGCTTTGCGAAAAATGGGCGCAATGGCCAAGCCAGATTGTA
TCATCACTTGTGATGGTAAAAACCTCACCATAAAAACTGAGAGCACTTTGAAAACAACA
CAGTTTTCTTGATACCCTGGGAGAGAAGTTTGAAGAAACCACAGCTGATGGCAGAAAAA
CTCAGACTGTCTGCAACTTTACAGATGGTGCATTGGTTCAGCATCAGGAGTGGGATGGG
AAGGAAAGCACAATAACAGCAAAATTGAAAGATGGGAAACTAGTGGTGGAGTGTGTCA
TGAACAATGTCACCTGTACTGCGATCTATGAAAAAGTAGAATAAAAAATTCATCATCACTT
TGGACAGGAGTTAATTAAGAGAACGACCAAGCTCAGTTCAATGAGCAAATCTCCATACT
GTTTCTTTCTTTTTTTTTTTCATTACTGTGTTCAATTATCTTTATCATAAACATTTTACATGCA
GCTATTTCAAAGTGTGTTGGATTAATTAGGATCATCCCTTTGGTTAATAAATAAATGTGTT
TGTGCTAAAGCCGAATTCCGCGGCCGCGAGGCCTCTAGAGTCGACCTGCAGCCCCGGGGG
ATCCACTAGTTCTAGAGCGGCCGCCACCGCGGTGGAGCTCCAGCTTTTGTTCCCTTAG
TGAGGGTTAATTGCGCGCTTGGCGTAATCATGGTCATAGCTGTTTCTGTGTGAAATTGT
TATCCGCTCACAATTCCACACAACATACGAGCCGGAAGCATAAAGTGTAAGCCTGGGG
TGCCTAATGAGTGAGCTAACTCACATTAATTGCGTTGCGCTCACTGCCCCTTTCAGTCG
GGAAACCTGTCGTGCCAG

```

**Figure 4.6: Insertion of C-FABP-R109/129A cDNA into pBluescript II SK cloning vector**

Sequence alignment was determined by using BioEdit for searching Genbank (BLAST) (appendix 3). The sequences marked in red colour are C-FABP-R109/129A (insert) while the sequences marked in black colour are pBluescript (vector). The sequences marked in blue colour are multiple restriction sites as GGTACC represents KpnI, CTCGAG represents XhoI and CTGCAG represents PstI. GC and GC represent double mutation (The Alanine GCA, mutated from Arginine AGA and the Alanine GCG, converted from Arginine CGG).

### 4.2.3 Cloning of wild type and mutant C-FABPs into an expression vector pQEs

The cDNAs for C-FABP-WT, C-FABP-109A and C-FABP-109/129A were excised from pBluescript II SK vector by restriction enzyme digestion using *KpnI* and *PstI*. The products of restriction enzyme digestion were separated by agarose gel electrophoresis (1%) as presented in Figure 4.7. The DNA fragments of C-FABP-WT, C-FABP-109A and C-FABP-109/129A were recovered from agarose gel respectively as described in Chapter 2. The expression vector pQE 30, 31 and 32 was linearized using *KpnI/PstI* restriction enzymes and purified from agarose gel. The purified DNA fragment of wild type and mutant C-FABPs were inserted into pQE vector respectively using T4 DNA ligase. The recombinant DNAs were transformed into *BL21* bacterial cells and plated onto LB plates in the presence of antibiotics (50µg/ml ampicillin). Single colonies of transformed *BL21* bacteria were transferred into flasks containing 10ml of LB medium with 50µg/ml ampicillin and left to grow overnight at 37°C, 225xg. The overnight cultured bacterial cells (5ml) were harvested and the pQE vectors containing C-FABP-WT, C-FABP-109A and C-FABP-109/129A were isolated from bacterial cells respectively using miniprep as described in Chapter 2. The ligation was examined using restriction enzyme digestion as shown in Figure 4.8. The expression and purification of C-FABP recombinant proteins conducted using QIAexpress Ni-NTA Fast Start kits (for purification and detection of recombinant 6xHis-tagged proteins. Protein were analysed by SDS-PAGE to confirm the presence of insertion in pQE vector. The sequencing analysis also confirmed the presence of the insertions in pQE vector as shown in Figure 4.11 - Figure 4.13.

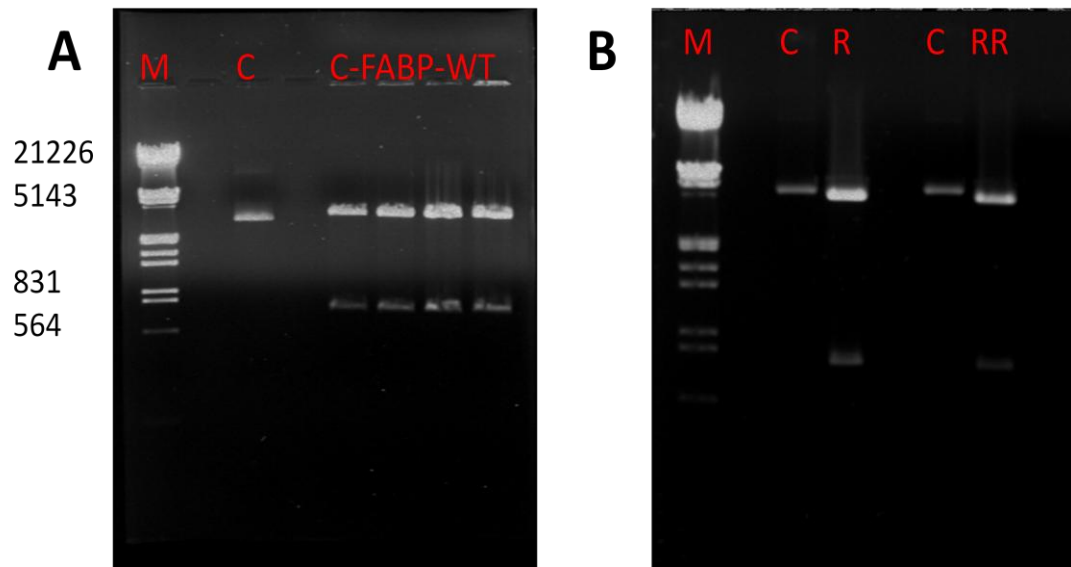


**Figure 4.7: the product of restriction enzyme digestion for the ligation reaction**

After DNA sequencing analysis, the pBluescript II SK vector containing C-FABP-WT (A), C-FABP-109A (B) and C-FABP-109/129A (C) was digested by KpnI/PstI for the ligation reaction. The control vector digested by KpnI/PstI is presented in control lanes. (A) The bottom band represents DNA fragment of C-FABP-WT. The top bands represent digested pQE vectors (3.4 kb). (B) The bottom bands represent DNA fragment of C-FABP-109A and C-FABP-109/129A, respectively. The top bands represent digested pQE vectors.

\*M: marker, C: Control, C-FABP-WT: Ligated pQE32 and C-FABP-WT, R & RR: Ligated pQE32 and C-FABP-R109 and C-FABP-R109/129A, respectively.

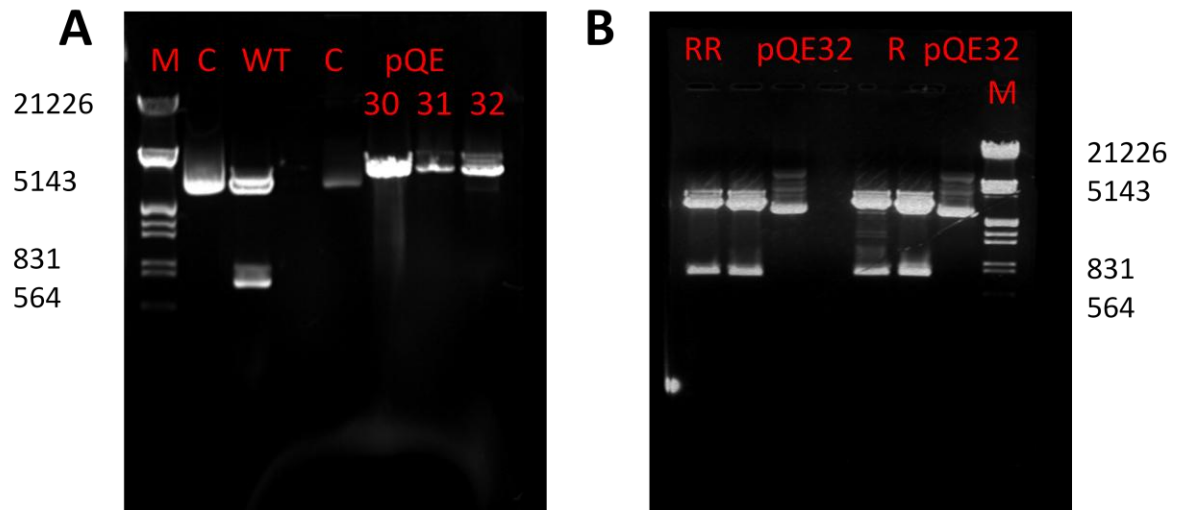


**Figure 4.8: Digestion of vector DNAs**

To generate a cohesive end with the insert, the DNAs were digested using *KpnI* /*PstI* which is complimentary to the sequence on both ends of the C-FABP CDNAs. After ligation reaction, the recombinant DNAs were double digested using *KpnI* /*PstI* to confirm that the DNA fragment of C-FABP-WT (A), C-FABP-109A and C-FABP-109/129A (B) was inserted into the vector. The undigested pQE vector was used as control as shown in control lanes. (A) The bottom band represents DNA fragment of C-FABP-WT. The top band represents digested pQE 30, 31 and 32 vectors. (B) The bottom bands represent DNA fragment of C-FABP-109A and C-FABP-109/129A, respectively. The top bands represent digested pQE 32 vector. In panel A and B, the DNA standard marker in lane M is denoted in number of base pairs.

## 4.2.4 Confirmation of successful insertion of wild type and mutant C-FABP cDNAs into pQEs expression vector

### 4.2.4.1 Sequences analysis of plasmid DNAs

The ligation reaction was transfected into *E.coli* cells and the colonies have the cloning vector was selected and the total DNA from *E.coli* cell purified and subjected to sequencing analysis. The sequence obtained from the cloning vector was shown in Figure 4.11, Figure 4.12 and Figure 4.13. The total DNAs were sent for sequencing at the Cogenics Technologies<sup>TM</sup> (Essex, UK), 100ng/μl (10μl) of each purified DNA was analysed. pQE Forward and pQE Reverse primers were used according to Cogenics Technologies. Sequence alignment was determined by using BioEdit for searching Genbank (BLAST).

Forward primer (pQEF)

5'-CCCGAAAAGTGCCACCTG-3'

Reverse primer (pQER)

5'-GTTCTGAGGTCATTACTGG-3'

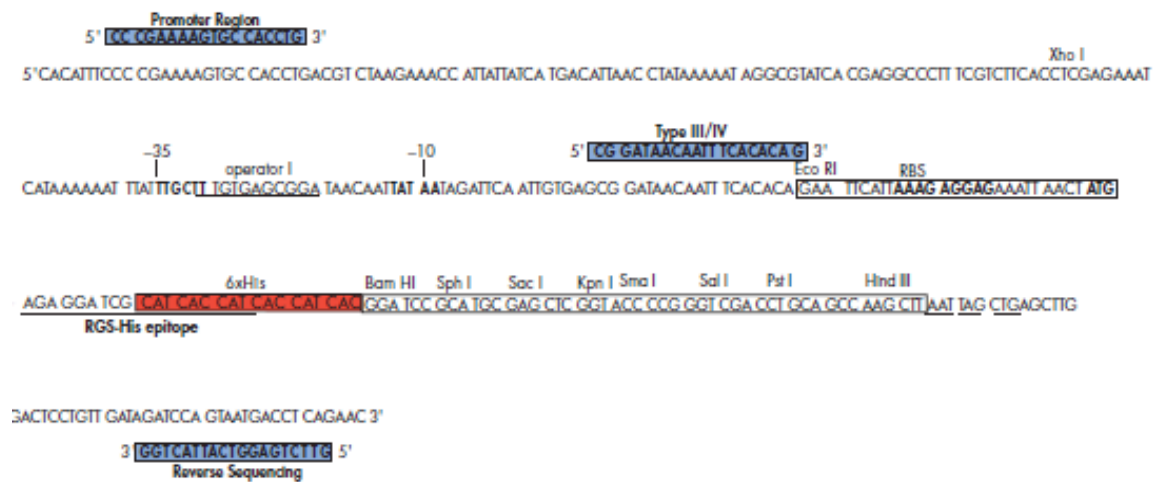


**Figure 4.9: Sequencing primers for pQE vectors**

#### 4.2.4.2 Confirmation of Correct reading frame for recombinant proteins production

Expression vectors pQE30, 31 and 32 plasmid DNA containing wild type and mutant types of C-FABP were sequenced in order to determine which plasmid ought to be used for recombinant protein production. It is important that the start codon (ATG) for the C-FABPs is in the same reading frame as the start codon (ATG) for the 6xhistage of the expression vector pQEs.

Sequencing results showed that pQE32 was the clone that achieved the correct reading frame for the C-FABP (wild type and mutants) as shown in Figure 4.10. Therefore, pQE32 was identified and chosen for protein induction.

**A**Start Codon6x HisTTAAAGAGGAGAAATTAACTATG AGA GGA TCG CAT CAC CAT CACKpnICAT CAC GGA TCC GCA TGC GAG CTC GGT ACC GGG CCC CCCC-FABP Sequences (Insert)CTC GAG ATC TTC GAA TTC GGC TTA CCG CCG ACG CAG ACCStart CodonCCT CTC TGC ACG CCA GCC CGC CCG CAC CCA CCATGG**B**Start Codon6x HisGAGGAGAAATTAACTATG AGA GGA TCT CAC CAT CAC CAT CAC CATKpnIACG GAT CCG CAT GCG AGC TCG GTA CCG GGC CCC CCC TCG AGAC-FABP Sequences (Insert)TCT TCG AAT TCG GCT TAC CGC CGA CGC AGA CCC CTC TCT GCA CGCStart CodonCAG CCC GCC CGC ACC CAC CACTGG

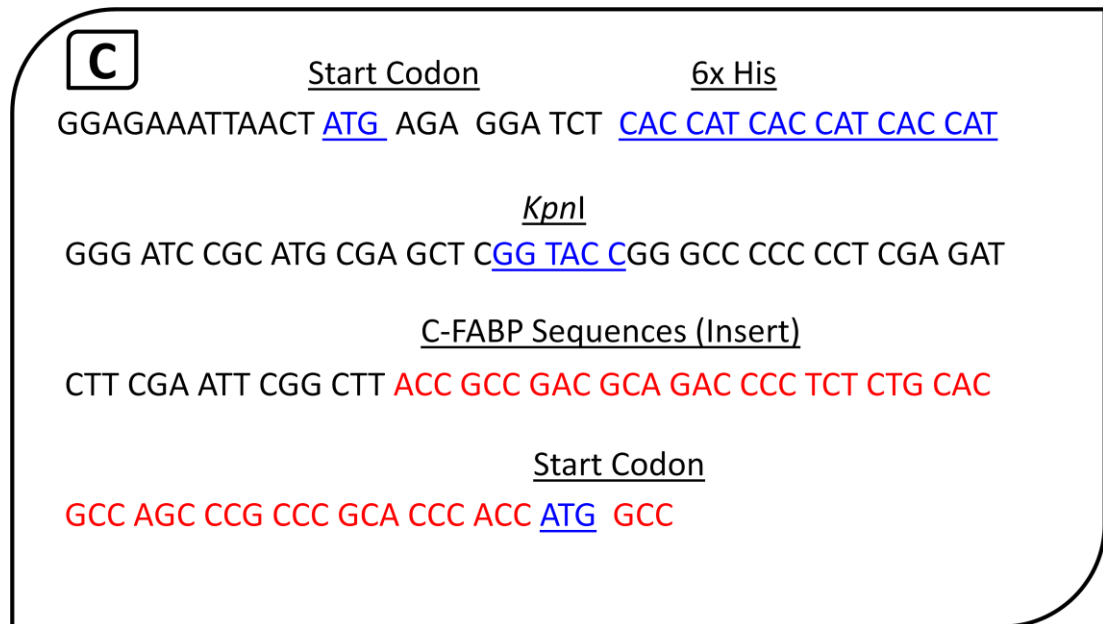


**Figure 4.10: confirmation of correct reading frame for recombinant C-FABP proteins production**

(A) Insertion of C-FABP-WT into expression vector pQE30. (B) Insertion of C-FABP-WT into pQE31. (C) Insertion of C-FABP-WT into pQE32. According to the sequencing analysis and the alignment of the codon, pQE32 has the correct reading frame that was identified and used for protein production.



```

GACTTACCTATAAAATAGGCGTATCACGAGGCCCTTTCGTCTTCACCTCGAGAAATCATA
AAAAATTTATTTGCTTTGTGAGCGGATAACAATTATAATAGATTCAATTGTGAGCGGATA
ACAATTTACACAGAATTCATTAAAGAGGAGAAATTAAGTATGAGAGGATCTCACCATC
ACCATCACCATGGGATCCGCATGCGAGCTCGGTACCGGGCCCCCCTCGAGATCTTCGA
ATTCGGCTTACCGCCGACGCAGACCCCTCTCTGCACGCCAGCCGCCCCGCACCCACCAT
GGCCACAGTTCAGCAGCTGGAAGGAAGATGGCGCCTGGTGGACAGCAAAGGCTTTG
ATGAATACATGAAGGAGCTAGGAGTGGGAATAGCTTTGCGAAAAATGGGCGCAATGG
CCAAGCCAGATTGTATCATCACTTGTGATGGTAAAAACCTCACCATAAAAACTGAGAGC
ACTTTGAAAACAACACAGTTTTCTTGTACCCTGGGAGAGAAGTTTGAAGAAACCACAG
CTGATGGCAGAAAACTCAGACTGTCTGCACTTTACAGATGGTGCATTGGTTCAGCAT
CAGGAGTGGGATGGGAAGGAAAGCACAATAACAAGAAAATTGAAAGATGGGAAACT
AGTGGTGGAGTGTGTCATGAACAATGTACCTGTACTCGGATCTATGAAAAAGTAGAAT
AAAAATTCATCATCACTTTGGACAGGAGTTAATTAAGAGAACGACCAAGCTCAGTTCA
ATGAGCAAATCTCCATACTGTTTCTTTCTTTTTTTTTTTCATTACTGTGTTCAATTATCTTTAT
CATAAACATTTTACATGCAGCTATTTCAAAGTGTGTTGGATTAATTAGGATCATCCCTTG
GTTAATAAATAAATGTGTTTGTGCTAAAGCCGAATTCCGCGGCCGCAGGCCTCTAGAGT
CGACCTGCAGCCAAGCTTAATNAGCTGAGCTTGGACTCCTGNTGATAGATCCAGTAAT
GACCTCANANCTCCATCTGGATTTGTTCAAAACGCTCGGTTGCCCCNGGCGTTTTTTT
TGGGNGAAAATCCAGCTAGCTGGGCGAGATTTTCAG

```

**Figure 4.11: Insertion of C-FABP-WT cDNA into pQE32 expression vector**

*Sequence alignment was determined by using BioEdit for searching Genbank (BLAST) (appendix 3). The sequences marked in red colour are C-FABP-WT (insert) while the sequences marked in black colour are pQE32 (vector). The sequences marked in blue colour are multiple restriction sites as GGTACC represents *KpnI* and CTGCAG represents *PstI*.*

```

CTGACTTACCTATAAAATAGGCGTATCACGAGGCCCTTTCGTCTTCACCTCGAGAAATCA
TAAAAAATTTATTTGCTTTGTGAGCGGATAACAATTATAATAGATTCAATTGTGAGCGGA
TAACAATTTACACAGAATTCATTAAAGAGGAGAAATTAAGTATGAGAGGATCTACCA
TCACCATCACCATGGGATCCGCATGCGAGCTCGGTACCGGGCCCCCCTCGAGATCTTC
GAATTCGGCTTACCGCCGACGCAGACCCCTCTCTGCACGCCAGCCCGCCCGCACCCAC
CATGGCCACAGTTCAGCAGCTGGAAGGAAGATGGCGCCTGGTGGACAGCAAAGGCTT
TGATGAATACATGAAGGAGCTAGGAGTGGGAATAGCTTTGCGAAAAATGGGCGCAAT
GGCCAAGCCAGATTGTATCATCACTTGTGATGGTAAAAACCTCACCATAAAAACTGAGA
GCACTTTGAAAAACAACAGTTTTCTGTACCCTGGGAGAGAAGTTTGAAGAAACCAC
AGCTGATGGCAGAAAACTCAGACTGTCTGCACTTTACAGATGGTGCATTGGTTCAG
CATCAGGAGTGGGATGGGAAGGAAAGCACAATAACAGCAAATTGAAAGATGGGAA
ACTAGTGGTGGAGTGTGTATGAACAATGTCACCTGTACTCGGATCTATGAAAAAGTAG
AATAAAAATTCATCATCACTTTGGACAGGAGTTAATTAAGAGAACGACCAAGCTCAGT
TCAATGAGCAAATCTCCATACTGTTTCTTTCTTTTTTTTTCATTACTGTGTTCAATTATCT
TTATCATAAACATTTTACATGCAGCTATTTCAAAGTGTGTTGGATTAATTAGGATCATCCC
TTTGGTTAATAATAAATGTGTTGTGCTAAAGCCGAATTCCGCGGCCGCAGGCCTCTA
GAGTCGACCTGCAGCCNAGCTNAATTAGCTGAGCTTGGACTCCTGTTGATAGATCCAG
TAATGACCTCAGAACTCCATCTGGATTGTTCAAACGCTCGGTTGCCGCCGGGCGTTTTT
ATTGGNGAAATCAGCTAGCTGGGCGAGATTTNCAGGAGCTANGGAGCTAAATGNAA
AAAAATTCCTGGATTNCCCCGTTGATTNTCCNATGGCTCGTAAANANATTTGA

```

**Figure 4.12: Insertion of C-FABP-R109A cDNA into pQE32 expression vector**

Sequence alignment was determined by using BioEdit for searching Genbank (BLAST) (appendix 3). The sequences marked in red colour are C-FABP-R109A (insert) while the sequences marked in black colour are pQE32 (vector). The sequences marked in blue colour are multiple restriction sites as GGTACC represents *KpnI* and CTGCAG represents *PstI*. GC represents single mutation (The Alanine GCA, mutated from Arginine AGA).

```

CTTTTCTGACTTACCTATAAAATAGGCGTATCACGAGGCCCTTTCGTCTTCACCTCGAG
AAATCATAAAAAATTTATTTGCTTTGTGAGCGGATAACAATTATAATAGATTCAATTGTGA
GCGGATAACAATTTACACAGAATTCATTAAAGAGGAGAAATTAAGTATGAGAGGATCT
CACCATCACCATCACCATGGGATCCGCATGCGAGCTCGGTACCGGGCCCCCCTCGAGA
TCTTCGAATTCGGCTTACCGCCGACGCAGACCCCTCTCTGCACGCCAGCCCGCCCGCAC
CCACCATGGCCACAGTTCAGCAGCTGGAAGGAAGATGGCGCCTGGTGGACAGCAAAG
GCTTTGATGAATACATGAAGGAGCTAGGAGTGGAATAGCTTTGCGAAAAATGGGCG
CAATGGCCAAGCCAGATTGTATCATCACTTGTGATGGTAAAAACCTCACCATAAAAACT
GAGAGCACTTTGAAAAACAACAGTTTTCTTGACCCTGGGAGAGAAGTTTGAAGAA
ACCACAGCTGATGGCAGAAAAACTCAGACTGTCTGCAACTTTACAGATGGTGCATTGG
TTCAGCATCAGGAGTGGGATGGGAAGGAAAGCACATAACAGCAAAATTGAAAGATG
GGAACTAGTGGTGGAGTGTGTCATGAACAATGTCACCTGTACTGCGATCTATGAAAA
GTAGAATAAAAAATTCCATCATCACTTTGGACAGGAGTTAATTAAGAGAACGACCAAGCT
CAGTTCAATGAGCAAATCTCCATACTGTTTCTTTCTTTTTTTTTCATTACTGTGTTCAATT
ATCTTTATCATAAACATTTTACATGCAGCTATTTCAAAGTGTTGGATTAATTAGGATCA
TCCCTTGGTTAATAATAAATGTGTTTGCTTAANGCCGAATCCGCGGCCCGCAGGCC
TCTAGAGTCGACCTGCAGCCNAGCTTAATTAGCTGAGCTGGGACTCCTGTTGATAGATC
CAGTAATGACCTCAGANCTCCATCTGGATTNGTTCAGANCGCTCGGTTGCCCGCCGGG
CGTTTTTTTTTGGTGAAATCCAGCTAGCTNNGCGAGATTNNNGGAGCTANGGAGCTAAA
TGGAAAAAAAATCCTGGATTACCCNGTTGATTTCCNATGGCTCGTAANA

```

**Figure 4.13: Insertion of C-FABP-R109/129A cDNA into pQE32 expression vector**

Sequence alignment was determined by using BioEdit for searching Genbank (BLAST) (appendix 3). The sequences marked in red colour are C-FABP-R109/129A (insert) while the sequences marked in black colour are pQE32 (vector). The sequences marked in blue colour are multiple restriction sites as GGTACC represents KpnI and CTGCAG represents PstI. GC and GC represent double mutation (The Alanine GCA, mutated from Arginine AGA and the Alanine GCG, converted from Arginine CGG).

## 4.2.5 Expression and purification of recombinant C-FABP proteins

### 4.2.5.1 Time course analysis of protein expression

To optimize the expression of a given protein construct, a time-course analysis of the level of protein expression is recommended (Figure 4.14). Intracellular protein content is often a balance between the amount of soluble protein in the cells, the formation of inclusion bodies, and protein degradation. By checking the 6xHis-tagged protein present at various times after induction in the soluble fractions, the optimal induction period can be established. The maximum amount of protein was achieved at 5 hours of IPTG induction as shown in Figure 4.14. However, continuous incubation after this time protein started to degrade.

A single colony was picked from selective antibiotic LB agar plate and inoculated into a 10ml LB medium containing 50µg/ml ampicillin in a 50ml flask and incubated at 37°C overnight. 250ml of pre-warmed media with ampicillin was inoculated with 10ml of the overnight culture and grown at 37°C with vigorous shaking until an OD<sub>600</sub> of 0.6 was reached (30-60 min). 0.5ml sample was taken immediately before induction (this sample is the non-induced control). Expression of wild type and mutant C-FABP proteins were induced by adding 1mM of IPTG. A second 0.5ml was collected (this sample is the induced control). Culture was incubated for an additional 4-5 hours with 0.5ml samples taken each hour. Cells were harvested by centrifugation at 4000xg for 20 min. Cell pellets were stored overnight at -20°C until further use.

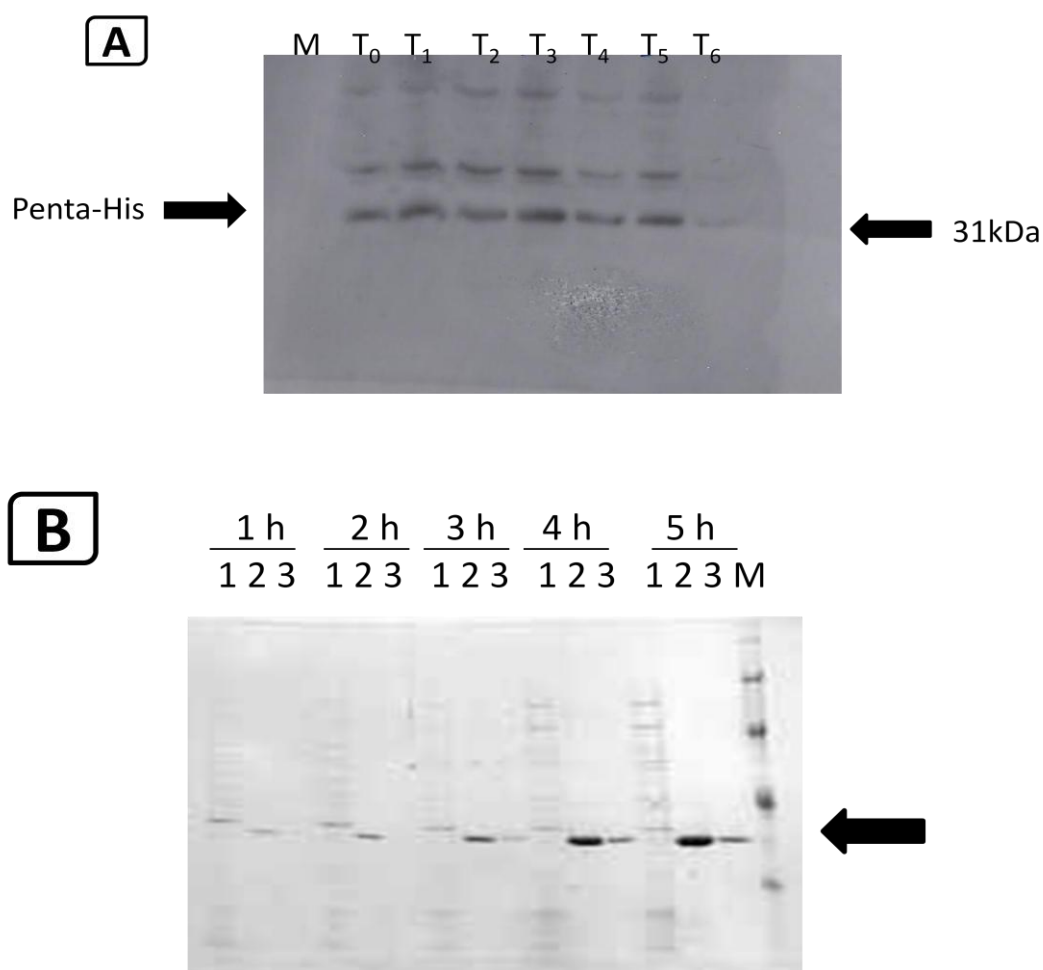


**Figure 4.14: protein expression and time course for C-FABP-WT**

Expression of 6xHis-tagged was induced with 1mM IPTG. Aliquots were removed at the times indicated purified on Ni-NTA agarose under denaturing conditions. Proteins were visualised by SDS-PAGE analysis. Yields per litre cultures were 2.9, 5.7, 12.6, 34 and 60.2 mg respectively. (A) Crude cell lysate. M: Marker, T<sub>0</sub>: non induced control, T<sub>1-6</sub>: IPTG induced after an hour to 6 hours, 6His-tagged pounded protein bands were recognised by Penta-His antibody (31 KDa). (B) Purification with Ni-NTA, C-FABP protein bands were recognized by a monoclonal anti-human C-FABP antibody and visualized as described in Chapter 2 (14 KDa). 1: flow through fraction, 2 & 3: first and second elutes.

#### 4.2.5.2 Purification of 6xHis-tagged C-FABP proteins

Cell pellets were resuspended in 10ml denaturing lysis buffer (pH 8.0). Cell suspensions were incubated at RT (15-25°C) for 60 min. After an hour cell suspensions were mixed 2-3 times by gently swirling the suspensions (lysis is completed when the suspension is translucent). Lysates were centrifuged at 14000xg for 30 min at RT to pellet the cellular debris (the supernatants contain the recombinant protein). 5µl 2x SDS-PAGE sample buffer was added to a 5µl aliquot of the supernatant and stored at -20°C for SDS-PAGE analysis. The resin in a fast star column was gently resuspended by inverting it several times. The seal at the outlet of the column was broken, screw cap was opened, and the storage buffer allowed draining out. The cell lysate supernatants were applied to the column. The flow-through fractions were collected and 5µl 2x SDS-PAGE sample buffer was added to a 5µl aliquot of the flow-through fractions and stored at -20°C for SDS-PAGE analysis. Columns were washed 2 times with 4ml of denaturing wash buffer (pH 6.3) and both wash fractions were collected. 5µl 2x SDS-PAGE sample buffer was added to a 5µl aliquot of each wash fraction and stored at -20°C for SDS-PAGE analysis. Bound 6xHis-tagged proteins were eluted with 1ml aliquots of denaturing elution buffer (pH 4.5) and each elution fraction was collected in a separate tube. 5µl 2x SDS-PAGE sample buffer was added to a 5µl aliquot of each elution fractions and stored at -20°C for SDS-PAGE analysis. All fractions were analysed by SDS-PAGE as shown in Figure 4.15.

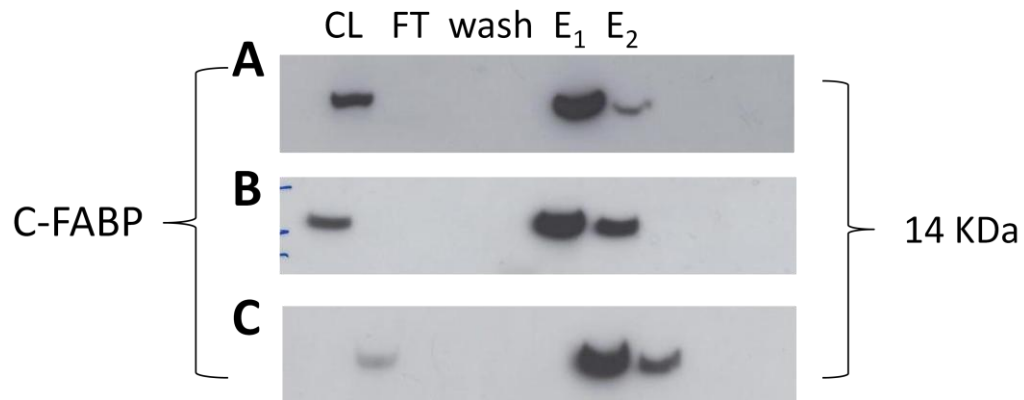


**Figure 4.15: Western blot analysis of the 6xHis-tagged wild type and mutant C-FABP proteins**

*After elution, un-bound 6xHis-tagged proteins were subjected to western blot analysis. C-FABP protein bands were recognized by a monoclonal anti-human C-FABP antibody and visualized as described in Chapter 2. (A) C-FABP-WT. (B) C-FABP-R109A. (C) C-FABP-R109/129A. CL: Cell lysate, FT: Flow-through fraction,  $E_1$  &  $E_2$ : first and second elutes.*

#### 4.2.6 Fatty acid binding assay for recombinant C-FABP proteins

Fatty acid binding capability of the three FABPs was examined by using the environment-sensitive fluorescent fatty acid analogue DAUDA (11-(Dansylamino)undecanoic acid) that alters its fluorescence emission spectra and intensities on entry into binding proteins. The blue shift of DAUDA fluorescence maximum from 542 to 537, 529 and 527 nm for C-FABP-WT, C-FABP-R109A and C-FABP-R109/129A, respectively, and the associated increase of its fluorescence emission (both indicative of the entry of DAUDA into a polar environment (Hagan *et*

*al.*, 2008)) confirmed the binding of the fluorescent fatty acid to the three C-FABP variants. These shifts are comparable with the result obtained from structurally related FABPs such as the heart FABP, brain FABP and adipocyte FABP where the fluorescence emission moves to 536, 531 and 530nm, respectively (Zimmerman *et al.*, 2001), value closer to what was observed for C-FABP. Interestingly, the dissociation constants ( $K_d$ ) for DAUDA binding to the three C-FABP variants were similar (0.65, 0.75 and 0.67 for C-FABP-WT, C-FABP-R109A and C-FABP-R109/129A, respectively) and the maximum fluorescence ( $F_{max}$ ) were also similar (125, 123 and 132 for C-FABP-WT, C-FABP-R109A and C-FABP-R109/129A, respectively) as shown in Figure 4.16. To highlight the possible differences in the binding affinities of the three C-FABP proteins for other fatty acids, we performed competitive experiments using DAUDA as a tracer and some natural fatty acids as competitor. The addition of myristic ( $C_{14}$ ), palmitic ( $C_{16}$ ), oleic ( $C_{18}$ ) and linoleic acids ( $C_{20}$ ) indeed revealed a diverse affinity of the three wild type and mutants C-FABP. The efficiency of each fatty acid to displace DAUDA from the C-FABP proteins binding pocket is shown in Figure 4.17. A value of 100% indicates the complete displacement of DAUDA. The data showed that C-FABP-WT has the higher affinity of DAUDA displacement and binding to natural fatty acids (80, 81, 84 and 92% for myristic, palmitic, oleic and linoleic acids, respectively). In contrast, when fatty acid binding ability of the C-FABP-WT is set at 1, the fatty acid binding ability of the C-FABP-R109A was significantly reduced to 0.35, 0.37, 0.39 and 0.43, respectively, when bound to natural fatty acids. The fatty acid binding ability of the C-FABP-R109/129A was further significantly reduced to 00, 0.08, 0.15 and 0.17, respectively (Student t-test,  $P < 0.001$ ).



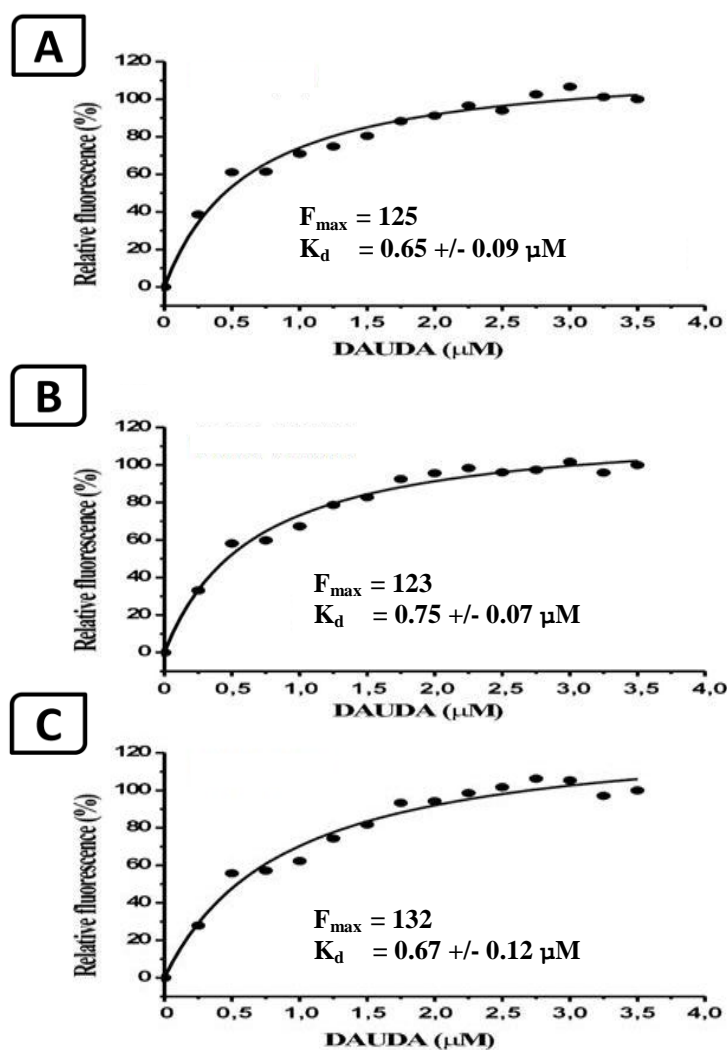


**Figure 4.16: Titration curves of DAUDA binding to C-FABP proteins.**

*Increasing amounts of DAUDA were added to a 2  $\mu\text{M}$  solution of the protein in PBS.*

*The enhancement of DAUDA fluorescence upon binding to the C-FABP variants was obtained by subtracting the fluorescence of the same concentration of DAUDA in the absence of the protein. All of the data were analyzed by a non-linear regression model according to Hill's function using the origin programme. (A) C-FABP-WT. (B) C-FABP-R109A. (C) C-FABP-R109/129A.*

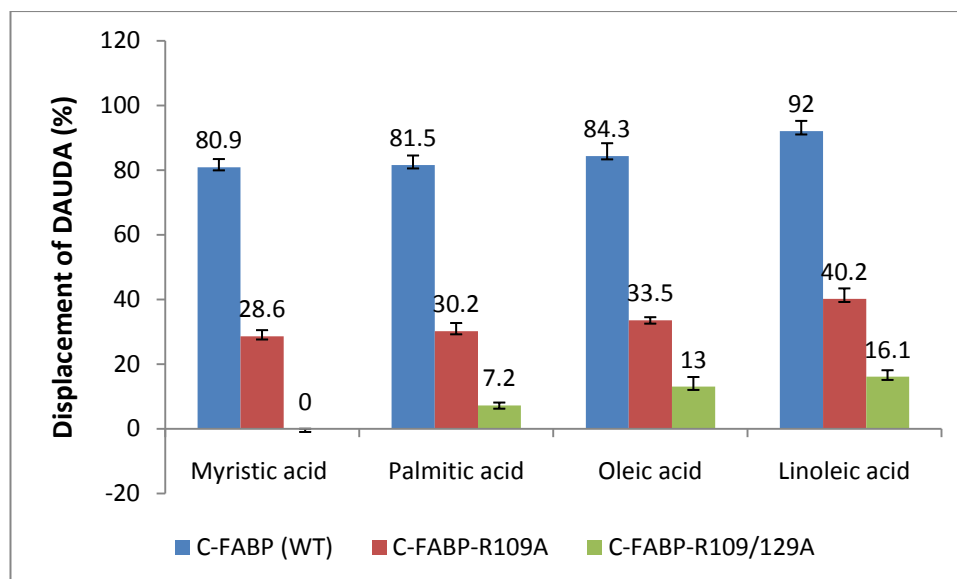


**Figure 4.17: Displacement of DAUDA binding to three C-FABP proteins by natural fatty acids.**

*The percentage of displacement is indicated above each bar. Competitive binding experiments were carried out using 2  $\mu$ M DAUDA in the presence of 2  $\mu$ M of each natural fatty acid and 2  $\mu$ M of each C-FABP proteins. Data expressed as means $\pm$ SD of three independent experiments.*

### 4.3 Discussion

In previous chapter, one or two site-directed point mutations into the C-FABP cDNA region containing the fatty acid-binding motif were successfully generated. The wild type and mutant C-FABP cDNAs were contained in the pIRES2-EGFP vector. When the wild type and mutant C-FABP cDNAs were cloned into an expression vector to produce recombinant C-FABPs, it was found that in the multiple cloning sites of this construct, there was no complimentary restriction site for the expression vector pQE. Therefore, before the C-FABP cDNAs were inserted into to the expression vector pQEs, it was necessary to generate complimentary restriction sites at both ends of the cDNAs. Thus, the C-FABP-cDNAs were excised from pIRES2-EGFP with restriction enzymes *XhoI* and *PstI* and inserted into cloning vector pBluescript which contains the multiple restriction sites (*KpnI* and *PstI*). The C-FABP cDNAs were then excised out from the pBluescript vector with *KpnI* and *PstI* and then inserted into the expression vector pQEs to form three constructions which will express the C-FABP-WT, C-FABP-R109, and C-FABP-R109/129A, respectively.

The insertion of C-FABP cDNAs into pQEs expression vector (Figure 4.11) were successful and confirmed by sequences analysis. Further analysis confirmed that pQE32 (Figure 4.10) is only vector that remain the ATG codon unchanged. Therefore, PQE32 was identifies and chosen as the construct to produce recombinant proteins.

When the recombinant protein is synthesised in *E.coli* cells, different expression systems have different efficiencies. Thus, it is necessary to found out the time point at which the maximum yield of protein is synthesised in *E.coli* cells. In this work, it was found that the amount of protein synthesis is increased as the increasing incubation time, and reached the maximum at five hours after IPTG induction. Once reached the maximum, any further induction and incubation was not accompanied with any further increment in protein synthesis. Instead, the yield of recombinant protein was reduced (Figure 4.14). This could due to either the cessation of production inside the *E. coli* cells or the degradation of the completed synthesised proteins. Therefore, the optimal time at which the maximum yield of protein production was achieved is 5 hours after IPTG induction.

C-FABP is a small molecule (14 KDa) and the protein produced in *E.coli* was soluble with the 6xHis-tagged system. The 6xHis affinity tag facilitates binding to Ni-NTA. Using pQE vectors it can be placed at the C- or N-terminus of the protein. It is poorly immunogenic, and at pH 8.0 the tag is small, uncharged, and therefore does not generally affect secretion, compartmentalization, or folding of the fusion protein within the cell. As well as, the 6xHis tag does not affect the structure or function of the purified protein as demonstrated for a wide variety of proteins, including C-FABP proteins.

After C-FABP was separate from the 6xhis-tagged using Ni-NTA Fast Start column and subjected to Western blot analysis (Figure 4.15), a single band at the correct site

of the blot was visualised. This result indicated that the separation of the recombinant C-FABP proteins from the *E. coli* bacterial proteins was very successful and the recombinant proteins obtained from purification procedures were very pure.

To test whether the recombinant proteins produced were biological active, we have tested the fatty acid binding ability of wild type and mutant C-FABPs. The fatty acid binding ability of the C-FABP-WT was 80%, 81%, 84% and 92%, respectively, when bind to natural fatty acids (myristic, palmitic, oleic and linoleic acids). When fatty acid binding ability of the wild type C-FABP is set at 1, the fatty acid binding ability of the C-FABP-R109A was reduced to 0.35, 0.37, 0.39 and 0.43, respectively, when bind to natural fatty acids. The fatty acid binding ability of the C-FABP-R109/129A was further reduced to 00, 0.08, 0.15 and 0.17, respectively, when bound to natural fatty acids (Figure 4.17). These result suggested that fatty acid binding ability of C-FABP depends on its structure integrity of the binding motif. Therefore, changing one amino acid in motif by site-directed point mutation significantly reduced the fatty acid binding ability and changing two amino acids by sites-directed mutations almost completely deprived the fatty acid binding ability of C-FABP.

In the experiments described in this chapter, the wild type and mutated C-FABP cDNAs have been successfully cloned into the expression vector and different recombinant protein expression constructs were successfully established. Using the pQE *E. coli* expression system, it is possible that 60.2mg of recombinant proteins can be produced and purified from 1 litre of bacterial cells. The availability of large amount of pure wild type and mutant C-FABPs provided an excellent opportunity to further study and compare their biological activities.

## **5 Effect of overexpression of recombinant wild type and mutant C-FABPs on tumorigenicity of prostate cancer cells**

## 5.1 Introduction

In Chapter 4, recombinant protein of mutant and wild type C-FABPs were produced in *E. coli* cells and successfully expressed and purified. To reveal whether the fatty acid binding ability is essential for C-FABP to promote cancer development progression, fatty acid binding ability of recombinant wild type and mutant C-FABPs were monitored. In this Chapter, to study further the effect of the structure changing of fatty acid binding motif of C-FABP on its ability of cancer promoting activity, we have further conducted experiments to study the relationship between fatty acid binding motif and tumorigenicity.

Cell proliferation and invasion ability are significant factors which contribute to tumorigenicity and metastasis. Morgan *et al* found that cell proliferation rate was significantly reduced by 2.5-fold in siRNA transfected prostate cancer cell line PC-3M, in which the expression level of C-FABP was suppressed, compared to the parental cell line (Morgan *et al*, 2008). Moreover, it has been showed that suppression of C-FABP expression resulted in a significant reduction of the cell invasiveness and inhibition of metastasis (Adamson *et al*, 2003; Morgan *et al*, 2008). In contrast, Fang *et.al* reported that overexpression of C-FABP in transfected human oral squamous carcinoma cells was associated with promoting the cancer cells growth rate and invasion ability (Fang *et al*, 2009) suggesting that increase expression of C-FABP may be related to malignant progression.

Tumour progression is complex, involving multiple mutations of tumour suppressor genes, and/or proto-oncogenes resulting in loss of control of cell proliferation. Several studies showed that androgen-dependent human prostate cancer LNCaP cells

hardly formed tumours with 0%-50% tumorigenicity rate when inoculated subcutaneous (SC) in immunodeficient nude mice (Gleave *et al*, 1991; Horoszewicz *et al*, 1983b) and even if the tumour was formed, the tumour growth was very slow. Morgan *et.al* showed that suppression of C-FABP expression level in PC-3M cells significantly reduced tumour formation ability of the cancer cells both *in vitro* and *in vivo* (Morgan *et al*, 2008). Similar results had been achieved by using antisense RNA to suppress C-FABP expression (Adamson *et al*, 2003). Nevertheless, the tumorigenicity of LNCaP cells with overexpression of C-FABP has not been reported. In contrast to PC-3M cells which express very high level of C-FABP, the weakly malignant LNCaP cells do not express detectable level of C-FABP. It is interesting to know whether the tumorigenicity of LNCaP can be increased by elevated C-FABP expression.

As mentioned in Chapter 4, the biological function of C-FABP in normal condition is to bind to fatty acids and to transport them into cells, it is important to understand whether the ability of binding to fatty acids is related to the tumorigenicity promoting function of C-FABP in experiments of this Chapter. The recombinant C-FABPs were subjected to different *in vitro* assessments to analyze the effect of overexpression of wild type and mutant C-FABPs on the cell properties associated with tumour development and malignancy.



## 5.2 Results

### 5.2.1 The effect of wild type and mutant C-FABPs on cellular fatty acid uptake

The orange-red fluorescence-labelled fatty acid BODIPY 558/568 C<sub>12</sub> [4, 4-difluoro-5- (2-thienyl)-4-bora-3a, 4a-diaza-s-indacene-3-dodecanoic acid], which act as the analogue of natural LCFA, was applied to examine the level of fatty acid uptake for each C-FABPs. The fluorescence intensity of each single cell before and 45 minutes after adding labelled LCFA was measured using an EPICS XL Cytometer at the wave length of 570 nm to assess the fatty acid uptake capacities as described in Chapter 2.

The fatty acid uptakes in LNCaP cells treated with C-FABP proteins were shown in Figure 5.1. The peaks in the each diagram represented the red fluorescence intensities which were quantified by manufacture's software as demonstrated in X-Mean. The number and proportion of cells in each cell line were also indicated in the diagram column number and %Gated respectively. Relative levels of LCFA uptake (Figure 5.2). When the level of fatty acid uptake in control was set at 1, levels in C-FABP-WT, C-FABP-R109A, and C-FABP-R109/129A were  $6.8 \pm 0.75$ ,  $3.5 \pm 0.5$  and  $2.7 \pm 0.8$  respectively. In comparison with the control, the fatty acid uptake by C-FABP-WT was significantly higher (Student t-test,  $P=0.005$ ). However, the fatty acid uptake between C-FABP-R109A and the control, or that between C-FABP-R109/129A and the control, was at similar level (Student t-test,  $P=0.013$ ,  $P=0.063$ , respectively). Further statistical analysis showed that a significant difference was observed in fatty acid uptakes between C-FABP-WT and C-FABP-R109A or C-

FABP-R109/129A (Student t-test,  $P=0.044$ ,  $P=0.026$ , respectively). However, no difference was observed in fatty acid uptakes between C-FABP-R109A and C-FABP-R109/129A (Student t-test,  $P=0.199$ ).

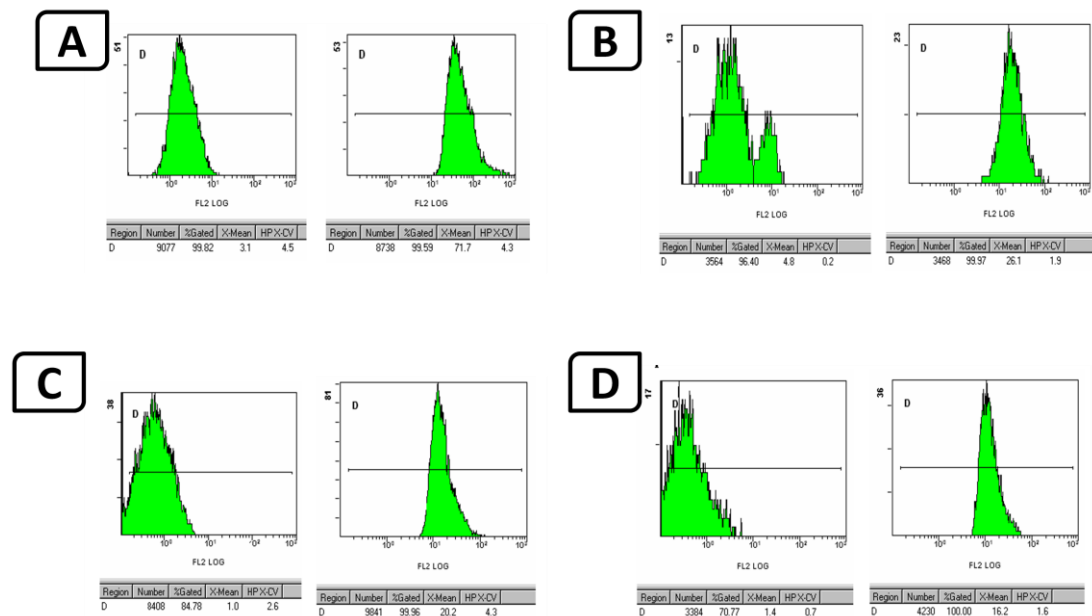


**Figure 5.1: Fatty acid uptakes by C-FABP cDNAs at absence and presence of red fluorescence labelled LCFA.**

*Flow cytometry analysis of LCFA uptake by LNCaP cell line. Fluorescence labelled BODIPY 558/568C<sub>12</sub> was added to the cultured cells and plated at  $1 \times 10^6$  cells/well in a 6-well plate. The fluorescence intensity of each transfected cell lines was assessed (X-Mean) and plotted as histogram before (left panel) and after 30min (right panel) incubation. A: C-FABP-WT; B: C-FABP-R109A; C: C-FABP-R109/129A and D: Control. X-Mean values were; 74.1, 27.1, 20.2 and 14.2, respectively.*

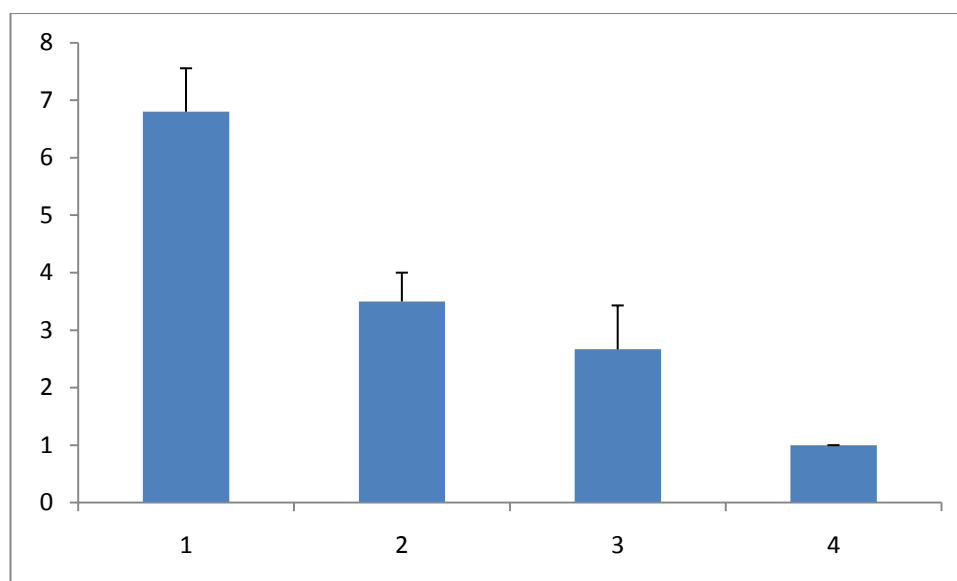


**Figure 5.2: Relative level of LCFA uptake by wild type and mutants C-FABP cDNAs.**

*Relative levels of LCFA uptake C-FABP-WT (Column 1), C-FABP-R109A (Column 2) and C-FABP-R109/129A (Column 3) and the control (Column 4) were measured by flow cytometer. C-FABP-WT had the highest fatty acid uptake capacity and significantly higher than the rest (Student *t*-test  $P < 0.05$ ). Data expressed as means  $\pm$  SD of three independent experiments.*

### 5.2.2 Effect of wild type and mutants C-FABPs on cell proliferation

A proliferation assay *in-vitro* was performed to determine the potential tumorigenic capacity of the wild type and mutant C-FABPs on the weakly malignant and androgen-dependent LNCaP, the androgen-independent but has androgen receptor 22RV1 and the highly malignant and androgen-independent LNCaP-C4<sub>2</sub> cell lines. Standard curve of each tested cell line was constructed as described in Chapter 2.

Diagrams in Figure 5.3, Figure 5.5 and Figure 5.7 presented standard curves for the three cell lines. The MTT forms crystals in cytoplasm and the crystals were dissolved by DMSO. The colorimetric measurement was performed at 570nm wavelength using a spectrophotometer. The values obtained from the plate reader were converted to cell numbers which were extrapolated from the standard curve.

#### 5.2.2.1 LNCaP cell line

The detailed proliferation assay results were shown in Figure 5.4. During the first two days, growth rates of all tested cells were very similar. However, from the 3rd day on, the proliferation rate of C-FABP-WT stimulated cells started to be higher than those of other lines. On the 4<sup>th</sup>, 5<sup>th</sup> the 6<sup>th</sup> day, the numbers of C-FABP-WT stimulated LNCaP cells without adding natural fatty acid were 25941, 28733 and 33608, respectively. At same time points, number of those cells with natural fatty acid stimulations were 31138, 34480 and 50412, respectively. Whereas in the same time points, numbers of cells from the control LNCaP cells only were 19691, 24608 and 27191, respectively and 23630, 29530 and 40787, respectively, of those cells with natural fatty acid stimulations. The proliferation rate of C-FABP-WT stimulated cells was significantly increased by 24% (Day 4), 14% (Day 5) and 19% (Day 6) compared with control cells (Student t-test,  $P=0.0399$ ). Similarly, number of cells stimulated by mutants C-FABP-R109A and C-FABP-R109/129A only were significantly reduced when compared to control cells during the 6 days culture (Student t-test,  $P=0.0069$  and  $P=0.0096$ , respectively ). In addition, number of those cell with natural fatty acid stimulations were also significantly reduced when

compared to control cells during 6 days culture ( $P=0.03$  and  $0.0344$ , respectively). The final cell counts on day 6 and statistical comparison were summarised in Table 5.1

To assess the difference between cells stimulated by C-FABPs only and cells stimulated by C-FABPs plus natural fatty acid, statistical analysis showed that the proliferation rate of cells stimulated by C-FABPs plus natural fatty acids were significantly increased by 20% (C-FABP-WT), 17% (C-FABP-R109A) and 15% (C-FABP-R109/129A) compared with cells stimulated by C-FABPs only (Student t-test,  $P>0.05$ ).

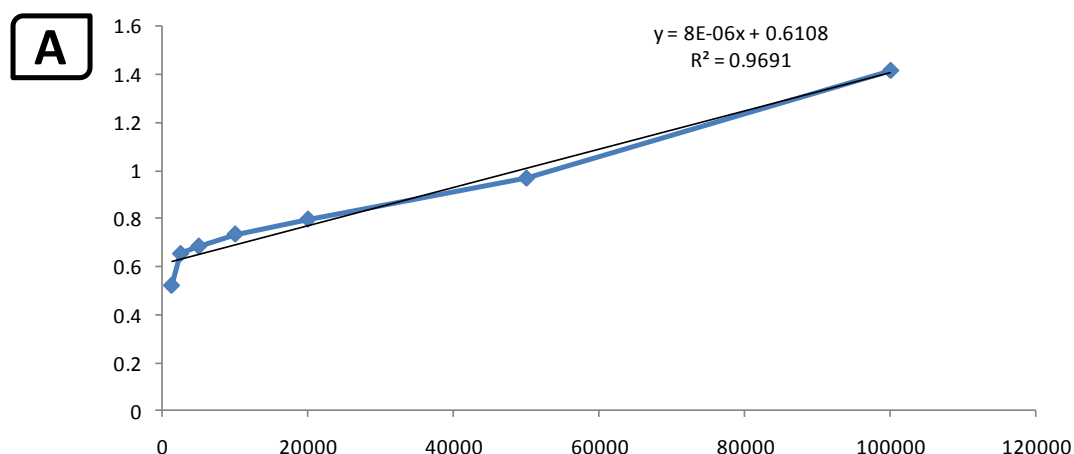


**Figure 5.3: Standard curve for LNCaP cell line**

*A standard curve was established by plotting absorbance (OD at 570nm) (Axis Y) against the number of cells (Axis X). The cell number of samples was determined by comparing serially diluted standard from the standard curve. The curve equation and regression value of standard curve are presented in the diagrams.*

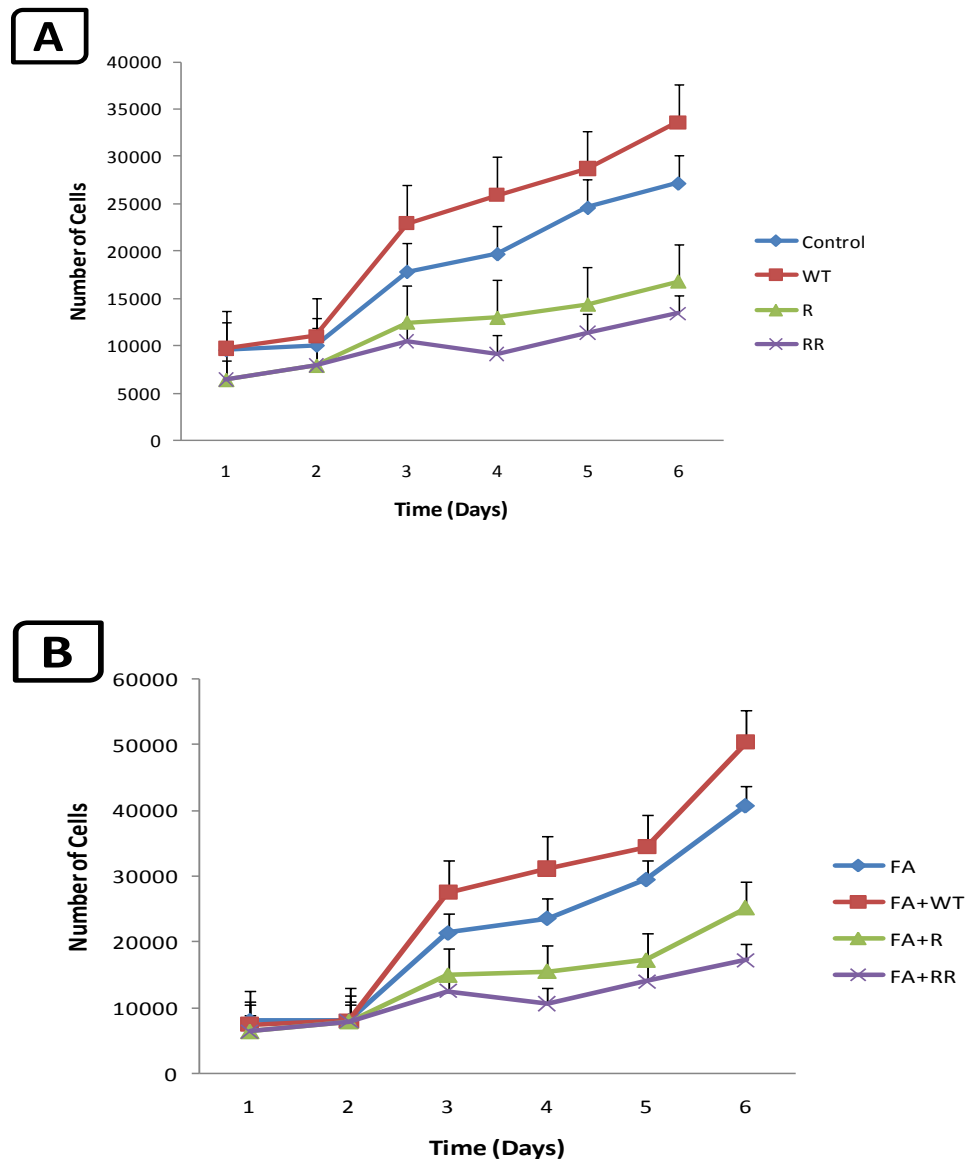


**Figure 5.4: Time course curve of proliferation rate for LNCaP cells stimulated by wild type and mutant C-FABP proteins**

*The numbers of cells stimulated with different C-FABPs, shown mean of three individual experiments were obtained every day during the 6 days period. (A) LNCaP cells were stimulated by recombinant C-FABPs only. (B) LNCaP cells were stimulated by recombinant C-FABPs plus natural fatty acid (Myristic acid). Data expressed as means $\pm$ SD of three independent experiments.*

<b>A</b> LNCaP	Mean number of cells $\pm$ SD	P Value
C-FABP-WT	21988 $\pm$ 9680	0.0165
C-FABP-R109A	11821 $\pm$ 3941	0.0069
C-FABP-R109/129A	9778 $\pm$ 2507	0.0096
Control	18136 $\pm$ 7308	---

<b>B</b> LNCaP	Mean number of cells $\pm$ SD	P Value
C-FABP-WT	26501 $\pm$ 16501	0.0399
C-FABP-R109A	14548 $\pm$ 6817	0.03
C-FABP-R109/129A	11437 $\pm$ 3985	0.0344
Control	21889 $\pm$ 12683	---

**Table 5.1: Cell counts of C-FABPs at the end point of proliferation assay**

*The final cell counts on day 6 and the statistic analyse were shown above. P values were obtained by comparing sample groups to control. (A) LNCaP cells were stimulated by recombinant C-FABPs only. (B) LNCaP cells were stimulated by recombinant C-FABPs plus natural fatty acid (Myristic acid).*

### 5.2.2.2 22RV1 Cell line

The detailed proliferation assay results were demonstrated in Figure 5.6. During the first two days, growth rates of tested cells were very similar. However, from the 3rd day on, the proliferation rate of C-FABP-WT stimulated cells started to be higher than those of other lines. On the 4<sup>th</sup>, 5<sup>th</sup> the 6<sup>th</sup> day, the numbers of C-FABP-WT stimulated LNCaP cells without adding natural fatty acid were 28535, 31606 and 36969, respectively. At same time points, number of those cells with natural fatty acid stimulations were 34243, 37928 and 55453, respectively. Whereas in the same time points, numbers of cells from the control LNCaP without adding fatty acids were 19691, 24608 and 33000, respectively, and number of those cells with natural fatty acid stimulations were 23630, 29530 and 40787, respectively. The proliferation rate of C-FABP-WT stimulated cells was significantly increased by 31% (Day 4), 22% (Day 5) and 26% (Day 6) compared with control cells (Student t-test,  $P=0.0310$ ). Similarly, cell numbers of cells stimulated by mutants C-FABP-R109A and C-FABP-R109/129A only were significantly reduced when compared to control cells during the 6 day culture (Student t-test,  $P=0.0017$  and  $P=0.001$ ). Moreover, number of those cells with natural fatty acid stimulations were also significantly reduced when compared to control cells during 6 days culture ( $P=0.0083$  and  $0.008$ ). The final cell counts on day 6 and statistical comparison were summarised in Table 5.2

To assess the difference between cells stimulated by C-FABPs only and cells stimulated by C-FABPs plus natural fatty acid, statistical analysis showed that the proliferation rate of cells stimulated by C-FABPs plus natural fatty acids were significantly increased by 23% (C-FABP-WT), 20% (C-FABP-R109A) and 16% (C-



FABP-R109/129A) compared with cells stimulated by C-FABPs only (Student t-test,  $P > 0.015$ ).

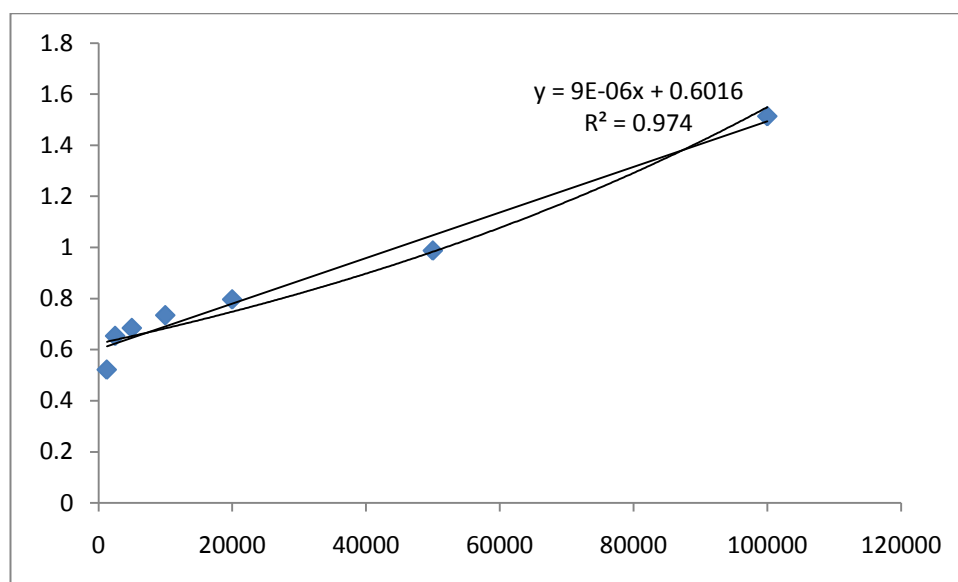


**Figure 5.5: Standard curve for 22RV1 cell line**

A standard growth curve was established by plotting absorbance (OD at 570nm) (Axis Y) against the number of cells (Axis X). The cell number of samples was determined by comparing serially diluted standard from the standard curve. The curve equation and regression value of standard curve are presented in the diagrams.

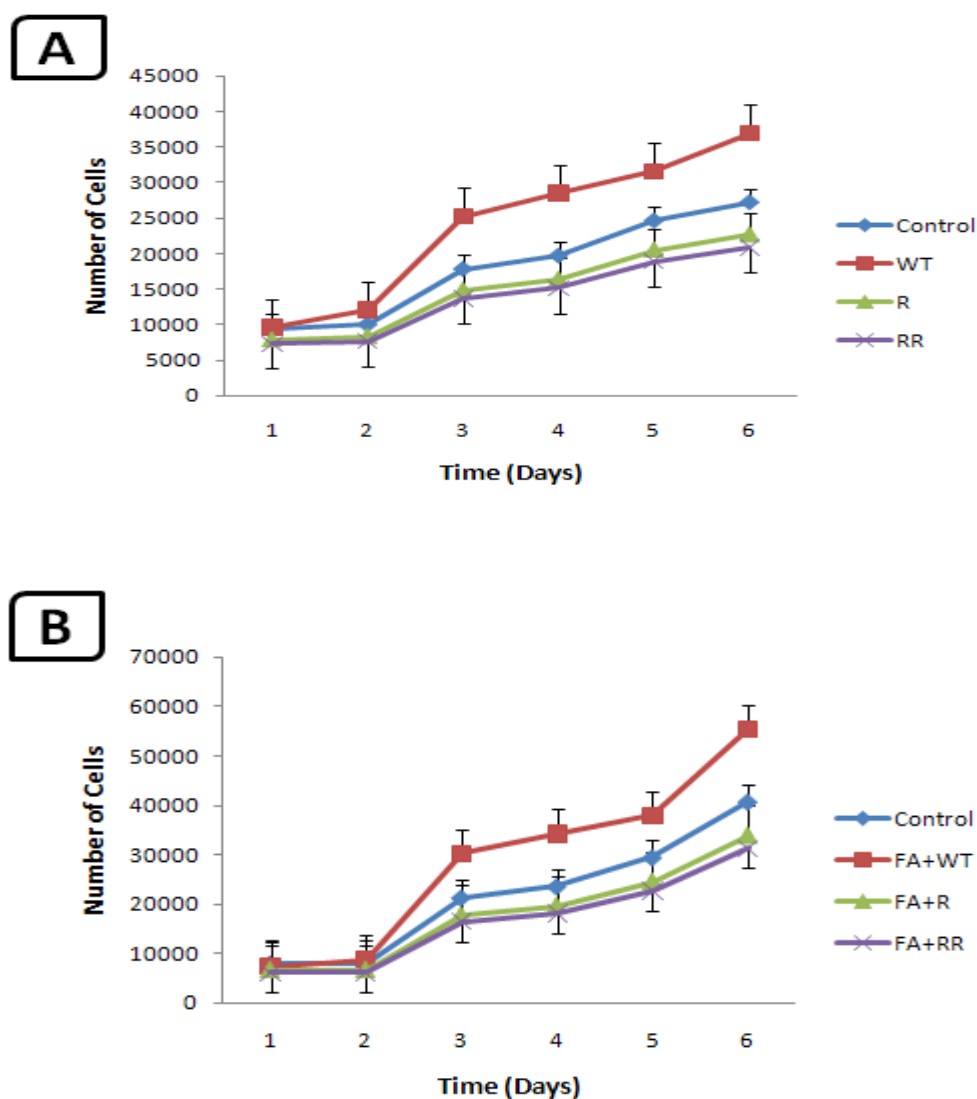


**Figure 5.6: Time course curve of proliferation rate for 22RV1 cells stimulated by wild type and mutant C-FABP proteins**

*The numbers of cells stimulated with different C-FABPs, shown mean of three individual experiments were obtained every day during the 6 days period. (A) 22RV1 cells were stimulated by recombinant C-FABPs only. (B) 22RV1 cells were stimulated by recombinant C-FABPs plus natural fatty acid (Myristic acid). Data expressed as means $\pm$ SD of three independent experiments.*

<b>A</b>	22RV1	Mean number of cells $\pm$ SD	P Value
	C-FABP-WT	24009 $\pm$ 10925	0.0139
	C-FABP-R109A	15113 $\pm$ 6090	0.0017
	C-FABP-R109/129A	13950 $\pm$ 5621	0.001
	Control	18136 $\pm$ 7308	---

<b>B</b>	22RV1	Mean number of cells $\pm$ SD	P Value
	C-FABP-WT	29027 $\pm$ 18334	0.0310
	C-FABP-R109A	18241 $\pm$ 10569	0.0083
	C-FABP-R109/129A	16837 $\pm$ 9756	0.008
	Control	21889 $\pm$ 12683	---

**Table 5.2: Cell counts of C-FABPs at the end point of proliferation assay**

The final cell counts on day 6 and the statistic analyse were shown above. P values were obtained by comparing sample groups to control. (A) 22RV1 cells were stimulated by recombinant C-FABPs only. (B) 22RV1 cells were stimulated by recombinant C-FABPs plus natural fatty acid (Myristic acid).

### 5.2.2.3 LNCaP-C4<sub>2</sub> cell line

The detailed proliferation assay results were demonstrated in Figure 5.8. During the first two days, growth rates of all tested cells were very similar. However, from the 3rd day on, the proliferation rate of C-FABP-WT stimulated cells started to be higher than those of other lines. On the 4th, 5th the 6th day, the numbers of C-FABP-WT stimulated LNCaP-C4<sub>2</sub> cells without adding natural fatty acids were 51883, 57466 and 67216, respectively. At same time points, number of those cells with natural fatty acid stimulations were 62260, 68960 and 100825, respectively. Whereas in the same time points, numbers of cells from the control LNCaP-C4<sub>2</sub> cells only were 39383, 49216 and 54383, respectively, and 47260, 59060 and 81575, respectively, of those cells with natural fatty acid stimulations. The proliferation rate of C-FABP-WT stimulated cells was significantly increased by 24% (Day 4), 15% (Day 5) and 20% (Day 6) compared with control cells (Student t-test,  $P=0.0399$ ). Similarly, number of cells stimulated by mutants C-FABP-R109A and C-FABP-R109/129A only were significantly reduced when compared to control cells during the 6 day culture (Student t-test,  $P=0.006$  and  $P=0.0096$ , respectively). Moreover, number of those cells with natural fatty acid stimulations were also significantly reduced when compared to control cells during 6 days culture ( $P=0.03$  and  $0.0344$ , respectively). The final cell counts on day 6 and statistical comparison were summarised in Table 5.3.

To assess the difference between cells stimulated by C-FABPs only and cells stimulated by C-FABPs plus natural fatty acid, statistical analysis showed that the proliferation rate of cells stimulated by C-FABPs plus natural fatty acids were significantly increased by 27% (C-FABP-WT), 19% (C-FABP-R109A) and 17% (C-

FABP-R109/129A) compared with cells stimulated by C-FABPs only (Student t-test,  $P > 0.05$ ).

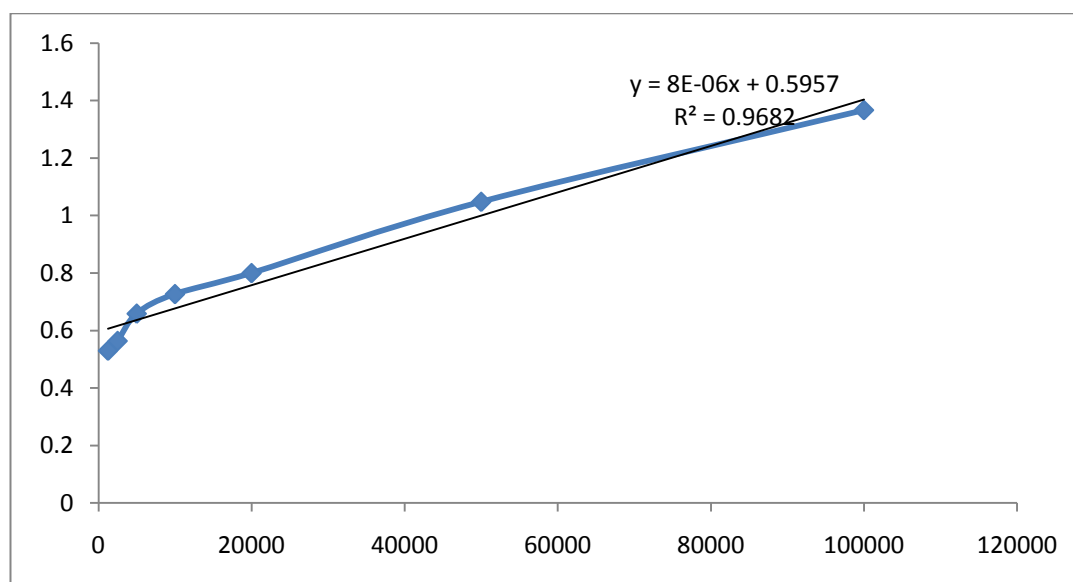


**Figure 5.7: Standard curve for LNCaP-C4<sub>2</sub> cell line**

A standard curve was established by plotting absorbance (OD at 570nm) (Axis Y) against the number of cells (Axis X). The cell number of samples was determined by comparing serially diluted standard from the standard curve. The curve equation and regression value of standard curve are presented in the diagrams.

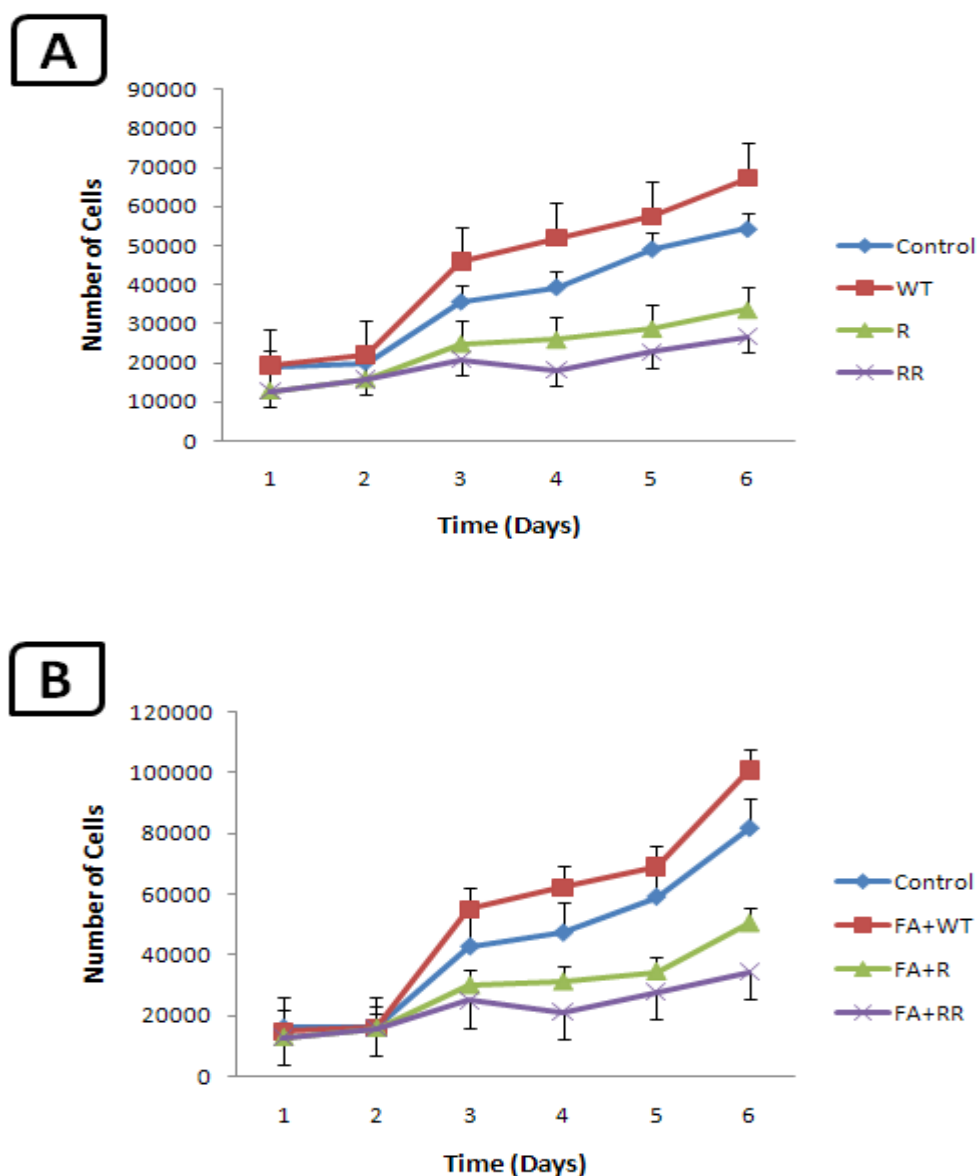


**Figure 5.8: Time course curve of proliferation rate for LNCaP-C4<sub>2</sub> cells stimulated by wild type and mutant C-FABP proteins**

*The numbers of cells for each C-FABP proteins, shown mean of three individual experiments were obtained every day during the 6 days period. (A) LNCaP-C4<sub>2</sub> cells were stimulated by recombinant C-FABPs only. (B) LNCaP-C4<sub>2</sub> cells were stimulated by recombinant C-FABPs plus natural fatty acid (Myristic acid). Data expressed as means±SD of three independent experiments.*

<b>A</b> LNCaP-C4 <sub>2</sub>	Mean number of cells $\pm$ SD	P Value
C-FABP-WT	43977 $\pm$ 19361	0.0165
C-FABP-R109A	23642 $\pm$ 7882	0.006
C-FABP-R109/129A	13950 $\pm$ 5621	0.0096
Control	36272 $\pm$ 14616	---

<b>B</b> LNCaP-C4 <sub>2</sub>	Mean number of cells $\pm$ SD	P Value
C-FABP-WT	53003 $\pm$ 33019	0.0399
C-FABP-R109A	29097 $\pm$ 13635	0.03
C-FABP-R109/129A	22875 $\pm$ 7971	0.0344
Control	43778 $\pm$ 25367	---

**Table 5.3: Cell counts of C-FABPs at the end point of proliferation assay**

*The final cell counts on day 6 and the statistic analyse were shown above. P values were obtained by comparing sample groups to control. (A) LNCaP-C4<sub>2</sub> cells were stimulated by recombinant C-FABPs only. (B) LNCaP-C4<sub>2</sub> cells were stimulated by recombinant C-FABPs plus natural fatty acid (Myristic acid).*

### 5.2.3 The effect of wild type and mutants C-FABPs on the invasiveness of the cells

The proliferation assay showed no significant differences of the effect of C-FABPs on LNCaP, 22RV1 and LNCaP-C42 cell line. Therefore, the invasion assay was conducted only on LNCaP cells.

A modified Boyden Chamber assay was applied to evaluate the invasiveness of LNCaP cell stimulated by different recombinant C-FABP proteins. This chemotactic directional migration assay was used widely to reveal the cell invasion ability which correlates well with the metastasis potential (Tuszynski *et al*, 1987). The cells were examined in a Boyden Chamber with 6.5mm diameter polycarbonate membrane coated with 30µg of matrigel to the upper compartment before the cells were seeded. After 24 hours incubation, cells remaining in the upper compartment of the filters were removed and the cells attached to the lower side of the filter were fixed and stained by crystal violet reagent. The numbers of migrated and invaded cells were counted under a light microscope at 10/0.25 magnification. On each filter, nine random fields were counted and the representatives of each cell line were shown in Figure 5.9.

The results were normalized by the cell number after 20 hours routine culture and were shown in Figure 5.10. All migrated cells remained attaching to the low surface of the membrane and no cells were found in the culture medium of the low chamber. The numbers of invading cells that pass through the membrane were shown in Table 5.4. The number of invaded C-FABP-WT stimulated cells was the highest in all cell lines and more than 2.6-fold higher than the number of invaded cells from control



(Student t-test,  $P=0.03$ ). The invasiveness of C-FABP-R109A stimulated cells was higher than LNCaP-R109/129A stimulated cells and control cells, but was significantly lower than that of C-FABP-WT stimulated cells (Student t-test,  $P=0.01$ ). The invasiveness of C-FABP-R109/129A stimulated cells was at similar level to that of the control cells (Student t-test,  $P=0.44$ ). Difference of invaded cells between C-FABP-R109A and C-FABP-R109/129A stimulated cells was considered to be a statistically significant (Student t-test,  $P=0.037$ ).

LNCaP cells	Mean number of invaded cells $\pm$ SD	P Value
C-FABP-WT	256 $\pm$ 40	0.03
C-FABP-R109A	163 $\pm$ 32	0.031
C-FABP-R109/129A	80 $\pm$ 26	0.44
Control	96.6 $\pm$ 15.2	---

**Table 5.4: The number of invading cells that pass through the membrane.**

*Number of invaded cells (Mean $\pm$ SD) produced by LNCaP stimulated by different C-FABPs proteins in three separate experiments were shown above and P values were calculated by comparing sample groups to control group.*

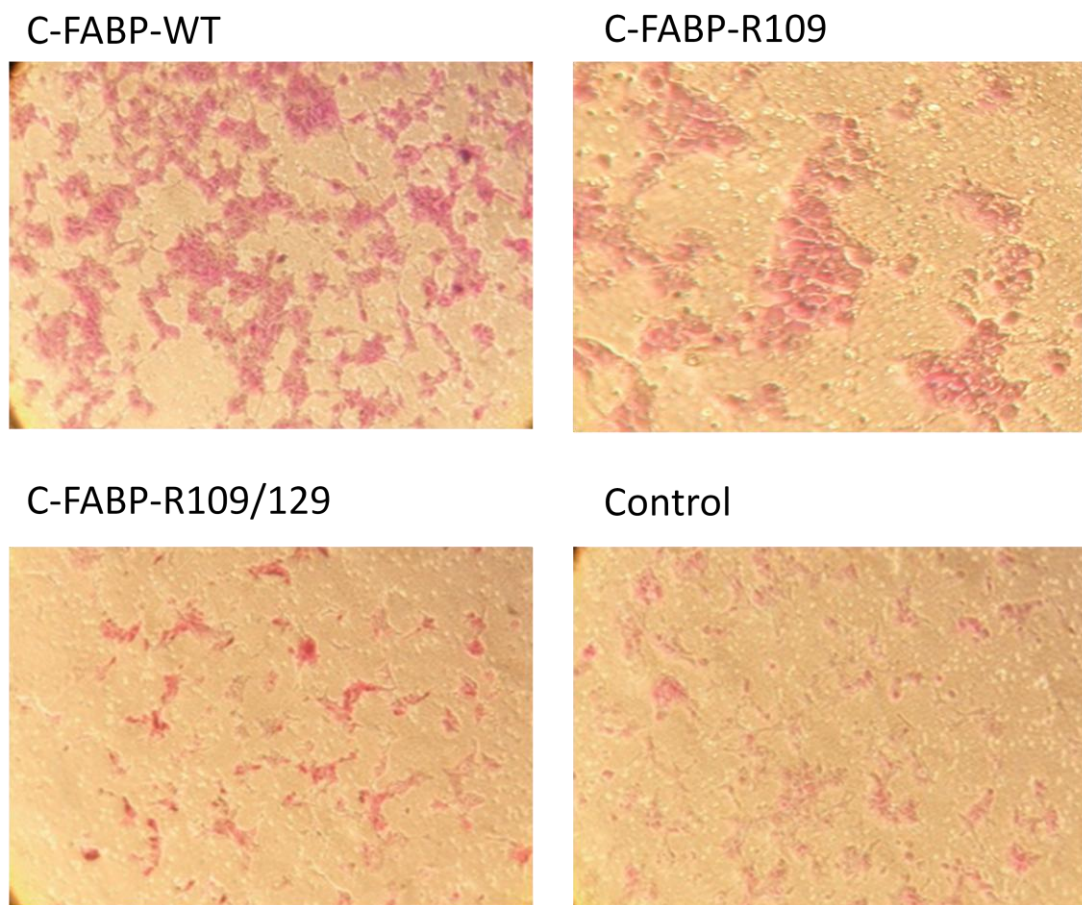


**Figure 5.9: The images of invaded cells stimulated by C-FABP proteins on the lower filter surface of the Boyden Chamber**

*The appearances of invaded cells from C-FABP-WT stimulated cells, C-FABP-R109A stimulated cells, C-FABP-R109/129A stimulated cells and the control, respectively.*

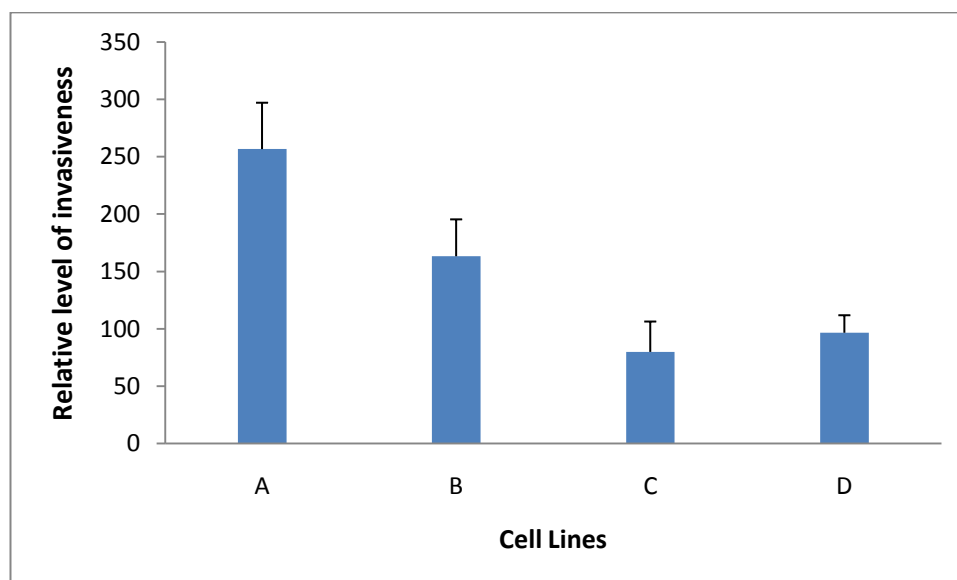


**Figure 5.10: Number of cells invaded per field in the invasion assay**

*The columns represent the invasiveness of C-FABP-WT stimulated cells (Column A), C-FABP-R109A stimulated cells (Column B), C-FABP-R109/129A stimulated (Column C) and control (Column D). The invasiveness of C-FABP-WT stimulated cells was significantly higher than those of C-FABP-R109A stimulated cells, C-FABP-R109/129A stimulated cells and the control cells. The results are the mean  $\pm$  SD of three individual experiments.*

## 5.2.4 Soft agar colony formation assay of recombinant C-FABP proteins

The tumorigenicity of the LNCaP, 22RV1 and LNCaP-C4<sub>2</sub> cell lines stimulated by C-FABP proteins were tested by examining their anchorage-independent growth in a soft agar.

### 5.2.4.1 LNCaP cell line

The images of soft agar for each cell stimulated by C-FABP proteins were shown in Figure 5.11 and the results of the soft agar were shown in Figure 5.12. The accurate quantitative assessment and *P* values of Student t-test for each tested cell line compared to control were presented in Table 5.5.

The number of colonies produced in the soft agar by LNCaP cells stimulated with C-FABP-WT, C-FABP-R109A, C-FABP-R109/129A and control cells were  $1050 \pm 132.29$ ,  $283 \pm 76.38$ ,  $157 \pm 38.1$  and  $155 \pm 68.74$ , respectively. In comparison with the control, the number of colonies produced by C-FABP-R109A stimulated cells was significantly increased by 45% (Student t-test,  $P=0.0183$ ) whereas the number of colonies produced by C-FABP-R109/129A stimulated cells was at same level as the control (Student t-test,  $P=0.5737$ ). The most significant change was observed in C-FABP-WT stimulated cells which produced more than 6.7-fold increase in the number of colonies formed in soft agar when compared to control. Further analysis showed that a significant difference was found between the number of colonies produced by control C-FABP-R109A stimulated cells and the number of colonies produced by C-FABP-R109/129A stimulated cells (Student t-test,  $P=0.0258$ ). However, the differences between the colony numbers produced by C-FABP-R109A

and C-FABP-109/129A stimulated cells were significantly reduced by 73% and 85% when compared to C-FABP-WT stimulated cells (Student t-test,  $P=0.0043$  and  $P=0.0077$ , respectively).

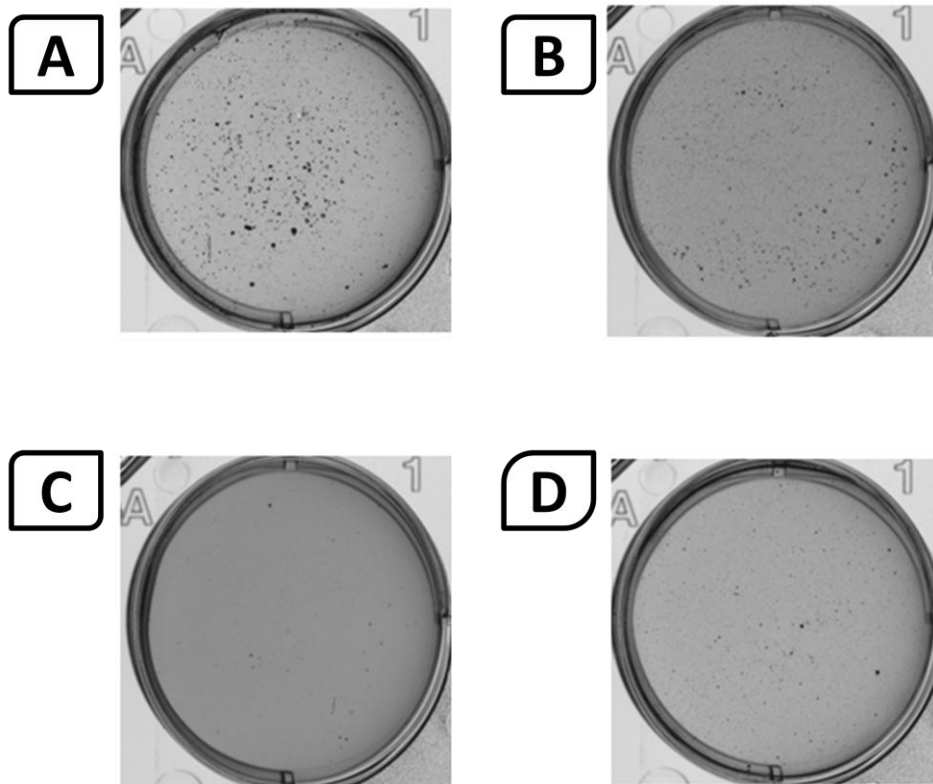


**Figure 5.11: The colonies produced in soft agar by LNCaP cell stimulated with different C-FABPs**

*After incubation for 5 weeks, 2 hours staining by MTT was performed on colonies developed from C-FABP-WT (Panel A), C-FABP-R109A (Panel B), C-FABP-R109/129A (Panel C) and Control (Panel D) were displayed above. All plates were stimulated by natural fatty acid (Myristic acid). Experiments were tested in three plates.*

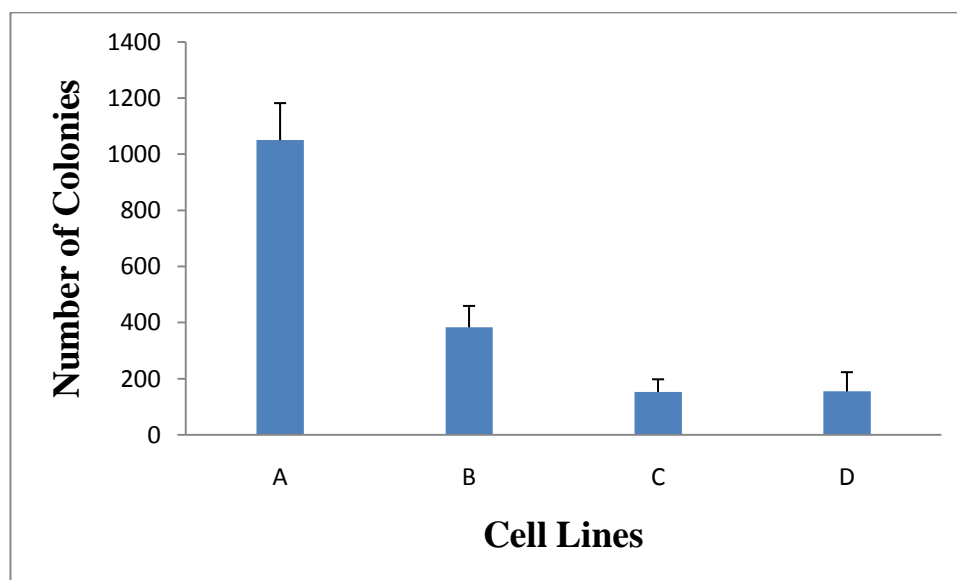


**Figure 5.12: The effect of wild and mutants C-FABPs on colonies formation ability of LNCaP cells in soft agar**

*The number of colonies was counted using GelCount with optimised setting: Edge detection: 30; Centre detection: 50; Colony diameter: 150 $\mu$ m-800 $\mu$ m; Circularity: 60; Density: 0.75. C-FABP-WT (Column A), C-FABP-R109A (Column B), C-FABP-R109/129A (Column C) and Control (Column D).*

LNCaP cells	Mean number of colonies $\pm$ SD	P Value
C-FABP-WT	1050 $\pm$ 132.29	0.0005
C-FABP-R109A	283 $\pm$ 76.38	0.0183
C-FABP-R109/129A	157 $\pm$ 38.1	0.5737
Control	155 $\pm$ 68.74	---

**Table 5.5: The numbers of colonies produced in soft agar by LNCaP cells stimulated by different C-FABPs**

*Numbers of colonies (mean  $\pm$  SD) produced by LNCaP cells stimulated with different C-FABP proteins in three separate soft agar assays were shown above and P values were obtained by comparing sample groups to control group (paired t test).*

#### 5.2.4.2 22RV1 cells line

The images of soft agar for cell stimulated by C-FABP proteins were shown in Figure 5.13 and the results of the soft agar assays were shown in Figure 5.14. The accurate quantitative assessment and P values of Student t-test for each tested cell line compared to control were presented in Table 5.6.

The number of colonies produced in the soft agar by 22RV1 cells stimulated with C-FABP-WT, C-FABP-R109A, C-FABP-R109/129A and control cells were 1183.33 $\pm$ 160.73, 408.33 $\pm$ 38.19, 197 $\pm$ 92.50 and 216.67 $\pm$ 73.38, respectively. In

comparison with the control, the number of colonies produced by C-FABP-R109A stimulated cells was significantly increased by 47% (Student t-test,  $P=0.0130$ ) whereas the number of colonies produced by C-FABP-R109/129A stimulated cells was at same level as control (Student t-test,  $P=0.1836$ ). The most significant change was observed in C-FABP-WT stimulated cells which produced more than 5.4-fold increase in the number of colonies formed in soft agar when compared to control. Further analysis showed that a significant difference was found between the number of colonies produced by control C-FABP-R109A stimulated cells and the number of colonies produced by C-FABP-R109/129A stimulated cells (Student t-test,  $P=0.0214$ ). However, the differences between the colony numbers produced by C-FABP-R109A and C-FABP-109/129A stimulated cells were significantly reduced by 65% and 83% when compared to C-FABP-WT stimulated cells (Student t-test,  $P=0.0092$  and  $P=0.0035$ , respectively).



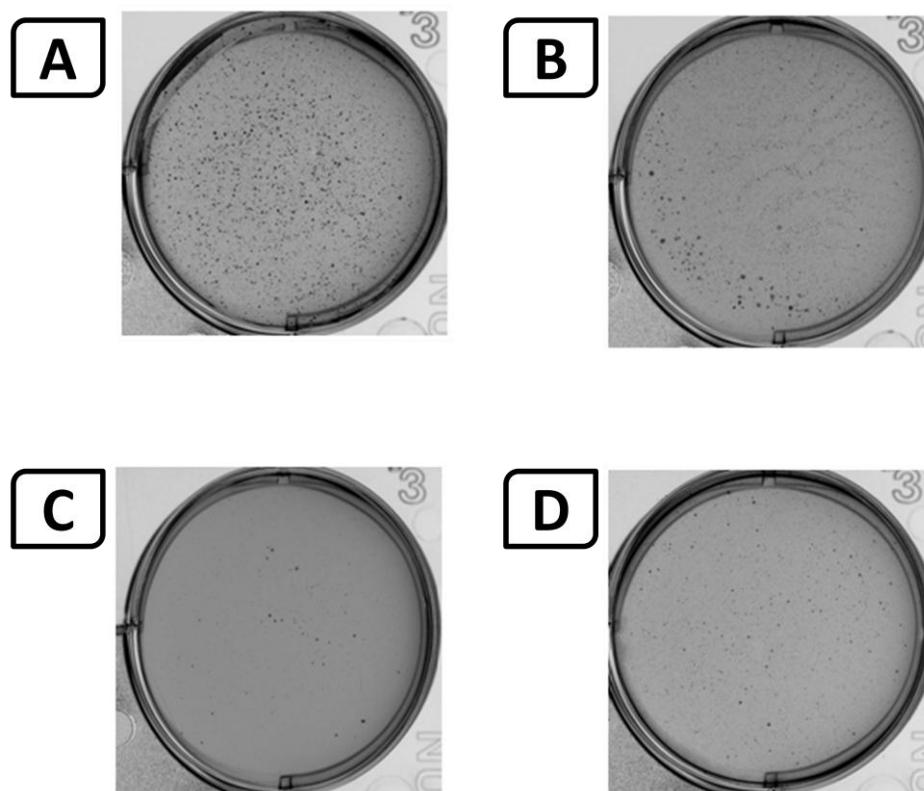


**Figure 5.13: The colonies produced in soft agar by 22RV1 cells stimulated with different C-FABPs**

*After incubation for 4 weeks, 2 hours staining by MTT was performed on colonies developed from C-FABP-WT (Panel A), C-FABP-R109A (Panel B), C-FABP-R109/129A (Panel C) and Control (Panel D) were displayed above. All plates were stimulated by natural fatty acid (Myristic acid). Experiments were tested in three plates.*

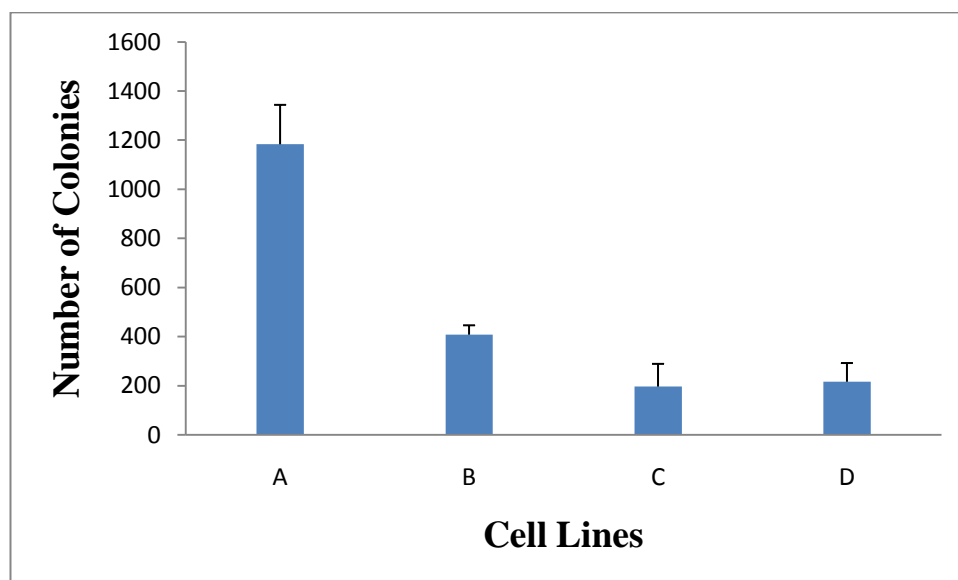


**Figure 5.14: The effect of wild and mutants C-FABPs on colonies formation ability of 22RV1 cells in soft agar**

*The number of colonies was counted using GelCount with optimised setting: Edge detection: 30; Centre detection: 50; Colony diameter: 150 $\mu$ m-800 $\mu$ m; Circularity: 60; Density: 0.75. C-FABP-WT (Column A), C-FABP-R109A (Column B), C-FABP-R109/129A (Column C) and Control (Column D).*

22RV1 cells	Mean number of colonies $\pm$ SD	P Value
C-FABP-WT	1183.33 $\pm$ 160.73	0.0038
C-FABP-R109A	408.33 $\pm$ 38.19	0.0130
C-FABP-R109/129A	197 $\pm$ 92.50	0.1836
Control	216.67 $\pm$ 73.38	---

**Table 5.6: The numbers of colonies produced in soft agar by 22RV1 cells stimulated with different C-FABPs**

*Numbers of colonies (mean  $\pm$  SD) produced by 22RV1 stimulated with different C-FABP proteins in three separate soft agar assays were shown above and P values were obtained by comparing sample groups to control group (paired t test).*

#### 5.2.4.3 LNCaP-C4<sub>2</sub> cell line

The images of soft agar assay for LNCaP-C4<sub>2</sub> stimulated with C-FABP proteins were shown in Figure 5.15 and the results of the soft agar assays were shown in Figure 5.16. The accurate quantitative assessment and P values of Student t-test for each tested cell line compared to control were presented in Table 5.7.

The number of colonies produced in the soft agar by LNCaP-c4<sub>2</sub> cells stimulated with C-FABP-WT, C-FABP-R109A, C-FABP-R109/129A and Control were  $1233 \pm 208.17$ ,  $443.33 \pm 60.28$ ,  $216.67 \pm 76.38$  and  $180.33 \pm 65.12$ , respectively. In comparison with the control, the number of colonies produced by C-FABP-R109A stimulated cells was significantly increased by 59% (Student t-test,  $P=0.0068$ ) whereas the number of colonies produced by C-FABP-R109/129A stimulated cells was at same level as the control (Student t-test,  $P=0.5647$ ). The most significant change was observed in C-FABP-WT stimulated cells which produced more than 7-fold increased in the number of colonies formed in soft agar when compared to control. Further analysis showed that a significant difference was found between the number of colonies produced by control C-FABP-R109A stimulated cells and the number of colonies produced by C-FABP-R109/129A stimulated cells (Student t-test,  $P=0.0157$ ). However, the differences between the colony numbers produced by C-FABP-R109A and C-FABP-109/129A stimulated cells were significantly reduced by 65% and 82% when compared to C-FABP-WT stimulated cells (Student t-test,  $P=0.0032$  and  $P=0.0014$ , respectively).

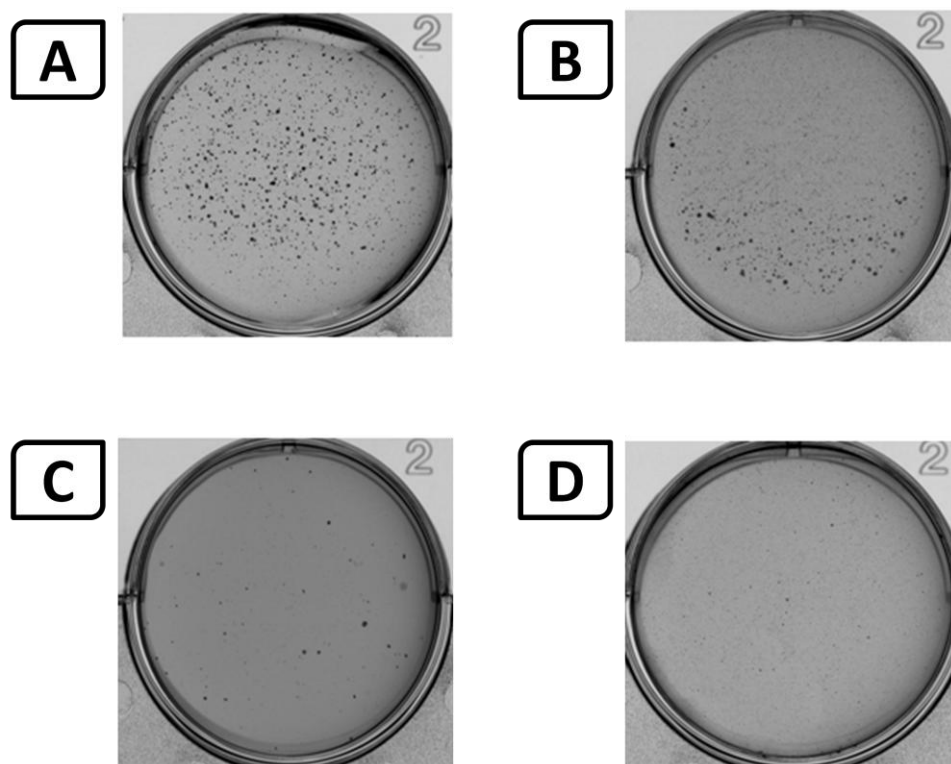


**Figure 5.15: The colonies produced in soft agar by LNCaP-C4<sub>2</sub> cells stimulated with different C-FABPs**

*After incubation for 4 weeks, 2 hours staining by MTT was performed on colonies developed from C-FABP-WT (Panel A), C-FABP-R109A (Panel B), C-FABP-R109/129A (Panel C) and Control (Panel D) were displayed above. All plates were stimulated by natural fatty acid (Myristic acid). Experiments were tested in three plates.*

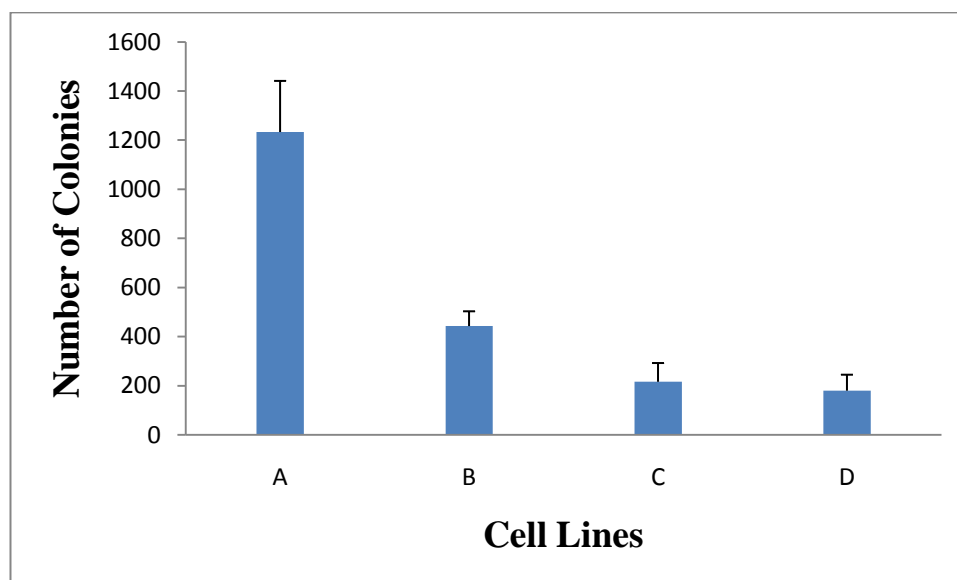


**Figure 5.16: The effect of wild type and mutants FABPs on colonies formation ability of LNCaP-C4<sub>2</sub> in soft agar**

*The number of colonies was counted using GelCount with optimised setting: Edge detection: 30; Centre detection: 50; Colony diameter: 150µm-800µm; Circularity: 60; Density: 0.75. C-FABP-WT (Column A), C-FABP-R109A (Column B), C-FABP-R109/129A (Column C) and Control (Column D).*

<b>LNCaP-C4<sub>2</sub></b>	<b>Mean number of colonies<math>\pm</math> SD</b>	<b>P Value</b>
<b>C-FABP-WT</b>	1233 $\pm$ 208.17	0.0011
<b>C-FABP-R109A</b>	443.33 $\pm$ 60.28	0.0068
<b>C-FABP-R109/129A</b>	216.67 $\pm$ 76.38	0.5647
<b>Control</b>	180.33 $\pm$ 65.12	---

**Table 5.7: The numbers of colonies produced in soft agar by LNCaP-C42 stimulated with different C-FABPs**

*Numbers of colonies (mean  $\pm$  SD) produced by different C-FABP proteins in three separate soft agar assays were shown above and P values were obtained by comparing sample groups to control group (paired t test).*

### 5.3 Discussion

In this chapter, the relationship between the tumourigenicity-promoting function of C-FABP and its fatty acid-binding ability was monitored. C-FABP binds to fatty acids through a binding motif which consists of three key amino acids (Arg<sup>109</sup>, Arg<sup>129</sup>, and Tyr<sup>131</sup>) and replacing any one of these key amino acids with another almost completely deprives C-FABP of its fatty acid binding ability (Vorum *et al*, 1998). Fatty acid uptake is a strictly regulated process and it is related to the levels of certain FABPs in LNCaP cells (Pinthus *et al*, 2007). The fatty acid uptake assay investigated in this chapter, our results showed that the fatty acid uptake capacity of LNCaP stimulated with C-FABP-WT was significantly increased when C-FABP was forced to be overexpressed. In contrast, the fatty acid uptake capacities stayed at same level between either LNCaP cells stimulated with single point mutated C-FABP (C-FABP-R109A) and control cells (LNCaP) or LNCaP cells stimulated with double points mutated C-FABP (C-FABP-R109/129A) and LNCaP cells. These results indicated that elevate the expression of C-FABP-WT in LNCaP cells can result in enhancing its fatty acid uptake capability. Moreover, it has been also demonstrated that expression of mutated recombinant C-FABPs generated by site-directed mutagenesis can not increase the fatty acid uptake capability compared to the control cells, which suggested that the ability of C-FABP to bind and to transport fatty acids into these cells depends on the structural integrity of its fatty acid-binding motif and changing amino acids in this part can result losing most fatty acid-binding and transporting capability.



To study the importance of the structural integrity of the fatty acid binding motif to the tumorigenicity-promoting activity of C-FABP in prostate cancer, the effect of wild type and mutant C-FABPs on cell proliferation, invasion and colony formation as indication of tumourigenicity were investigated. The average growth rate of cells stimulated with C-FABP-WT was significantly increased by 17% (Student t-test,  $P<0.05$ ) when compared to control cells. Whereas, the average growth rate of cells stimulated with C-FABP-R109A and C-FABP-R109/129A were significantly reduced by 33% and 47%, respectively (Student t-test,  $P<0.005$ ) when compared to control cells. Further statistical analysis showed that the proliferation rate of cells stimulated by C-FABPs plus natural fatty acids were significantly increased by 27% (C-FABP-WT), 19% (C-FABP-R109A) and 17% (C-FABP-R109/129A) when compared with cells stimulated by C-FABPs only (Student t-test,  $P>0.05$ ). The invasiveness of cells stimulated with C-FABP-WT, C-FABP-R109, C-FABP-R109/129A and the control cells were  $256\pm40$ ,  $163\pm32$ ,  $80\pm26$  and  $96.6\pm15.2$ , respectively. The number of invaded cells stimulated with C-FABP-WT was the highest in all cell lines and more than 2.6-fold higher than the number of invaded cells from control (Student t-test,  $P<0.05$ ). The average number of colonies produced in the soft agar by selected cells stimulated with C-FABP-WT, C-FABP-R109A, C-FABP-R109/129A and control were  $1050\pm132.29$ ,  $283\pm76.38$ ,  $157\pm38.1$  and  $155\pm68.74$ , respectively. In comparison with the control, the average number of colonies produced by C-FABP-R109A stimulated cells was increased by 45% (Student t-test,  $P<0.01$ ) whereas the average number of colonies produced by C-FABP-R109/129A stimulated cells was at same level as the control cells (Student t-test,  $P>0.5$ ). The most significant change was observed in C-FABP-WT stimulated

cells which produced more than 6.7-fold (85%) increase in the number of colonies formed in soft agar assay comparing to the control (Student t-test,  $P < 0.001$ ). These results showed that, the increased wild type C-FABP stimulation in prostate cell lines significantly increased cell proliferation, invasiveness, and tumorigenicity. Whereas, the increased expression of both mutant forms of C-FABP did not significantly effect these characteristics.

*In-vitro* findings in this chapter were consistent with our recently *in-vivo* results, when inoculated in nude mice, 7 out of 8 (88.9%) mice inoculated with LNCaP-WT cells developed tumours, but only 3 out of 8 (37.5%) mice inoculated with LNCaP-R109/129A and LNCaP-V cells respectively produced tumours. At the end of the test, the average weight of the tumours produced by LNCaP-WT was 5.8- and 7.3-times of those produced respectively by LNCaP-R109/129A and LNCaP-V cells (Malki *et al*, 2011). This result showed that not only that the wild type C-FABP-expressing cells produced more but also larger tumours than those cells either not expressing C-FABP or expressing mutated C-FABP which was not able to bind and transport fatty acids. Furthermore, consistent with this finding, our previous work established that suppressing expression of C-FABP by either antisense mRNA or RNA interference in the highly malignant prostate cancer cell line PC3M has greatly inhibited its ability of forming tumours in nude mouse (Adamson *et al*, 2003; Forootan *et al*, 2010; Morgan *et al*, 2008). Therefore, The results of the current and previous work *in-vitro* and *in-vivo* further confirmed that C-FABP promotes malignant progression of prostate cancer by its binding and transporting intracellular fatty acids into the cancer cells.

## **6 GENERAL DISCUSSION AND CONCLUSION**

## 6.1 Discussion

Prostate cancer is the most frequently diagnosed non-cutaneous male malignancy and is the second cause of cancer-related death in men in most Western countries. In the UK, more than 35,000 men are diagnosed with prostate cancer and around 10,000 men die from prostate cancer each year. Current understanding of the molecular pathology of prostate cancer is limited. At present, clinical therapy focuses on androgen blockage by physical or pharmaceutical castration. However, prostate cancer often returns exhibiting more aggressive hormone independent phenotype. Therefore, it is important to improve the understanding of the specific molecular mechanisms involved in the malignant progression of prostate cancer in order to develop new therapies.

The risk factors for prostate cancer include age, ethnicity, family history and diet. It has been reported that prostate cancer onset may be attributed to a variety of dietary factors ranging from lack of selenium supplementations (Quiner *et al*, 2011) to vitamin D (Stewart *et al*, 2005) and high dairy fat intake was also associated with increased risk of prostate cancer (Crowe *et al*, 2008; Kurahashi *et al*, 2008). A long-term study demonstrated high blood levels of trans-fatty acids to be associated with an increased prostate cancer risk (Chavarro *et al*, 2008).

C-FABP is a 15 KDa cytosolic protein within the family of fatty acid binding protein. It binds with high affinity to long chain fatty acid. Increased expression of C-FABP has been detected in malignant tumours of breast, bladder and pancreas

(Celis *et al*, 1999; Sinha *et al*, 1999). Our previous studies in the molecular pathology laboratory have established the relationship between over-expression of C-FABP in breast and prostate cancer cells. A study by (Jing *et al*, 2000) found the *C-FABP* gene to be over-expressed in malignant breast and prostate epithelial cell lines. When the *C-FABP* gene was transfected into the rat benign Rama 37 model cells and the tranfectants subsequently inoculated into Wistar Furth rats, a significant number of animals developed metastasis. Suppression of *C-FABP* expression by antisense transfection in PC-3M cells decreased the invasive capacity *in vitro* and reduced the tumourigenicity *in vivo*. Moreover, suppression of *VEGF* has also been detected in these transfected cell lines (Adamson *et al*, 2003). These results indicated that over-expression of *C-FABP* may stimulate the expression of *VEGF* and subsequently promote the angiogenesis to facilitate tumour formation and metastasis. Recent studies by Morgan *et.al* (2008) confirmed that suppressing the expression of *C-FABP* in PC-3M cells using siRNA silencing technique resulted the significant reduction of tumourigenicity both *in-vitro* and *in-vivo* (Morgan *et al*, 2008). However, the mechanism of C-FABP elevating the expression of VEGF remains unclear.

Overall, the aims of this thesis were to investigate the relationship between the tumorigenicity-promoting function of C-FABP and its fatty acid-binding ability, so as to ascertain that the tumorigenicity promoting activity of C-FABP depends on its structural integrity of its fatty acid-binding motif and hence its fatty acid-binding ability in prostate cancer cells.

In common with other FABP family proteins, C-FABP binds to fatty acids through a binding motif which consists of 3 key amino acids (Arg<sup>109</sup>, Arg<sup>129</sup>, and Tyr<sup>131</sup>). We used site-directed mutagenesis to convert Arg<sup>109</sup> or Arg<sup>109</sup> and Arg<sup>129</sup> into Ala<sup>109</sup> or Ala<sup>109</sup> and Ala<sup>129</sup> to generate two mutant cDNAs (Figure 3.1) and transfected them together with wild type cDNA into the LNCaP cells to generate modified transfectant cell lines. Real-time PCR measurement on C-FABP mRNA showed that the C-FABP mRNA level in LNCaP-WT cells to be increased 137.5-fold comparing with control cells (Figure 3.5). Western blot also confirmed the overexpression of C-FABP in LNCaP-WT cells (Figure 3.6). From the results obtained by our previous studies, it was demonstrated that the biological function of C-FABP is promote malignant progression of cancer cells. In this study, the effect of high level increment of C-FABP expression on cell malignant properties such as proliferation rate, invasiveness and anchorage-independent growth as an indication of tumourigenecity, was investigated. It is also showed that the mutant C-FABP mRNA levels expressed, respectively, in LNCaP-R109A and LNCaP-R109/129A cells were also increased to levels similar to that in LNCaP-WT cells. Thus these transfectants were ideal cell lines used for comparing biological functions exerted by wild type and mutant C-FABPs.

The wild type and mutant C-FABP cDNAs were contained in the pIRES2-EGFP vector. When the wild type and mutant C-FABP cDNAs were cloned into an expression vector to produce recombinant C-FABPs, it was found that in the multiple cloning sites of this construct, there was no complimentary restriction site for the expression vector pQE. Therefore, before the C-FABP cDNAs were inserted into to

the expression vector pQEs, it was necessary to generate complimentary restriction sites at both ends of the cDNAs. Thus, the C-FABP-cDNAs were excised from pIRES2-EGFP with restriction enzymes *XhoI* and *PstI* (Figure 4.1 - Figure 4.3) and inserted into cloning vector pBluescript that contains the multiple restriction sites (*KpnI* and *PstI*). Sequences analysis successfully confirmed the insertion of C-FABP cDNAs into the cloning vector pBluescript (Figure 4.4 - Figure 4.6). The C-FABP cDNAs were then excised out from the pBluescript vector with *KpnI* and *PstI* (Figure 4.7 and Figure 4.8) and then inserted into the expression vector pQEs to form three constructions which will express the wild type and mutant C-FABPs (C-FABP-WT, C-FABP-R109A and C-FABP-R109/129A, respectively). Sequence analysis successfully confirmed the insertion of C-FABP cDNAs into the pQEs expression vector (Figure 4.11 - Figure 4.13). Further analysis confirmed that pQE32 is the only vector that remains the ATG codon unchanged as shown in Figure 4.10. Therefore, pQE32 was identified and chosen as the construct to produce recombinant proteins. When the recombinant proteins are synthesised in *E.coli* cells, different expression systems exhibit different efficiencies. Thus, it is necessary to establish the time point at which the maximum yield of protein is synthesised in *E.coli* cells. In this work, it was found that protein synthesis is increased with increased incubation time, and reached a maximum at five hours after IPTG induction. Once at the maximum, any further induction and incubation was not accompanied with any further increment in protein synthesis. Instead, the yield of recombinant protein was reduced. This could be due to either the cessation of production inside the *E. coli* cells or the degradation of the completed synthesised proteins. Therefore, the optimal time at which the maximum yield of protein production was achieved was 5 hours after IPTG

induction (Figure 4.14). After C-FABP was separated from the 6xhis-tagged using Ni-NTA Fast Start column and subjected to Western blot analysis, a single band at the correct site of the blot was visualised (Figure 4.15). This result indicated that the separation of the recombinant C-FABP proteins from the *E. coli* bacterial proteins was very successful and the recombinant proteins obtained from purification procedures were very pure.

To test whether the recombinant proteins produced were biologically active, the fatty acid binding ability of wild type and mutant C-FABPs were tested. The fatty acid binding ability of the C-FABP-WT was on average 85% when exposed to natural fatty acids (myristic, palmitic, oleic and linoleic acids). However, the average fatty acid binding ability of the C-FABP-R109A was significantly reduced to 33% (Student t-test,  $P < 0.001$ ) when exposed to natural fatty acids and the average fatty acid binding ability of the C-FABP-R109/129A was further significantly reduced to 10% (Student t-test,  $P < 0.001$ ) (Figure 4.17). These results suggested that fatty acid binding ability of C-FABP depends on its structural integrity of the binding motif. Therefore, changing one amino acid in motif by site-directed point mutation significantly reduced the fatty acid binding ability and changing two amino acids by sites-directed mutations almost completely deprived the fatty acid binding ability of C-FABP. These findings are comparable to the results of the study by Hagan *et al* (2008) who tested the fatty acid binding ability of wild type and mutant Liver fatty acid binding protein (L-FABP) (Hagan *et al*, 2008). The study concluded that the fatty acid binding ability of mutant L28W and M74W were significantly reduced by 80% and 87%, respectively, when exposed to linoleic acids comparing to wild type



protein. Therefore mutant forms of fatty acid binding proteins seemed to reduce the ability to bind to fatty acids compared to wild type proteins as found in this work and by others.

To analyze the possible expression of C-FABP proteins in prostate carcinogenesis and tumour progression, we examined the effect of wild type and mutant C-FABPs on cell proliferation, invasiveness and soft agar colony formation assays as indication of tumorigenicity of prostate cells. The average proliferation rate of C-FABP-WT stimulated LNCaP cells was significantly increased by 19% when compared to control cells (Student t-test,  $P=0.03$ ). However, the average proliferation rate of C-FABP-R109 and C-FABP-R109/129A stimulated LNCaP cells were significantly reduced by 33% and 47% when compared to the control cells (Student t-test,  $P<0.005$ ) (Figure 5.4). Similarly, the average proliferation rate of C-FABP-WT stimulated 22RV1 and LNCaP-C4<sub>2</sub> were significantly increased by 25% and 20%, respectively, when compared with control cells (Student t-test,  $P<0.005$  and  $P<0.001$ , respectively) (Figure 5.6 and Figure 5.7). To analyze the differences between the growth rate of selected cells stimulated by C-FABP proteins plus fatty acid and selected cells stimulated by recombinant protein only, further statistical analysis showed that the average proliferation rate of tested cells stimulated by C-FABPs plus selected natural fatty acids were significantly increased by 23% (C-FABP-WT), 18% (C-FABP-R109A) and 16 % (C-FABP-R109/129A) compared with cells stimulated by C-FABPs only (Student t-test,  $P<0.05$ ). Thus, this finding may support the hypothesis that the elevated expression of *C-FABP* may give rise to

an increased total uptake of fatty acids, and hence an enhanced fatty acid signalling activity.

With respect to cell invasions, the number of LNCaP cells stimulated with C-FABP-WT that invaded through the trans-well membrane was 2.6-fold higher (student t-test,  $P < 0.05$ ) than the number of cells in the LNCaP control group (Figure 5.9). The invasiveness of C-FABP-R109A stimulated cells was higher than C-FABP-R109/129A stimulated cells and control group, but was significantly lower than that of C-FABP-WT stimulated cells (Student t-test,  $P < 0.01$ ) (Figure 5.10). The invasiveness C-FABP-R109/129A stimulated LNCaP cells was at similar level to that of the control cells (Student t-test,  $P = 0.44$ ). Further statistic showed that the invasiveness of LNCaP cells stimulated with C-FABP-R109A was significantly increased by 2-fold than the number of invaded cells in the LNCaP stimulated with C-FABP-R109/129A (Student t-test,  $P < 0.05$ ) (Table 5.4). The expression level of three C-FABP proteins in prostate cancer cells was proportional to their invasive abilities, which suggests that the change one or two amino acids by site-directed point mutation might be associated with the metastatic potential of prostate cancer cells. These findings are consistent with previously reported associations of C-FABP with tumorigenesis and metastasis in prostate cancer and breast cancer *in-vitro* and *in-vivo* (Adamson *et al*, 2003; Fang *et al*, 2010; Fujii *et al*, 2005; Jing *et al*, 2000; Morgan *et al*, 2008). Over-expression of the *C-FABP* gene in non-metastatic rat-cell models induced the metastatic phenotype (Jing *et al*, 2000). Transfecting a vector expressing an antisense C-FABP transcript into PC-3M prostatic cancer cells significantly inhibited tumorigenicity *in-vivo* (Adamson *et al*, 2003).

Several studies have reported that FABP expression regulates cell proliferation. Alter one or two amino acids of liver-FABP resulted in remarkably inhibited cell proliferation and induced apoptosis of prostate and breast cancer cells (Hammamieh *et al*, 2005; Hammamieh *et al*, 2004). Several genes correlating with cell growth and proliferation were down-regulated, and antiproliferative genes were up-regulated in response to L-FABP antisense oligonucleotide (Hammamieh *et al*, 2005). Conversely, overexpressed adipocyte-FABP in DU145 prostate cancer cells caused apoptosis, perhaps because it down-regulated essential autocrine growth factors, such as transforming growth factor- $\alpha$ , and upregulated pro-apoptotic factors, such as tumour necrosis factor- $\alpha$  (De Santis *et al*, 2004). Antisense oligonucleotide blocking C-FABP expression has increased proliferation in DU145 prostate cancer cells (Das *et al*, 2001). Homozygous C-FABP-null mouse keratinocytes showed no difference in proliferation compared with wild-type mouse keratinocytes (Kusakari *et al*, 2006). However, the transport and metabolism of fatty acids in prostate cancer cells might be important to maintain cell growth, and altered lipid metabolism may affect proliferation. The exact mechanism used by C-FABP in increased cell proliferation and invasion is worthy of further investigation *in-vitro* and clarification *in-vivo*.

The tumorigenicity of the LNCaP, 22RV1 and LNCaP-C4<sub>2</sub> cells stimulated by wild type and mutant C-FABPs were tested by examining their anchorage-independent growth in soft agar. The number of colonies produced by in soft agar by LNCaP cells stimulated with C-FABP-WT was significantly increased by 85% comparing to the control cells (Student t-test,  $P < 0.001$ ) (Figure 5.11 and Figure 5.12). Similarly, the

number of colonies produced by LNCaP cells stimulated with C-FABP-R109 was significantly increased by 45% comparing to the control cells (Student t-test,  $P < 0.05$ ). Nevertheless, it was significantly reduced by 3.7-fold comparing to C-FABP-WT stimulated cells (Student t-test,  $P < 0.005$ ) (Table 5.5). No statistically significant difference were observed between the number of colonies produced by LNCaP cells stimulated with C-FABP-R109/129A and the number of colonies produced by control group (Student t-test,  $P = 0.57$ ). At same time points, the numbers of colonies produced by 22RV1 cells stimulated with C-FABP-WT, and C-FABP-R109A were significantly increased by 82% and 47%, respectively, comparing to the control group (Student t-test,  $P < 0.005$ ,  $P < 0.05$ , respectively) (Figure 5.13 and Figure 5.14). Whereas, no differences were found between the number of colonies produced by C-FABP-R109/129A stimulated cells and the number of colonies produced by the control group (Student t-test,  $P = 0.18$ ) (Table 5.6). Further statistic showed that the number of colonies produced by 22RV1 stimulated with C-FABP-R109A and C-FABP-R109/129A were significantly reduced by 2.9-fold and 6-fold, respectively, when compared to the number of colonies produced by 22RV1 cells stimulated with C-FABP-WT (Student t-test,  $P < 0.05$ ,  $P < 0.005$ , respectively). The number of colonies produced by LNCaP-C4<sub>2</sub> cells stimulated with C-FABP-WT and C-FABP-R109A were significantly increased by 85% and 59%, respectively, when compared to the control group (Student t-test,  $P < 0.001$  and  $P < 0.05$ , respectively) (Figure 5.15 and Figure 5.16). Whereas, no differences were found between the number of colonies produced by LNCaP-C4<sub>2</sub> cells stimulated with C-FABP-R109/129A and the number of colonies produced by the control group (Student t-test,  $P = 0.56$ ) (Table 5.7). Further statistic showed that the number of colonies produced by LNCaP-C4<sub>2</sub>

stimulated with C-FABP-R109A and C-FABPR109/129A were significantly reduced by 2.8-fold and 5.7-fold, respectively, when compared to the number of colonies produced by LNCaP-C4<sub>2</sub> cells stimulated with C-FABP-WT (Student t-test,  $P < 0.005$ ,  $P < 0.001$ , respectively). These results suggested that changing one or two amino acids in motif of C-FABP by site-directed point mutation significantly reduced the tumorigenicity of prostate cancer cells.

The results obtained from *in-vitro* assays in this work were consistent with our recent *in-vivo* assays, when inoculated with LNCaP-WT cells, 88.9% nude mice developed tumours. In contrast, only 50%, 37.5% and 37.5% of the mice inoculated with LNCaP-R109A, LNCaP-R109/129A and LNCaP-V cells respectively yielded tumours. The average weight of the tumours produced by LNCaP-WT was 5.8- and 7.3- times of those produced respectively by LNCaP-R109/129A and LNCaP-V cells (Malki *et al*, 2011). This result showed that not only that the wild type C-FABP-expressing cells produced more but also larger tumours than those cells either not expressing C-FABP or expressing mutated C-FABP which was not able to bind and transport fatty acids. Furthermore, consistent with this finding, our previous work established that suppressing expression of C-FABP by either antisense mRNA or RNA interference in the highly malignant prostate cancer cell line PC3M has greatly inhibited its ability of forming tumours in nude mouse (Adamson *et al*, 2003; Forootan *et al*, 2010; Morgan *et al*, 2008). Therefore, The results of the current and previous work *in-vitro* and *in-vivo* further confirmed that C-FABP promotes malignant progression of prostate cancer by its binding and transporting intracellular fatty acids into the cancer cells.

Angiogenesis is a process involving the growth of new capillaries from pre-existing blood vessels. It has been difficult to identify and characterize the earliest molecular changes that facilitate angiogenesis in clinical prostate cancer mostly because of the limited availability and access to human tissue representing early-stage disease. A number of studies have demonstrated that human prostate tumours and cell lines can express VEGF; however, VEGF has also been detected in normal prostate and BPH, which reveals the difficulty inherent in a comprehensive analysis of human prostate cancer specimens. For example, in one study, the level of VEGF mRNA was found to be overexpressed 3-fold or more in 29% of prostate cancer when compared with normal prostate (Montecinos *et al*, 2012). In another study, VEGF protein was detected in 90% of prostate cancers and 100% of BPH specimens (Lynch *et al*, 2012). However, in a separate study, VEGF protein was detected in 80% of prostate cancer, 18% of BPH, and 0% normal prostate samples (Huss *et al*, 2001). Clearly there is some degree of controversy regarding the relationship between VEGF expression and prostate disease, complicated by the fact that prostate cancer is a heterogeneous disease of a heterogeneous population. Clinical studies revealed that the level of VEGF expression in serum, plasma or urine was correlated with higher Gleason grade, metastasis and disease-specific survival (Bok *et al*, 2001; Hudson *et al*, 2012). On the other hand, inhibition of VEGFR-1 and VEGFR-2 using AZD-2171 (Cediranib, AstraZeneca) induced tumour shrinkage in 56.5% of patients (13 out of 23 patients with measurable disease) with 4 meeting the criteria for partial response (Aragon-Ching & Dahut, 2009). These results indicated that VEGF played a dual role in prostate cancer at both the early initiating stage and the later stage for tumour progression and metastasis. VEGF interacts with VEGF-2 to stimulate endothelial

cell proliferation through the mitogen activated protein kinase (MAPK) pathway and promote vascular permeability, and subsequently with VEGFR-1 to assist the organization of new capillary tubes. The current studies showed that angiogenesis-associated genes such as VEGF significantly increased the prostate cancer risk. Our recent unpublished data (Malki *et al*, 2011) showed that increased expression of biologically active VEGF was detected in wild type C-FABP transfectants, but not in the mutant types of the transfectant cells. These results suggested that increased VEGF expression may be caused by wild type C-FABP and that the ability of C-FABP to increase VEGF depends on its fatty acid-binding ability.

Indeed, we have showed that increased wild type C-FABP stimulation in prostate cell line significantly increased cell invasiveness which correlates well with the metastasis potential of prostate cancer cells. Cancer metastasis is a complicated process, which involves a number of changes in the expression patterns of different genes. These changes include the diminished activity of metastasis-suppressing genes or the increased activity of metastasis-inducing genes. One such metastasis-inducing gene identified recently is that for C-FABP, which, when over-expressed, is able to cause Rama 37 cells to metastasize. Our current and previous work showed that transfection of the C-FABP gene into non-metastatic rat mammary Rama 37 model cells (Jing *et al*, 2000) and inoculation of the transfectants into syngeneic Wistar Furth rats demonstrated that over-expression of the C-FABP gene can induce the non-metastatic Rama 37 cells to metastasize to the lungs and lymph nodes. Therefore, the C-FABP gene is suggested to be a metastasis-inducing gene (Jing *et al*, 2001). In addition to blocking invasion, angiogenesis and metastasis, targeting C-

FABP blocked the growth and proliferation of prostate cancer cells. The growth inhibition seen in PC3M cells expressing C-FABP RNAi suggests that, not only does targeting C-FABP block the ability of PC3M cells to metastasize, but also the ability of primary tumours to expand and secondary metastases to establish at distant sites (Lynch *et al*, 2012). It is possible that reducing C-FABP in prostate cancer cells induced defects in growth, invasion and angiogenesis, all contributing to inhibition of bone metastasis. C-FABP silencing in the mouse breast cancer cell line 4T1 inhibited metastatic nodules to lungs but, did not inhibit primary tumour growth (Liu *et al*, 2011). Thusly, targeting C-FABP therapeutically may impair growth at the primary tumour site, the ability of cancer cells to escape primary tumours, as well as the ability of cancer cells to establish and colonize secondary sites. A recent study showed that C-FABP was over-expressed in oral squamous cell carcinoma (OSCC) during early carcinogenesis and tumour metastasis. By increasing or silencing C-FABP expression in OSCC cells, they found that C-FABP levels were positively correlated with *in-vitro* cell growth, MMP-9 expression and invasiveness (Fang *et al*, 2010). MMPs, a family of metalloproteases that degrade extracellular matrix proteins, have been associated with cancer cell invasion and metastasis (Deryugina & Quigley, 2006). The expression of MMPs, particularly the gelatinases (MMP-2 and MMP-9), has been associated with a high potential for metastasis in several human carcinomas, including prostate cancer (Shin & Kim, 2012). Fang *et al* (2010) demonstrated that C-FABP overexpression increases MMP-9 expression and OSCC invasion. However, the molecular mechanisms through which C-FABP regulates MMP-9 expression and OSCC invasion remain unknown. Other studies have shown that C-FABP interacted directly with PPAR and S100A7 (Psoriasin) and then



modulated their activities (Kwon *et al*, 2010; Schug *et al*, 2007b). C-FABP regulated the transcriptional activities of PPAR by governing their ligands to target the receptor, thereby enabling PPAR to exert its biological functions, such as the PPAR-mediated induction of keratinocyte differentiation (Lee *et al*, 2011). Activated PPARs by their ligands or agonists inhibited K562 human erythroleukemia cells and the adhesion and invasion of HL-60 human leukaemia cell as well as down-regulated the expression of MMP-9 and MMP-2 (Eberhardt *et al*, 2002). Down-regulation of S100A7 expression by RNA silencing in a human invasive breast carcinomas cell line up-regulates MMP-13 expression and increases cell migration and invasion (Krop *et al*, 2005; West & Watson, 2010). These data suggested that the effects of C-FABP on the enhanced MMP-9 production and cancer cells invasion might not be associated with these interactions. Therefore, the exact molecular mechanisms of the role of C-FABP on cancer invasion and metastasis remain to be explored.

## 6.2 Conclusion

Subsequent to the results of this study, it is reasonable to hypothesise that there may be fatty acid-initiated signalling pathways are involved in the malignant progression of prostate cancer cells. The order of these pathways is suggested as: the elevated expression of C-FABP gives rise to increased total uptake of fatty acid thus enhancing the fatty acid signalling activity. Therefore, it may be possible that elevated levels of free fatty acids are transported by C-FABP into the cancer cell nuclei to activate downstream mechanisms that might initiate a chain of molecular reactions resulting in promotion of cancer growth and expansion. One of such actions regulated through this unknown mechanism is to up-regulate some important downstream “cancer-promoting” genes, such as VEGF (Adamson *et al*, 2003; Chen *et al*, 2000; Forootan *et al*, 2010), and hence contribute to carcinogenesis. Thus C-FABP which acted as an intercellular fatty acids transporter may play a key role during this process. A schematic hypothesis for the involvement of C-FABP in cancer malignant progression is shown in Figure 6.1.

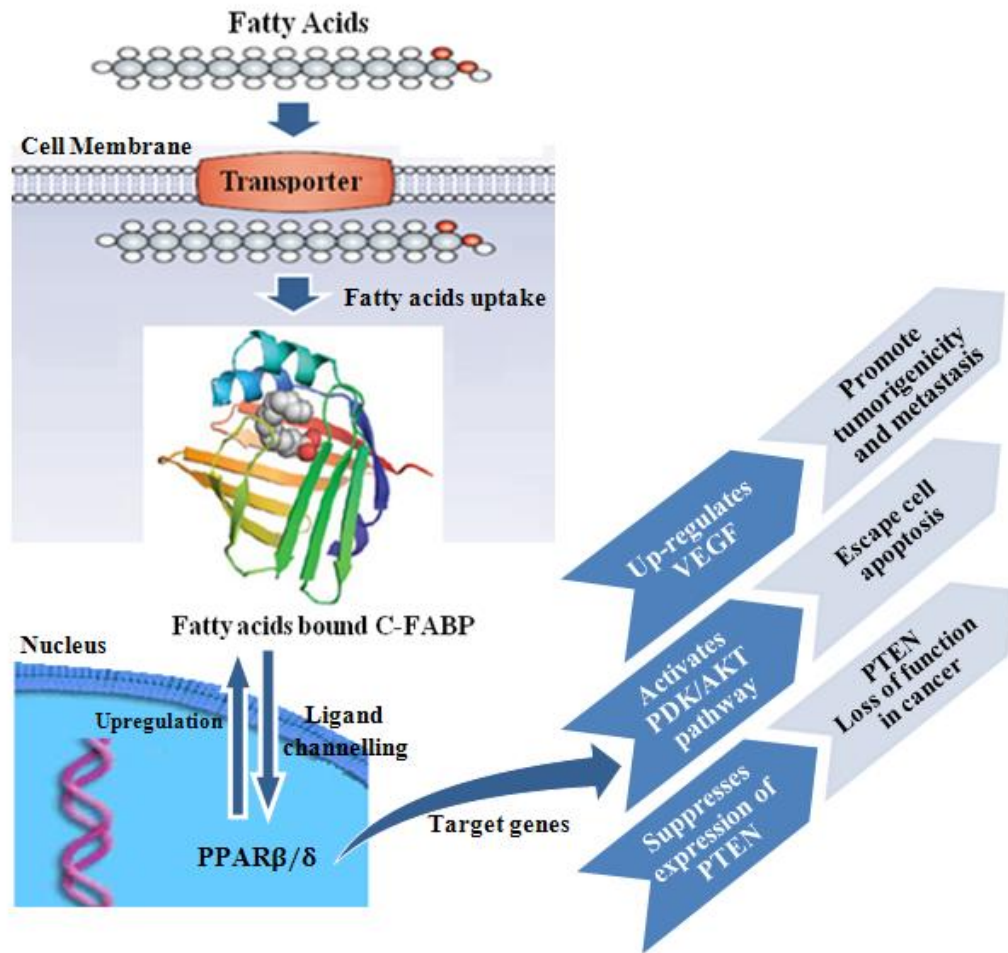


**Figure 6.1: Model for possible C-FABP signalling pathways in prostate cancer malignant progression.**

Upon binding to a cognate ligand, C-FABP translocates to the nucleus where it directly delivers the ligand to its cognate nuclear receptor, PPAR $\beta/\delta$ . Activation of PPAR $\beta/\delta$  results in upregulation of C-FABP. A positive feedback loop is thus established: PPAR $\beta/\delta$  activation induces the expression of C-FABP which, in turn, enhances the transcriptional activity of the receptor. The FABP5/PPAR $\beta/\delta$  pathway induces the expression of PPAR $\beta/\delta$  target genes involved in cell survival, for example, PDK1, and growth and angiogenesis, for example, VEGF, and thus contributes to prostate cancer development.

The free fatty acids move into the blood stream where they are bound by serum albumin and transported to the tissue needing fuel (Hajri & Abumrad, 2002). In these cells, excessive level C-FABP binds to and to transport intracellular fatty acids into cells, its tumor-promoting activity may be related to its fatty acid-transporting ability. Fatty acids have been identified as signalling molecules which can be recognised by their nuclear receptor PPARs (Morgan *et al*, 2010). The elevated expression of *C-FABP* may give rise to an increased total uptake of fatty acids, and hence an enhanced fatty acid signalling activity. Moreover, excessive levels of free fatty acids may be translocated into the nucleus to activate target genes by PPARs through their PPAR recognition (*AGGGCANAGGTCA*) elements (PPRE). Thus, the roles played by FABPs and medium and long chain fatty acids in modulating nuclear receptors and gene transcription may have contributed significantly to carcinogenesis (Schug *et al*, 2007b). One of such actions regulated through this unknown mechanism is to up-regulate some important down-stream “cancer-promoting” genes, such as VEGF (Adamson *et al*, 2003; Chen *et al*, 2000; Forootan *et al*, 2010), and hence to facilitate angiogenesis and contribute to carcinogenesis. Angiogenesis plays an important role in growth, malignant progression and metastasis by promoting endothelial cell proliferation, invasion and capillary differentiation. In addition, it has reported that the pathological surrogate for angiogenesis (microvessel density) is correlated with malignancy of prostate cancer. The current studies showed that angiogenesis-associated genes such as VEGF significantly increased the prostate cancer risk. Our recent unpublished data showed that increased expression of biologically active VEGF was detected in wild type C-FABP transfectants, but not in the mutant types of the transfectant cells. These results suggested that increased

VEGF expression may be caused by wild type C-FABP and that the ability of C-FABP to increase VEGF depends on its fatty acid-binding ability. Other downstream genes leading to suppression of apoptosis through up-regulation of PDK/AKT pathway may be involving in this pathway, strong evidence suggests that ligand activation of PPAR  $\beta/\delta$  can enhance the expression of 3-phosphoinositide dependent protein kinase 1 (PDK1) and subsequently activate the downstream protein kinase B (AKT) by phosphorylation (Di Paola *et al*, 2011). Activation of the PDK1/AKT signalling pathway has a direct effect on cell apoptosis through phosphorylation of the *BCL-2* family member *BCL-2* associated death promoter (BAD) thereby suppressing cell apoptosis and promoting cell survival. Schug *et al*. also suggested that PDK1/AKT anti-apoptosis signalling pathway regulated by PPAR  $\beta/\delta$  (Schug *et al*, 2007a).

### 6.3 Future work

As a first step towards testing the hypothesis, we investigated the relationship between the tumorigenicity-promoting function of C-FABP and its ability of binding to and transporting fatty acid and demonstrated that fatty acid binding and transporting ability is essential for C-FABP to promote tumour growth and expansion. To fully establish this proposed route of fatty acids signalling pathways, further studies are needed to:

- ❖ Investigate how exactly PPAR regulated VEGF leading to angiogenesis. To achieve the answer to this question, gene targeting and reporter gene technique will be employed to establish whether PPAR can directly activate VEGF through its PPAR responsible element (PPRE) located in 5'- untranslated region.
- ❖ Studies also needed to investigate how PPAR regulate down-stream genes leading to suppression of apoptosis in prostate cancer cells. This can be achieved by identification of the major down-stream genes through Gene-Chip micro-array analysis.
- ❖ When assessing the results from micro-array, effort should also be made to investigate whether there are any other cancer-promoting molecules up-regulated.

## **7 REFERENCES**

- Aaltomaa S, Lipponen P, Viitanen J, Kankkunen JP, Ala-Opas M, Kosma VM (2000) Prognostic value of CD44 standard, variant isoforms 3 and 6 and -catenin expression in local prostate cancer treated by radical prostatectomy. *Eur Urol* 38(5): 555-62
- Abate-Shen C, Shen MM (2000) Molecular genetics of prostate cancer. *Genes Dev* 14(19): 2410-34
- Abeele FV, Skryma R, Shuba Y, Van Coppenolle F, Slomianny C, Roudbaraki M, Mauroy B, Wuytack F, Prevarskaya N (2002) Bcl-2-dependent modulation of Ca<sup>2+</sup> homeostasis and store-operated channels in prostate cancer cells. *Cancer cell* 1(2): 169-179
- Adamson J, Morgan EA, Beesley C, Mei Y, Foster CS, Fujii H, Rudland PS, Smith PH, Ke Y (2003) High-level expression of cutaneous fatty acid-binding protein in prostatic carcinomas and its effect on tumorigenicity. *Oncogene* 22(18): 2739-49
- Ali IU (2000) Gatekeeper for Endometrium: the PTEN Tumor Suppressor Gene. *Journal of the National Cancer Institute* 92(11): 861-863
- Amirghofran Z, Monabati A, Gholijani N (2005) Apoptosis in prostate cancer: bax correlation with stage. *Int J Urol* 12(4): 340-5
- Aragon-Ching JB, Dahut WL (2009) VEGF inhibitors and prostate cancer therapy. *Curr Mol Pharmacol* 2(2): 161-8
- Arya M, Bott SR, Shergill IS, Ahmed HU, Williamson M, Patel HR (2006) The metastatic cascade in prostate cancer. *Surg Oncol* 15(3): 117-28
- Attar RM, Takimoto CH, Gottardis MM (2009) Castration-resistant prostate cancer: locking up the molecular escape routes. *Clin Cancer Res* 15(10): 3251-5
- Ayala AG, Ro JY (2007) Prostatic intraepithelial neoplasia: recent advances. *Arch Pathol Lab Med* 131(8): 1257-66
- Baade PD, Youlten DR, Krnjacki LJ (2009) International epidemiology of prostate cancer: geographical distribution and secular trends. *Mol Nutr Food Res* 53(2): 171-84



Balendiran GK, Schnutgen F, Scapin G, Borchers T, Xhong N, Lim K, Godbout R, Spener F, Sacchettini JC (2000) Crystal structure and thermodynamic analysis of human brain fatty acid-binding protein. *J Biol Chem* 275(35): 27045-54

Balk SP (2002) Androgen receptor as a target in androgen-independent prostate cancer. *Urology* 60(3 Suppl 1): 132-8; discussion 138-9

Banham AH, Boddy J, Launchbury R, Han C, Turley H, Malone PR, Harris AL, Fox SB (2007) Expression of the forkhead transcription factor FOXP1 is associated both with hypoxia inducible factors (HIFs) and the androgen receptor in prostate cancer but is not directly regulated by androgens or hypoxia. *Prostate* 67(10): 1091-8

Bastide C, Bagnis C, Mannoni P, Hassoun J, Bladou F (2002) A Nod Scid mouse model to study human prostate cancer. *Prostate Cancer Prostatic Dis* 5(4): 311-5

Bennett S, Joshua A, Russell PJ (1997) Reliable method of isolating transfected clones from the LNCaP human prostatic cell line. *Biotechniques* 23(1): 66, 68, 70

Berry PA, Maitland NJ, Collins AT (2008) Androgen receptor signalling in prostate: effects of stromal factors on normal and cancer stem cells. *Mol Cell Endocrinol* 288(1-2): 30-7

Boddy JL, Fox SB, Han C, Campo L, Turley H, Kanga S, Malone PR, Harris AL (2005) The androgen receptor is significantly associated with vascular endothelial growth factor and hypoxia sensing via hypoxia-inducible factors HIF-1a, HIF-2a, and the prolyl hydroxylases in human prostate cancer. *Clin Cancer Res* 11(21): 7658-63

Bok RA, Halabi S, Fei DT, Rodriguez CR, Hayes DF, Vogelzang NJ, Kantoff P, Shuman MA, Small EJ (2001) Vascular endothelial growth factor and basic fibroblast growth factor urine levels as predictors of outcome in hormone-refractory prostate cancer patients: a cancer and leukemia group B study. *Cancer Res* 61(6): 2533-6

Bonkhoff H, Remberger K (1996) Differentiation pathways and histogenetic aspects of normal and abnormal prostatic growth: a stem cell model. *Prostate* 28(2): 98-106

Bookstein R, Shew JY, Chen PL, Scully P, Lee WH (1990) Suppression of tumorigenicity of human prostate carcinoma cells by replacing a mutated RB gene. *Science* 247(4943): 712-715

Bosetti C, Bertuccio P, Levi F, Lucchini F, Negri E, La Vecchia C (2008) Cancer mortality in the European Union, 1970–2003, with a joinpoint analysis. *Annals of Oncology* 19(4): 631-640

Bratt O (2002) Hereditary prostate cancer: clinical aspects. *J Urol* 168(3): 906-13

Brewster DH, Fraser LA, Harris V, Black RJ (2000) Rising incidence of prostate cancer in Scotland: increased risk or increased detection? *BJU Int* 85(4): 463-72; discussion 472-3

Brooks JD, Bova GS, Ewing CM, Piantadosi S, Carter BS, Robinson JC, Epstein JI, Isaacs WB (1996) An uncertain role for p53 gene alterations in human prostate cancers. *Cancer Res* 56(16): 3814-22

Bui M, Reiter RE (1998) Stem Cell Genes in Androgen-independent Prostate Cancer. *Cancer and Metastasis Reviews* 17(4): 391-399

Burchardt M, Burchardt T, Shabsigh A, Ghafar M, Chen M-W, Anastasiadis A, de la Taille A, Kiss A, Buttyan R (2001) Reduction of wild type p53 function confers a hormone resistant phenotype on LNCaP prostate cancer cells\*. *The Prostate* 48(4): 225-230

Cairns P, Okami K, Halachmi S, Halachmi N, Esteller M, Herman JG, Jen J, Isaacs WB, Bova GS, Sidransky D (1997) Frequent inactivation of PTEN/MMAC1 in primary prostate cancer. *Cancer Res* 57(22): 4997-5000

Carmeliet P, Jain RK (2000) Angiogenesis in cancer and other diseases. *Nature* 407(6801): 249-257

Catz SD, Johnson JL (2003) BCL-2 in prostate cancer: A minireview. *Apoptosis* 8(1): 29-37

Celis A, Rasmussen HH, Celis P, Basse B, Lauridsen JB, Ratz G, Hein B, Ostergaard M, Wolf H, Orntoft T, Celis JE (1999) Short-term culturing of low-grade superficial bladder transitional cell carcinomas leads to changes in the expression levels of several proteins involved in key cellular activities. *Electrophoresis* 20(2): 355-61

Cerveira N, Ribeiro FR, Peixoto A, Costa V, Henrique R, Jeronimo C, Teixeira MR (2006) TMPRSS2-ERG gene fusion causing ERG overexpression precedes chromosome copy number changes in prostate carcinomas and paired HGPIN lesions. *Neoplasia* 8(10): 826-32

Chan JM, Stampfer MJ, Giovannucci E, Gann PH, Ma J, Wilkinson P, Hennekens CH, Pollak M (1998) Plasma Insulin-Like Growth Factor-I and Prostate Cancer Risk: A Prospective Study. *Science* 279(5350): 563-566

Chavarro JE, Stampfer MJ, Campos H, Kurth T, Willett WC, Ma J (2008) A prospective study of trans-fatty acid levels in blood and risk of prostate cancer. *Cancer Epidemiol Biomarkers Prev* 17(1): 95-101

Chen C, Lewis SK, Voigt L, Fitzpatrick A, Plymate SR, Weiss NS (2005) Prostate carcinoma incidence in relation to prediagnostic circulating levels of insulin-like growth factor I, insulin-like growth factor binding protein 3, and insulin. *Cancer* 103(1): 76-84

Chen HJ, Treweek AT, Ke YQ, West DC, Toh CH (2000) Angiogenically active vascular endothelial growth factor is over-expressed in malignant human and rat prostate carcinoma cells. *Br J Cancer* 82(10): 1694-701

Chi KN (2005) Targeting Bcl-2 with oblimersen for patients with hormone refractory prostate cancer. *World J Urol* 23(1): 33-7

Chmurzyńska A (2006) The multigene family of fatty acid-binding proteins (FABPs): Function, structure and polymorphism. *Journal of Applied Genetics* 47(1): 39-48

Coe NR, Bernlohr DA (1998) Physiological properties and functions of intracellular fatty acid-binding proteins. *Biochim Biophys Acta* 1391(3): 287-306

Coffey DS, Isaacs JT (1981) Control of prostate growth. *Urology* 17(Suppl 3): 17-24

Collett GP, Betts AM, Johnson MI, Pulimood AB, Cook S, Neal DE, Robson CN (2000) Peroxisome Proliferator-activated Receptor  $\alpha$  Is an Androgen-responsive Gene in Human Prostate and Is Highly Expressed in Prostatic Adenocarcinoma. *Clinical Cancer Research* 6(8): 3241-3248

Collins AT, Maitland NJ (2006) Prostate cancer stem cells. *European journal of cancer (Oxford, England : 1990)* 42(9): 1213-1218

Craft N, Shostak Y, Carey M, Sawyers CL (1999) A mechanism for hormone-independent prostate cancer through modulation of androgen receptor signaling by the HER-2/neu tyrosine kinase. *Nat Med* 5(3): 280-285

Crowe FL, Allen NE, Appleby PN, Overvad K, Aardestrup IV, Johnsen NF, Tjønneland A, Linseisen J, Kaaks R, Boeing H, Kroger J, Trichopoulou A, Zavitsanou A, Trichopoulos D, Sacerdote C, Palli D, Tumino R, Agnoli C, Kiemeny LA, Bueno-de-Mesquita HB, Chirlaque MD, Ardanaz E, Larranaga N, Quiros JR, Sanchez MJ, Gonzalez CA, Stattin P, Hallmans G, Bingham S, Khaw KT, Rinaldi S, Slimani N, Jenab M, Riboli E, Key TJ (2008) Fatty acid composition of plasma phospholipids and risk of prostate cancer in a case-control analysis nested within the European Prospective Investigation into Cancer and Nutrition. *Am J Clin Nutr* 88(5): 1353-63

Culig Z, Bartsch G (2006) Androgen axis in prostate cancer. *J Cell Biochem* 99(2): 373-81

Culig Z, Hobisch A, Cronauer MV, Radmayr C, Hittmair A, Zhang J, Thurnher M, Bartsch G, Klocker H (1996) Regulation of prostatic growth and function by peptide growth factors. *Prostate* 28(6): 392-405

Culig Z, Hobisch A, Cronauer MV, Radmayr C, Trapman J, Hittmair A, Bartsch G, Klocker H (1994a) Androgen receptor activation in prostatic tumor cell lines by insulin-like growth factor-I, keratinocyte growth factor, and epidermal growth factor. *Cancer Res* 54(20): 5474-8

Culig Z, Hobisch A, Cronauer MV, Radmayr C, Trapman J, Hittmair A, Bartsch G, Klocker H (1994b) Androgen receptor activation in prostatic tumor cell lines by insulin-like growth factor-I, keratinocyte growth factor, and epidermal growth factor. *Cancer Research* 54(20): 5474-8

Das R, Hammamieh R, Neill R, Melhem M, Jett M (2001) Expression pattern of fatty acid-binding proteins in human normal and cancer prostate cells and tissues. *Clin Cancer Res* 7(6): 1706-15

Davies MA, Koul D, Dhesi H, Berman R, McDonnell TJ, McConkey D, Yung WK, Steck PA (1999) Regulation of Akt/PKB activity, cellular growth, and apoptosis in prostate carcinoma cells by MMAC/PTEN. *Cancer Res* 59(11): 2551-6

de Jong FH, Reuvers PJ, Bolt-de Vries J, Mulder E, Blom JH, Schroeder FH (1992) Androgens and androgen-receptors in prostate tissue from patients with benign prostatic hyperplasia: effects of cyproterone acetate. *J Steroid Biochem Mol Biol* 42(1): 49-55

De Marzo AM, Bradshaw C, Sauvageot J, Epstein JI, Miller GJ (1998) CD44 and CD44v6 downregulation in clinical prostatic carcinoma: Relation to Gleason grade and cytoarchitecture. *The Prostate* 34(3): 162-168

De Santis ML, Hammamieh R, Das R, Jett M (2004) Adipocyte-fatty acid binding protein induces apoptosis in DU145 prostate cancer cells. *J Exp Ther Oncol* 4(2): 91-100

Demichelis F, Fall K, Perner S, Andren O, Schmidt F, Setlur SR, Hoshida Y, Mosquera JM, Pawitan Y, Lee C, Adami HO, Mucci LA, Kantoff PW, Andersson SO, Chinnaiyan AM, Johansson JE, Rubin MA (2007) TMPRSS2:ERG gene fusion associated with lethal prostate cancer in a watchful waiting cohort. *Oncogene* 26(31): 4596-9

Deryugina EI, Quigley JP (2006) Matrix metalloproteinases and tumor metastasis. *Cancer Metastasis Rev* 25(1): 9-34

Dhanasekaran SM, Barrette TR, Ghosh D, Shah R, Varambally S, Kurachi K, Pienta KJ, Rubin MA, Chinnaiyan AM (2001) Delineation of prognostic biomarkers in prostate cancer. *Nature* 412(6849): 822-826

Di Paola R, Briguglio F, Paterniti I, Mazzon E, Oteri G, Militi D, Cordasco G, Cuzzocrea S (2011) Emerging role of PPAR-beta/delta in inflammatory process associated to experimental periodontitis. *Mediators Inflamm* 2011: 787159

Dong JT, Lamb PW, Rinker-Schaeffer CW, Vukanovic J, Ichikawa T, Isaacs JT, Barrett JC (1995) KAI1, a metastasis suppressor gene for prostate cancer on human chromosome 11p11.2. *Science* 268(5212): 884-6

Dong JT, Li CL, Sipe TW, Frierson HF, Jr. (2001) Mutations of PTEN/MMAC1 in primary prostate cancers from Chinese patients. *Clin Cancer Res* 7(2): 304-8

Dorff TB, Quek ML, Daneshmand S, Pinski J (2006) Evolving treatment paradigms for locally advanced and metastatic prostate cancer. *Expert Rev Anticancer Ther* 6(11): 1639-51

Du Z, Fujiyama C, Chen Y, Masaki Z (2003) Expression of hypoxia-inducible factor 1alpha in human normal, benign, and malignant prostate tissue. *Chin Med J (Engl)* 116(12): 1936-9

Duque JL, Loughlin KR, Adam RM, Kantoff PW, Zurakowski D, Freeman MR (1999) Plasma levels of vascular endothelial growth factor are increased in patients with metastatic prostate cancer. *Urology* 54(3): 523-7

Eberhardt W, Akool el S, Rebhan J, Frank S, Beck KF, Franzen R, Hamada FM, Pfeilschifter J (2002) Inhibition of cytokine-induced matrix metalloproteinase 9 expression by peroxisome proliferator-activated receptor alpha agonists is indirect and due to a NO-mediated reduction of mRNA stability. *J Biol Chem* 277(36): 33518-28

Edwards BK, Brown ML, Wingo PA, Howe HL, Ward E, Ries LA, Schrag D, Jamison PM, Jemal A, Wu XC, Friedman C, Harlan L, Warren J, Anderson RN, Pickle LW (2005) Annual report to the nation on the status of cancer, 1975-2002, featuring population-based trends in cancer treatment. *J Natl Cancer Inst* 97(19): 1407-27

Fang L-Y, Wong T-Y, Chiang W-F, Chen Y-L (2010) Fatty-acid-binding protein 5 promotes cell proliferation and invasion in oral squamous cell carcinoma. *Journal of Oral Pathology & Medicine* 39(4): 342-348

Fang LY, Wong TY, Chiang WF, Chen YL (2009) Fatty-acid-binding protein 5 promotes cell proliferation and invasion in oral squamous cell carcinoma. *J Oral Pathol Med*

Fauconnet S, Lascombe I, Chabannes E, Adessi GL, Desvergne B, Wahli W, Bittard H (2002) Differential regulation of vascular endothelial growth factor expression by peroxisome proliferator-activated receptors in bladder cancer cells. *J Biol Chem* 277(26): 23534-43

Feldman BJ, Feldman D (2001) The development of androgen-independent prostate cancer. *Nat Rev Cancer* 1(1): 34-45

Ferrara N (2004) Vascular endothelial growth factor: basic science and clinical progress. *Endocr Rev* 25(4): 581-611

Folkman J (2002) Role of angiogenesis in tumor growth and metastasis. *Semin Oncol* 29(6 Suppl 16): 15-8

Forootan SS, Bao ZZ, Forootan FS, Kamalian L, Zhang Y, Bee A, Foster CS, Ke Y (2010) Atelocollagen-delivered siRNA targeting the FABP5 gene as an experimental therapy for prostate cancer in mouse xenografts. *Int J Oncol* 36(1): 69-76

Fosslien E (2000) Biochemistry of Cyclooxygenase (COX)-2 Inhibitors and Molecular Pathology of COX-2 in Neoplasia. *Critical Reviews in Clinical Laboratory Sciences* 37(5): 431-502

Foster, Cornford, Forsyth, Djamgoz, Ke (1999) The cellular and molecular basis of prostate cancer. *BJU International* 83(2): 171-194

Foster CS, Ke Y (1997) Stem cells in prostatic epithelia. *Int J Exp Pathol* 78(5): 311-29

Fujii K, Kondo T, Yokoo H, Yamada T, Iwatsuki K, Hirohashi S (2005) Proteomic study of human hepatocellular carcinoma using two-dimensional difference gel electrophoresis with saturation cysteine dye. *Proteomics* 5(5): 1411-22

Furuhashi M, Hotamisligil GS (2008) Fatty acid-binding proteins: role in metabolic diseases and potential as drug targets. *Nat Rev Drug Discov* 7(6): 489-503

Gillilan RE, Ayers SD, Noy N (2007) Structural basis for activation of fatty acid-binding protein 4. *J Mol Biol* 372(5): 1246-60

Gioeli D (2005) Signal transduction in prostate cancer progression. *Clin Sci* 108(4): 293-308

Glatz JF, van der Vusse GJ (1996) Cellular fatty acid-binding proteins: their function and physiological significance. *Prog Lipid Res* 35(3): 243-82

Gleave M, Hsieh JT, Gao CA, von Eschenbach AC, Chung LW (1991) Acceleration of human prostate cancer growth in vivo by factors produced by prostate and bone fibroblasts. *Cancer Res* 51(14): 3753-61

Grandori C, Cowley SM, James LP, Eisenman RN (2000) THE MYC/MAX/MAD NETWORK AND THE TRANSCRIPTIONAL CONTROL OF CELL BEHAVIOR. *Annual Review of Cell and Developmental Biology* 16(1): 653-699

Gregory CW, Fei X, Ponguta LA, He B, Bill HM, French FS, Wilson EM (2004) Epidermal growth factor increases coactivation of the androgen receptor in recurrent prostate cancer. *J Biol Chem* 279(8): 7119-30

Gregory CW, Johnson RT, Jr., Mohler JL, French FS, Wilson EM (2001) Androgen receptor stabilization in recurrent prostate cancer is associated with hypersensitivity to low androgen. *Cancer Res* 61(7): 2892-8

Gumerlock PH, Poonamallee UR, Meyers FJ, deVere White RW (1991) Activated ras Alleles in Human Carcinoma of the Prostate Are Rare. *Cancer Research* 51(6): 1632-1637

Gurel B, Iwata T, M Koh C, Jenkins RB, Lan F, Van Dang C, Hicks JL, Morgan J, Cornish TC, Sutcliffe S, Isaacs WB, Luo J, De Marzo AM (2008) Nuclear MYC protein overexpression is an early alteration in human prostate carcinogenesis. *Mod Pathol* 21(9): 1156-1167

Haapala K, Kuukasjarvi T, Hyytinen E, Rantala I, Helin HJ, Koivisto PA (2007) Androgen receptor amplification is associated with increased cell proliferation in prostate cancer. *Hum Pathol* 38(3): 474-8

Hagan RM, Worner-Gibbs J, Wilton DC (2008) The interaction of liver fatty-acid-binding protein (FABP) with anionic phospholipid vesicles: is there extended phospholipid anchorage under these conditions? *Biochem J* 410(1): 123-9

Hajra KM, Fearon ER (2002) Cadherin and catenin alterations in human cancer. *Genes Chromosomes Cancer* 34(3): 255-68

Hajri T, Abumrad NA (2002) FATTY ACID TRANSPORT ACROSS MEMBRANES: Relevance to Nutrition and Metabolic Pathology1. *Annual Review of Nutrition* 22(1): 383-415

Hammamieh R, Chakraborty N, Barmada M, Das R, Jett M (2005) Expression patterns of fatty acid binding proteins in breast cancer cells. *J Exp Ther Oncol* 5(2): 133-43

Hammamieh R, Chakraborty N, Das R, Jett M (2004) Molecular impacts of antisense complementary to the liver fatty acid binding protein (FABP) mRNA in DU 145 prostate cancer cells in vitro. *J Exp Ther Oncol* 4(3): 195-202

Han JK, Lee HS, Yang HM, Hur J, Jun SI, Kim JY, Cho CH, Koh GY, Peters JM, Park KW, Cho HJ, Lee HY, Kang HJ, Oh BH, Park YB, Kim HS (2008) Peroxisome proliferator-activated receptor-delta agonist enhances vasculogenesis by regulating endothelial progenitor cells through genomic and nongenomic activations of the phosphatidylinositol 3-kinase/Akt pathway. *Circulation* 118(10): 1021-33



Harmon GS, Dumlao DS, Ng DT, Barrett KE, Dennis EA, Dong H, Glass CK (2010) Pharmacological correction of a defect in PPAR-[gamma] signaling ameliorates disease severity in Cftr-deficient mice. *Nat Med* 16(3): 313-318

Hartsough MT, Steeg PS (2000) Nm23/nucleoside diphosphate kinase in human cancers. *J Bioenerg Biomembr* 32(3): 301-8

Haslmayer P, Thalhammer T, Jager W, Aust S, Steiner G, Ensinger C, Obrist P (2002) The peroxisome proliferator-activated receptor gamma ligand 15-deoxy-Delta12,14-prostaglandin J2 induces vascular endothelial growth factor in the hormone-independent prostate cancer cell line PC 3 and the urinary bladder carcinoma cell line 5637. *Int J Oncol* 21(4): 915-20

Haunerland NH, Spener F (2004) Fatty acid-binding proteins--insights from genetic manipulations. *Prog Lipid Res* 43(4): 328-49

Hermans KG, van Marion R, van Dekken H, Jenster G, van Weerden WM, Trapman J (2006) TMPRSS2:ERG fusion by translocation or interstitial deletion is highly relevant in androgen-dependent prostate cancer, but is bypassed in late-stage androgen receptor-negative prostate cancer. *Cancer Res* 66(22): 10658-63

Hertzel AV, Bennaars-Eiden A, Bernlohr DA (2002) Increased lipolysis in transgenic animals overexpressing the epithelial fatty acid binding protein in adipose cells. *J Lipid Res* 43(12): 2105-11

Holen I, Croucher PI, Hamdy FC, Eaton CL (2002) Osteoprotegerin (OPG) is a survival factor for human prostate cancer cells. *Cancer Res* 62(6): 1619-23

Horoszewicz JS, Leong SS, Kawinski E, Karr JP, Rosenthal H, Chu TM, Mirand EA, Murphy GP (1983a) LNCaP Model of Human Prostatic Carcinoma. *Cancer Research* 43(4): 1809-1818

Horoszewicz JS, Leong SS, Kawinski E, Karr JP, Rosenthal H, Chu TM, Mirand EA, Murphy GP (1983b) LNCaP model of human prostatic carcinoma. *Cancer Res* 43(4): 1809-18

Hotamisligil GS (2006) Inflammation and metabolic disorders. *Nature* 444(7121): 860-7

Hsing AW (2001) Hormones and Prostate Cancer: What's Next? *Epidemiologic Reviews* 23(1): 42-58

Hudson TS, Perkins SN, Hursting SD, Young HA, Kim YS, Wang TC, Wang TT (2012) Inhibition of androgen-responsive LNCaP prostate cancer cell tumor xenograft growth by dietary phenethyl isothiocyanate correlates with decreased angiogenesis and inhibition of cell attachment. *Int J Oncol* 40(4): 1113-21

Hughes-Fulford M, Chen Y, Tjandrawinata RR (2001) Fatty acid regulates gene expression and growth of human prostate cancer PC-3 cells. *Carcinogenesis* 22(5): 701-7

Humphrey PA (2004) Gleason grading and prognostic factors in carcinoma of the prostate. *Mod Pathol* 17(3): 292-306

Huss WJ, Hanrahan CF, Barrios RJ, Simons JW, Greenberg NM (2001) Angiogenesis and prostate cancer: identification of a molecular progression switch. *Cancer Res* 61(6): 2736-43

Hynes NE, Lane HA (2005) ERBB receptors and cancer: the complexity of targeted inhibitors. *Nat Rev Cancer* 5(5): 341-354

Igawa M, Urakami S, Shiina H, Ishibe T, Usui T, Chodak GW (1996) Association of nm23 protein levels in human prostates with proliferating cell nuclear antigen expression at autopsy. *Eur Urol* 30(3): 383-7

Isaacs JT (1999) The biology of hormone refractory prostate cancer. Why does it develop? *Urol Clin North Am* 26(2): 263-73

Isaacs SD, Kiemeny LA, Baffoe-Bonnie A, Beaty TH, Walsh PC (1995) Risk of cancer in relatives of prostate cancer probands. *J Natl Cancer Inst* 87(13): 991-6

Isaacs WB, Carter BS, Ewing CM (1991) Wild-type p53 suppresses growth of human prostate cancer cells containing mutant p53 alleles. *Cancer Res* 51(17): 4716-20

Jackson MW, Roberts JS, Heckford SE, Ricciardelli C, Stahl J, Choong C, Horsfall DJ, Tilley WD (2002) A potential autocrine role for vascular endothelial growth factor in prostate cancer. *Cancer Res* 62(3): 854-9

Jackson P, Ow K, Yardley G, Delprado W, Quinn D, Yang JL, Russell PJ (2003) Downregulation of KAI1 mRNA in localised prostate cancer and its bony metastases does not correlate with p53 overexpression. *Prostate Cancer Prostatic Dis* 6(2): 174-181

Jemal A, Siegel R, Ward E, Hao Y, Xu J, Murray T, Thun MJ (2008) Cancer Statistics, 2008. *CA Cancer J Clin* 58(2): 71-96

Jing C, Beesley C, Foster CS, Chen H, Rudland PS, West DC, Fujii H, Smith PH, Ke Y (2001) Human cutaneous fatty acid-binding protein induces metastasis by up-regulating the expression of vascular endothelial growth factor gene in rat Rama 37 model cells. *Cancer Res* 61(11): 4357-64

Jing C, Beesley C, Foster CS, Rudland PS, Fujii H, Ono T, Chen H, Smith PH, Ke Y (2000) Identification of the messenger RNA for human cutaneous fatty acid-binding protein as a metastasis inducer. *Cancer Res* 60(9): 2390-8

Joniau S, Goeman L, Pennings J, Van Poppel H (2005) Prostatic intraepithelial neoplasia (PIN): importance and clinical management. *Eur Urol* 48(3): 379-85

Joseph IB, Nelson JB, Denmeade SR, Isaacs JT (1997) Androgens regulate vascular endothelial growth factor content in normal and malignant prostatic tissue. *Clin Cancer Res* 3(12 Pt 1): 2507-11

Kassis J, Moellinger J, Lo H, Greenberg NM, Kim HG, Wells A (1999) A role for phospholipase C-gamma-mediated signaling in tumor cell invasion. *Clin Cancer Res* 5(8): 2251-60

Katsumata M, Siegel RM, Louie DC, Miyashita T, Tsujimoto Y, Nowell PC, Greene MI, Reed JC (1992) Differential effects of Bcl-2 on T and B cells in transgenic mice. *Proceedings of the National Academy of Sciences of the United States of America* 89(23): 11376-11380

Kauffman EC, Robinson VL, Stadler WM, Sokoloff MH, Rinker-Schaeffer CW (2003) Metastasis suppression: the evolving role of metastasis suppressor genes for regulating cancer cell growth at the secondary site. *J Urol* 169(3): 1122-33

Keller H, Dreyer C, Medin J, Mahfoudi A, Ozato K, Wahli W (1993) Fatty acids and retinoids control lipid metabolism through activation of peroxisome proliferator-activated receptor-retinoid X receptor heterodimers. *Proc Natl Acad Sci U S A* 90(6): 2160-4

Kingsley LA, Fournier PG, Chirgwin JM, Guise TA (2007) Molecular biology of bone metastasis. *Mol Cancer Ther* 6(10): 2609-17

Kitagawa Y, Dai J, Zhang J, Keller JM, Nor J, Yao Z, Keller ET (2005) Vascular endothelial growth factor contributes to prostate cancer-mediated osteoblastic activity. *Cancer Res* 65(23): 10921-9

Knudson AG (2001) Two genetic hits (more or less) to cancer. *Nat Rev Cancer* 1(2): 157-62

Knudson AG, Jr. (1971) Mutation and cancer: statistical study of retinoblastoma. *Proc Natl Acad Sci U S A* 68(4): 820-3

Koivisto P, Kononen J, Palmberg C, Tammela T, Hyytinen E, Isola J, Trapman J, Cleutjens K, Noordzij A, Visakorpi T, Kallioniemi OP (1997) Androgen receptor gene amplification: a possible molecular mechanism for androgen deprivation therapy failure in prostate cancer. *Cancer Res* 57(2): 314-9

Krop I, März A, Carlsson H, Li X, Bloushtain-Qimron N, Hu M, Gelman R, Sabel MS, Schnitt S, Ramaswamy S, Kleer CG, Enerbäck C, Polyak K (2005) A Putative Role for Psoriasin in Breast Tumor Progression. *Cancer Research* 65(24): 11326-11334

Kurahashi N, Inoue M, Iwasaki M, Sasazuki S, Tsugane AS (2008) Dairy product, saturated fatty acid, and calcium intake and prostate cancer in a prospective cohort of Japanese men. *Cancer Epidemiol Biomarkers Prev* 17(4): 930-7

Kusakari Y, Ogawa E, Owada Y, Kitanaka N, Watanabe H, Kimura M, Tagami H, Kondo H, Aiba S, Okuyama R (2006) Decreased keratinocyte motility in skin wound on mice lacking the epidermal fatty acid binding protein gene. *Mol Cell Biochem* 284(1-2): 183-8

Kwon YW, Chang IH, Kim KD, Kim YS, Myung SC, Kim MK, Kim TH (2010) Significance of S100A2 and S100A4 Expression in the Progression of Prostate Adenocarcinoma. *Korean J Urol* 51(7): 456-62

Labrie F, Belanger A, Luu-The V, Labrie C, Simard J, Cusan L, Gomez J, Candas B (2005) Gonadotropin-releasing hormone agonists in the treatment of prostate cancer. *Endocr Rev* 26(3): 361-79

Lee SY, Park SY, Kim SH, Choi EC (2011) Expression of matrix metalloproteinases and their inhibitors in squamous cell carcinoma of the tonsil and their clinical significance. *Clin Exp Otorhinolaryngol* 4(2): 88-94

Levitt NC, Hickson ID (2002) Caretaker tumour suppressor genes that defend genome integrity. *Trends Mol Med* 8(4): 179-86

Lichtenstein P, Holm NV, Verkasalo PK, Iliadou A, Kaprio J, Koskenvuo M, Pukkala E, Skytthe A, Hemminki K (2000) Environmental and heritable factors in the causation of cancer--analyses of cohorts of twins from Sweden, Denmark, and Finland. *N Engl J Med* 343(2): 78-85

Lilien J, Balsamo J, Arregui C, Xu G (2002) Turn-off, drop-out: Functional state switching of cadherins. *Developmental Dynamics* 224(1): 18-29

Lindstrom S, Wiklund F, Jonsson BA, Adami HO, Balter K, Brookes AJ, Xu J, Zheng SL, Isaacs WB, Adolfsson J, Gronberg H (2005) Comprehensive genetic evaluation of common E-cadherin sequence variants and prostate cancer risk: strong confirmation of functional promoter SNP. *Hum Genet* 118(3-4): 339-47

Liu RZ, Graham K, Glubrecht DD, Germain DR, Mackey JR, Godbout R (2011) Association of FABP5 expression with poor survival in triple-negative breast cancer: implication for retinoic acid therapy. *Am J Pathol* 178(3): 997-1008

Liu Y, Jiang C, Tan Y (2002) [Pathological study on the expression of cell adhesion molecules and metastasis suppressor gene in thyroid follicular carcinoma and papillary carcinoma]. *Zhonghua Bing Li Xue Za Zhi* 31(4): 322-6

Lombardi D (2006) Commentary: nm23, a metastasis suppressor gene with a tumor suppressor gene aptitude? *J Bioenerg Biomembr* 38(3-4): 177-80

Lunenfeld B (2002) The ageing male: demographics and challenges. *World J Urol* 20(1): 11-6

Lynch TP, Ferrer CM, Jackson SR, Shahriari KS, Vosseller K, Reginato MJ (2012) Critical role of O-GlcNAc transferase in prostate cancer invasion, angiogenesis and metastasis. *J Biol Chem*

Ma X, Ziel-van der Made AC, Autar B, van der Korput HA, Vermeij M, van Duijn P, Cleutjens KB, de Krijger R, Krimpenfort P, Berns A, van der Kwast TH, Trapman J (2005) Targeted Biallelic Inactivation of Pten in the Mouse Prostate Leads to

Prostate Cancer Accompanied by Increased Epithelial Cell Proliferation but not by Reduced Apoptosis. *Cancer Research* 65(13): 5730-5739

Maeda K, Uysal KT, Makowski L, Görgün CZ, Atsumi G, Parker RA, Brüning J, Hertzel AV, Bernlohr DA, Hotamisligil GS (2003) Role of the Fatty Acid Binding Protein mal1 in Obesity and Insulin Resistance. *Diabetes* 52(2): 300-307

Makridakis NM, Reichardt JK (2004) Molecular epidemiology of androgen-metabolic loci in prostate cancer: predisposition and progression. *J Urol* 171(2 Pt 2): S25-8; discussion S28-9

Malki MI, Bao ZZ, Forootan S, Adamson J, Kamalian L, Zhang Y, Foster C, Rudland P, Ke Y (2011) Tumorigenicity-promoting activity of C-FABP in prostate cancer cells depends on its fatty acid-binding capability. pp 1-18. *Molecular and Clinical Cancer Medicine: The University of Liverpool*

Marcelli M, Ittmann M, Mariani S, Sutherland R, Nigam R, Murthy L, Zhao Y, DiConcini D, Puxeddu E, Esen A, Eastham J, Weigel NL, Lamb DJ (2000) Androgen Receptor Mutations in Prostate Cancer. *Cancer Research* 60(4): 944-949

Masouye I, Saurat JH, Siegenthaler G (1996) Epidermal fatty-acid-binding protein in psoriasis, basal and squamous cell carcinomas: an immunohistological study. *Dermatology* 192(3): 208-13

Matsushima H, Hosaka Y, Suzuki M, Mizutani T, Ishizuka H, Kawabe K (1996) bcl-2 Expression on Prostate Cancer and its Relationship to Cell Cycle and Prognosis. *International Journal of Urology* 3(2): 113-117

McCall P, Gemmell LK, Mukherjee R, Bartlett JM, Edwards J (2008) Phosphorylation of the androgen receptor is associated with reduced survival in hormone-refractory prostate cancer patients. *Br J Cancer* 98(6): 1094-101

McDonnell TJ, Troncoso P, Brisbay SM, Logothetis C, Chung LW, Hsieh JT, Tu SM, Campbell ML (1992) Expression of the protooncogene bcl-2 in the prostate and its association with emergence of androgen-independent prostate cancer. *Cancer Res* 52(24): 6940-4

McMenamin ME, Soung P, Perera S, Kaplan I, Loda M, Sellers WR (1999) Loss of PTEN expression in paraffin-embedded primary prostate cancer correlates with high Gleason score and advanced stage. *Cancer Res* 59(17): 4291-6

Medinger M, Adler CP, Schmidt-Gersbach C, Soltau J, Droll A, Unger C, Dreys J (2003) Angiogenesis and the ET-1/ETA receptor system: immunohistochemical expression analysis in bone metastases from patients with different primary tumors. *Angiogenesis* 6(3): 225-31

Merrill RM, Bird JS (2002) Effect of young age on prostate cancer survival: a population-based assessment (United States). *Cancer Causes and Control* 13(5): 435-443

Miyamoto H, Messing EM, Chang C (2004) Androgen deprivation therapy for prostate cancer: current status and future prospects. *Prostate* 61(4): 332-53

Molinie V (2008) [Gleason's score: update in 2008]. *Ann Pathol* 28(5): 350-3

Montecinos VP, Godoy A, Hinklin J, Vethanayagam RR, Smith GJ (2012) Primary xenografts of human prostate tissue as a model to study angiogenesis induced by reactive stroma. *PLoS One* 7(1): e29623

Montironi R, Mazzucchelli R, Algaba F, Lopez-Beltran A (2000) Morphological identification of the patterns of prostatic intraepithelial neoplasia and their importance. *J Clin Pathol* 53(9): 655-65

Morgan E, Kannan-Thulasiraman P, Noy N (2010) Involvement of Fatty Acid Binding Protein 5 and PPARbeta/delta in Prostate Cancer Cell Growth. *PPAR Res* 2010

Morgan EA, Forootan SS, Adamson J, Foster CS, Fujii H, Igarashi M, Beesley C, Smith PH, Ke Y (2008) Expression of cutaneous fatty acid-binding protein (C-FABP) in prostate cancer: potential prognostic marker and target for tumorigenicity-suppression. *Int J Oncol* 32(4): 767-75

Mori K, Le Goff B, Charrier C, Battaglia S, Heymann D, Redini F (2007) DU145 human prostate cancer cells express functional receptor activator of NFkappaB: new insights in the prostate cancer bone metastasis process. *Bone* 40(4): 981-90

Mostaghel EA, Montgomery B, Nelson PS (2009) Castration-resistant prostate cancer: Targeting androgen metabolic pathways in recurrent disease. *Urologic Oncology: Seminars and Original Investigations* 27(3): 251-257

Myers RB, Srivastava S, Oelschläger DK, Brown D, Grizzle WE (1996) Expression of nm23-H1 in prostatic intraepithelial neoplasia and adenocarcinoma. *Human Pathology* 27(10): 1021-1024

Nam RK, Sugar L, Yang W, Srivastava S, Klotz LH, Yang LY, Stanimirovic A, Encioiu E, Neill M, Loblaw DA, Trachtenberg J, Narod SA, Seth A (2007) Expression of the TMPRSS2:ERG fusion gene predicts cancer recurrence after surgery for localised prostate cancer. *Br J Cancer* 97(12): 1690-5

Newberry EP, Kennedy SM, Xie Y, Sternard BT, Luo J, Davidson NO (2008) Diet-induced obesity and hepatic steatosis in L-Fabp / mice is abrogated with SF, but not PUFA, feeding and attenuated after cholesterol supplementation. *Am J Physiol Gastrointest Liver Physiol* 294(1): G307-14

Newberry EP, Xie Y, Kennedy SM, Luo J, Davidson NO (2006) Protection against Western diet-induced obesity and hepatic steatosis in liver fatty acid-binding protein knockout mice. *Hepatology* 44(5): 1191-205

Noordzij MA, van Steenbrugge GJ, Schroder FH, Van der Kwast TH (1999) Decreased expression of CD44 in metastatic prostate cancer. *Int J Cancer* 84(5): 478-83

Noordzij MA, van Steenbrugge GJ, Verkaik NS, Schroder FH, van der Kwast TH (1997) The prognostic value of CD44 isoforms in prostate cancer patients treated by radical prostatectomy. *Clin Cancer Res* 3(5): 805-15

Nowak DG, Woolard J, Amin EM, Konopatskaya O, Saleem MA, Churchill AJ, Lodomery MR, Harper SJ, Bates DO (2008) Expression of pro- and anti-angiogenic isoforms of VEGF is differentially regulated by splicing and growth factors. *J Cell Sci* 121(Pt 20): 3487-95

Omara-Opyene AL, Qiu J, Shah GV, Iczkowski KA (2004) Prostate cancer invasion is influenced more by expression of a CD44 isoform including variant 9 than by Muc18. *Lab Invest* 84(7): 894-907

Orth P, Weimer A, Kaul G, Kohn D, Cucchiarini M, Madry H (2008) Analysis of novel nonviral gene transfer systems for gene delivery to cells of the musculoskeletal system. *Mol Biotechnol* 38(2): 137-44

Penno H, Nilsson O, Brandstrom H, Winqvist O, Ljunggren O (2009) Expression of RANK-ligand in prostate cancer cell lines. *Scand J Clin Lab Invest* 69(1): 151-5



Peters JM, Gonzalez FJ (2009) Sorting out the functional role(s) of peroxisome proliferator-activated receptor-beta/delta (PPARbeta/delta) in cell proliferation and cancer. *Biochim Biophys Acta* 1796(2): 230-41

Pfaffl MW (2001) A new mathematical model for relative quantification in real-time RT-PCR. *Nucleic Acids Res* 29(9): e45

Pich A, Chiusa L, Navone R (2004) Prognostic relevance of cell proliferation in head and neck tumors. *Annals of Oncology* 15(9): 1319-1329

Pino MV, Kelley MF, Jayyosi Z (2004) Promotion of colon tumors in C57BL/6J-APC(min)/+ mice by thiazolidinedione PPARgamma agonists and a structurally unrelated PPARgamma agonist. *Toxicol Pathol* 32(1): 58-63

Pinthus JH, Lu JP, Bidaisee LA, Lin H, Bryskine I, Gupta RS, Singh G (2007) Androgen-dependent regulation of medium and long chain fatty acids uptake in prostate cancer. *Prostate* 67(12): 1330-8

Piqueras L, Reynolds AR, Hodivala-Dilke KM, Alfranca A, Redondo JM, Hatae T, Tanabe T, Warner TD, Bishop-Bailey D (2007) Activation of PPARbeta/delta induces endothelial cell proliferation and angiogenesis. *Arterioscler Thromb Vasc Biol* 27(1): 63-9

Ponta H, Sherman L, Herrlich PA (2003) CD44: from adhesion molecules to signalling regulators. *Nat Rev Mol Cell Biol* 4(1): 33-45

Quigley CA, De Bellis A, Marschke KB, el-Awady MK, Wilson EM, French FS (1995) Androgen receptor defects: historical, clinical, and molecular perspectives. *Endocr Rev* 16(3): 271-321

Quiner TE, Nakken HL, Mason BA, Lephart ED, Hancock CR, Christensen MJ (2011) Soy Content of Basal Diets Determines the Effects of Supplemental Selenium in Male Mice. *The Journal of Nutrition* 141(12): 2159-2165

Quinn DI, Henshall SM, Sutherland RL (2005) Molecular markers of prostate cancer outcome. *Eur J Cancer* 41(6): 858-87

Rachet B, Maringe C, Nur U, Quaresma M, Shah A, Woods LM, Ellis L, Walters S, Forman D, Steward J, Coleman MP (2009) Population-based cancer survival trends

in England and Wales up to 2007: an assessment of the NHS cancer plan for England. *Lancet Oncol* 10(4): 351-69

Raffo AJ, Perlman H, Chen MW, Day ML, Streitman JS, Buttyan R (1995) Overexpression of bcl-2 protects prostate cancer cells from apoptosis in vitro and confers resistance to androgen depletion in vivo. *Cancer Research* 55(19): 4438-4445

Reddy GP, Barrack ER, Dou QP, Menon M, Pelley R, Sarkar FH, Sheng S (2006) Regulatory processes affecting androgen receptor expression, stability, and function: potential targets to treat hormone-refractory prostate cancer. *J Cell Biochem* 98(6): 1408-23

Revelos K, Petraki C, Gregorakis A, Scorilas A, Papanastasiou P, Koutsilieris M (2005) Immunohistochemical expression of Bcl2 is an independent predictor of time-to-biochemical failure in patients with clinically localized prostate cancer following radical prostatectomy. *Anticancer Res* 25(4): 3123-33

Rizzo S, Attard G, Hudson DL (2005) Prostate epithelial stem cells. *Cell Proliferation* 38(6): 363-374

Rosenblatt KA, Wicklund KG, Stanford JL (2001) Sexual Factors and the Risk of Prostate Cancer. *American Journal of Epidemiology* 153(12): 1152-1158

Rubin MA, Mucci NR, Figurski J, Fecko A, Pienta KJ, Day ML (2001) E-cadherin expression in prostate cancer: a broad survey using high-density tissue microarray technology. *Hum Pathol* 32(7): 690-7

Rubin SJ, Hallahan DE, Ashman CR, Brachman DG, Beckett MA, Virudachalam S, Yandell DW, Weichselbaum RR (1991) Two prostate carcinoma cell lines demonstrate abnormalities in tumor suppressor genes. *J Surg Oncol* 46(1): 31-6

Ruizeveld de Winter JA, Janssen PJ, Sleddens HM, Verleun-Mooijman MC, Trapman J, Brinkmann AO, Santerse AB, Schroder FH, van der Kwast TH (1994) Androgen receptor status in localized and locally progressive hormone refractory human prostate cancer. *Am J Pathol* 144(4): 735-46

Ruscica M, Dozio E, Motta M, Magni P (2007) Role of neuropeptide Y and its receptors in the progression of endocrine-related cancer. *Peptides* 28(2): 426-434

Sasagawa I, Nakada T (2001) EPIDEMIOLOGY OF PROSTATIC CANCER IN EAST ASIA. *Systems Biology in Reproductive Medicine* 47(3): 195-201

Sausville J, Naslund M (2010) Benign prostatic hyperplasia and prostate cancer: an overview for primary care physicians. *Int J Clin Pract* 64(13): 1740-5

Schroder FH (2008) Progress in understanding androgen-independent prostate cancer (AIPC): a review of potential endocrine-mediated mechanisms. *Eur Urol* 53(6): 1129-37

Schroder FH, Hugosson J, Roobol MJ, Tammela TL, Ciatto S, Nelen V, Kwiatkowski M, Lujan M, Lilja H, Zappa M, Denis LJ, Recker F, Berenguer A, Maattanen L, Bangma CH, Aus G, Villers A, Rebillard X, van der Kwast T, Blijenberg BG, Moss SM, de Koning HJ, Auvinen A (2009) Screening and prostate-cancer mortality in a randomized European study. *N Engl J Med* 360(13): 1320-8

Schug TT, Berry DC, Shaw NS, Travis SN, Noy N (2007a) Opposing effects of retinoic acid on cell growth result from alternate activation of two different nuclear receptors. *Cell* 129(4): 723-33

Schug TT, Berry DC, Shaw NS, Travis SN, Noy N (2007b) Opposing Effects of Retinoic Acid on Cell Growth Result from Alternate Activation of Two Different Nuclear Receptors. *Cell* 129(4): 723-733

Schulz WA, Burchardt M, Cronauer MV (2003) Molecular biology of prostate cancer. *Molecular Human Reproduction* 9(8): 437-448

Serhan CN (2007) Resolution phase of inflammation: novel endogenous anti-inflammatory and proresolving lipid mediators and pathways. *Annu Rev Immunol* 25: 101-37

Shaneyfelt T, Husein R, Bubley G, Mantzoros CS (2000) Hormonal predictors of prostate cancer: a meta-analysis. *J Clin Oncol* 18(4): 847-53

Shi XB, Gandour-Edwards R, Beckett LA, Deitch AD, de Vere White RW (2004) A modified yeast assay used on archival samples of localized prostate cancer tissue improves the detection of p53 abnormalities and increases their predictive value. *BJU International* 94(7): 996-1002

Shi XB, Nesslinger NJ, Deitch AD, Gumerlock PH, deVere White RW (2002) Complex functions of mutant p53 alleles from human prostate cancer. *Prostate* 51(1): 59-72

Shields JM, Pruitt K, McFall A, Shaub A, Der CJ (2000) Understanding Ras: '[i]t ain't over 'til it's over'. *Trends in Cell Biology* 10(4): 147-154

Shin YJ, Kim JH (2012) The Role of EZH2 in the Regulation of the Activity of Matrix Metalloproteinases in Prostate Cancer Cells. *PLoS One* 7(1): e30393

Sinha P, Hutter G, Kottgen E, Dietel M, Schadendorf D, Lage H (1999) Increased expression of epidermal fatty acid binding protein, cofilin, and 14-3-3-sigma (stratifin) detected by two-dimensional gel electrophoresis, mass spectrometry and microsequencing of drug-resistant human adenocarcinoma of the pancreas. *Electrophoresis* 20(14): 2952-60

Slamon DJ, Leyland-Jones B, Shak S, Fuchs H, Paton V, Bajamonde A, Fleming T, Eiermann W, Wolter J, Pegram M, Baselga J, Norton L (2001) Use of Chemotherapy plus a Monoclonal Antibody against HER2 for Metastatic Breast Cancer That Overexpresses HER2. *New England Journal of Medicine* 344(11): 783-792

Sobel RE, Sadar MD (2005) Cell lines used in prostate cancer research: a compendium of old and new lines--part 1. *The Journal of Urology* 173(2): 342-359

Soker S, Kaefer M, Johnson M, Klagsbrun M, Atala A, Freeman MR (2001) Vascular endothelial growth factor-mediated autocrine stimulation of prostate tumor cells coincides with progression to a malignant phenotype. *Am J Pathol* 159(2): 651-9

Sowery RD, So AI, Gleave ME (2007) Therapeutic options in advanced prostate cancer: present and future. *Curr Urol Rep* 8(1): 53-9

Stanbrough M, Bubley GJ, Ross K, Golub TR, Rubin MA, Penning TM, Febbo PG, Balk SP (2006) Increased expression of genes converting adrenal androgens to testosterone in androgen-independent prostate cancer. *Cancer Res* 66(5): 2815-25

Stephen RL, Gustafsson MC, Jarvis M, Tatoud R, Marshall BR, Knight D, Ehrenborg E, Harris AL, Wolf CR, Palmer CN (2004) Activation of peroxisome proliferator-activated receptor delta stimulates the proliferation of human breast and prostate cancer cell lines. *Cancer Res* 64(9): 3162-70

Stewart LV, Lyles B, Lin MF, Weigel NL (2005) Vitamin D receptor agonists induce prostatic acid phosphatase to reduce cell growth and HER-2 signaling in LNCaP-derived human prostate cancer cells. *J Steroid Biochem Mol Biol* 97(1-2): 37-46

Syed S, Tolcher A (2003) Innovative therapies for prostate cancer treatment. *Rev Urol* 5 Suppl 3: S78-84

Tanaka N, Fujimoto K, Hirayama A, Yoneda T, Yoshida K, Hirao Y (2010) Trends of the Primary Therapy for Patients with Prostate Cancer in Nara Uro-oncological Research Group (NUORG): A Comparison Between the CaPSURE Data and the NUORG Data. *Japanese Journal of Clinical Oncology* 40(6): 588-592

Taneja SS, Ha S, Garabedian MJ (2001) Androgen stimulated cellular proliferation in the human prostate cancer cell line LNCaP is associated with reduced retinoblastoma protein expression. *J Cell Biochem* 84(1): 188-99

Taplin ME, Bubley GJ, Ko YJ, Small EJ, Upton M, Rajeshkumar B, Balk SP (1999) Selection for androgen receptor mutations in prostate cancers treated with androgen antagonist. *Cancer Res* 59(11): 2511-5

Taplin ME, Rajeshkumar B, Halabi S, Werner CP, Woda BA, Picus J, Stadler W, Hayes DF, Kantoff PW, Vogelzang NJ, Small EJ (2003) Androgen receptor mutations in androgen-independent prostate cancer: Cancer and Leukemia Group B Study 9663. *J Clin Oncol* 21(14): 2673-8

Tell G, Pines A, Arturi F, Cesaratto L, Adamson E, Puppini C, Presta I, Russo D, Filetti S, Damante G (2004) Control of Phosphatase and Tensin Homolog (PTEN) Gene Expression in Normal and Neoplastic Thyroid Cells. *Endocrinology* 145(10): 4660-4666

Tomita K, van Bokhoven A, van Leenders GJLH, Ruijter ETG, Jansen CFJ, Bussemakers MJG, Schalken JA (2000) Cadherin Switching in Human Prostate Cancer Progression. *Cancer Research* 60(13): 3650-3654

Tomlins SA, Rhodes DR, Perner S, Dhanasekaran SM, Mehra R, Sun XW, Varambally S, Cao X, Tchinda J, Kuefer R, Lee C, Montie JE, Shah RB, Pienta KJ, Rubin MA, Chinnaiyan AM (2005) Recurrent fusion of TMPRSS2 and ETS transcription factor genes in prostate cancer. *Science* 310(5748): 644-8

Tulinius H, Egilsson V, Olafsdottir GH, Sigvaldason H (1992) Risk of prostate, ovarian, and endometrial cancer among relatives of women with breast cancer. *BMJ* 305(6858): 855-7

Tuszynski GP, Gasic TB, Rothman VL, Knudsen KA, Gasic GJ (1987) Thrombospondin, a potentiator of tumor cell metastasis. *Cancer Res* 47(15): 4130-3

Umbas R, Isaacs WB, Bringuier PP, Xue Y, Debruyne FM, Schalken JA (1997) Relation between aberrant alpha-catenin expression and loss of E-cadherin function in prostate cancer. *Int J Cancer* 74(4): 374-7

van Bokhoven A, Varella-Garcia M, Korch C, Johannes WU, Smith EE, Miller HL, Nordeen SK, Miller GJ, Lucia MS (2003) Molecular characterization of human prostate carcinoma cell lines. *Prostate* 57(3): 205-25

van der Kwast TH, Schalken J, Ruizeveld de Winter JA, van Vroonhoven CC, Mulder E, Boersma W, Trapman J (1991) Androgen receptors in endocrine-therapy-resistant human prostate cancer. *Int J Cancer* 48(2): 189-93

Veldscholte J, Berrevoets CA, Ris-Stalpers C, Kuiper GG, Jenster G, Trapman J, Brinkmann AO, Mulder E (1992) The androgen receptor in LNCaP cells contains a mutation in the ligand binding domain which affects steroid binding characteristics and response to antiandrogens. *J Steroid Biochem Mol Biol* 41(3-8): 665-9

Verhagen PC, van Duijn PW, Hermans KG, Looijenga LH, van Gurp RJ, Stoop H, van der Kwast TH, Trapman J (2006) The PTEN gene in locally progressive prostate cancer is preferentially inactivated by bi-allelic gene deletion. *J Pathol* 208(5): 699-707

Verkaik NS, van Steenbrugge GJ, van Weerden WM, Bussemakers MJ, van der Kwast TH (2000) Silencing of CD44 expression in prostate cancer by hypermethylation of the CD44 promoter region. *Lab Invest* 80(8): 1291-8

Vlietstra RJ, van Alewijk DCJG, Hermans KGL, van Steenbrugge GJ, Trapman J (1998) Frequent Inactivation of PTEN in Prostate Cancer Cell Lines and Xenografts. *Cancer Research* 58(13): 2720-2723

Vorum H, Madsen P, Svendsen I, Cells JE, Honore B (1998) Expression of recombinant psoriasis-associated fatty acid binding protein in Escherichia coli: gel electrophoretic characterization, analysis of binding properties and comparison with human serum albumin. *Electrophoresis* 19(10): 1793-802

Weinstein IB, Joe AK (2006) Mechanisms of Disease: oncogene addiction[mdash]a rationale for molecular targeting in cancer therapy. *Nat Clin Prac Oncol* 3(8): 448-457

West NR, Watson PH (2010) S100A7 (psoriasin) is induced by the proinflammatory cytokines oncostatin-M and interleukin-6 in human breast cancer. *Oncogene* 29(14): 2083-2092

Williams K, Fernandez S, Stien X, Ishii K, Love HD, Lau Y-F, Roberts RL, Hayward SW (2005) Unopposed c-MYC expression in benign prostatic epithelium causes a cancer phenotype. *The Prostate* 63(4): 369-384

Wise G, Ostad E (2001) Hormonal treatment of patients with benign prostatic hyperplasia: Pros and cons. *Current Urology Reports* 2(4): 285-291

Yu M, Leav BA, Leav I, Merk FB, Wolfe HJ, Ho SM (1993) Early alterations in ras protooncogene mRNA expression in testosterone and estradiol-17 $\beta$  induced prostatic dysplasia of Noble rats. *Laboratory Investigation* 68(1): 33-44

Zhang X, Lee C, Ng P-Y, Rubin M, Shabsigh A, Buttyan R (2000) Prostatic neoplasia in transgenic mice with prostate-directed overexpression of the c-myc oncoprotein. *The Prostate* 43(4): 278-285

Zheng X, Cui XX, Gao Z, Zhao Y, Lin Y, Shih WJ, Huang MT, Liu Y, Rabson A, Reddy B, Yang CS, Conney AH (2010) Atorvastatin and celecoxib in combination inhibits the progression of androgen-dependent LNCaP xenograft prostate tumors to androgen independence. *Cancer Prev Res (Phila)* 3(1): 114-24

Ziada A, Barqawi A, Glode LM, Varella-Garcia M, Crighton F, Majeski S, Rosenblum M, Kane M, Chen L, Crawford ED (2004) The use of trastuzumab in the treatment of hormone refractory prostate cancer; phase II trial. *Prostate* 60(4): 332-7

Zimmer JS, Dyckes DF, Bernlohr DA, Murphy RC (2004) Fatty acid binding proteins stabilize leukotriene A4: competition with arachidonic acid but not other lipoxygenase products. *J Lipid Res* 45(11): 2138-44

Zimmerman AW, van Moerkerk HTB, Veerkamp JH (2001) Ligand specificity and conformational stability of human fatty acid-binding proteins. *The International Journal of Biochemistry & Cell Biology* 33(9): 865-876

Zimmerman AW, Veerkamp JH (2002) New insights into the structure and function of fatty acid-binding proteins. *Cell Mol Life Sci* 59(7): 1096-116



## **8 Appendices**

## 8.1 Appendix 1

### 8.1.1 Materials for general molecular Biology

Reagents	Supplier
.....	
Absolute ethanol	BDH
Agarose	Geneflow
Bromophenol blue	Sigma
Calcium Chloride	Sigma
DEPC	Sigma
DNA Marker III	Roche
DNA Marker XIV	Roche
Ethidium bromide	Sigma
Glycerol	Sigma
Isopropanol	BDH
Microcentrifuge	Beckman Coulter
NanoDrop ND-1000	NanoDrop Technologies
Potassium acetate	Sigma
Potassium chloride	Sigma
QIAprep Spin Miniprep Kit	Qiagen

QIAprep Spin Midiprep Kit	Qiagen
QIAshredder spin column	Qiagen
Restriction enzymes	New England BioLabs
Restriction enzyme buffers	New England BioLabs
SDS	Sigma
Sodium chloride	Sigma
Sodium acetate	Sigma
Sonicator	Bandelin
Wizard DNA Clean-up System	Promega
Xylene cyanol FF	Sigma
Ni-NTA fast start kit	Qiagen

### 8.1.2 Materials for transformation of competent bacteria

Reagents	Supplier
.....	
Ampicillin	Sigma
Bacto-tryptone	Sigma
DH5 $\alpha$ <i>E.coli</i> bacteria	Invitrogen

Glucose	Sigma
Kanamycin	Sigma
LB agar	Sigma
LB broth	Sigma
Magnesium chloride	Sigma
Magnesium sulphate	Sigma
MOPS	Sigma
Yeast extract	Fisher Scientific

### 8.1.3 Materials for point mutation

Reagents	Supplier
.....	
10x annealing solution	Ambion
10x T4 DNA ligase buffer	Ambion
10x T4 Polynucleotide Kinase Buffer	New England BioLabs
IPTG	Sigma
Mutagenic and selection primers	Invitrogen
T4 DNA ligase	Ambion

T4 DNA polymerase	Clontech
T4 Polynucleotide Kinase	New England BioLabs
Transformer <sup>™</sup> Site-Directed Mutagenesis Kit	Clontech

#### 8.1.4 Materials for PCR, RT-PCR and Real-time PCR

Reagents	Supplier
.....	
5x First strand buffer	Stratagene
10x PCR buffer	Promega
Brilliant II SYBR green Q-PCR master mix	Stratagene
dNTPs	ABgene
DTT	Invitrogen
Oligo (dT) <sub>20</sub>	Stratagene
PCR primers	Invitrogen
RNaseOUT	Invitrogen
SuperScriptIII reverse transcriptase	Stratagene
Taq DNA polymerase	Promega
Thermo-Cycler PTC-200	MJ Research

### 8.1.5 Materials for cell culture

Reagents	Supplier
.....	
Cell culture plates and filter cap flasks	Nunc
Labofuge 400R (Centrifuge)	Heraeus
Cryogenic vials	Nunc
DMSO	Sigma
EndoGRO basal medium	Millipore
EndoGRO LS supplement kit	Millipore
Eppendorf tubes (1.5ml)	Sarstedt
Fetal calf serum	Biosera
PixCell II (fluorescence microscope)	Arcturus
GeneJammer transfection reagent	Stratagene
Geneticin (G418)	PAA
Hemocytometer slide	Weber scientific international
Hydrocortisone	Sigma
Incubator (Cell culture)	Thermo Scientific
L-Glutamine	BioWhittaker
Penicillin/Streptomycin	BioWhittaker

Phosphate buffered saline (Tablet)	Gibco
XGI 1640	PAA
Sodium pyruvate	Sigma
Testosterone	Sigma
Tissue culture pipettes (5ml – 25ml)	Greiner bio-one
Trypsin	Gibco
Universal tube (25ml)	Greiner bio-one
Versene	Gibco
Water bath	Grant Instruments

### 8.1.6 Materials for Western blot

Reagents	Supplier
.....	
$\beta$ -mercaptoethanol	Sigma
Next gel 12.5%	Pro Pure
Next gel running buffer	Pro Pure
Bradford reagent	Sigma
CellLytic-M	Sigma
Coomassie brilliant blue	Bio-Rad

ECL detection kit	GE Healthcare
Hyper films	Amersham Biosciences
Kodak Developer	Sigma
Reagents	Supplier
Kodak Fixer	Sigma
Pro Sieve colour protein marker	Cambrex
Methanol	Fisher Scientific
Nitrocellulose membrane	Amersham biosciences
Problock reagent A &B	ACTG (National diagnostics)
Roller mixer SRT1	Stuart
TEMED	Sigma
Tween-20	Sigma

### 8.1.7 Materials for fatty acid uptake assay

Reagents	Supplier
.....	
BSA	Sigma
BODIPY 558/568C <sub>12</sub>	Invitrogen
EPICS XL Flow Cytometer	Beckman Coulter



### 8.1.8 Materials for fatty acid Binding assay

Reagents	Supplier
.....	
Myristic acid	Sigma
Palmitic acid	Sigma
Oleic acid	Sigma
Linoleic acid	Sigma
DAUDA	Cayman Chemical

### 8.1.9 Materials for cell proliferation assay

Reagents	Supplier
.....	
96-well plate	Nunc
MTT	Sigma
Multiscan plate reader	Labsystem

**8.1.10 Materials for cell invasion assay****Reagents****Supplier**

.....

Multiwell 24-well Boyden chamber plate

BD

Boyden chamber

BD

Crystal violet

Sigma

Matrigel

BD

**8.1.11 Materials for soft agar assay****Reagents****Supplier**

.....

GelCount

Oxford Optronix

Low melting point agarose

Geneflow

Autoclave

Boxer Laboratory Equipment

## 8.2 Appendix 2

### 8.2.1 Media and Stock Solutions

#### 8.2.1.1 Tissue culture

##### Routine cell culture medium

- XGI medium 1640 500ml
- Foetal calf serum 10% (v/v)
- Pen-Strep (5000U/ml) 5ml
- L-Glutamine (200mM) 5ml
- Testosterone (5µg/ml) 5ml
- Sodium pyruvate (100mM) 5ml

##### Freezing medium

- Routin cell culture medium 92% (v/v)
- DMSO 8% (v/v)

##### Trypsin/EDTA solution (2.5%)

- Versene 100ml
- Trypsin 2.5ml

##### MTT solution (5mg/ml)

- MTT 50mg
- PBS 10ml

#### Molecular Biology

##### LB medium

- LB broth 10g
- dH<sub>2</sub>O 500ml

##### LB agar

- LB agar 17.5g
- dH<sub>2</sub>O 500ml

##### RF1 buffer (pH 6.8)

- KCl 100mM
- MgCl<sub>2</sub>.4H<sub>2</sub>O 50mM
- K-acetate 30mM
- CaCl<sub>2</sub> 10mM
- Glycerol 15% v/v

**RF2 buffer (pH 6.8)**

- MOPS 10mM
- KCl 10mM
- CaCl<sub>2</sub>.2H<sub>2</sub>O 75mM
- Glycerol 15% v/v

**SOB medium (pH 7.0)**

- Trypon 2% (w/v)
- Yeast Extract 0.5% (w/v)
- NaCl 10mM
- KCl 2.5mM
- MgCl<sub>2</sub> 10mM
- MgSO<sub>4</sub> 10mM

**SOC medium (pH 7.0)**

- Trypon 2% (w/v)
- Yeast Extract 0.5% (w/v)
- NaCl 10mM
- KCl 2.5mM
- MgCl<sub>2</sub> 10mM
- MgSO<sub>4</sub> 10mM
- Glucose 20mM

**Stock medium for bacteria**

- Glycerol 50% (v/v)
- LB medium with bacteria 50% (v/v)

**8.2.1.2 Qiagen Midi-prep plasmid extraction buffers****Buffer P1 – Resuspension buffer**

- Tris-HCl (pH 8.0) 50mM
- EDTA 10mM
- RNaseA 100µg/ml

**Buffer P2 – Lysis buffer**

- NaOH 200mM
- SDS 1% (w/v)

**Buffer P3 – Neutralising buffer**

- K-acetate (pH 5.5) 3.0M

**Buffer QBT – Equilibration buffer**

- NaCl 750mM
- MOPS (pH 7.0) 50mM
- Isopropanol 15% (v/v)
- Triton X-100 15% (v/v)

**Buffer QC – Wash buffer**

- NaCl 1.0M
- MOPS (pH7.0) 50mM
- Isopropanol 15% (v/v)

**Buffer QF – Elution buffer**

- NaCl 1.25M
- Tris-HCl (pH 8.5) 50mM
- Isopropano 15% (v/v)

**TE buffer (pH 7.5)**

- Tris-HCl 10 mM
- EDTA 1 mM

**8.2.1.3 Wizard SV gel and PCR clean-up system buffers****Membrane binding solution**

- Guanidine isothiocyanate 4.5M
- K-acetate (pH5.0) 0.5M

**Membrane wash solution**

- K-acetate (pH5.0) 10mM
- Ethanol 80% (v/v)
- EDTA (pH8.0) 16.7μM

**DNA loading buffer**

- Bromophenol blue 0.25% (w/v)
- Xylene cyanol FF 0.25% (w/v)
- Glycerol 30% (v/v)
- dH<sub>2</sub>O 70% (v/v)

**10x TBE buffer (pH 8.0)**

- Tris base 890mM
- Boric acid 890mM
- EDTA 20mM

#### 8.2.1.4 Western blot buffers

##### 5x SDS-PAGE sample loading buffer

- |                             |        |
|-----------------------------|--------|
| • 1M Tris-HCl (pH 6.8)      | 1.25ml |
| • 40% (v/v) Glycerol        | 15ml   |
| • 10% SDS                   | 5ml    |
| • 1% (w/v) Bromophenol blue | 2.5ml  |
| • $\beta$ -mercaptoethanol  | 1.25ml |

##### Running Buffer

- |                           |       |
|---------------------------|-------|
| • Next gel running buffer | 25ml  |
| • Distilled water         | 500ml |

##### Transfer Buffer

- |             |           |
|-------------|-----------|
| • Glycine   | 192mM     |
| • Methanol  | 20% (v/v) |
| • Tris base | 25mM      |

##### 10x TBS (pH 7.5)

- |             |        |
|-------------|--------|
| • Tris base | 500mM  |
| • NaCl      | 1500mM |

##### TBS-Tween (Washing Buffer)

- |            |        |
|------------|--------|
| • 1x TBS   | 1000ml |
| • Tween 20 | 1ml    |

##### Blocking Buffer

- |                   |       |
|-------------------|-------|
| • 5% Skimmed milk | 5mg   |
| • TBST            | 100ml |

### 8.3 Appendix 3

#### Sequences alignment of the wild type and mutant C-FABP cDNAs

```

Score = 1212 bits (656), Expect = 0.0
Identities = 662/662 (100%), Gaps = 0/662 (0%)
Strand=Plus/Plus

Query 250 CGCCGACGCAGACCCCTCTCTGCACGCCAGCCCGCCCGCACCCACCATGGCCACAGTTCA 309
          |||
Sbjct 68 CGCCGACGCAGACCCCTCTCTGCACGCCAGCCCGCCCGCACCCACCATGGCCACAGTTCA 127

Query 310 GCAGCTGGAAGGAAGATGGCGCCTGGTGGACAGCAAAGGCTTTGATGAATACATGAAGGA 369
          |||
Sbjct 128 GCAGCTGGAAGGAAGATGGCGCCTGGTGGACAGCAAAGGCTTTGATGAATACATGAAGGA 187

Query 370 GCTAGGAGTGGGAATAGCTTTGCGAAAAATGGGCGCAATGGCCAAGCCAGATTGTATCAT 429
          |||
Sbjct 188 GCTAGGAGTGGGAATAGCTTTGCGAAAAATGGGCGCAATGGCCAAGCCAGATTGTATCAT 247

Query 430 CACTTGTGATGGTAAAAACCTCACCATAAAAACTGAGAGCACTTTGAAAACAACACAGTT 489
          |||
Sbjct 248 CACTTGTGATGGTAAAAACCTCACCATAAAAACTGAGAGCACTTTGAAAACAACACAGTT 307

Query 490 TTCTTGTACCTGGGAGAGAAGTTTGAAGAAACCACAGCTGATGGCAGAAAACTCAGAC 549
          |||
Sbjct 308 TTCTTGTACCTGGGAGAGAAGTTTGAAGAAACCACAGCTGATGGCAGAAAACTCAGAC 367

Query 550 TGTCTGCAACTTTACAGATGGTGCATTGGTTCAGCATCAGGAGTGGGATGGGAAGGAAAG 609
          |||
Sbjct 368 TGTCTGCAACTTTACAGATGGTGCATTGGTTCAGCATCAGGAGTGGGATGGGAAGGAAAG 427

Query 610 CACAATAACAAGAAAAATTGAAAGATGGGAAATTAGTGGTGGAGTGTGTCATGAACAATGT 669
          |||
Sbjct 428 CACAATAACAAGAAAAATTGAAAGATGGGAAATTAGTGGTGGAGTGTGTCATGAACAATGT 487

Query 670 CACCTGTACTCGGATCTATGAAAAAGTAGAATAAAAAATCCATCATCACTTTGGACAGGA 729
          |||
Sbjct 488 CACCTGTACTCGGATCTATGAAAAAGTAGAATAAAAAATCCATCATCACTTTGGACAGGA 547

Query 730 GTTAATTAAGAGAATGACCAAGCTCAGTTCAATGAGCAAATCTCCATACTGTTTCTTTCT 789
          |||
Sbjct 548 GTTAATTAAGAGAATGACCAAGCTCAGTTCAATGAGCAAATCTCCATACTGTTTCTTTCT 607

Query 790 TTTTTTTTTCATTACTGTGTTCAATTATCTTTATCATAAACATTTTACATGCAGCTATTT 849
          |||
Sbjct 608 TTTTTTTTTCATTACTGTGTTCAATTATCTTTATCATAAACATTTTACATGCAGCTATTT 667

Query 850 CAAAGTGTGTTGGATTAATTAGGATCATCCCTTTGGTTAATAAATAAATGTGTTTGTGCT 909
          |||
Sbjct 668 CAAAGTGTGTTGGATTAATTAGGATCATCCCTTTGGTTAATAAATAAATGTGTTTGTGCT 727

Query 910 AA 911
          ||
Sbjct 728 AA 729

```

#### Figure 8.1: Confirmation of insertion of C-FABP-WT cDNA into pQE32

*Sequence alignment was determined by using BioEdit for searching Genbank (BLAST). The sequences alignment showed a 100% sequences match between Query (C-FABP-WT) and subject (database sequence).*

Score = 1201 bits (650), Expect = 0.0  
 Identities = 661/663 (99.5%), Gaps = 2/663 (0%)  
 Strand=Plus/Plus

```

Query  252  CGCCGACGCAGACCCCTCTCTGCACGCCAGCCCGCCCGCACCACCATGGCCACAGTTCA 311
      |||
Sbjct  68    CGCCGACGCAGACCCCTCTCTGCACGCCAGCCCGCCCGCACCACCATGGCCACAGTTCA 127

Query  312  GCAGCTGGAAGGAAGATGGCGCCTGGTGGACAGCAAAGGCTTTGATGAATACATGAAGGA 371
      |||
Sbjct  128  GCAGCTGGAAGGAAGATGGCGCCTGGTGGACAGCAAAGGCTTTGATGAATACATGAAGGA 187

Query  372  GCTAGGAGTGGGAATAGCTTTGCGAAAAATGGGCGCAATGGCCAAGCCAGATTGTATCAT 431
      |||
Sbjct  188  GCTAGGAGTGGGAATAGCTTTGCGAAAAATGGGCGCAATGGCCAAGCCAGATTGTATCAT 247

Query  432  CACTTGTGATGGTAAAAACCTCACCATAAAAACTGAGAGCACTTTGAAAACAACACAGTT 491
      |||
Sbjct  248  CACTTGTGATGGTAAAAACCTCACCATAAAAACTGAGAGCACTTTGAAAACAACACAGTT 307

Query  492  TTCTTGTACCCTGGGAGAGAAGTTTGAAGAAACCACAGCTGATGGCAGAAAAACTCAGAC 551
      |||
Sbjct  308  TTCTTGTACCCTGGGAGAGAAGTTTGAAGAAACCACAGCTGATGGCAGAAAAACTCAGAC 367

Query  552  TGTCTGCAACTTTACAGATGGTGCATTGGTTTCAGCATCAGGAGTGGGATGGGAAGGAAAG 611
      |||
Sbjct  368  TGTCTGCAACTTTACAGATGGTGCATTGGTTTCAGCATCAGGAGTGGGATGGGAAGGAAAG 427

Query  612  CACAATAACAAGCAAAAAATTGAAAGATGGGAAACTAGTGGTGGAGTGTGTCATGAACAATG 670
      |||
Sbjct  428  CACAATAACAAGCAAAAAATTGAAAGATGGGAAACTAGTGGTGGAGTGTGTCATGAACAATG 486

Query  671  TCACCTGTACTCGGATCTATGAAAAAGTAGAATAAAAAATCCATCATCACTTTGGACAGG 730
      |||
Sbjct  487  TCACCTGTACTCGGATCTATGAAAAAGTAGAATAAAAAATCCATCATCACTTTGGACAGG 546

Query  731  AGTTAATTAAGAGAATGACCAAGCTCAGTTCAATGAGCAAATCTCCATACTGTTTCTTTC 790
      |||
Sbjct  547  AGTTAATTAAGAGAATGACCAAGCTCAGTTCAATGAGCAAATCTCCATACTGTTTCTTTC 606

Query  791  TTTTTTTTTTCATTACTGTGTCAATTATCTTTATCATAAACATTTTACATGCAGCTATT 850
      |||
Sbjct  607  TTTTTTTTTTCATTACTGTGTCAATTATCTTTATCATAAACATTTTACATGCAGCTATT 666

Query  851  TCAAAGTGTGTGGATTAATTAGGATCATCCCTTTGGTTAATAAATAAATGTGTTTGTGC 910
      |||
Sbjct  667  TCAAAGTGTGTGGATTAATTAGGATCATCCCTTTGGTTAATAAATAAATGTGTTTGTGC 726

Query  911  TAA  913
      |||
Sbjct  727  TAA  729

```

### Figure 8.2: Confirmation of insertion of C-FABP-R109A cDNA into pQE32

Sequence alignment was determined by using BioEdit for searching Genbank (BLAST) (appendix 3). The sequences marked in red colour confirmed the location of single mutation (The Alanine GCA, mutated from Arginine AGA). The sequences alignment showed a 99.5% sequences match between Query (C-FABP-R109A) and subject (database sequence). The 0.5% gap confirmed the location of Single mutant.



Score = 1190 bits (644), Expect = 0.0  
 Identities = 660/664 (99%), Gaps = 4/664 (1%)  
 Strand=Plus/Plus

```

Query  258  CGCCGACGCAGACCCCTCTCTGCACGCCAGCCCGCCCGCACCCACCATGGCCACAGTTCA 317
      |||
Sbjct  68    CGCCGACGCAGACCCCTCTCTGCACGCCAGCCCGCCCGCACCCACCATGGCCACAGTTCA 127

Query  318  GCAGCTGGAAGGAAGATGGCGCCTGGTGGACAGCAAAGGCTTTGATGAATACATGAAGGA 377
      |||
Sbjct  128  GCAGCTGGAAGGAAGATGGCGCCTGGTGGACAGCAAAGGCTTTGATGAATACATGAAGGA 187

Query  378  GCTAGGAGTGGGAATAGCTTTGCGAAAAATGGGCGCAATGGCCAAGCCAGATTGTATCAT 437
      |||
Sbjct  188  GCTAGGAGTGGGAATAGCTTTGCGAAAAATGGGCGCAATGGCCAAGCCAGATTGTATCAT 247

Query  438  CACTTGTGATGGTAAAAACCTCACCATAAAAACTGAGAGCACTTTGAAAACAACACAGTT 497
      |||
Sbjct  248  CACTTGTGATGGTAAAAACCTCACCATAAAAACTGAGAGCACTTTGAAAACAACACAGTT 307

Query  498  TTCTTGTACCCTGGGAGAGAAGTTTGAAGAAACCACAGCTGATGGCAGAAAACTCAGAC 557
      |||
Sbjct  308  TTCTTGTACCCTGGGAGAGAAGTTTGAAGAAACCACAGCTGATGGCAGAAAACTCAGAC 367

Query  558  TGTCTGCAACTTTACAGATGGTGCATTGGTTCAGCATCAGGAGTGGGATGGGAAGGAAAG 617
      |||
Sbjct  368  TGTCTGCAACTTTACAGATGGTGCATTGGTTCAGCATCAGGAGTGGGATGGGAAGGAAAG 427

Query  618  CACAATAACAAGCAAAAAATTGAAAGATGGGAAACTAGTGGTGGAGTGTGTCATGAACAATG 676
      |||
Sbjct  428  CACAATAACAAGCAAAAAATTGAAAGATGGGAAACTAGTGGTGGAGTGTGTCATGAACAATG 486

Query  677  TCACCTGTACT--GATCTATGAAAAAGTAGAATAAAAAATTCATCATCACTTTGGACAGG 735
      |||
Sbjct  487  TCACCTGTACTCGGATCTATGAAAAAGTAGAATAAAAAATTCATCATCACTTTGGACAGG 545

Query  736  GAGTTAATTAAGAGAACGACCAAGCTCAGTTCAATGAGCAAAATCTCCATACTGTTTCTTT 795
      |||
Sbjct  546  GAGTTAATTAAGAGAATGACCAAGCTCAGTTCAATGAGCAAAATCTCCATACTGTTTCTTT 605

Query  796  CTTTTTTTTTTCATTACTGTGTCAATTATCTTTATCATAAACATTTTACATGCAGCTAT 855
      |||
Sbjct  606  CTTTTTTTTTTCATTACTGTGTCAATTATCTTTATCATAAACATTTTACATGCAGCTAT 665

Query  856  TTCAAAGTGTGTGGATTAATTAGGATCATCCCTTTGGTTAATAAATAAATGTGTTTGTG 915
      |||
Sbjct  666  TTCAAAGTGTGTGGATTAATTAGGATCATCCCTTTGGTTAATAAATAAATGTGTTTGTG 725

Query  916  CTAA  919
      |||
Sbjct  726  CTAA  729

```

**Figure 8.3: Confirmation of insertion of C-FABP-R109/129A into pQE32**

Sequence alignment was determined by using BioEdit for searching Genbank (BLAST). The sequences marked in red colour confirmed the location of the double mutations (The Alanine GCA, mutated from Arginine AGA and the Alanine GCG, converted from Arginine CGG). The sequences alignment showed a 99% sequences match between Query (C-FABP-R109/129A) and subject (database sequence). The 1% gap confirmed the location of Single and double mutations.

#### **8.4 Appendix 4**

### **AWARDS, CONFERENCES & PUBLICATIONS**



Mr Mohammed Molki  
5 Dunworth Street  
Rusholme  
Manchester  
M14 7WH

18 August 2008

GS/ORS08 200484581

Dear Mr Molki

**ORSAS Scholarship**

On behalf of the University's Scholarship Committee, I am pleased to inform you that you have been awarded an ORSAS scholarship. The scholarship is tenable for up to three years and will pay the difference between the overseas student tuition fee and the home student tuition fee. In conjunction with this award you will also receive an additional award which pays the remainder of your tuition fee and provides a stipend of £1,000 (per annum) towards your living costs and maintenance.

The above scholarship and awards are conditional upon your registration with the University at the start of the 2008/09 session. They will not be credited to you until you have registered as a student for that session. Once your registration is completed, arrangements will be made for the payment of your stipend into your UK bank account (you will be sent an electronic version of the student bank details form before you commence your studies, which you must complete and return to me by hard copy once you have opened a UK bank account).

Please note, that if you register at the University before the 1 October 2008, you will be liable for tuition fees up until the starting date of the ORSAS.

If you haven't already done so, I should be grateful if you would email or write to me to confirm whether or not you intend to take up these awards. If you do not intend to do so, then please write and inform me so that they may be offered to another student.

On behalf of the Scholarships Committee and the University, may I congratulate you on winning these awards and wish you success in your forthcoming studies.

Yours sincerely

A handwritten signature in black ink, appearing to be 'Rebecca Morton'.

Rebecca Morton  
Graduate School Administrator

Tel: 0151 795 4697  
Email: [r.morton@liverpool.ac.uk](mailto:r.morton@liverpool.ac.uk)

Cc: Supervisors  
Faculty of Medicine



## EXCELLENCE AWARD

*Presented to*

**Mohammed Imad Malki**

---

*EACR Prize for Best Presentation (C-FABP & Prostate Cancer)*

*the 53rd Annual Meeting of the Italian Cancer Society (SIC) Back to the Future: Translating Cancer  
Research from Bedside to Bench and Back*

22 October 2011



A handwritten signature in black ink, reading 'Anne-Lise Børresen-Dale'.

Anne-Lise Børresen-Dale



## CERTIFICATE OF ATTENDANCE

This is to certify that **Dr. MOHAMMED IMAD MALKI** has attended the "Cell Death in Cancer" Conference held in Amsterdam, the Netherlands from 26<sup>th</sup> to 28<sup>th</sup> January 2012.

The Accreditation Council of Oncology in Europe (ACOE) has appraised and approved the "Cell Death in Cancer" Conference. ACOE accreditation acknowledges the quality of the scientific programme and its educational value.

ACOE is a multidisciplinary body of full time specialists practicing in the field of oncology and all recognised for their experience in education and expertise in their field.

The "Cell Death in Cancer" Conference is designated for a maximum of 12 educational hours.

ACOE credits have been endorsed by the European Accreditation Council for Continuing Medical Education (EACCME) – a body of the European Union of Medical Specialists (UEMS).

These credits are also recognised as Physician's Recognition Award (AMA PRA Category 1 credits) by the American Medical Association.

The above mentioned participant has earned **12** European CME credits at this event (1 ECMEC (European Continuous Medical Education Credit) per full educational hour attended with a maximum of 6 ECMEC's for a full day and 3 ECMEC's for a half day)

This conference operates an honour system. Each medical specialist should claim only those hours of credit that he/ she actually spent in the educational activity.

Prof. Verena Jendrossek

Prof. Simone Fulda

Chairs of the EACR Conference on Cell Death in Cancer



SOCIETÀ ITALIANA DI CANCEROLOGIA

## CERTIFICATE OF ATTENDANCE

MALKI Mohammed (Imad)

has participated in the 53<sup>rd</sup> Meeting of the Italian Cancer Society

**BACK TO THE FUTURE**  
**Translating cancer research**  
**from bedside to bench and back**

organized by SIC (Società Italiana di Cancerologia)  
from 19<sup>th</sup> to 22<sup>nd</sup> October 2011, in Turin, Italy

Turin, October 2011

For the organizing committee:  
Silvia Giordano

A handwritten signature in dark ink, appearing to read 'S. Giordano'.





## CERTIFICATE OF ATTENDANCE

This is to certify that Dr Mohammed Imad Malki has attended the **1st EACR-OECI Joint Training Course "Molecular PATHOLOGY approach to cancer"** held in Amsterdam from 7 to 9 March 2011.

The Accreditation Council of Oncology in Europe (ACOE) has appraised and approved the **1st EACR-OECI Joint Training Course "Molecular PATHOLOGY approach to cancer"**. ACOE accreditation acknowledges the quality of the scientific programme and its educational value.

ACOE is a multidisciplinary body of full time specialists practicing in the field of oncology and all recognised for their experience in education and expertise in their field.

The **1st EACR-OECI Joint Training Course "Molecular PATHOLOGY approach to cancer"** is designated for a maximum of 13 educational hours.

ACOE credits have been endorsed by the European Accreditation Council for Continuing Medical Education (EACCME) – a body of the European Union of Medical Specialists (UEMS).

These credits are also recognised as Physician's Recognition Award (AMA PRA Category 1 credits) by the American Medical Association.

The above mentioned participant has earned 13 ECMEC's at this event (1 ECMEC (European Continuous Medical Education Credit) per full educational hour attended with a maximum of 6 ECMEC's for a full day and 3 ECMEC's for a half day)

This conference operates an honour system. Each medical specialist should claim only those hours of credit that he/ she actually spent in the educational activity.

Marc van de Vijver

Jorge Reis-Filho

Antonio Llombart-Bosch

Angelo Paradiso

c/o ECCO - the European CanCER Organisation • Avenue E. Mounier 83 • B-1200 Brussels • Belgium  
Telephone: + 32 (0) 2 775 02 07 • Telefax: + 32 (0) 2 775 02 00 • e-mail: [accreditation@acoe.be](mailto:accreditation@acoe.be) • [www.acoe.be](http://www.acoe.be)



### CERTIFICATE OF ATTENDANCE

This is to certify that *Malki, M.I. - United Kingdom* has attended the **21st meeting of the European Association for Cancer Research (EACR-21)** held in Oslo, Norway from 26 to 29 June 2010.

The Accreditation Council of Oncology in Europe (ACOE) has appraised and approved the **EACR-21**. ACOE accreditation acknowledges the quality of the scientific programme and its educational value.

ACOE is a multidisciplinary body of full time specialists practicing in the field of oncology and all recognised for their experience in education and expertise in their field.

The **EACR-21** has been designated a maximum of **21** educational hours.

ACOE credits have been endorsed by the European Accreditation Council for Continuing Medical Education (EACCME) - a body of the European Union of Medical Specialists (UEMS).

These credits are also recognised as Physician's Recognition Award (AMA PRA Category 1 credits) by the American Medical Association.

The above mentioned participant has earned ..... out of 21 ECMEC's at this event (1 ECMEC per full educational hour attended with a maximum of 6 ECMEC's for a full day and 3 ECMEC's for a half day)

This conference operates an honour system. Each medical specialist should claim only those hours credit that he/she actually spent in the educational activity.

**Prof. Anne-Lise Børresen-Dale**  
EACR President and Conference Chair

c/o ECCO - the European CanCER Organisation □ Avenue E. Mounier 83 □ B-1200 Brussels □ Belgium  
Telephone: + 32 (0) 2 775 02 07 □ Telefax: + 32 (0) 2 775 02 00 □ e-mail: [accreditation@acoe.be](mailto:accreditation@acoe.be) □ [www.acoe.be](http://www.acoe.be)

<http://www.ecco-org.eu/cm.net.webui/cm.net.webui.zone/eacr/logoncertificate.aspx>

01/07/2010